



HAL
open science

Impact of D-2HG on the Tumor Microenvironment of IDH-mutated Gliomas

Alice Laurence-Leprince

► **To cite this version:**

Alice Laurence-Leprince. Impact of D-2HG on the Tumor Microenvironment of IDH-mutated Gliomas. Cellular Biology. Université Paris-Saclay, 2024. English. NNT : 2024UPASL096 . tel-04905906

HAL Id: tel-04905906

<https://theses.hal.science/tel-04905906v1>

Submitted on 22 Jan 2025

HAL is a multi-disciplinary open access archive for the deposit and dissemination of scientific research documents, whether they are published or not. The documents may come from teaching and research institutions in France or abroad, or from public or private research centers.

L'archive ouverte pluridisciplinaire **HAL**, est destinée au dépôt et à la diffusion de documents scientifiques de niveau recherche, publiés ou non, émanant des établissements d'enseignement et de recherche français ou étrangers, des laboratoires publics ou privés.

Impact of D-2HG on the Tumor Microenvironment of IDH-mutated Gliomas

*Impact du D-2HydroxyGlutarate sur le micro-environnement tumoral
des gliomes avec mutation IDH*

Thèse de doctorat de l'Université Paris-Saclay

École doctorale n° 582 : oncologie : biologie - médecine - santé (CBMS)
Spécialité de doctorat : Sciences du Cancer
Graduate school : Sciences de la vie et santé. Référent : Faculté de médecine

Thèse préparée à l'**Institut du Cerveau** (CNRS, Inserm, Sorbonne Université),
sous la direction de **Marc Sanson**, Professeur des universités – praticien hospitalier,
et le co-encadrement de **Luis Castro-Vega**, Chercheur.

Thèse présentée et soutenue à Paris-Saclay, le 13 décembre 2024, par

Alice LAURENCE-LEPRINCE

Composition du Jury

Membres du jury avec voix délibérative

Alexandre Boissonnas

Directeur de recherche, Inserm, Sorbonne Université

Président & Examineur

François Ducray

PU-PH, Université Claude Bernard Lyon 1

Rapporteur & Examineur

Morgane Thion

Chargée de recherche HDR, CNRS, Université PSL

Rapporteuse & Examinatrice

Sophie Postel-Vinay

Praticienne hospitalière HDR, Université Paris-Saclay

Examinatrice

Remerciements

Je tiens à exprimer mes sincères remerciements à M^{me} Morgane Thion, M^r François Ducray, M^{me} Sophie Postel-Vinay, et M^r Alexandre Boissonnas d'avoir accepté d'évaluer ce travail.

Merci à M^r Marc Sanson de m'avoir donné l'opportunité de réaliser ce travail, pour son encadrement toujours bienveillant, pour ses encouragements et son soutien sans faille,

Merci à M^r Luis Castro-Vega pour son encadrement, sa disponibilité et son indulgence (pourtant mises à rude épreuve pour la rédaction de ce manuscrit), pour nos discussions répétées et constructives,

Merci à M^r Michel Mallat pour son aide suivie, patiente, et attentive, bienveillante, qui aura été fondamentale pendant ces quatre années.

Merci à M^{me} Marie-Anne Debily, M^{me} Violetta Zujovic, et M^r Aymeric Silvin, membres de mon CSI, de leurs critiques bienveillantes, et d'avoir réussi à transformer ce qui me semblait initialement être rébarbatif en un moment constructif et stimulant.

Merci à toute l'équipe de génétique et développement des tumeurs cérébrales de l'ICM de son soutien quotidien, en particulier à :

Pietro Pugliese, Quentin Richard, et Stéphanie Jouannet, pour leur participation active à la réalisation de ce travail,

Karim Labreche, et Agusti Alentorn pour leur aide si précieuse et appréciée sur les aspects bioinformatiques de ce travail,

Franck Bielle, Karima Mokhtari, Suzanne Tran, pour leur appui indispensable à la fois scientifique et organisationnel, et à tous les membres de l'équipe de neuropathologie de la Pitié-Salpêtrière, pour leur disponibilité et leur gentillesse, Sarah Scuderi, et Yvette Hayat qui ont pris ma suite pour les expériences in vitro.

Merci à Isabelle Leroux, Emmanuelle Huillard, et Mehdi Touat pour leur soutien et leurs critiques constructives,

Merci à Nathalie Magne, pour son appui à la fois scientifique, pratique, humain, et amical qui aura été décisif pour la conduite de ce travail,

Merci également à Sandra Joppé et Bertille Bance pour leur soutien scientifique et humain, ainsi qu'à Maïte Verreault,

Merci à la grande équipe de doctorants que nous formons ou avons formée, pour nos échanges constructifs et parfois amicaux, en particulier à Cristina Birzu, Charlotte Bellamy, Nina Potier, Alberto Picca, Lisa Salhi, Alexa Saliou, Irma Segoviano, Diego Prost, Isaias Hernandez, Noémie Barrillot, Rana Salam, Sofia Archontidi, ainsi qu'à Mercedes Otero Pizarro

Merci à Julie Lameth, Marine Giry, Julie Lerond, Sophie Paris, Emie Quissac, Eva Kirasic, Amel Dridi-Aloulou, Catherine Carpentier, pour leur soutien et leur aide dans la réalisation de ce travail

Merci aux membres des différentes plateformes de l'ICM de leur aide et de leur disponibilité, en particulier à David Akbar et Yannick Marie, avec lesquels c'est toujours un plaisir d'interagir et qui ont été d'une grande aide pour la réalisation de ce travail.

Merci à toute l'équipe de neuro-chirurgie de la Pitié-Salpêtrière qui nous confie chaque semaine de précieux échantillons, à la base même de ce travail.
Une pensée particulière et émue pour Laurent Capelle, qui n'est plus parmi nous aujourd'hui, sans qui ce travail n'aurait pas été possible, pour sa bienveillance, son soutien, sa bonne humeur.
Un grand merci également à Bertrand Mathon et Pauline Marijon pour nos échanges enrichissants et leur aide très active qui a été indispensable.

Merci à Gilles Huberfeld et son équipe, notamment Giampaolo Milior et Richard Barrillet, pour leur regard extérieur et leur aide dans la réalisation de ce travail.

Merci à l'ensemble des membres de cette belle et grande équipe de neuro-oncologie au sein de laquelle j'ai la chance d'exercer, pour leur soutien et leurs encouragements.
Merci aux patients et à leurs familles, qui nous communiquent au quotidien leur énergie et leur combativité si précieuses.

Merci à ma famille et mes amis pour leur présence et leur soutien, en particulier à mon mari et à nos trois formidables enfants, dont les aînées s'émerveillent toujours de mes « histoires de microglie ».

Résumé substantiel

Contexte

Les gliomes diffus sont les tumeurs primitives malignes du système nerveux central les plus fréquentes. Certains présentent une mutation du gène codant pour l'isocitrate déshydrogénase 1 ou 2 (IDH) qui leur confère la néo-activité de transformer l'alpha-cétoglutarate (α -KG) produit par l'enzyme non mutée en D-2hydroxyglutarate (D-2HG). L'accumulation de cet oncométabolite entraîne l'inhibition compétitive des dioxygénases dépendantes de l' α -KG, incluant la famille TET (Ten Eleven Translocase) des ADN hydroxylases, et les JmjC/KMDs histone déméthylases, qui conduit elle-même à l'hyperméthylation des histones et de l'ADN des cellules tumorales. Les macrophages et microglies associés aux tumeurs (TAMs) sont des cellules myéloïdes très abondantes dans les gliomes, dont le phénotype et la réponse immunitaire sont déterminés par l'ontogenèse et le microenvironnement. Les TAMs présentent des caractéristiques différentes en fonction du statut IDH du gliome, mais les mécanismes de régulation sous-jacents restent largement méconnus. Le D-2HG relargué dans le microenvironnement par les cellules de gliomes IDH-mutants (IDH-m) pourrait influencer le phénotype et la fonction de ces TAMs. Nous avons émis l'hypothèse que le D-2HG pourrait modifier l'épigénome des TAMs, comme dans le cas des cellules tumorales.

Matériel et méthodes

Nous avons comparé le méthylome (puce EPIC de méthylation) et le transcriptome des TAMs (CD11B+ isolés par tri cellulaire activé par magnétisme) de 25 gliomes IDH-m et 11 gliomes IDH-wildtype (IDH-wt), ainsi que de tissu cérébral contrôle non tumoral. Pour déterminer les effets directs du D-2HG sur la microglie, nous avons mis au point des cultures primaires de microglie humaine obtenues à partir d'une chirurgie de gliome ou d'épilepsie. Nous avons d'abord dosé le D-2HG dans la microglie traitée par D-2HG par spectrométrie de masse par chromatographie en phase liquide (LC-MS) afin d'évaluer l'entrée du métabolite dans ces cellules, et avons évalué l'activité enzymatique de TET. Des cellules IDH-m et IDH-wt ont été utilisées comme contrôles externes. Nous avons exposé ou non des cellules microgliales au D-2HG pendant 14 jours et analysé leur méthylome et leur transcriptome. Les ratios de 5mC/5hmC ont été analysés à une résolution de base unique. Nous avons évalué la réponse transcriptomique et la respiration mitochondriale après stimulation au LPS de la microglie pré-traitée par D-2HG. Enfin, nous avons analysé par snRNA-seq le transcriptome microglial d'un échantillon apparié de gliome IDH-m avant et après traitement par l'inhibiteur d'IDH-m ivosidenib, qui diminue les concentrations intratumorales de D-2HG.

Résultats

Nous montrons que les cellules myéloïdes CD11B+ des gliomes IDH-m humains présentent une hyperméthylation de l'ADN principalement au niveau des enhanceurs. Cette hyperméthylation est liée à une diminution de l'expression des gènes impliqués dans les réponses inflammatoires et le métabolisme glycolytique, et à l'inactivation des facteurs de transcription qui régulent la réponse microgliale aux stimuli environnementaux. L'exposition prolongée de la microglie primaire humaine au D-2HG inhibe l'oxydation de 5mC médiée par TET, ce qui entraîne une accumulation réduite des niveaux globaux de 5hmC. Nous avons observé des rapports 5mC/5hmC élevés, en particulier au niveau d'enhancers spécifiquement actifs dans ces cellules. Conformément à la modulation des enhanceurs, la microglie traitée au D-2HG présente une capacité pro-inflammatoire réduite et une augmentation de la phosphorylation oxydative. À l'inverse, la diminution des niveaux de D-2HG après traitement par ivosidenib chez un patient atteint de gliome IDH-m est associée à la restauration de l'expression génique liée à l'activation microgliale.

Conclusion

Nos résultats fournissent une base mécanistique de l'état hyporéactif de la microglie dans les gliomes IDH-m et élargissent le concept selon lequel les oncométabolites peuvent perturber la fonction des cellules immunitaires du microenvironnement tumoral.

Contents

1	Background	13
1.1	Adult-type diffuse gliomas	13
1.1.1	Histo-molecular classification	13
1.1.2	The neomorphic function of IDH mutations	15
1.1.3	Epidemiology	16
1.1.4	Standard-of-care and emerging therapies	16
1.2	Effects of the oncometabolite D-2HG in IDH-mutant cells	18
1.2.1	D-2HG inhibits 2OG-dependent enzymes	18
1.2.2	D-2HG inhibits TET-mediated DNA demethylation	20
1.2.3	D-2HG effects on histone demethylation	21
1.2.4	D-2HG blocks cell differentiation	23
1.2.5	D-2HG impairs DNA repair	25
1.2.6	Other actions of D-2HG in tumor cells	26
1.3	Myeloid immune tumor microenvironment of gliomas	26
1.3.1	Myeloid cell populations in the central nervous system	27
1.3.2	Tumor-associated macrophages and microglia	28
1.3.3	TAMs heterogeneity beyond M1/M2 phenotypes	30
1.4	Immunomodulatory roles of D-2HG	34
1.4.1	Hypermethylation in IDH-mutant cells promotes immune evasion	34
1.4.2	Cell-extrinsic effects D-2HG in TME cells	36
1.4.2.1	D-2HG accumulates in the TME	36
1.4.2.2	Effects of D-2HG in lymphocytes	38
1.4.2.3	Effects of D-2HG in dendritic cells	39
1.4.2.4	Effects of D-2HG in TAMs	40
1.4.2.5	Effects of D-2HG in non-immune cells	40
1.4.3	Role of D-2HG in inflammation	41
2	Statement of the problem	43
2.1	Rationale and working hypothesis	43
2.2	Objectives	44
2.2.1	<i>Ex vivo</i> study	44
2.2.2	<i>In vitro</i> study	44
2.2.3	D-2HG depletion	45
3	Results	47

4 Discussion and Perspectives	129
4.1 <i>Ex vivo</i> study	129
4.1.1 Heterogeneity of CD11B+ cell populations	129
4.1.2 TAM patterning by the TME	130
4.1.3 Link between DNA hypermethylation and transcription factor binding	130
4.1.4 Inhibition of TET-mediated demethylation	131
4.2 <i>In vitro</i> study	132
4.2.1 <i>In vitro</i> model	132
4.2.2 D-2HG selectively affects lineage-specific enhancers	134
4.2.3 Effects of D-2HG beyond the methylome	135
4.2.4 Impact of D-2HG on microglial function	136
4.3 Conclusion	138
A Abstract presented to the EANO 2024 conference	141
B Articles and reviews related to this PhD	143
C Research articles and reviews not directly related to this PhD that I co-authored	209
D Clinical articles not directly related to this PhD that I co-authored	211

List of Figures

1.1	Anatomopathology of a grade II oligodendroglioma	14
1.2	Mutant IDH enzymes produce D-2hydroxyglutarate	15
1.3	TET-mediated active DNA demethylation	20
1.4	D-2HG leads to immunomodulatory effects on cells in the tumor micro-environment	35
1.5	Production of D-2hydroxyglutarate (D-2HG)	36
1.6	D-2hydroxyglutarate accumulates in the tumor microenvironment . . .	37

List of Tables

1.1	IC50 values of 2OG-dependent enzymes for D-2hydroxyglutarate . . .	19
1.2	Summary of TAM clusters in human gliomas established from single- cell transcriptomics data	32

List of abbreviations

2OG	2-oxoglutarate
5hmC	5-hydroxymethylcytosine
5mC	5-methylcytosine
ADHFE1	alcohol dehydrogenase iron containing 1
AHR	aryl-hydrocarbon receptor
AML	acute myeloid leukemia
AMPK	adenosine 5'-monophosphate-activated protein kinase
AMPK	adenosine monophosphate-activated protein kinase
ATAC-seq	assay for transposase-accessible chromatin using sequencing
ATP	adenosine triphosphate
ATRX	ATP-dependent helicase
BAM	border-associated macrophage
CAR-T cells	chimeric antigen receptors T cells
CDKN2A	cyclin dependent kinase inhibitor
CNS	central nervous system
CTCF	CCCTC-binding factor
CXCL10	C-X-C motif chemokine ligand 10
CYTOF	single-cell mass cytometry
ChIP	chromatin immunoprecipitation
ChIP-seq	ChIP-sequencing
D-2HGA	D-2-hydroxyglutaric aciduria
D-2HG	D-2hydroxyglutarate
D2HGDH	D-2-hydroxyglutarate dehydrogenase
DAM	disease-associated microglia
DDR	DNA damage response
DIM	disease inflammatory macrophage
DMRs	differentially methylated regions
DNMT	DNA methyltransferase
EGFR	epidermal growth factor receptor
EPO	erythropoietin

ESC	embryonic stem cell
FDA	food and drug administration
G-CIMP	CpG island methylator phenotype
G-CSF	granulocyte colony-stimulating factor
GFAP	glial fibrillary acidic protein
GM-CSF	granulocyte-macrophage colony-stimulating factor
HIF	hypoxia-inducible factor
HLA-DR	human leukocyte antigen – DR isotype
HOT	hydroxyacid–oxoacid transhydrogenase
IC50	half maximal inhibitory concentration
ICI	immune checkpoint inhibitors
IDH	isocitrate dehydrogenase
IDH-m	IDH mutant
IDH-wt	IDH wildtype
IFN-γ	interferon gamma
IL-4	interleukin-4
iPSC	induced pluripotent stem cell
KDM	histone lysine demethylase
LDH	lactate dehydrogenase
LINE	long interspersed nuclear element
LPS	lipopolysaccharides
MHC	major histocompatibility complex
MRS	magnetic resonance spectroscopy
MSC	mesenchymal stem cells
mTOR	mammalian target of rapamycin
NFAT	nuclear factor of activated T cells
NMDA	N-methyl-D-aspartic acid
ORR	objective response rate
OS	overall survival
PCV	procarbazine, CCNU, vincristine
PD1	programmed cell death protein 1 receptor
PDGFRA	platelet-derived growth factor receptor A
PHGDH	3-phosphoglycerate dehydrogenase
PKCδ	protein kinase C δ
carRNA	chromatin-associated retrotransposon RNA
eRNA	enhancer RNA
lncRNA	long non-coding RNA

scRNAseq single-cell RNA sequencing
shRNA short hairpin RNA
siRNA small interfering RNA
SLC13A3 sodium-dependent dicarboxylate transporter 3
snRNAseq single-nuclei RNA sequencing
STAT1 signal transducer and activator of transcription 1
TAM-MDMs infiltrating monocyte derived macrophages
TAM-MGs microglia
TAMs tumor-associated microglia and macrophages
TCGA the cancer genome atlas
TERT telomerase reverse transcriptase
TET ten-eleven translocation
TME tumor microenvironment
TMZ temozolomide
VEGF vascular endothelial growth factor
WHO world health organization
YAM youth-associated microglia

Chapter 1

Background

1.1 Adult-type diffuse gliomas

Diffuse gliomas constitute the most common primary malignant tumor of the central nervous system (CNS) in adults: they represent around 70% of primary malignant tumors of the CNS and approximately 20% of all tumors of the CNS in the United States, which corresponds to an annual age-adjusted incidence rate of about 4.8 per 100,000 population (Ostrom et al. 2022).

Diffuse gliomas are glial tumors characterized by a diffuse infiltration of the CNS, due to the migration of tumor cells away from the initial tumor site along preexisting structures (such as bundles of white matter or vessels), as opposed to circumscribed gliomas. They infiltrate the nervous tissue without distinct limits, making their total excision impossible. Consequently, almost all of these tumors relapse despite current treatments combining surgery, radiotherapy and chemotherapy. A better understanding of the mechanisms underlying the initiation and progression of these tumors is thus essential to allow the development of new therapeutic strategies.

1.1.1 Histo-molecular classification

The 2021 World Health Organization (WHO) classification (Louis et al. 2021) distinguishes between diffuse gliomas primarily affecting adults (adult-type) and those predominantly affecting children (pediatric-type), reflecting clinically and biologically distinct entities. Hereafter, I will not address the pediatric types, as they fall outside the scope of this work.

The 2021 WHO classification integrates molecular and pathological criteria to divide adult diffuse gliomas into three groups, based on the mutational status of the isocitrate dehydrogenase (IDH) 1 and 2 genes, and the status of chromosomes 1p and 19q (ibid.):

- IDH-mutant (IDH-m) astrocytomas without 1p/19q codeletion, grade 2 to 4.
IDH-m grade 2 astrocytomas are composed of well-differentiated fibrillar glial cells that infiltrate the brain parenchyma. Cytonuclear atypia is mild, and mitotic activity is low (with no clearly defined threshold) (Komori 2022). Neither necrosis nor microvascular proliferation is present, and there is no homozygous deletion of the cyclin dependent kinase inhibitor 2A or 2B (*CDKN2A* or *2B*) genes (a criterion defining grade 4). IDH-m grade 3 astrocytomas are characterized by increased cellular density, elevated mitotic activity and a

Figure under copyright,
see Capper et al. (2011).

Figure 1.1: **Anatomopathology of a grade II oligodendroglioma**, from Capper et al. (2011). **a.** Hematoxylin and eosin (HE) stained slide of grade II oligodendroglioma, with round cells with a clear halo surrounding a round, central core (appearance of “fried egg” or “honeycomb”). **b.** Anti-IDH1R132H immunohistochemistry of the same area showing strongly positive tumor cells.

more pronounced cytonuclear atypia. IDH-m grade 4 astrocytomas exhibit necrosis and/or microvascular proliferation and/or homozygous deletion of the *CDKN2A* or *CDKN2B* genes. IDH-m grade 2–4 are also characterized by loss-of-function mutations in the gene of the ATP-dependent helicase (*ATRX*).

- IDH-m oligodendrogliomas with 1p/19q codeletion, grade 2 to 3.

Oligodendroglioma cells typically appear in paraffin sections as uniform round cells with a clear halo surrounding a round, central core, resembling a “fried egg” or “honeycomb” (see Figure 1.1). The vascularization is sparse, and microcalcifications are common. IDH-m grade 2 oligodendrogliomas typically exhibit a Ki67 proliferation index of less than 5% (with no clearly defined threshold), and fewer than 2.5 mitoses/mm² (Pouget et al. 2020). They do not show microvascular proliferation nor necrosis. IDH-m grade 3 oligodendrogliomas exhibit higher cellularity, marked cytonuclear atypia, microvascular proliferation, and/or necrosis. IDH-m grade 2-3 oligodendrogliomas may also harbor somatic mutations in the promoter of the gene of the telomerase reverse transcriptase (*TERT*) and absence of *ATRX* mutations.

- Glioblastoma without IDH mutation (IDH wildtype, IDH-wt), grade 4.

Glioblastomas have a variable histological presentation but are typically composed of a high density of poorly differentiated pseudo-astrocytic cells with marked cytonuclear atypia. Mitotic activity is generally high. Microvascular proliferation and necrosis are characteristic features, with the presence of either being sufficient to make the diagnosis in the context of a diffuse glioma without IDH or H3 mutation. Other frequent molecular alterations in glioblastomas include *TERT* promoter mutations, amplification of the gene of the epidermal growth factor receptor (*EGFR*), and chromosome 7 gain/chromosome 10 loss (chr +7/-10).

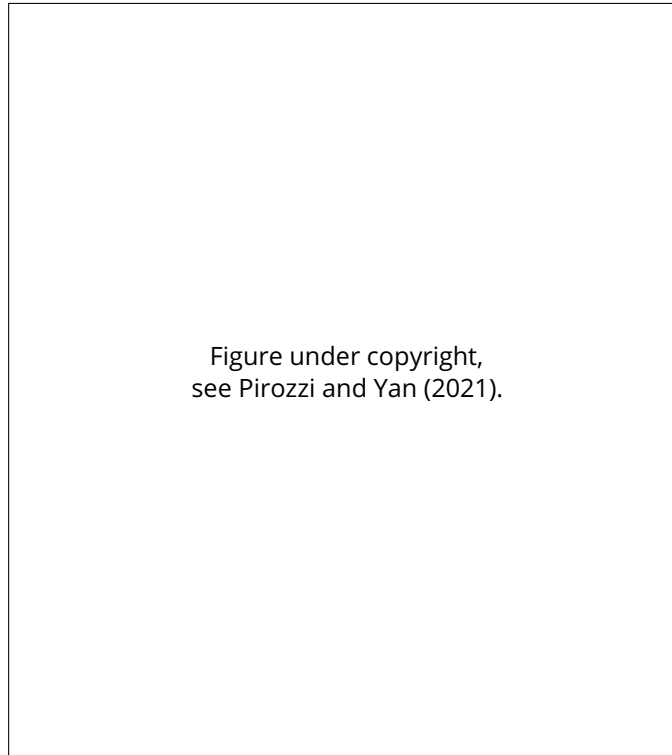


Figure 1.2: **Mutant IDH enzymes produce D-2hydroxyglutarate**, from Pirozzi and Yan (2021). IDH1 and IDH2 are homologous enzymes that catalyze the reversible oxidative decarboxylation of isocitrate to α -ketoglutarate (or 2-oxoglutarate) while reducing NADP⁺ to NADPH, respectively in the cytoplasm and in the peroxisome / in the mitochondrion. The presence of a heterozygous somatic point mutation of codons 132 or 172, which corresponds to the active site, gives them the ability to catalyze the transformation of α -ketoglutarate into D-2hydroxyglutarate. These two compounds have structural homology.

The appendix section B.1 (page 143) includes a detailed article on the WHO classification, written during the course of my PhD: A. Laurence, S. Tran, M. Peyre, and A. Idbaih (Feb. 15, 2023). *Classification OMS 2021 des tumeurs du système nerveux central*. In: *EM-Consulte*. URL: <https://www.em-consulte.com/article/1573026/classification-oms-2021-des-tumeurs-du-systeme-ner>.

1.1.2 The neomorphic function of IDH mutations

IDH1 and IDH2 are homologous enzymes that catalyze the reversible conversion of isocitrate to α -ketoglutarate (also known as 2-oxoglutarate, 2OG) while reducing NADP⁺ to NADPH, with IDH1 functioning in the cytoplasm and IDH2 in the peroxisome and mitochondrion (Figure 1.2). The catalytic activity of IDH requires homodimerization, along with a conformational change in the enzyme; binding of isocitrate transforms the enzyme structure from an open to a closed conformation. Substrate recognition depends on the amino acid residues present in the active site. Heterozygous missense mutations at codons 132 or 172, which correspond to the active site, result in the replacement of a strong, positively charged arginine (R) residue with lower polarity amino acids such as histidine (H), lysine (K) or cysteine (C), which im-

pedes the formation of hydrogen bonds with the α -carboxyl and β -carboxyl sites of isocitrate. The mutant IDH enzyme therefore exhibits decreased affinity for isocitrate and instead exhibits a neomorphic activity to catalyze the conversion of 2OG into the oncometabolite D-2hydroxyglutarate (D-2HG) (Dang et al. 2009). Notably, as only one copy of the *IDH* gene is mutated in tumors, the main forms of IDH dimers are presumed to be heterodimers of wild-type and mutant IDH. The more frequent mutation is IDH1 R132H. Non-canonical mutations are associated with even higher D-2HG levels (Pusch et al. 2014). While IDH-m is believed to be an early genetic event that confers a growth advantage for glioma initiation, circumstantial evidence suggests that it is no longer necessary for tumor progression (M. Touat et al. 2015; Favero et al. 2015; Ehret et al. 2023).

1.1.3 Epidemiology

IDH-m astrocytomas account for more than 13% of gliomas (Ostrom et al. 2022). The median age at diagnosis is 38 years, with patients diagnosed with grade 4 being significantly older (Reuss et al. 2015). The patients are predominantly men, with a male-to-female ratio of 1.5 (Cancer Genome Atlas Research Network et al. 2015).

IDH-m oligodendrogliomas account for more than 5% of gliomas (Ostrom et al. 2022). The median age at diagnosis is 43 years for grade 2 and 50 years for grade 3. The patients are primarily men, with a male-to-female ratio of 1.2 for grades 3 (Bauchet and Ostrom 2019).

IDH-wt glioblastomas are the most common diffuse glioma, accounting for almost 60% of gliomas (Ostrom et al. 2022). They usually occur between the ages of 55 and 85 years and mainly affect men, with a male-to-female ratio of 1.60 (Bauchet and Ostrom 2019).

The 2021 WHO classification identifies subgroups of patients that have different prognoses. For instance, the five-year relative survival rates in the United States are as follows (Ostrom et al. 2022):

- oligodendroglioma grade 2: 83.6%,
- oligodendroglioma grade 3: 62.5%,
- astrocytoma grade 2: 51.8%,
- astrocytoma grade 3: 30.9%,
- glioblastoma grade 4: 6.6%.

1.1.4 Standard-of-care and emerging therapies

The therapeutic management of diffuse glioma is outlined in international recommendations (Weller et al. 2021; Vargas López 2021; Miller et al. 2023).

The first step of treatment involves maximal safe resection. For patients not eligible for surgical resection, a biopsy is performed to histologically confirm the diagnosis and may also include additional molecular tests.

- For patients with grade 4 tumors (astrocytomas and glioblastomas), radiotherapy with concomitant and adjuvant chemotherapy by temozolomide (TMZ) is recommended, according to the EORTC-NCIC trial (Stupp, Hegi, et al. 2009). The addition of tumor-treating fields to maintenance chemotherapy is recommended, based on the results of a phase III trial (Stupp, Taillibert, et al. 2017).

- For patients with grade 3 IDH-m gliomas (astrocytoma and oligodendroglioma), radiotherapy followed by adjuvant alkylating agent chemotherapy is recommended, based on the RTOG 9402, EORTC 26951 and CATNON trials (Cairncross et al. 2013; Bent, Brandes, et al. 2013; Bent, Tesileanu, et al. 2021; Lassman et al. 2022). Two different protocols can be used: temozolomide or polychemotherapy with procarbazine, CCNU, vincristine (PCV), with this first-line radiotherapy/PCV being associated with better progression-free survival (PFS) and overall survival (OS) (Kacimi et al. 2024).
- For patients with grade 2 IDH-m gliomas (astrocytoma and oligodendroglioma), management depends on the presence or absence of high-risk criteria that were retrospectively defined. For young patients (< 40 years) who have undergone gross total resection, a “watch and wait” approach can be proposed. In patients with residual or recurrent disease not requiring radiation and chemotherapy, the INDIGO trial recently highlighted the benefit of the IDH1/2 inhibitor vorasidenib (Mellinghoff, Bent, et al. 2023). In a subset of patients with grade 2 IDH-m glioma, radiation followed by adjuvant chemotherapy (PCV or sometimes TMZ) is recommended according to the RTOG 9802 trial and by extrapolation of results in grade 3 tumors (Buckner et al. 2016).

Unfortunately, almost all patients with diffuse glioma will experience relapse after first line treatment with surgery, radiotherapy and alkylating agent chemotherapy. Treatment options at recurrence are limited to second surgery, alkylating chemotherapy not used in first line treatment, re-irradiation, or the anti-vascular endothelial growth factor (anti-VEGF) bevacizumab (Weller et al. 2021). The benefit of IDH1/2 inhibitors appears more limited at the recurrence compared to earlier disease stages (Mellinghoff, M. Lu, et al. 2023). Patients often succumb to tumor progression.

Emerging therapeutic strategies are actively being tested. I will focus on IDH-m gliomas which constitute the subject of this work. The mutant IDH presents an attractive target for treatment due to its early occurrence in gliomagenesis and the homogeneous expression of this mutant enzyme throughout tumor evolution in most patients.

Two phase I trials evaluated the IDH1-m inhibitor ivosidenib (Mellinghoff, Ellingson, et al. 2020) and the dual IDH1/IDH2-m inhibitor vorasidenib (Mellinghoff, Penas-Prado, et al. 2021). The results showed a favorable safety profile for both molecules, with an objective response rate (ORR) of 2.9% for ivosidenib and 18% for vorasidenib in non-enhancing (MRI profile) gliomas. A phase I peri-operative study explored vorasidenib and ivosidenib to select a candidate for phase III evaluation (Mellinghoff, M. Lu, et al. 2023). The primary endpoint, which was the concentration of the oncometabolite D-2HG in the tumor after vorasidenib or ivosidenib treatment, was reduced by more than 90%. Based on this data, vorasidenib, which inhibits both IDH1/IDH2-m and demonstrated more favorable brain penetration properties than ivosidenib, was selected for the phase III INDIGO study in non-enhancing grade 2 gliomas. This double-blind, randomized, placebo-controlled trial investigated the efficacy and safety of vorasidenib in patients with recurrent or residual WHO grade 2 IDH-m gliomas (Mellinghoff, Bent, et al. 2023). Median PFS was significantly longer in the vorasidenib group compared to the placebo group, and the safety profile was acceptable. Following these results, vorasidenib has been approved by the US Food

and Drug Administration (FDA) for the treatment of patients with grade 2 IDH-m glioma following surgery. Approval is under review in several other countries. Other IDH-m inhibitors are currently being evaluated (Fuente et al. 2023; Natsume et al. 2023; Wick et al. 2021).

Another approach to target the IDH mutation is vaccination. Encouraging results have been reported with IDH1-R132H peptide vaccines alone (Platten et al. 2021, trial NCT02193347), and in combination with immune checkpoint inhibitors (ICI) (Bunse, Rupp, et al. 2022). However, phase III trials are necessary before these vaccines can be used in routine clinical care.

Immune checkpoint inhibitors are part of the standard of care for many tumors, such as melanoma (Tawbi et al. 2018), including brain metastases, where concordant responses are observed in both extracerebral disease and brain lesions (Goldberg et al. 2016; Kluger et al. 2019; Tawbi et al. 2018). However, this therapeutic class failed to meet endpoints in phase III trials for IDH-wt gliomas (Andersen and Reardon 2022; Arrieta et al. 2023). These divergent responses to treatment of tumors located in the same organ may be driven by intrinsic properties of the tumor cells, or by differences in the tumor microenvironment (Keenan, Burke, and Van Allen 2019). Only a selective group of patients has shown clear benefit from immunotherapy (Daniel et al. 2019; Johanns et al. 2016; Bouffet et al. 2016). In IDH-m gliomas, ICI were hypothesized to provide increased benefit at relapse after alkylating agents, due to the high rate of post-treatment hypermutation and mismatch repair deficiency in this population (Mehdi Touat et al. 2020). The REVOLUMAB study tested the anti-programmed cell death protein 1 receptor (anti-PD1) nivolumab in recurrent IDH-m gliomas of grade 2 to 4, but the primary endpoint was not achieved (Picca et al. 2024).

The appendix section B.2 (page 161) includes a detailed review article on the new treatments of IDHm gliomas, written during the course of my PhD: Chooyoung Baek, Alice Laurence, and Mehdi Touat (Sept. 12, 2024). "Advances in the treatment of IDH-mutant gliomas". In: *Current Opinion in Neurology*. ISSN: 1473-6551. DOI: 10.1097/WCO.0000000000001316.

The development of effective therapeutic strategies to improve disease control after first-line treatment or at recurrence represents an unmet clinical need. A better understanding of the mechanisms underlying gliomagenesis and tumor progression is crucial to pave the way for novel therapeutic modalities.

1.2 Effects of the oncometabolite D-2HG in IDH-mutant cells

1.2.1 D-2HG inhibits 2OG-dependent enzymes

As discussed, D-2HG is produced by mutated IDH. It is the reduced form and a structural analogue of 2OG (2-oxoglutarate) as depicted in Figure 1.2. D-2HG acts as a competitive inhibitor of 2OG-dependant enzymes. Xu et al. established that D-2HG is a weak inhibitor, requiring a 100-fold molar excess over 2OG to cause a significant inhibitory effect toward 2OG-dependent dioxygenases (W. Xu et al. 2011; Chowdhury et al. 2011). These enzymes target various substrates such as proteins, DNA, RNA, and fatty acids, but share a common reaction mechanism: they require dioxygen, divalent iron, and 2OG as co-substrates, producing a hydroxylated product, CO₂, and succinate (Losman, Koivunen, and Kaelin 2020).

2OG-dep enzymes	IC50 (μmol/l)
ABH2	420–500
ABH3	500
BBOX1	13200
EGLN1	300-7300
EGLN2	210
FIH1	1100–1500
KDM2A	110
KDM4A	2–160
KDM4B	150
KDM4C	80
KDM5B	3600–10870
KDM6A	18
KDM6B	350
P4HA1	1800
TET1	4000
TET2	5000

Table 1.1: **IC50 values of 2OG-dependent enzymes for D-2hydroxyglutarate**, from Losman, Koivunen, and Kaelin (2020).

Chowdhury et al. observed no significant increase in half maximal inhibitory concentration (IC50) values even at 10-fold iron concentrations (for KDM4A and BBOX-1), suggesting that the inhibition of these enzymes by D-2HG does not predominantly rely on iron sequestration (Chowdhury et al. 2011). Crystallographic analyses of FIH and JMJD2A showed that D-2HG can bind to the active site Fe(II) and compete with 2OG for binding (ibid.).

2OG-dependant enzymes comprise more than 70 different enzymes, several of which have been extensively studied due to their importance in key biological processes. These include (Losman, Koivunen, and Kaelin 2020):

- Nucleic acid oxygenases: ALKBH1, ALKBH2, ALKBH3, ALKBH5 (RNA demethylase), ALKBH8 (tRNA methyltransferase), FTO (ALKBH9), ten-eleven translocation (TET) 1–3 and TYW5,
- Histone demethylases: KDM2A, KDM2B, KDM3A, KDM3B, KDM4A, KDM4B, KDM4C, KDM4D, KDM5A, KDM5B, KDM5C, KDM5D, KDM6A, KDM6B, KDM6C, KDM7A, KDM7B and KDM9,
- Prolyl or Lysyl hydroxylases: ASPH, hypoxia-inducible factor (HIF) prolyl 4-hydroxylases EGLN1–3, FIH1, JMJD4–7, LEPRE1, LEPREL1, LEPREL2, MINA53, NO66, OGFOD1, P4HA1–3, P4HTM and PLOD1–3,
- Fatty acid and small-molecule oxygenases: γ -butyrobetaine hydroxylase 1 (BBOX1), PHYH and TMLHE.

These enzymes participate in diverse processes like epigenetic regulation, hypoxia response, and collagen biosynthesis. Losman et al. reviewed the known IC50 of D-2HG for these different enzymes (ibid.), cf Table 1.1. Considering these values and the high amount of D-2HG, at the millimolar level, reported in glioma, the vast majority of these enzymes can theoretically be competitively inhibited in

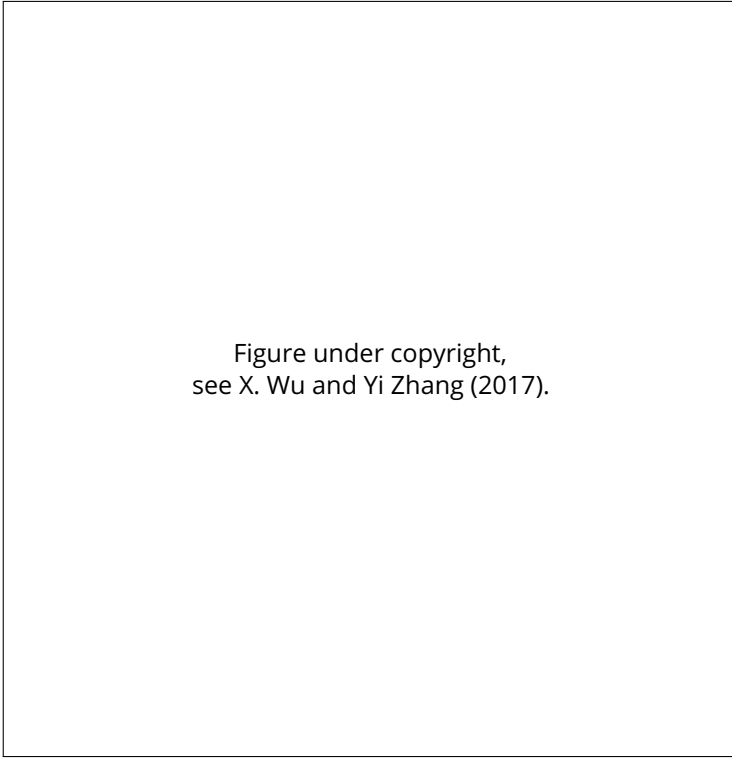


Figure under copyright,
see X. Wu and Yi Zhang (2017).

Figure 1.3: **TET-mediated active DNA demethylation**, from X. Wu and Yi Zhang (2017). DNA methyltransferases (DNMTs) convert unmodified cytosine to 5-methylcytosine (5mC). 5mC can be converted back to unmodified cytosine by TET-mediated oxidation to 5-hydroxymethylcytosine (5hmC), 5-formylcytosine (5fC) and 5-carboxylcytosine (5caC), followed by excision of 5fC or 5caC mediated by thymine DNA glycosylase (TDG) coupled with base excision repair (BER).

IDH-m cells. The effects of D-2HG have indeed been observed in various tumors beyond gliomas, particularly in contexts where IDH mutations are prevalent, where it affects cellular differentiation, gene expression, and tumor microenvironment. These tumors include acute myeloid leukemia (AML, about 20%, and precursor conditions that can progress to AML: myelodysplastic syndromes and myeloproliferative neoplasms), cartilaginous tumors (about 75%), thyroid carcinoma (17%), intrahepatic cholangiocarcinoma (10%–23%), and other cancers to a lesser extent (< 5% of prostate cancers, acute B-lymphoblastic leukemia, paragangliomas, colorectal carcinomas, melanoma) (reviewed by Oermann et al. 2012).

1.2.2 D-2HG inhibits TET-mediated DNA demethylation

Figueroa et al. analyzed the DNA methylation profile of a large cohort of acute myeloid leukemia (AML) samples and reported that IDH-m samples clustered together into two groups based on their DNA methylation profile (Figueroa et al. 2010). All differentially methylated regions (DMRs) between IDH-m vs IDH-wt samples were universally hypermethylated in IDH-m AMLs. They evaluated the level of 5-methylcytosine (5mC) in immortalized cells expressing either mutated or wild type *IDH* and reported a significant increase in 5mC levels in IDH-m expressing cells, with a positive correlation between the levels of 2-HG measured in the cells (ibid.). This sug-

gests that 2-HG production leads to increased 5mC levels in IDH-m cells.

TET enzymes are known to be DNA hydroxylases that convert 5mC to 5-hydroxymethylcytosine (5hmC) (Ito et al. 2010) as illustrated in Figure 1.3. The expression of *TET1* or *TET2* in cellular systems leads to a decrease in 5-mC levels (ibid.). 5mC is established by *de novo* DNA methyltransferases DNMT3A and DNMT3B (Okano et al. 1999). The methyl group is covalently attached to the cytosine base through a stable carbon-carbon bond. This methyl group is then maintained after DNA replication by the maintenance methyltransferase DNMT1, which recognizes hemi-methylated CpG (Hermann, Goyal, and Jeltsch 2004). A dysfunction in this maintenance system can lead to the dilution of 5mC during DNA replication, constituting *passive* DNA demethylation. In contrast, TET enzymes are responsible for *active* DNA demethylation, by mediating the oxidation of 5mC to 5hmC (Ito et al. 2010), with the dilution of this form of 5mC after replication resulting in demethylation (X. Wu and Yi Zhang 2017). Exploratory analyses of tumor tissues following treatment with an IDH-m inhibitor showed that the reduction of D-2HG was associated with increased levels of DNA 5-hydroxymethylcytosine (Mellinghoff, M. Lu, et al. 2023).

Figuroa et al. showed that mutations in *IDH1/2* are mutually exclusive with mutations in *TET2* in AML (Figuroa et al. 2010), suggesting that *IDH1/2* mutations and *TET2* mutations display overlapping roles in the pathophysiology of AML. Consistent with this hypothesis, they reported an overlapping hypermethylation signature of IDH-m and *TET2*-m AMLs (ibid.).

In glioma, Noushmehr et al. identified a subgroup of patients exhibiting highly concordant DNA methylation across a large subset of loci, indicative of a CpG island methylator phenotype (G-CIMP). This pattern is associated with IDH-m glioma (Noushmehr et al. 2010; Turcan, Rohle, et al. 2012), and corresponds to patients that are younger at the time of diagnosis and experience significantly improved outcomes (Noushmehr et al. 2010). Turcan et al. further introduced the mutated *IDH* into immortalized primary human astrocytes and demonstrated that this mutation was sufficient to increase levels of H3K9me3, and to induce DNA hypermethylation (evident from passage #12 and #22, respectively), thus mimicking the observed changes in G-CIMP gliomas (Turcan, Rohle, et al. 2012). They found that the expression of wild-type *IDH1* in the same cells leads to DNA hypomethylation at specific loci, suggesting that both D-2HG production and modulation of 2OG levels affect the methylome (ibid.). They hypothesized that the inhibition of *TET2* by D-2HG could be a mechanistic basis for the accumulation of DNA methylation, leading to the G-CIMP pattern (ibid.). Subsequently, it was shown that IDH-m gliomas exhibit hyper-methylation at CCCTC-binding factor (CTCF) binding sites, resulting in loss of insulation between topological domains. This permits a constitutive enhancer to aberrantly interact with the oncogene platelet-derived growth factor receptor A (PDGFRA) (Flavahan et al. 2016).

A hypermethylation signature is not only known in IDH-m AMLs and glioma, but also in IDH-m cholangiocarcinoma (P. Wang et al. 2013) and chondrosarcoma (Guilhamon et al. 2013).

1.2.3 D-2HG effects on histone demethylation

Besides *TET2*, the inhibition of histone lysine demethylases (KDMs) appears to play a significant role in the biology of IDH-m tumors. Studies have shown that D-2HG can inhibit various KDM enzymes both *in vitro* and *in vivo* (C. Lu et al. 2012; Kernysky et

al. 2015; Sasaki, Knobbe, Munger, et al. 2012; Turcan, Makarov, et al. 2018; Laukka et al. 2018), and that these enzymes are more sensitive to inhibition by D-2HG than TET2. Furthermore, KDM enzymes are known to be mutated or downregulated in cancer (reviewed by Losman, Koivunen, and Kaelin 2020), suggesting that they may function as tumor suppressors. Their inhibition by D-2HG could contribute to the transformation of IDH-m cells.

Laukka et al. systematically assessed the catalytic and inhibitory properties of several human KDM enzymes, including KDM4A, KDM4B, KDM5B, KDM6A, and KDM6B (Laukka et al. 2018). They show that KDM enzymes display substrate specificity: KDM4A/B demethylated peptides with H3K9me3 or H3K27me3, whereas KDM5B targeted peptides with H3K4me3 or H3K4me2, and KDM6A/B specifically acted on H3K27me3. Among the cancer-associated 2-OG analogues fumarate, succinate, D-2HG and L-2HG, as well as the metabolic regulators citrate and oxaloacetate, D-2HG emerged as the most effective inhibitor of KDM4A, KDM4B and KDM6A. In contrast, KDM5B was particularly resistant to inhibition by D-2HG (ibid.). Consistent with these findings, they reported an accumulation of the histone marks H3K9me3 and H3K27me3 in cells treated with cell-permeable D-2HG (ibid.).

Lu et al. reported an increase of the repressive histone methylation marks, specifically trimethylation of H3K9 (H3K9me3) and trimethylation of H3K27 (H3K27me3), in IDH-m gliomas compared to IDH-wt gliomas (C. Lu et al. 2012). Similarly, they observed a global increase in H3K9 methylation in murine 3T3-L1 cells expressing the mutated *IDH* compared to IDH-wt (ibid.). They also retrovirally transduced immortalized normal human astrocytes with IDH-m or IDH-wt and observed higher H3K9me3 levels by passage #12 in IDH-m cells (ibid.).

Complementary observations have been made in hematopoietic cells. Immunoblotting of lysates from control and IDH-m murine myeloid cells revealed an increase in the methylation of multiple H3 lysine residues in IDH-m cells (Sasaki, Knobbe, Munger, et al. 2012). Intriguingly, another mouse model of IDH-m exhibited DNA hypermethylation but did not show histone hypermethylation (Bardella et al. 2016), which cannot be explained by different concentrations of D-2HG required to inhibit these enzymes (estimated to be 5 mM for TET vs 75-150 μ M for KDM). Kernytsky et al. assessed the histone methylation changes at the hemoglobin γ promoter (*HBG*, a marker of early fetal differentiation states), using chromatin immunoprecipitation (ChIP) with an H3K9me3 antibody, in TF-1 cells (Kernytsky et al. 2015). In IDH-wt cells treated with the erythroid differentiation inducer erythropoietin (EPO), they observed a reduction of the association between H3K9me3 histones and the *HBG* promoter, alongside an increase of *HBG* mRNA expression, and a color change indicative of erythroid differentiation. In contrast, they reported that IDH-m cells retained a high level of H3K9me3 at the *HBG* promoter under EPO treatment and failed to express *HBG* mRNA or undergo color change. This observation was reversed upon treatment with an IDH-m-specific small-molecule inhibitor (ibid.).

Turcan et al. analyzed the impact of the IDH mutation on histone modifications by ChIP-sequencing (ChIP-seq) analysis in immortalized human astrocytes (Turcan, Makarov, et al. 2018). They reported a progressive enrichment of the activating histone mark H3K4me3, as well as the repressive marks H3K9me3 and H4K20me3, after successive passages. Notably, the increase in H3K9me3 and H3K36me3 methylation was not uniform across the genome but occurred at specific regions (ibid.).

Altogether, these studies allow to conclude that D-2HG leads to histone hyper-

methylation in IDH-m cells, through the competitive inhibition of KDM enzymes.

1.2.4 D-2HG blocks cell differentiation

Due to the fact that both IDH and TET2 alterations are reported to occur at early stages during glioma and leukemia development (Delhommeau et al. 2009; Lange-meijer et al. 2009; Watanabe et al. 2009), it has been hypothesized that IDH-m could contribute to tumorigenesis by altering epigenetic profiles and conferring features of stem or progenitor cells (W. Xu et al. 2011). For instance, the expression of IDH-m into murine primary bone marrow cells leads to an increase of expression of stem cell markers such as C-Kit and impairs myeloid differentiation, as evidenced by reduced expression of mature myeloid markers Gr-1 and Mac-1 (Figueroa et al. 2010). Similar observations were made in the context of TET2 knockdown (ibid.).

Sasaki et al. generated a conditional *Idh1* knock-in mouse model in which IDH R132H is expressed under the *LysM* promoter, activated early during myeloid development (Sasaki, Knobbe, Munger, et al. 2012). They observed an accumulation of lineage-restricted progenitors in the spleen and bone marrow of knocked-in mice, with near-normal peripheral blood counts (ibid.). In a different context, Klug et al. showed that the differentiation of post-proliferative monocytes into dendritic cells is accompanied by the appearance of 5hmC, followed by the loss of DNA methylation (Klug et al. 2013), suggesting that TET is essential for the differentiation of human monocytes.

Losman et al. transduced TF-1 cells, a human erythroleukemia cell line that remains cytokine-dependent and retains the ability to differentiate in response to EPO, to express either IDH1 R132H or an inactive IDH enzyme. The cells transduced with IDH1 R132H became cytokine-independent four passages after transduction. By the tenth passage in culture, these cells no longer differentiated in response to EPO (Losman, Looper, et al. 2013). Similar results were obtained by treating TF-1 cells with cell permeable D-2HG. To establish the mechanism of action of D-2HG, the authors subsequently used a pool of several hundred lentiviral short hairpin RNAs (shRNAs) vectors targeting 2-OG-dependent dioxygenases and monitored the abundance of each individual vector by next-generation DNA sequencing. They found that shRNAs targeting *TET2* were significantly enriched over time in culture in the absence of Granulocyte-macrophage colony-stimulating factor (GM-CSF), suggesting that these shRNAs confer cytokine-independence (ibid.). Notably, the acquired growth factor independence was reversed after the removal of cell permeable D-2HG, with the time required for restoration depending on the intensity (duration × dose) of D-2HG exposure. Withdrawal of D-2HG restored the ability of TF-1 cells to differentiate in response to EPO, even after long-term exposure to D-2HG (ibid.).

TET2 is not the only target of D-2HG that contributes to differentiation blockade. Gunn et al. later demonstrated that treatment of TF-1 cells with cell permeable D-2HG at concentrations that do not inhibit TET2 can still induce cytokine independence (Gunn et al. 2023). They identified the inhibition of the 2-OG dependent H3K4 histone lysine demethylases KDM5A, KDM5C, and KDM5D as a mechanism underlying cytokine-independence proliferation. The deletion of these three enzymes in TF-1 cells reproduced the effects of IDH-m expression on cell proliferation (ibid.). Furthermore, they showed that inhibiting H3K4 methyltransferase activity can reverse the cytokine independence induced by IDH-m expression in these cells (ibid.).

Lu et al. studied the impact of IDH mutation onto the maturation of murine 3T3-

L1 cells into adipocytes upon stimulation with a differentiation cocktail. They found that IDH-m cells exhibited visibly reduced lipid droplet accumulation compared to IDH-wt cells (C. Lu et al. 2012). Treatment with cell-permeable 2HG led to similar observations. They reported an increase in H3K9me3, and to a lesser extent in H3K27me3, at the promoter of *Cebpa*, a transcription factor essential for executing adipogenesis, in IDH-m cells (ibid.). They also blocked the induction of KDM4C in 3T3-L1 cells, which typically removes H3K9me2 and H3K9me3 in the presence of 2-OG, using small interfering RNAs (siRNAs). This intervention resulted in enhanced expression of H3K9me3 coupled with a reduced ability to differentiate into adipocytes, demonstrating that the inability to erase repressive H3K9 methylation is sufficient to block the differentiation of non-transformed cells (ibid.). Consistent observations were made for murine primary neurosphere cultures, where IDH-m cells failed to express glial fibrillary acidic protein (GFAP) under conditions that promote astrocyte differentiation, including treatment with retinoic acid, as opposed to IDH-wt cells (ibid.).

A blockade of differentiation is also observed in other cell types. Suijker et al. showed that D-2HG affects the differentiation of mesenchymal stem cells (MSC) (Suijker et al. 2015). *In vitro*, they observed a drastic inhibition of calcification after 3 weeks of MSC culture under osteogenic differentiation conditions in the presence of D-2HG. They reported an increase in differentiation towards the chondrogenic lineage. *In vivo*, they observed an impaired development of vertebral rings in zebrafish exposed to D-2HG. They conclude that IDH mutations block osteogenic differentiation during skeletogenesis, which leads to the development of cartilaginous tumors such as enchondromas (ibid.).

Ma et al. showed that on one hand D-2HG accumulation in IDH-m human sarcoma cell lines (HT1080 cells) *in vitro* does not affect cell proliferation, even after 20 passages, nor does it impact cell migration (S. Ma et al. 2015). On the other hand, they found that D-2HG leads to a lower rate of colony formation in soft-agar by these cells, suggesting that this compound plays a role in promoting anchorage-independent cell growth, which is known to correlate with tumorigenic and metastatic potential *in vivo* (ibid.). In a concordant manner, the tumor volume of nude mice injected with IDH-m HT1080 cells was larger compared to cells that do not produce D-2HG (knockout of the endogenous mutant *IDH1* gene). Furthermore, tumor cell growth was suppressed by the expression of D-2HG dehydrogenase (D2HGDH), which inhibits D-2HG production, indicating that D-2HG promotes the tumorigenicity of HT1080 cells *in vivo* (ibid.).

Koivunen et al. showed in independent experiments that the expression of IDH-m confers increased proliferation at confluence and the ability to form macroscopic colonies in soft agar to immortalized human astrocytes around passage #14 (Koivunen et al. 2012). They suggested that, although EGLN enzymes were initially reported to be inhibited by D-2HG (Chowdhury et al. 2011), EGLN activation by D-2HG, leading to the downregulation of HIF1 α , contributes to this capability. Specifically, the downregulation of HIF1 α by shRNAs, or the overproduction of wild-type EGLN1 promoted soft agar growth after approximately 15 passages. Conversely, the downregulation of EGLN1 by shRNAs inhibited the proliferation of late-passage IDH-m cells (Koivunen et al. 2012). Gunn et al. later showed that the inhibition of KDM5 enzymes is sufficient to induce soft-agar colony formation, phenocopying the effect induced by IDH-m in immortalized human astrocytes (Gunn et al. 2023). This suggests that the competitive inhibition of these 2-OG

enzymes could be a mechanism of action of D-2HG participating in this effect.

Although there are no reported IDH mutations in breast cancers, 2HG accumulates at high levels in a subset of these tumors with MYC activation (Terunuma et al. 2014). Kusi et al. showed that 2HG disrupts nucleosome positioning in breast cancer cells and promotes cell-to-cell variability (Kusi et al. 2022). Furthermore, they showed that ascorbate-2-phosphate limits heterogeneity and growth of high 2HG-producing breast cancer cells. These findings suggest that 2HG plays a prominent role in cancer cell plasticity (ibid.).

Consistent with all these observations, exploratory analyses of tumor tissues upon treatment with IDH-m inhibitors indicated that D-2HG reduction was associated with transcriptomic changes consistent with lineage differentiation (Mellinghoff, Ellingson, et al. 2020; Mellinghoff, Penas-Prado, et al. 2021; Mellinghoff, M. Lu, et al. 2023; Spitzer et al. 2024).

1.2.5 D-2HG impairs DNA repair

Wang et al. reported that D-2HG inhibits the ALKBH DNA repair enzymes (Pu Wang et al. 2015). They showed that glioma cells U87-MG transduced with the IDH-m display reduced DNA repair kinetics after treatment with methyl methane sulfonate compared with U87-MG IDH-wt cells, leading to the accumulation of DNA double-strand breaks (DSBs). The sensitization to methyl methane sulfonate conferred by R132H IDH1-m was abolished upon introducing secondary mutations that eliminate 2-HG production. Wang et al. suggested that the impairment of DNA repair caused by D-2HG accumulation contributes to tumorigenesis (ibid.).

Phosphorylation of the Ser-139 residue of the histone H2AX, known as γ H2AX, is recognized as an early cellular response to DSBs. The detection of this phosphorylation event is currently used as a marker to monitor DNA damage (Mah, El-Osta, and Karagiannis 2010). Inoue et al. studied mice expressing IDH1 R132H in myeloid cells and observed that γ H2AX accumulates with age in undifferentiated hematopoietic cells from these mice compared to cells from IDH-wt mice (Inoue et al. 2016). This finding suggests a defect in DNA damage response signaling in IDH-m cells. Concordantly, Kusi et al. showed that breast tumor cells with low levels of endogenous 2HG treated with 2HG accumulate DSBs, as evidenced by γ H2AX detection (Kusi et al. 2022). Following 2HG withdrawal, there was a substantial decrease in H2AX phosphorylation. These data indicate that 2HG impairs DNA repair mechanisms, leading to the accumulation of DNA damage, potentially through the competitive inhibition of ALKBH enzymes, as hypothesized by Pu Wang et al. (2015).

Active DNA demethylation via TET enzymes is also linked to DNA repair. TET enzymes catalyze the oxidation of 5mC to 5hmC, but can further mediate the iterative oxidation of 5hmC to 5-formylcytosine (5fC) and 5-carboxylcytosine (5caC), see Figure 1.3 (X. Wu and Yi Zhang 2017). The latter two oxidized forms can be excised by thymine DNA glycosylase (TDG), resulting in demethylation facilitated by the base excision repair (BER) system (ibid.). Different lines of evidence suggest that TET enzymes participate in DNA repair in various ways. For instance, TET1 depletion leads to the accumulation of γ H2AX in mouse oocytes (Yamaguchi et al. 2012), while *TET1* knockout results in genomic instability in mouse embryonic fibroblasts, possibly due to the downregulation of DNA-repair-associated genes (Zhong et al. 2017). Moreover, double knockout of *TET2* and *TET3* results in a progressive γ H2AX increase in mouse bone marrow and spleen (An et al. 2015). Given these findings, the com-

petitive inhibition of TET enzymes by D-2HG could contribute to the impairment of DNA repair mechanisms.

Recently, Sulkowski et al. provided evidence for another mechanism by which D-2HG impairs DNA repair (Sulkowski, Oeck, et al. 2020). They first observed that IDH-m induces a defect in homologous recombination, which can be reversed by treatment with IDH-m inhibitors and recapitulated by D-2HG treatment (Sulkowski, Corso, et al. 2017). They demonstrated that the competitive inhibition of the histone demethylase KDM4B leads to hypermethylation of H3K9 at loci surrounding DNA breaks, masking the local H3K9me3 signal essential for the recruitment of Tip60 and MRE11, two key factors in the homology-dependent repair pathway (Sulkowski, Oeck, et al. 2020).

1.2.6 Other actions of D-2HG in tumor cells

D-2HG may also impact hypoxia-inducible factors (HIFs), which are crucial for adaptation to hypoxia, through the inhibition of the 2OG-dependent HIF prolyl hydroxylases (PHD/EGLN). Zhao et al. reported that the over-expression of IDH-m led to an early elevation of HIF-1 α levels, while 2-OG supplementation diminished this effect (Zhao et al. 2009). In contrast, other studies observed a reduction in HIF-1 α levels upon IDH-m expression and reported that D-2HG can promote EGLN activity (Koivunen et al. 2012; Tarhonskaya et al. 2014). Consistent with this latter observation, bioinformatics analysis of the cancer genome atlas (TCGA) data revealed that IDH-m glioma exhibit decreased expression of HIF1A targets and downstream biological functions such as angiogenesis and vasculogenesis (Kickingreder et al. 2015).

D-2HG also inhibits the 2OG-dependent collagen prolyl 4-hydroxylases, enzymes responsible for hydroxylating collagen (Myllyharju and Kivirikko 2004), which stabilizes its helical structure. Sasaki et al. reported defects in collagen maturation and basement membrane function in an IDH-m knock-in mouse model, leading to increased invasiveness (Sasaki, Knobbe, Itsumi, et al. 2012). Hydroxylated collagen is an essential component of the extracellular matrix, crucial for interactions between tumor cells and their surrounding environment (see page 33). Thus, D-2HG could alter the structure of the extracellular matrix via inhibition of these hydroxylases, potentially modifying cell interactions (Cairns and Mak 2013).

Lastly, IDH-m tumor cells may also display alterations of glutaminolytic and reductive carboxylation, NAD⁺ salvage pathways, redox control capacity, phospholipid profile, and ATP supply (Leonardi et al. 2012; Grassian et al. 2014; Sasaki, Knobbe, Itsumi, et al. 2012; Tateishi et al. 2015; Reitman et al. 2011; Esmaeili et al. 2014; Chan et al. 2015; Su et al. 2018). These alterations may not only be linked to a direct effect of D-2HG but also to the fact that while IDH-wt produce NADPH, IDH-m cells consume NADPH to produce D-2HG, thus decreasing NADPH/NADP⁺ ratio.

1.3 Myeloid immune tumor microenvironment of gliomas

Gliomas are composed of both tumor cells and cells residing in the tumor microenvironment (TME), including astrocytes, neurons, immune cells, endothelial cells, pericytes, and fibroblasts. Cellular interactions within the TME are the focus of intense

research aimed at identifying potential therapeutic targets. Compared to other tumor types, gliomas exhibit a poor lymphocytic infiltration (Rossi et al. 1987). The low mutation burden, limited antigen repertoire, and antigen presentation deficiency are thought to contribute to the “cold” immune TME of these tumors. While lymphoid cells are scarce in gliomas, tumor-associated microglia and macrophages (TAMs) are myeloid cells that constitute nearly 40% of the tumor mass and play critical roles in tumor progression (reviewed in Hambardzumyan, Gutmann, and Kettenmann 2016). As such, these cells may serve as prognostic biomarkers and therapeutic targets (Shan et al. 2020; Khan et al. 2023). In the following sections, I will focus on myeloid cells of the central nervous system. Subsequently, I will delve into the characterization of the immune TME of IDH-m gliomas, with emphasis on the myeloid compartment.

1.3.1 Myeloid cell populations in the central nervous system

Microglia are the main resident immune cells in the brain, accounting for 5% to 12% of all brain cells, depending on the region in healthy mice (Lawson et al. 1990). In humans, the proportion of microglia reaches values ranging from 0.5% to 16.5% according to brain regions (Mittelbronn et al. 2001). Both in mouse and human species, microglia derive from mesodermal macrophage progenitors generated in the yolk sac (Alliot, Godin, and Pessac 1999; Ginhoux et al. 2010; Z. Wang et al. 2023), and then self-renew within the brain under homeostatic conditions (Ajami, Bennett, et al. 2011; Askew et al. 2017). In the human brain, microglia were estimated to renew at a median rate of 28% per year (Réu et al. 2017). Microglia specialize within the unique brain environment, displaying a phenotype distinct from other tissue macrophages (Gosselin, Link, et al. 2014; Lavin et al. 2014). Different microglial subtypes have been associated with age, brain region, and disease stage (Silvin, Uderhardt, et al. 2022). While microglia are long-lived and terminally differentiated, they can undergo proliferation following stimulation (Prinz, Jung, and Priller 2019). Studying human microglia is particularly challenging, as these cells are difficult to obtain and maintain in culture (ibid.). As a result, most studies rely on rodent microglia, either primary or immortalized cells, which do not fully recapitulate the properties of human microglia (Masopust, Sivula, and Jameson 2017; Mestas and Hughes 2004; Seok et al. 2013; Smith and Dragunow 2014; Wolf, Boddeke, and Kettenmann 2017). Current efforts are focused on implementing induced pluripotent stem cell (iPSC)-derived systems in combination with gene editing strategies.

Other myeloid cells present in the homeostatic brain include border-associated macrophages (BAMs), which are located in border structures such as meninges, choroid plexuses, and perivascular spaces of the central nervous system (Mrdjen et al. 2018). BAMs are of embryonic origin and derive from a distinct macrophage lineage present in the yolk sac (Utz et al. 2020). Silvin et al. demonstrated that the renewal of BAMs during adulthood and aging involves monocyte recruitment (Silvin, Uderhardt, et al. 2022). In inflammatory conditions, monocyte-derived macrophages are recruited (Ajami, Samusik, et al. 2018; Mrdjen et al. 2018). In addition, recently described disease-associated microglia (DAM) are found at sites of neurodegeneration, where they are believed to play a protective role (Deczkowska et al. 2018; Keren-Shaul et al. 2017).

Silvin et al. integrated datasets from various stages of development (Hammond et al. 2019; Keren-Shaul et al. 2017; Van Hove et al. 2019; Zeisel et al. 2015), in both

physiological and pathological contexts to map different myeloid populations in the brain of mice and subsequently in humans (Silvin, Uderhardt, et al. 2022). This analysis led to the identification of youth-associated microglia (YAM), which emerge in the developing murine brain at embryonic day 14 and persist for only a few weeks during the early post-natal period, likely contributing to proper brain myelination (Hagemeyer et al. 2017). While YAM represent a physiological population associated with brain development, DAMs appear in pathological conditions to potentially restore brain homeostasis. Notably, Silvin et al. demonstrated that YAM and DAM share common patterns of gene expression (Silvin, Uderhardt, et al. 2022). These embryonically derived cells are not observed during normal aging, but emerge only in the context of neurodegeneration (ibid.). Alongside these protective cells, the authors described disease inflammatory macrophages (DIMs), which are monocyte derived. In contrast to DAMs, DIMs not only increase in frequency in the context of neurodegeneration but also accumulate during normal aging (ibid.), possibly due to a lack of integrity in the blood brain barrier with age (Rustenhoven and Kipnis 2019). Silvin et al. showed that the transcriptomic profiles of YAM, DAM and DIM described in mice can be extended to humans (Silvin, Uderhardt, et al. 2022).

Different myeloid populations coexist in the brain in a physiological manner. However, each population is also heterogeneous; microglial transcriptomic profiles vary notably depending on the brain region in which they reside (Grabert et al. 2016). Furthermore, studies have shown that microglia undergo transcriptional, functional, and metabolic shifts with aging that are specific to their brain region of residence (Grabert et al. 2016; Flowers et al. 2017). Geirsdottir et al. combined bulk and single cell transcriptomic approaches to evaluate microglial heterogeneity across different species (Geirsdottir et al. 2019). This analysis revealed that the homeostatic gene signature of microglia is conserved among species, including *C1QC*, *P2RY12*, and *TARDBP*. However, they observed significant heterogeneity in humans, with an organization into several microglial subtypes, in contrast to mice, macaques, marmosets, hamsters, or sheep, which exhibit only one dominant microglial type under steady-state, non-pathological conditions.

In summary, various myeloid populations of different origins coexist in the brain in a physiological state and evolve with aging and pathological conditions. Notably, significant heterogeneity within each population is observed in humans.

1.3.2 Tumor-associated macrophages and microglia

Myeloid cells in gliomas comprise the so-called tumor associated macrophages and microglia (TAMs). Despite similarities between resident microglia (TAM-MGs) and infiltrating monocyte derived macrophages (TAM-MDMs), these cells have distinct ontological origins and localization within the tumor core, and consequently, they can contribute in different ways to tumor initiation and progression. However, the different roles of these myeloid populations remain poorly understood, particularly due to the difficulty in reliably distinguishing them. TAM-MGs undergo phenotypical and functional changes that complicate their identification. Historically, cells displaying CD11b+/CD45-high expression correspond to MDMs, whereas CD11b+/CD45-low cells are classified as microglia (Sedgwick et al. 1991). However, upregulation of CD45 in TAM-MGs was also observed in a glioma mouse model (A. Müller et al. 2015). Other authors compared steady-state microglia and macrophages and proposed CX3CR1 and CCR2 as markers to distinguish these cell populations; however, they

seem to be less reliable in the context of glioma (Andersen, Faust Akl, et al. 2021). P2RY12 was identified as a marker of TAM-MGs and CD49d as a marker of TAM-MDMs using lineage-tracing studies in mice, both of which were validated in human glioma tissues (Bowman et al. 2016; A. Müller et al. 2015). However, P2RY12 was subsequently reported to be downregulated in the glioma context (Qian et al. 2021), alongside other markers for microglia in homeostatic conditions, such as *Cx3cr1*, *Sall1*, and *Tmem119* (ibid.). *Hexb* also appeared to be specifically expressed in microglial cells, but only in mice, not in humans (Masuda et al. 2020). In the absence of a single marker, combinations of markers are used to distinguish ontogenetically different populations (Klemm et al. 2020; Friebel et al. 2020; Andersen, Faust Akl, et al. 2021). Pombo-Antunes et al. identified different surface proteins that delineate both populations using CITE-seq (Cellular Indexing of Transcriptomes and Epitopes by Sequencing): CD44, CD49d, and CD9 in TAM-MDMs versus CD69, CD151, TMEM119 in TAM-MGs (Pombo Antunes et al. 2021). In murine glioma, staining for TMEM119 and GAL-3 was shown to delineate between TAM-MGs and TAM-MDMs (Ochocka, Segit, Walentynowicz, et al. 2021).

The composition of the immune TME differs according to the IDH mutation status. Amankulor et al. observed a significantly lower content in CD45+ cells in IDH-m gliomas compared with IDH-wt gliomas (Amankulor et al. 2017). They created a syngeneic pair mouse model for IDH-m and IDH-wt glioma, which allowed them to observe a decrease in microglia, macrophages, monocytes, and polymorphonuclear leukocytes in IDH-m tumors (ibid.). Two landmark studies analyzed the extent of leukocyte diversity in surgical resections of IDH-wt, IDH-m gliomas, and brain metastases by using multiparameter fluorescence-activated cell sorting followed by RNA sequencing (Klemm et al. 2020) and single-cell mass cytometry (CYTOF) (Friebel et al. 2020).

Klemm et al. isolated different cell types from IDH-m gliomas, IDH-wt gliomas, brain metastases and non-tumor tissue by flow-cytometry (Klemm et al. 2020). These studies reported a predominance of myeloid cells in gliomas regardless of the IDH status and few T cells, thus supporting the notion that gliomas are immunologically “cold” (Jackson, J. Choi, and Lim 2019). At the opposite, the majority of metastases exhibited a substantial content of T cells and neutrophils. Friebel et al. also reported that TAMs and monocytes comprise about 80% ($\pm 18\%$) of leukocytes in glioma and in non-tumor control tissue, and 40% in metastases (Friebel et al. 2020).

They observed a predominance of TAM-MGs with low numbers of other immune cells in non-tumor tissues and IDH-m gliomas, whereas IDH-wt gliomas were for their part rich on TAM-MDMs and, to a lesser extent, on neutrophils (Klemm et al. 2020; Friebel et al. 2020). When present, the lymphocyte compartment was mostly composed of T cells with few natural killer cells and B cells. These observations were further confirmed by other studies using single cell techniques (Gupta et al. 2024). The invading myeloid cells in IDH-m glioma were composed mainly of monocytes, and a lesser proportion of TAM-MDMs.

Friebel et al. further studied the localization of both TAM-MGs and TAM-MDMs within the glioma micro-environment by immunofluorescence and immunohistochemistry. They observed that TAM-MGs (Iba1+, CD163- P2Y12+) were diffusely scattered throughout gliomas, whereas Iba1+ CD163+ TAM-MDMs were in close proximity to VE-cadherin-positive blood vessels. Other authors previously reported a predominance of TAM-MDMs in the tumor core, and of TAM-MGs in the tumor

periphery of IDH-wt gliomas (Darmanis et al. 2017; S. Müller et al. 2017; K. Yu et al. 2020). The spatial distribution of both cell types may vary according to the type and location of glioma. They examined the expression level of markers considered as “reactivity” markers (Keren-Shaul et al. 2017; Mrdjen et al. 2018; Walker and Lue 2015). Human leukocyte antigen – DR isotype (HLA-DR) expression was comparable between TAM-MGs from both IDH-m and IDH-wt gliomas, whereas CD14 and CD64 were upregulated in IDH-wt gliomas but not in IDH-m gliomas (Friebel et al. 2020).

Friedrich et al. used mouse models (GL261 glioma cells that episomally overexpressed IDH-wt or IDH-m were inoculated in mice) to show that the recruitment of myeloid cells differs according to the IDH status (Friedrich, Sankowski, et al. 2021).

Subsequent studies demonstrated that the composition in TAMs differs not only according to the IDH-m status but also tumor grade (Miller et al. 2023; Gupta et al. 2024). Experimental evidence indicate that glioma progression leads to a process of cellular competition, wherein TAM-MDMs invade the niche previously occupied by resident TAM-MGs (Pombo Antunes et al. 2021; Yeo et al. 2022).

The appendix section B.3 (page 171) includes a detailed review article on the differences in the immune TME of gliomas according to the IDH mutational status, written during the course of my PhD: Quentin Richard, Alice Laurence, Michel Mal-lat, Marc Sanson, and Luis Jaime Castro-Vega (Dec. 1, 2022). “New insights into the Immune TME of adult-type diffuse gliomas”. In: *Current Opinion in Neurology* 35.6, pp. 794–802. ISSN: 1473-6551. DOI: 10.1097/WCO.0000000000001112.

1.3.3 TAMs heterogeneity beyond M1/M2 phenotypes

To understand the diversity of TAMs phenotypes, two main models are often discussed: the dichotomic and multi-faceted (continuum) models. The dichotomic model suggests that TAMs exist in two polarized states: either pro-inflammatory and tumor-suppressive (M1-like) or anti-inflammatory and tumor-promoting (M2-like). This binary classification has been useful in early studies of macrophage behavior in the TME, as it captures some of the functional extremes of TAM activity. However, emerging evidence increasingly supports a more nuanced, multi-faceted model. Klemm et al. also assessed the M1 and M2 polarization markers of TAM-MGs and TAM-MDMs using a panel of marker genes (Murray et al. 2014). Rather than a defined M1 or M2 phenotype, they observed a multifaceted response associating canonical M1 markers as interferon gamma (IFN- γ) and M2 markers as interleukin-4 (IL-4). According to this continuum model, TAMs exhibit a spectrum of phenotypes, adapting dynamically to the local cues within the TME. This plasticity underscores the diversity of TAM functions, ranging from immune suppression to support for tumor growth and invasion, rather than fitting into rigid categories.

Recent studies using single-cell and spatial transcriptomic modalities have revealed the diversity of the myeloid compartment of gliomas in mice and humans by unveiling distinct subsets of TAM-MG and TAM-MDMs (Pombo Antunes et al. 2021; Ochocka, Segit, Walentynowicz, et al. 2021; Abdelfattah et al. 2022; V. M. Ravi et al. 2022; Blanco-Carmona et al. 2023; Evans et al. 2023; Greenwald et al. 2024; Mirzaei et al. 2023). It is believed that the newly identified subsets of TAM-MGs and TAM-MDMs may play distinct roles in tumor evolution. For instance, immunosuppressive macrophages and inflammatory microglial cells correlate with worse and better prognosis, respectively (Abdelfattah et al. 2022).

Below are examples of TAMs subsets that were delineated using single-cell or

single-nuclei RNA sequencing (scRNA-Seq, snRNA-Seq). Markers of these subsets can be used to deconvolve bulk RNA-Seq data from tumors:

- Homeostatic TAM-MGs with high expression of microglia-enriched genes, observed in human and murine glioma of both IDH-m and IDH-wt status (Ochocka, Segit, Walentynowicz, et al. 2021; Abdelfattah et al. 2022; Blanco-Carmona et al. 2023),
- Transitory TAM-MDMs, that express monocyte-related genes (*EREG*, *S100A6* and *LYZ*) together with mature macrophage markers at low levels (*C1QA* and *IGF1*) suggestive of an ongoing monocyte-to-macrophage differentiation (Pombo Antunes et al. 2021; Abdelfattah et al. 2022),
- TAM-MDMs with adoptive features of MGs, with expression of many microglial signature genes (*CX3CR1*) (Pombo Antunes et al. 2021; Abdelfattah et al. 2022),
- Proliferating TAMs with high level of *MKI67* (Abdelfattah et al. 2022),
- Both phagocytosing TAM-MDMs and TAM-MGs whose gene signature is associated with phagocytosis and lipid metabolism (*GPNMB*, *LGALS3* and *FABP5*) (Pombo Antunes et al. 2021; Blanco-Carmona et al. 2023),
- Both hypoxic TAM-MDMs and TAM-MGs (expression of *BNIP3*, *ADAM8*, *MIF* and *SLC2A1*) (Pombo Antunes et al. 2021; Abdelfattah et al. 2022),
- Both TAM-MDMs and TAM-MGs with an IFN- γ signature (Pombo Antunes et al. 2021; Blanco-Carmona et al. 2023),
- Immunosuppressive subsets of TAM-MGs and TAM-MDMs. Miller et al. defined notably immunosuppressive programs found across TAM-MGs and TAM-MDMs (Miller et al. 2023).

A summary of TAM clusters in human gliomas established from single-cell transcriptomics data (scRNA-Seq and snRNA-Seq data) is provided in Table 1.2.

DAM-like TAM-MGs, similar to DAMs found in Alzheimer's disease expressing *SPP1*, *GPNMB* and *CST7*, may also be present in glioma (Pombo Antunes et al. 2021; Qian et al. 2021; Silvin, Qian, and Ginhoux 2023).

More recently, Gupta et al. described additional subsets of TAMs. The authors notably observed a subpopulation of TAM-MGs expressing the cytotoxic peptide granulysin, previously thought to be expressed only in lymphocytes (Gupta et al. 2024). Mirzaei et al. reported a new subtype of TAM-MGs expressing the protein kinase $\text{C}\delta$ (*PKC\delta*) in IDH-wt gliomas, which seems to present anti-tumor functions (Mirzaei et al. 2023).

Friedrich et al. conducted scRNA-Seq of myeloid cells from human IDH-m and IDH-wt gliomas, as well as control brain tissues (Friedrich, Sankowski, et al. 2021). They identified ten clusters of myeloid cells, with the cluster correlating with cells that upregulate genes encoding chemokines being enriched in IDH-m gliomas. Two clusters were more prominent in IDH-wt gliomas, identified as acutely infiltrating myeloid cells, which exhibited upregulation of interferon signaling and hypoxia-associated genes. In contrast, control-enriched clusters displayed an upregulation of genes associated with homeostatic microglia. These observations were further confirmed at the protein level (ibid.). Genes coding for major histocompatibility complex (MHC) class I and II were significantly more expressed in TAMs from IDH-wt gliomas than in those from IDH-m gliomas, which, in contrast, expressed higher levels of genes associated with steady-state microglia and inflammatory mediators

Source	Type of tumor	Clusters	Top 10 DE genes	Comparison
Pombo Antunes et al. (2021)	human ND GBM (scRNA-Seq)	Mg-TAM 1 Mg-TAM 2 Phago/lipid Mg-TAM IFN Mg-TAM Mg-TAM 5 Transitory Mo-TAM IFN Mo-TAM SEPP1+ Mo-TAM Hypoxic Mo-TAM Lipid Mo-TAM Prol. TAM 12 Prol. TAM 13 Monocytes Unknown	<i>VIM, S100A10, TGFBI, CD163, ANXA1, FTL, S100A4, LGALS1, ANXA2, TYMP, HAMP, FCGBP, SPP1, CD14, BIN1, C1QB, FSCN1, SCIN, ALOX5AP, VSIG4, FABP3, RAMP1, LRRRC39, TREM2, MYOZ1, LILRA4, LINC01235, GLDN, OLFM2, LPL, ISG15, IFI44L, IFIT1, MX1, IFI6, IFIT3, LY6E, IFITM3, OAS1, B2M, CD83, PPP1R15A, BAG3, NR4A1, IL1B, KLF6, DNAB1, DUSP1, DUSP2, IER3, TGFBI, S100A10, CXCL3, LGALS1, CXCL2, TREM2, VCAN, THBS1, ANPEP, S100A6, CXCL11, CXCL10, IFITM1, RSAD2, ISG20, IFIT3, IFIT2, IFIT1, GBP4, HAPLN3, HLA-DPB1, CST3, SPP1, HLA-DRB1, HLA-DPA1, CD74, HLA-DRA, TMIGD3, LYZ, HLA-DQB1, GAPDH, LDHA, ALDOA, BNIP3, S100A10, MIF, VIM, PLIN2, CSTB, TPI1, ALDH1A1, ACP5, LGALS3, SDS, GPNMB, CTSD, ADAMDEC1, OTOA, TSPAN4, BLVRA, TK1, TYMS, H2AFZ, MCM7, KIAA0101, CENPM, CLSPN, GINS2, PCNA, STMN1, BIRC5, PTTG1, MKI67, CENPF, CDKN3, TROAP, CDC20, HMGB3, TOP2A, CCNB1, FCN1, S100A12, VCAN, CFP, IL1R2, CD52, EREG, S100A6, LYZ, S100A8, HLA-DRB1, NEAT1, KLF6, HLA-DRA, HLA-DPA1, MALAT1, CD74, PSAP, DUSP1, GAPDH</i>	vs All
		Transitory Mo-TAM Lipid Mo-TAM Hypoxic Mo-TAM a Hypoxic Mo-TAM b SEPP1-lo Mo-TAM SEPP1-hi Mo-TAM IFN Mo-TAM Prol. TAM 7 Prol. TAM 8 monocytes Mg-TAM	<i>HLA-DPB1, HLA-DRA, HLA-DPA1, HLA-DQB1, LYZ, JUNB, HLA-DQA1, CXCR4, HLA-DRB1, RSG2, LGALS3, ACP5, CTSD, PLA2G7, OTOA, SDS, S100A11, FTL, GRN, LYZ, GAPDH, BNIP3, ALDOA, LDHA, MIF, ENO1, ADM, PLIN2, VIM, TPI1, ENO1, PKM, GAPDH, LGALS1, TPI1, LDHA, PGK1, PFN1, MIF, ANXA2, C3, FCGBP, C1QC, C1QA, NPC2, CX3CR1, OLFML3, CD74, LTC4S, YWHAH, SEPP1, CD74, HLA-DPA1, HLA-DRB1, HLA-DPB1, HLA-DRA, HLA-DQA1, HLA-DQB1, HLA-DMA, HLA-DMB, CXCL10, GBP1, CXCL11, GBP4, STAT1, RSAD2, IFIT2, ISG15, PSMB9, IFIT3, IRC5, STMN1, PTTG1, HMGN2, HMGB1, CENPF, MKI67, CDKN3, HMGB3, CKS1B, MCM7, TYMS, GINS2, CLSPN, KIAA0101, PCNA, CDT1, TK1, HELLS, H2AFZ, C1QC, FCN1, S100A6, C1QB, C1QA, APOE, TREM2, S100A4, APOC1, S100A9, VIM, LYZ, TMIGD3, S100A4, SPP1, PTMA, S100A6, ANXA1, AP1S2, VSIG4</i>	vs All
Abdelfattah et al. (2022)	2 LGG, 11 newly diagnosed glioblastoma, and 5 recurrent glioblastoma (scRNA-Seq)	MC01: activated microglia MC02: homeostatic microglia MC03: s-mac 1 MC04: MDSC MC05: s-mac 2 MC06: AP-microglia MC07: a-microglia MC08: DCs MC09: proliferating MDM	<i>CCL3L1, CCL4L2, CCL4, CCL3, EGR3, IL1B, EGR2, CD83, BTG2, CH25H, APOC2, C3, GPR34, LTC4S, ITM2B, LINC01736, HLA-DPA1, C1QC, HLA-DRB5, HBB, RNASE1, SELENOP, CXCL2, CTSD, CXCL3, GPNMB, TGFBI, CD163, LGALS3, GCHFR, MT1G, MT1X, MT2A, MT1H, MT1E, C15orf48, CSTB, MIF, BNIP3, G0S2, S100A9, S100A8, VCAN, LYZ, THBS1, TIMP1, S100A12, FCN1, AREG, IL1R2, ISG15, CXCL10, IFIT1, IFIT3, IFI6, IFI44L, MX1, IFIT2, IFITM3, LY6E, MALAT1, DDX5, SLC1A3, MT-ND3, NEAT1, RGS1, MEF2C, ARGLU1, HNRNPA2B1, TRA2B, AREG, HLA-DQA1, FCER1A, HLA-DPB1, PPA1, HLA-DRB1, HLA-DPA1, HLA-DQB1, JAML, HLA-DRA, HIST1H4C, STMN1, MKI67, TOP2A, HIST1H1D, TUBB, CENPF, PCLAF, HIST1H1E, HIST1H1B</i>	vs myeloid
Blanco-Carmona et al. (2023)	primary IDH-m glioma (snRNA-Seq)	BAMs BMD Anti-inflammatory TAMs Mg Activated Mg Homeostatic Mg IFN-γ TAMs Mg Inflammatory ICAM1+ Mg Inflammatory TAMs Mg Phagocytic Mg Resident-like TAMs Mg Stressed TAMs	<i>F13A1, COLEC12, SCN9A, TTN, LILRB5, CCDC141, CD28, CD36, FGF13, SELENOP, VAV3, SELENOP, ITGA4, SLC40A1, MS4A4E, CD163, MRC1, AC100849.1, CD163L1, MS4A6A, CX3CR1, SYNDIG1, DOCK8, P2RY12, RITN, PLXDC2, NAV3, RASGEF1C, C3, CACNA1A, LINGO1, PCDH15, C3, DLGAP1, CADM2, SLC26A3, INO80D, LRP1B, CIRBP, RASGEF1B, IFIT2, IFIT3, EPST11, SAMD9L, MX2, IFIT1, IFI44L, ZBP1, MX1, PARP14, RELB, ICAM1, NFKB2, AC011511.2, TNFAIP3, GCH1, BCL3, IL4I1, IL1B, IL1A, NR4A3, IL1B, NR4A1, EGR3, CCL4L2, CCL4, EGR2, CCL3L1, NFKBID, CD83, GPNMB, STARD13, MYO1E, RGCC, PLA2G7, DENND4C, PPARG, FNIP2, MITF, LPL, NHSL1, SERPINE1, ELMO1, ARHGAP24, DOCK5, FKBP5, AQP1, CTTNBP2, PLCL1, FRMD4A, HSPA1B, HSPA1A, SORCS2, FP236383.1, FP671120.1, AL355838.1, AJ009632.2, OR3A2, HSP90AA1, AC007319.1</i>	vs TAMs

Table 1.2: Summary of TAM clusters in human gliomas established from single-cell transcriptomics data

(Friedrich, Sankowski, et al. 2021). Functional validation of the TAM subsets described in the aforementioned scRNA-Seq studies has not yet been achieved; however, these studies advanced our understanding of the reprogramming of TAMs within the tumor microenvironment (Silvin, Qian, and Ginhoux 2023).

The IDH mutational status of the tumor may influence this reprogramming as previously discussed. Recently, Blanco-Carmona et al. used snRNA-Seq and assay for transposase-accessible chromatin using sequencing (ATAC-seq) to explore epigenetic changes underlying the diversity of TAMs in IDH-m gliomas. They highlighted notable differences between astrocytomas and oligodendrogliomas, finding that astrocytomas contained inflammatory TAMs expressing phosphorylated signal transducer and activator of transcription 1 (STAT1) (Blanco-Carmona et al. 2023). Sex-related factors may also influence the reprogramming of TAMs. Ochocka et al. observed significantly higher expression levels of MHC-II and PD-L1 in TAM-MDMs from male individuals (Ochocka, Segit, Walentynowicz, et al. 2021; Ochocka, Segit, Wojnicki, et al. 2023), suggesting that male TAMs could be more tumor-supportive than their female counterparts. Additionally, scRNA-Seq analysis revealed that both recurrent IDH-wt and recurrent IDH-m gliomas exhibit a greater abundance of infiltrating TAMs compared to primary tumors (Pombo Antunes et al. 2021; Gupta et al. 2024).

Beyond the identification of subsets of TAMs at single-cell resolution, recent studies have further characterized immunomodulatory programs within TAMs, emphasizing their spatial localization and response to environmental stressors like hypoxia. Miller et al. integrated scRNA-Seq data from 85 diverse gliomas, including primary and recurrent IDH-m and IDH-wt tumors (Miller et al. 2023). This analysis allowed them to identify consensus gene activity in inflammatory and immunosuppressive programs present across IDH-m, IDH-wt, primary, and recurrent gliomas, as well as across different myeloid cell types. They proposed that myeloid cells are plastic cells whose transcriptomic programs are determined not only by their ontology but also by cell-extrinsic factors in the tumor microenvironment (ibid.). The authors noted few differences in these immunomodulatory programs between myeloid cells from IDH-m and IDH-wt gliomas when comparing tumors of equivalent histological grade. Strikingly, they demonstrated convergent phenotypes of resident TAM-MGs and TAM-MDMs, with the latter adopting a microglia-like phenotype upon tumor colonization. All these observations support the concept of TAMs education by the TME (ibid.). Furthermore, it has been shown that TAMs and other immune cells in IDH-wt gliomas are spatially organized along a hypoxia gradient, whereas in IDH-m gliomas, the distribution of these cells is sparse and less structured (V. M. Ravi et al. 2022; Haley et al. 2024; Motevasseli et al. 2024; Greenwald et al. 2024).

Finally, TAMs actively modulate glioma biology while being influenced by tumor cells. Glioma cells and TAMs engage in bidirectional interactions through secretion of chemokines, cytokines, neurotrophic factors, and even microRNAs. D-2HG produced by IDH-m glioma cells plays critical roles in this cellular crosstalk. Both glioma cells and TAMs also modulate the extracellular matrix, affecting cell adhesion, migration, or proliferation. Through this crosstalk, glioma cells shape the spatial organization, polarization, and metabolic reprogramming of TAMs, which in turn influence tumor growth, migration, and invasion.

The appendix section B.4 (page 181) includes a detailed book chapter reviewing the interaction of TAMs with tumor cells, written during the course of my PhD:

Laurence A., Castro-Vega LJ, Huberfeld G. *Reciprocal interactions between glioma and tissue-resident cells fueling tumor progression*. Handbook of Clinical Neurology. 2024 (in press).

1.4 Immunomodulatory roles of D-2HG

While D-2HG drives malignant transformation, at least in part through epigenetic remodeling of IDH-m cells, the accumulation of this oncometabolite seems to diminish cellular fitness (Bralten et al. 2011; Losman, Looper, et al. 2013). Nonetheless, the extremely low rate of loss of the IDH mutation during tumor evolution suggests that D-2HG confers some benefits to tumor cells through indirect effects. As previously discussed, accumulating evidence suggests that the IDH mutation significantly shapes the immune tumor microenvironment. Mechanistically, the intrinsic accumulation of D-2HG in IDH-m cells, coupled with the associated epigenetic remodeling, has been shown to indirectly influence the composition of the immune TME. Additionally, emerging evidence indicates that D-2HG, which also accumulates in the TME, directly impacts immune cell function, primarily through non-canonical effects on the epigenome. In the following section, I will examine these two mechanisms separately.

1.4.1 Hypermethylation in IDH-mutant cells promotes immune evasion

Epigenetic modifications of IDH-m cells have been shown to lead to the modulation of the expression of key factors in the interrelation between tumor cells and immune cells of the TME:

- NKG2D ligands: Zhang et al. showed that IDH-m glioma cells acquire resistance to natural killer cells through epigenetic silencing inducing the down-regulation of NKG2D ligands (ULBP1 and ULBP3), which can be rescued by hypomethylating agents (X. Zhang et al. 2016).
- CXCL10: Kohanbash et al. reported reduced expression of genes involved in cytotoxic T cell function and recruitment (Kohanbash et al. 2017). In particular, they demonstrated in immortalized normal human astrocytes and syngeneic mouse glioma models, that D-2HG can directly suppress the expression of C-X-C motif chemokine ligand 10 (CXCL10), by reducing STAT1 levels. This effect was reversed by inhibiting the mutant IDH1 enzyme and was enhanced with vaccine immunotherapy in mice bearing IDH-m gliomas. Thus, these authors revealed for the first time a mechanism through which IDH mutations suppress the accumulation of T cells in these tumors (ibid.).
- PD-L1: Mu et al. revealed that D-2HG leads to a hypermethylation of the promoter of Programmed death-ligand 1 (PD-L1) and to the decreased expression of PD-L1 (Mu et al. 2018).
- MHC-I-type HLA genes: Luoto et al. showed that HLA genes were more methylated in IDH-m than IDH-wt gliomas, with decreased expression of the HLA components of MHC-I at the protein level (Luoto et al. 2018), which could impair the recognition of malignant cells by CD8+ cytotoxic T cells.

Figure under copyright,
see Foskolou, Bunse, and Van den Bossche (2023).

Figure 1.4: **D-2HG leads to immunomodulatory effects on cells in the tumor micro-environment**, from Foskolou, Bunse, and Van den Bossche (2023). D-2HG is produced physiologically in activated macrophages. It also accumulates in pathological context in acidurias and cancer. D-2HG is found in IDH-m tumors and can also increase in breast cancers with upregulation of PHGDH and ADHFE1.

- G-CSF: Alghamri et al. observed a change in the peak enrichment for H3K4me3 mark around the promoter region in IDH-m neurospheres compared with IDH-wt ones (Alghamri et al. 2021). Consistently, they reported a down-regulation of H3K4me3 deposition at the gene promoter region in IDH-m cells treated with an IDH-m inhibitor. In addition, they showed that *CSF3* gene expression was significantly up-regulated in patients with IDH-m glioma, with an increase of granulocyte colony-stimulating factor (G-CSF) level in serum (ibid.). They reported a subsequent expansion of non-immunosuppressive cells (CD45high/CD11b+/Ly6G+ cells) in IDH-m gliomas.
- cGAS-STING pathway: Wu et al. recently showed that IDH-m leads to a hypermethylation and silencing of the cytoplasmic double-stranded DNA sensor cGAS, which stimulates antitumor immunity (M.-J. Wu, Kondo, et al. 2024). Inhibiting mutant IDH1 activates TET2-mediated demethylation, leading to re-activation of genes in the cGAS-STING pathway, ultimately promoting immune responses against the tumor including restoration of INF- γ response and recruitment of CD8+ T cells.

These examples show that the hypermethylation of DNA or histones generated by D-2HG in IDH-m glioma cells leads to the modulation of the interactions of these tumor cells with the immune TME.

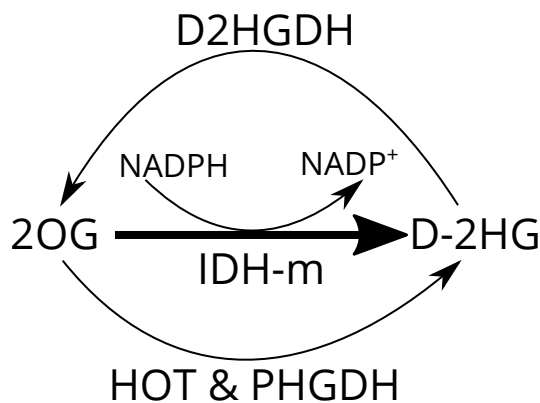


Figure 1.5: **Production of D-2hydroxyglutarate (D-2HG)**, from Kranendijk et al. (2012). D-2HG is physiologically formed from 2OG via hydroxyacid-oxoacid transhydrogenase (HOT), or d-3-phosphoglycerate dehydrogenase (PHGDH). D-2-hydroxyglutarate dehydrogenase (D-2HGDH) catalyzes the conversion of D-2HG to 2OG. Mutant isocitrate deshydrogenase converts 2OG into D-2HG.

1.4.2 Cell-extrinsic effects D-2HG in TME cells

D-2HG is indeed also released by tumor cells at high levels, through an uncharacterized mechanism, enabling paracrine effects, see Figure 1.4.

1.4.2.1 D-2HG accumulates in the TME

2HG is a five-carbon dicarboxylic acid with a chiral center at the second carbon atom, allowing two possible enantiomers: D-2HG and L-2HG. While L-2HG accumulates in acidic conditions and also plays physiological roles in T cells (Tyrakis et al. 2016; Foskolou, Bunse, and Van den Bossche 2023), basal levels of D-2HG are barely detected in normal cells but increase significantly as a product of the IDH-m in gliomas or by mutations in the D-2-hydroxyglutarate dehydrogenase (*D2HGDH*) gene in a rare metabolic disorder called D-2-hydroxyglutaric aciduria (D-2HGA). Other enzymes that account for the accumulation of D-2HG in the absence of IDH-m include 3-phosphoglycerate dehydrogenase (PHGDH), and hydroxyacid-oxoacid transhydrogenase (HOT) encoded by alcohol dehydrogenase iron containing 1 (*ADHFE1*), see Figure 1.5. PHGDH is a key enzyme of the serine synthesis pathway, which catalyzes the transformation of 2-OG into D-2HG as a side reaction. Amplification of the PHGDH locus has been associated to increased levels of D-2HG in breast cancer (Fan et al. 2015). The gene *ADHFE1* has also been reported to play an oncogenic role in breast cancer where its overexpression leads to the increase of D-2HG (Mishra et al. 2018).

In general, it is estimated that in IDH-m cells D-2HG levels are up to 100 times higher than L-2HG, reaching concentrations between 10 and 30 mM (Dang et al. 2009), as measured using GC/MS. This can also be determined non-invasively through proton magnetic resonance spectroscopy (MRS) (C. Choi et al. 2012), as depicted in Figure 1.6. Additionally, D-2HG can be detected in the cerebrospinal fluid of IDH-m glioma patients, where levels can reach up to 100 μ M (with a mean around 7 μ M) (Kalinina et al. 2016). While studies have demonstrated that D-2HG traffics out of tumor cells in both *in vitro* and *in vivo* settings through unknown

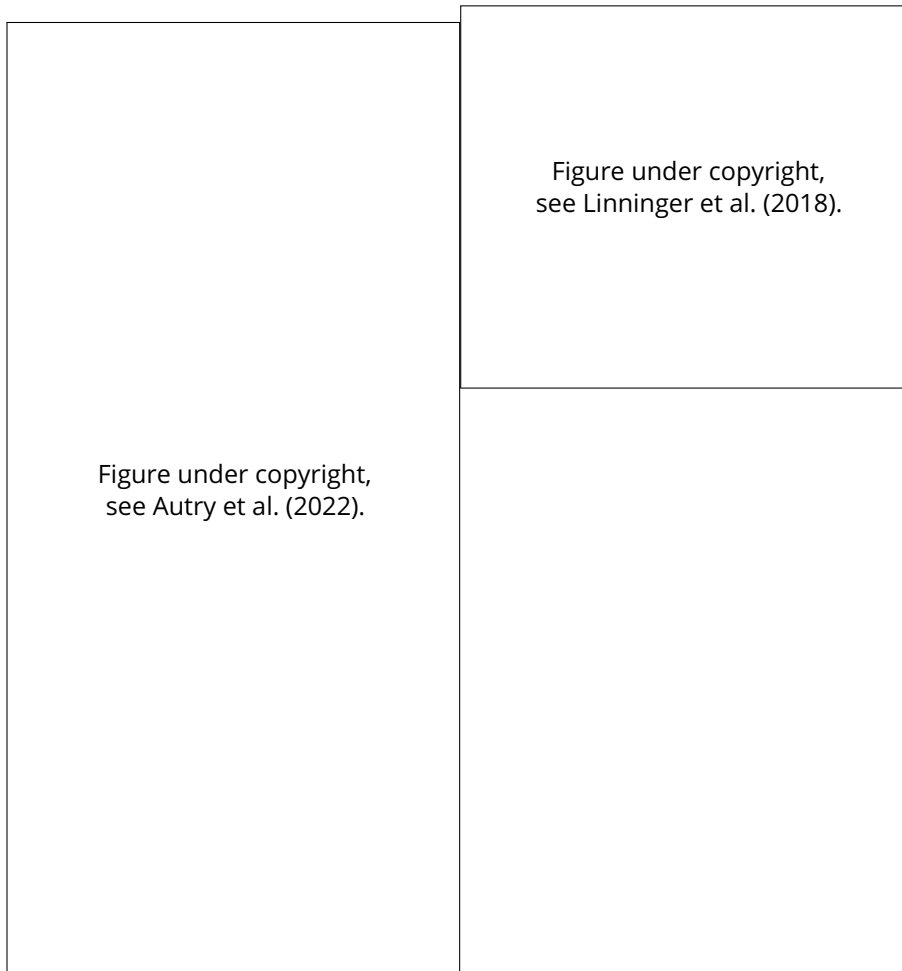


Figure 1.6: **D-2hydroxyglutarate accumulates in the tumor microenvironment.** **Left:** Spectral MRI data acquired prior to surgery from a patient with IDH-m grade 2 astrocytoma (CNI map overlaid on a T2-FLAIR image). Spectra reconstructed at the site of tissue sampling highlight the 2HG resonance among other brain metabolites, from Autry et al. (2022). **Right:** Predicted D-2HG concentration profiles around a IDH-m glioma, from Linninger et al. (2018).

mechanisms (Dang et al. 2009; Luchman et al. 2012), accurately quantifying D-2HG levels in the interstitial and extracellular compartments remains challenging.

Linninger et al. estimated the D-2HG concentration gradient in the extracellular fluid surrounding IDH-m gliomas (Linninger et al. 2018). They quantified D-2HG by liquid chromatography–mass spectrometry in conditioned medium from patient-derived IDH-wt and IDH-m glioma cells, finding a release rate of 3.7–97.0 pg per cell per week. For an average-sized tumor (30 mL glioma volume and 10^8 tumor cells/mL), they estimated a D-2HG release of $3.2\text{--}83.0 \times 10^{-12}$ mol/mL/s. Using a mathematical model of fluid flow throughout the intracerebral compartment, they also calculated the D-2HG release rate necessary to generate cerebrospinal fluid concentrations similar to those observed clinically. Their second approach yielded consistent results with the first one ($2.9\text{--}12.9 \times 10^{-12}$ mol/mL/s). They concluded that D-2HG extracellular concentrations exceed 3 mM within a 2 cm radius from the center of an IDH-m glioma (ibid.), as depicted in Figure 1.6.

Consistent with these observations, emerging evidence indicates that D-2HG may affect the function of cells residing in the TME. It has been shown that D-2HG enters murine and human T lymphocytes (Bunse, Pusch, et al. 2018). Murine and human dendritic cells also uptake D-2HG (Bunse, Pusch, et al. 2018; Ugele et al. 2019), as do murine (Chuntova et al. 2022) and human macrophages (Friedrich, Sankowski, et al. 2021), murine B cell blasts, murine splenocytes, murine microglia (Bunse, Pusch, et al. 2018), and human endothelial cells (Xiaomin Wang et al. 2022). However, D-2HG is highly hydrophilic (W. Xu et al. 2011) and must cross hydrophobic membranes to be transported between tumor cells and surrounding cells. Sodium-dependent dicarboxylate transporter 3 (SLC13A3) and organic anion transporters (SLC22A6 and SLC22A11) have been shown to transport D-2HG in renal cells and astrocytes (Mühlhausen et al. 2008). Bunse et al. reported evidence of D-2HG uptake by T cells through SLC13A3 (Bunse, Pusch, et al. 2018), whereas endothelial cells seem to use SLC1A1, a Na^+ -dependent glutamate transporter also known as EAAC1 (Xiaomin Wang et al. 2022).

1.4.2.2 Effects of D-2HG in lymphocytes

Bunse et al. reported an inhibition of T cell proliferation by D-2HG in a concentration-dependent manner (Bunse, Pusch, et al. 2018). They observed suppression of T cell capacity to produce the effector cytokines IFN- γ and IL-2 following activation by D-2HG, a finding that was subsequently confirmed by others (L. Zhang et al. 2018). Notably, they did not observe any significant epigenetic reprogramming of human T cells after D-2HG treatment, as assessed by 850k DNA methylation array and histone methylation analyses (Bunse, Pusch, et al. 2018). Instead, the authors showed that D-2HG can interfere with cytosolic calcium influx and the nuclear translocation of transcription factors NFAT and NF- κ B p65, in activated T cells, impairing T cell receptor-signaling. They also reported that D-2HG inhibits mitochondrial adenosine triphosphate (ATP) production, leading to the activation of adenosine monophosphate-activated protein kinase (AMPK) ultimately inhibiting polyamine synthesis, which supports cell proliferation under physiological conditions (ibid.). Afsari et al. found that D-2HG inhibits the Ca^{2+} -regulated phosphatase calcineurin, which is normally required for the dephosphorylation of nuclear factor of activated T cells (NFAT) and subsequent nuclear translocation (Afsari and McIntyre 2023).

Complementary to these observations, Bottcher et al. showed that D-2HG trig-

gers the destabilization of HIF-1 α protein, which skews T cells towards oxidative phosphorylation, favoring regulatory T cell development at the expense of T helper 17 polarization (Böttcher et al. 2018). Moreover, Notarangelo et al. found that D-2HG alters the metabolism and the capacity to release IFN- γ of CD8+ T cells by limiting the glycolytic flux of glucose into lactate through direct inhibition of the glycolytic enzyme lactate dehydrogenase (LDH) (Notarangelo et al. 2022). Additionally, the migration capability of T cells has also been reported to be restricted by D-2HG (L. Zhang et al. 2018).

In complement to these findings regarding the limitation of T cell functions in the presence of D-2HG, T lymphocytes from IDH-m tumors have been studied following the treatment with IDH-m inhibitors, which lead to D-2HG depletion. Chuntova et al. treated IDH-m glioma-bearing mice with an IDH-m inhibitor and reported a restriction in glioma progression during treatment, which was CD4+ and CD8+ cell-dependent. They observed enhanced proinflammatory IFN- γ -related gene expression and an increased number of CD4+ tumor-infiltrating T-cells in treated tumors (Chuntova et al. 2022). Another group reported an increase of PD-L1 expression levels on IDH-m glioma cells after treatment with an IDH-m inhibitor in a mouse model, achieving similar levels to those observed in IDH-wt gliomas (Kadiyala et al. 2021). Upon administering anti-PDL1 immune checkpoint blockade, they observed a reduction in T cell exhaustion and facilitation of memory CD8+ T cell generation (ibid.). Consistent findings were reported in IDH-m cholangiocarcinoma: IDH-m inhibition stimulated CD8+ T-cell recruitment and interferon γ expression in a murine model (M.-J. Wu, Shi, et al. 2022). Notably, in humans, inhibition of IDH-m in low-grade IDH-m gliomas was also associated with signs of immune cell activation (Mellinghoff, Ellingson, et al. 2020; Mellinghoff, Penas-Prado, et al. 2021; Mellinghoff, M. Lu, et al. 2023).

Finally, Yang et al. employed a complementary approach to IDH-m inhibition by enhancing D-2HG catabolism in T cells (Yang et al. 2022). They engineered chimeric antigen receptors T cells (CAR-T cells) that overexpress D2HGDH, the enzyme that catalyzes the conversion of D-2HG back into 2-OG (Figure 1.5), and reported an improvement of CAR-T cell-mediated killing of cancer cells. Treatment of IDH-m glioma-bearing mice with D2HGDH-overexpressing CAR-T cells resulted in enhanced T cell expansion and improved overall survival.

Collectively, these results provide evidence that D-2HG directly contributes to reduced T cell functionality, coupled with increased T cell exhaustion.

1.4.2.3 Effects of D-2HG in dendritic cells

The effects of D-2HG on myeloid cells have also been studied. Zhang et al. first reported that D-2HG did not modulate the differentiation of murine dendritic cells (L. Zhang et al. 2018). They also found no influence of D-2HG *in vitro* on the capability of dendritic cells to stimulate antigen-specific T-cell proliferation or production of IFN- γ (CD4+) or granzyme B (CD8+) by T cells (ibid.), suggesting that D-2HG does not impair antigen processing or presentation by dendritic cells. However, Ugele et al. later reported that D-2HG affects the activation and maturation of human monocyte-derived dendritic cells (Ugele et al. 2019): CD83 expression after lipopolysaccharides (LPS) stimulation was reduced in presence of D-2HG, as was IL-12 secretion. Mechanistically, they showed that D-2HG altered LPS-induced metabolic changes and increased oxygen consumption (ibid.). Friedrich et al. subsequently reported

that IDH-m can impair the microenvironmental education of dendritic cells *in vivo* in a murine model, leading to dysfunctional immature dendritic cells with poor antigen presentation capacity (Friedrich, Hahn, et al. 2023). Consistent with these findings, Hammon et al. also reported that D-2HG impairs human but not murine dendritic cell differentiation, leading to a more tolerogenic phenotype with decreased expression of MHC II and function (IFN- γ and IL12 secretion), thus reducing T cell stimulation and favoring the immune escape of AML cells (Hammon et al. 2024). Contrary to prior observations in T cells (Notarangelo Science 2022), treatment with D-2HG accelerated glucose metabolism (evidenced by lower glucose and higher lactate levels in culture supernatants) and led to an increase of LDH subunit A expression. Additionally, a 7-day D-2HG treatment also increased the basic oxygen consumption (routine respiration) of dendritic cells (ibid.). Importantly, the authors reported delayed DNA demethylation during differentiation of monocytes to dendritic cells upon D-2HG treatment, at loci that normally become demethylated during differentiation (ibid.). Intriguingly, however, reactivation of TET2 with vitamin C restored DNA demethylation and oxygen consumption but did not alter lactate levels or MHC II antigen expression.

1.4.2.4 Effects of D-2HG in TAMs

Friedrich et al. provided evidence that D-2HG also impairs the functions of TAMs. They co-cultured human T lymphocytes with D-2HG pretreated monocytes or macrophages and observed a dose-dependent suppression of T cell proliferation (Friedrich, Sankowski, et al. 2021). They reported a dose-dependent downregulation of HLA-DR and the costimulatory ligands CD80, CD86 by macrophages following D-2HG treatment, suggesting an alteration in antigen presentation capacity. This effect was shown to be mediated by the induction of L-tryptophan uptake and its conversion into L-kynurenine, which acts as an endogenous ligand of the aryl-hydrocarbon receptor (AHR). The activation of this receptor leads to increased secretion of the anti-inflammatory cytokine interleukin-10 and transforming growth factor- β (ibid.). On the other hand, Han et al. studied the effects of D-2HG on murine microglia (both immortalized BV2 and primary cells) (C.-J. Han et al. 2019). They showed that cell permeable octyl-2HG (1 mM) suppresses proinflammatory responses. Specifically, they observed that this compound inhibited LPS-induced nuclear translocation of the p65 subunit of NF- κ B and NF- κ B transcriptional activity. They hypothesized that activation of AMPK and subsequent inhibition of mammalian target of rapamycin (mTOR) signaling contribute to this inhibitory effect (ibid.).

1.4.2.5 Effects of D-2HG in non-immune cells

A recent study by Wang et al. showed no significant impact of D-2HG on endothelial cell growth (Xiaomin Wang et al. 2022). However, D-2HG enhanced the mobility and the lumen-forming ability of these cells *in vitro*. Consistent observations were made *in vivo*, where a higher intra-tumoral blood vessel intensity was reported after inoculation of IDH-m GL261 cells compared to IDH-wt GL261 cells, both in immunocompetent and immune-deficient mice (ibid.). Mechanistically, they showed that the influx of D-2HG into endothelial cells promotes mitochondrial $\text{Na}^+/\text{Ca}^{2+}$ exchange, which in turn fuels mitochondrial respiration, allowing a rapid production

of ATP (*ibid.*). ATP hydrolysis then facilitates the remodeling of the actin cytoskeleton necessary for changes in cell mobility. However, contradictory observations were subsequently reported by others, who noted a reduced micro-vessel density in IDH-m tumors, along with a decrease in endothelial cell migration and proliferation due to D-2HG (Cao et al. 2023). Regarding the effects on platelets, D-2HG has been reported to inhibit platelet aggregation and blood clotting through a calcium-dependent, methylation-independent mechanism (Unruh et al. 2016).

Direct effects of D-2HG on astrocytes and neurons have been little studied so far. Ravi et al. showed that the inoculation of IDH-m glioma cells into human neocortical sections or treatment with D-2HG leads to a transcriptional shift towards inflammation in astrocytes (V. M. Ravi et al. 2022). This was however found to be mediated by myeloid cell polarization rather to a direct effect of D-2HG on astrocytes (*ibid.*). They also reported an increased neuronal activity and changes in local field potentials after D-2HG treatment (V. Ravi et al. 2021). Indeed, previous studies also noted that D-2HG may promote epileptogenesis by co-opting glutamate activity on the N-methyl-D-aspartic acid (NMDA) receptor (H. Chen et al. 2017) and by modifying the metabolic profile of neurons through the upregulation of mTOR signaling (Mortazavi et al. 2022).

1.4.3 Role of D-2HG in inflammation

Strikingly, de Goede et al. found that 2HG is one of the most significantly increased immune metabolites following LPS stimulation (100 ng/ml) in both mouse and human macrophages, with D-2HG being the most prevalent enantiomer (Goede et al. 2022). This finding was confirmed by others (Williams et al. 2022). The study reported that D-2HG is induced at later time points (24 hours), coinciding with the transition from an inflammatory state toward resolution (Goede et al. 2022; Williams et al. 2022). The increase in D-2HG followed the induction of the immune-responsive enzyme HAT and was accompanied by a decrease in the expression of D2HGDH, which converts D-2HG back into 2-OG (Goede et al. 2022), see Figure 1.5.

Supporting these observations and a potential role of D-2HG during the resolution of inflammation, Han et al. had shown that a pre-treatment of microglia (BV-2 or murine primary microglia) with 2HG suppresses the expression of proinflammatory genes after LPS stimulation (C.-J. Han et al. 2019). They found that 2HG impairs the LPS-induced phosphorylation of I κ B kinase α/β (IKK α/β), I κ B α and p65, as well as the degradation of I κ B, and the nuclear translocation of the p65 subunit of NF- κ B, ultimately decreasing the transcriptional activity of NF- κ B (*ibid.*). The authors suggested that the activation of AMPK, leading to the inhibition of mTOR signaling, contributes to the observed inhibitory effect of 2HG on the NF- κ B signaling pathway in BV-2 cells (*ibid.*).

Besides, TET2 was shown to be upregulated upon various inflammatory stimuli in microglia cells, where it regulates early gene transcriptional changes, leading to metabolic alterations, as well as a later inflammatory response (Carrillo-Jimenez et al. 2019). Given that D-2HG competitively inhibits TET enzymes, it could also modulate this mechanism of response to inflammatory stimuli.

Chapter 2

Statement of the problem

2.1 Rationale and working hypothesis

Although IDH-m gliomas have a better prognosis compared to IDH-wt glioblastomas, nearly all patients experience relapse. Furthermore, these tumors develop resistance to standard-of-care therapies, and patients ultimately succumb to tumor progression. A deeper understanding of the mechanisms governing tumor initiation and progression is critical for developing novel and effective therapeutic strategies for these tumors. The TME is increasingly recognized as a key driver of tumor progression and therapeutic response. The characterization of the immune TME has led to the development of immunotherapies that are highly effective in some cancers, but these approaches have shown disappointing results in gliomas. This is in line with the fact that gliomas exhibit a cold immune TME, characterized by a scarcity of T cells and an abundance of myeloid cells, primarily TAMs. Indeed, these cells constitute up to 40% of the tumor mass and play roles in immunosuppression, thus favoring tumor progression.

TAMs are plastic cells, with their phenotype and immune responses shaped by the TME. While microglial cells are highly abundant in IDH-m gliomas, the effects of this particular environment on their transcriptional programs and cell states remain largely unknown. We hypothesized that the high levels of D-2HG released into the TME by IDH-m glioma cells could reshape the DNA methylome of myeloid cells by disrupting TET-mediated DNA demethylation, as opposed to the non-epigenetic effects observed in other immune cells within TME. To address this issue, a former PhD student conducted an *ex vivo* study aimed at characterizing the DNA methylome and transcriptome of CD11B+ myeloid cells isolated from a large series of IDH-m and IDH-wt gliomas for comparison. Although the CD11B+ cells in IDH-m gliomas displayed a striking bias towards hypermethylation, similar to IDH-m cells, only limited changes linked to gene expression were observed. Furthermore, it remained unclear whether these results reflect differences in the composition of the myeloid compartment between IDH-m and IDH-wt gliomas, as it is known that the former are enriched in TAM-MGs while the latter contain a higher proportion of TAM-MDMs.

On the other hand, while TET-mediated demethylation at enhancer regions occurs during the differentiation of monocytes to macrophages, prior studies demonstrated that D-2HG affects the metabolism of infiltrating macrophages through non-epigenetic mechanisms. We reasoned that resident microglia, which are expected to be chronically exposed to this oncometabolite from tumor initiation in IDH-m

gliomas, could readily undergo the DNA methylome changes observed *ex vivo*. Considering the roles of both D-2HG and TET-mediated demethylation at enhancer regions in macrophages upon activation, I reasoned that epigenetic priming of microglia induced by D-2HG could explain the longstanding hyporesponsive phenotype of these cells observed in IDH-m gliomas. Specifically, I aimed to determine the impact of D-2HG on the methylome of these cells as well as its potential consequences for microglial function.

2.2 Objectives

2.2.1 *Ex vivo* study

Our first objective was to **evaluate the effect of the IDH mutation on DNA methylation of TAMs**, and its impact at the transcriptomic level, while excluding differences due to cell composition. To achieve this goal, we proposed:

a) Comparing the DNA methylome (EPIC arrays) and transcriptome (RNA-Seq) of CD11B+ cells purified by magnetic cell sorting from IDH-m gliomas with CD11B+ cells from non-tumor brain tissues, both predominantly composed of microglial cells.

b) Considering the potential impact of DNA methylation on distal enhancer elements, we also proposed extending the analysis to these regulatory regions. Specifically, we aimed to identify transcription factor binding motifs affected by hypermethylation and infer their potential impact on the expression of target genes.

c) Additionally, since the methylome profiling method used does not discriminate 5hmC from 5mC, which could provide valuable insights into impaired TET function, I aimed to validate global levels of these epigenetic modifications using LC/MS in CD11B- (glioma cells) and corresponding CD11B+ (myeloid cells) fractions isolated from another series of IDH-m gliomas and non-tumor brain tissues.

2.2.2 *In vitro* study

My second objective was to **ascertain the direct effect of D-2HG on the DNA methylome of human microglial cells**, and evaluate its consequences on the response to LPS inflammatory stimulation. Prior circumstantial evidence suggested effects of D-2HG and roles of TET in microglial function, but these studies were conducted on primary and/or immortalized murine cells. Given the importance of excluding potential interspecies differences to draw accurate conclusions, my first goal was to establish primary human microglia cultures. Once I confirmed the functionality of these cultures, my aims were to:

a) Evaluate the uptake of non-permeable D-2HG by these cells using LC/MS and fluorimetric assays, and verify whether it reaches comparable levels exhibited by *bona fide* IDH-m cells. Next, I aimed to assess the inhibition of TET enzymatic activity and function by analyzing global levels of 5mC and 5hmC using LC/MS.

b) Determine the extent of D-2HG-driven methylome changes using EPIC arrays, followed by a more comprehensive analysis of 5mC and 5hmC levels at enhancers using a single-nucleotide resolution approach.

c) Examine how D-2HG-treated microglia respond to LPS stimulation, specifically by evaluating cytokine expression and mitochondrial respiration.

2.2.3 D-2HG depletion

Finally, we aimed to **investigate the impact of D-2HG depletion on the microglial response in IDH-m glioma**. To achieve this, we leveraged snRNA-Seq data of a paired IDH-m glioma sample we collected before and after treatment with the IDH-m inhibitor ivosidenib, which was administered in our institution.

Chapter 3

Results

The results of this research work, along with a detailed description of the experiments and analyses, are presented in the article reproduced in the following section. This work has already been published as a preprint (bioRxiv) and is currently under review:

<https://www.biorxiv.org/content/10.1101/2024.08.23.608811v1.abstract>

This work was accepted for oral presentation at the Congress of the European Association of Neuro-Oncology (EANO), held in Glasgow (UK) in October 2024. The abstract is reproduced in the Appendix A (page 141).

The Appendix B (page 143) also includes four review articles in connection with this PhD to which I made major contributions, as well as abstracts of articles where I am co-author (Appendix C, page 209), all written during the course of my PhD.

Notice

I contributed to completing the *ex vivo* study in close collaboration with Pietro Pugliese (co-first author). In parallel, I carried out the entire *in vitro* study to test the hypothesis regarding the effect of D-2HG on the DNA methylation landscape of microglial cells, as observed in IDH-m gliomas. Additionally, I set up a pipeline for the bioinformatics analyses of the methylation and transcriptomic data generated from *in vitro* experiments. The data reported in the article were reprocessed by Pietro Pugliese to formally ensure the accuracy of my analyses. Further *in vitro* validations, primarily Seahorse and RT-qPCR, were completed by a team engineer, Sarah Scuderi, while I had returned to working full-time at the hospital. To complete these analyses, I secured 12 k€ in funding from the Assistance Publique-Hôpitaux de Paris.

The oncometabolite D-2-hydroxyglutarate promotes DNA hypermethylation at lineage-specific enhancers controlling microglial activation in IDH^{mut} gliomas

Alice Laurence^{1,2*}, Pietro Pugliese^{1*}, Quentin Richard¹, Bertrand Mathon³, Stéphanie Jouannet¹, Yvette Hayat¹, Sarah Scuderi¹, Laurent Capelle^{3†}, Pauline Marijon³, Karim Labreche¹, Agustí Alentorn^{1,2}, Maïté Verreault¹, Ahmed Idbaih^{1,2}, Cristina Birzu^{1,2}, Emmanuelle Huillard¹, Nina Pottier¹, Aurore Desmons⁴, Inès Fayache⁴, Garrett A. Kaas⁵, Philip J. Kingsley⁶, Lawrence J. Marnett⁷, Eric Duplus⁸, Elias El-Habr⁹, Lucas A. Salas¹⁰, Karima Mokhtari^{1,11}, Suzanne Tran^{1,11}, Mehdi Touat^{1,2}, Franck Bielle^{1,11}, Mario L. Suvà^{12,13}, Antonio Iavarone¹⁴, Michele Ceccarelli¹⁵, Michel Mallat¹, Marc Sanson^{1,2,16}, Luis Jaime Castro-Vega¹

¹Sorbonne Université UMR5175, CNRS UMR7225, Inserm U1127, ICM - Paris Brain Institute, F-75013 Paris, France; Équipe Labellisée Par La Ligue Nationale Contre Le Cancer.

²Service de Neuro-Oncologie, AP-HP, Hôpital Pitié-Salpêtrière, F-75013 Paris, France.

³Department of Neurosurgery, AP-HP, Hôpital Pitié Salpêtrière, F-75013 Paris, France.

⁴Clinical Metabolomic Department, AP-HP, Hôpital Saint Antoine, Sorbonne Université, Paris, France.

⁵Division of Genetic Medicine, Vanderbilt University Medical Center, Nashville, TN, USA.

⁶Department of Biochemistry, Vanderbilt University, Nashville, TN, USA.

⁷Departments of Biochemistry, Chemistry, and Pharmacology, Vanderbilt Institute of Chemical Biology, Vanderbilt-Ingram Cancer Center, Vanderbilt University School of Medicine, Nashville, TN, USA.

⁸Sorbonne Université, IBPS, CNRS UMR8256, INSERM ERL1114, Biological Adaptation and Aging, Paris, France.

⁹Sorbonne Université, IBPS, CNRS UMR8246, Inserm U1130, Neuroscience Paris Seine Laboratory, Paris, France.

¹⁰Geisel School of Medicine at Dartmouth, Dartmouth Cancer Center, Lebanon, NH, 03756, USA.

¹¹Department of Neuropathology, AP-HP, Hôpital Pitié Salpêtrière, F-75013 Paris, France.

¹²Department of Pathology and Krantz Family Center for Cancer Research, Massachusetts General Hospital and Harvard Medical School, Boston, MA, 02114, USA.

¹³Broad Institute of Harvard and MIT, Cambridge, MA 02142, USA.

¹⁴Department of Neurological Surgery and Department of Biochemistry, Sylvester Comprehensive Cancer Center, University of Miami Miller School of Medicine, Miami, FL, USA.

¹⁵Department of Public Health Sciences and Sylvester Comprehensive Cancer Center, University of Miami Miller School of Medicine, Miami, FL, USA.

¹⁶Onconeurotek Tumor Bank, AP-HP, Hôpital Pitié-Salpêtrière, F-75013 Paris, France.

*These authors contributed equally to this work

†Dr. Laurent Capelle passed away in June 2023. This work is dedicated to his memory.

Corresponding authors:

Marc Sanson, M.D., Ph.D.

Email address: marc.sanson@aphp.fr

Genetics & Development of Brain Tumors

ICM - Paris Brain Institute, 75013, Paris, France

Luis J. Castro-Vega, M.D., Ph.D.

Email address: luis.castrovega@icm-institute.org

Genetics & Development of Brain Tumors

ICM - Paris Brain Institute, 75013, Paris, France

Summary

Tumor-associated macrophages and microglia (TAMs) are highly abundant myeloid cells in gliomas, with their phenotype and immune response determined by ontogeny and microenvironment. TAMs display distinctive transcriptional programs according to the IDH mutation status but the underlying regulatory mechanisms remain largely unknown. Herein, we uncover that CD11B⁺ myeloid cells in human IDH^{mut} gliomas exhibit DNA hypermethylation predominantly at distal enhancers. This hypermethylation was linked to decreased expression of genes involved in inflammatory responses and glycolytic metabolism, and the inactivation of transcription factors that regulate microglial responses to environmental stimuli. Prolonged exposure of human primary microglia to D-2-hydroxyglutarate (D-2HG) inhibited TET-mediated 5mC oxidation, resulting in a reduced accumulation of global 5hmC levels. We confirmed high 5mC/5hmC ratios at lineage-specific enhancers, by analyzing CpGs at single-base resolution. D-2HG-treated microglia show reduced proinflammatory capacity and enhanced oxidative phosphorylation, consistent with the remodeled enhancer landscape. Conversely, depletion of D-2HG following treatment of a glioma patient with an IDH mutant inhibitor was associated with enhanced microglial responses, as assessed by snRNA-seq. Our findings provide a mechanistic rationale for the hyporesponsive state of microglia in IDH^{mut} gliomas and support the concept that oncometabolites may disrupt the function of immune cells residing in the tumor microenvironment.

Keywords: D-2HG, 5mC, 5hmC, Glioma, TAMs, IDH mutation, Tumor Microenvironment

Introduction

Diffuse gliomas are the most frequent malignant primary brain tumors and are refractory to standard therapies¹. A high proportion of these tumors bear an IDH mutation, which confers a neomorphic ability to convert α -ketoglutarate (α -KG) to (D)-2-hydroxyglutarate (D-2HG)². It is believed that D-2HG drives cellular transformation by inhibiting α -KG-dependent dioxygenases, including the TET family of DNA demethylases, KDMs histone demethylases, and FTO/ALKBH RNA demethylases, ultimately leading to widespread epigenomic dysregulations and blocking of cell differentiation³. Much less is known about the tumor cell-extrinsic effects of this oncometabolite, which accumulates in the tumor microenvironment (TME)^{4,5}. Emerging evidence indicates that D-2HG released by IDH^{mut} cells suppresses T cells and impairs the metabolism of infiltrating macrophages, dendritic cells, and CD8⁺ T cells by non-epigenetic mechanisms⁶⁻¹⁰. It remains to be determined whether D-2HG is able to reshape the epigenetic landscape of the TME, particularly in resident microglia, which are abundant in IDH^{mut} gliomas and are exposed to this oncometabolite from tumor initiation.

Tumor-associated macrophages and microglia (TAMs) represent almost 40% of the tumor mass and play critical roles in tumor progression¹¹. As such, these cells may represent prognostic biomarkers and therapeutic targets^{12,13}. TAMs are plastic cells, with their phenotype and immune response determined by both ontogeny and microenvironment^{14,15}. Previous studies in IDH^{wt} glioma models uncovered that resident microglia and monocyte-derived macrophages (MDMs) display distinctive transcriptional and chromatin landscapes¹⁶. Transcriptional differences have also been observed in the myeloid compartment of gliomas as a function of the IDH mutation status^{17,18}. In IDH^{wt} tumors, MDMs and microglial cells exhibit expression changes associated with activation, including high expression of MHC class genes¹⁷. On the other hand, in IDH^{mut} gliomas, these cells display a hyporeactive phenotype similar to that of homeostatic microglia in non-tumor tissues¹⁷.

The relative proportion of MDMs and microglial cells differs according to the IDH^{mut} status¹⁷⁻²¹ and/or tumor grade^{22,23}. Glioma progression entails a process of cellular competition, wherein infiltrating macrophages overtake the niche occupied by resident microglia^{24,25}. Recent single-cell RNA-seq studies of the myeloid compartment in human gliomas have further unveiled subsets of MDMs with mesenchymal-like, lipid, and hypoxic/glycolytic signatures, as well as subsets of inflammatory and oxidative phosphorylation (OXPHOS)-related microglia^{20-22,24,26}, some of which have been associated with clinical outcomes. Additionally, it has been reported that myeloid cells express superimposed immunomodulatory activity programs, irrespective of the ontological origin²³. The epigenetic changes, i.e., DNA methylation, that drive the transcriptional programs and cell states of TAMs in human glioma, and the effects of tumor-derived signals on the TAM methylome, remain largely uncharacterized.

Inhibition of TET-mediated demethylation by D-2HG in tumor cells accounts for DNA hypermethylation characteristic of IDH^{mut} gliomas²⁷. Considering the elevated concentrations of this oncometabolite in the TME and its uptake by myeloid cells^{9,28}, we hypothesized that such a mechanism could be also at play in CD11B⁺ myeloid cells of these tumors, thus contributing to both epigenetic intratumoral heterogeneity and altered immune functions. Herein, to investigate whether and how TAMs in IDH^{mut} gliomas display functional DNA methylation changes, we first profiled the bulk transcriptome and methylome of CD11B⁺ myeloid cells isolated from a well-characterized series of human gliomas and non-tumor tissues. Our findings reveal that myeloid cells in IDH^{mut} tumors exhibit DNA hypermethylation at enhancer elements that regulate gene networks involved in microglia activation. We demonstrate the direct effects of D-2HG on TET-mediated DNA demethylation at lineage-specific enhancers in primary cultures of human microglia, thereby providing a mechanistic foundation for the hyporesponsive behavior of these cells in IDH^{mut} gliomas. These results have implications for therapeutics aimed at inhibiting the IDH mutant enzyme or repolarizing TAMs.

Results

Study design

To determine the mechanistic underpinnings of TAM phenotype linked to the IDH status, we analyzed bulk DNA methylome and/or transcriptome of CD11B⁺ myeloid cells isolated by magnetic sorting from adult-type human diffuse gliomas (n=36) comprising IDH^{wt}, IDH^{mut} oligodendrogliomas and IDH^{mut} astrocytomas. In addition, we analyzed available methylome data of CD11B⁺ cells from normal brains, isolated using a similar method and profiled with the same technology²⁹ (Fig. 1a). To adjust for potential confounding variables, samples were matched by age and sex while being fully characterized for their clinical, pathological and genetic features (Supplementary Table 1). The contamination of CD11B⁺ fractions by tumor cells was assessed by analysis of IDH1 R132H or TERT C228T/C250T promoter mutations through droplet digital PCR (ddPCR) and further verified by RNA-seq-based analysis of IDH variant allelic frequency (Extended Data Fig. 1a and 1b). The estimated purity of the CD11B⁺ samples included in downstream analyses reached ~95%. This analysis rules out the possibility that TAMs from our study cohort harbored the IDH1 R132H mutation to a significant extent, as previously reported³⁰.

CD11B⁺ myeloid cells in human IDH^{mut} gliomas display global DNA hypermethylation

To confirm the DNA methylation status of the cohort in relation to the IDH mutation, we first profiled glioma cell-enriched CD11B⁻ fractions isolated from both IDH^{wt} and IDH^{mut} tumors (n=17, Supplementary Table 1) using MethylationEPIC (EPIC) arrays. Analysis of methylation levels across all probes targeting CpG sites confirmed that IDH^{mut} tumors display global hypermethylation, yet with a high degree of heterogeneity as previously reported³¹⁻³³ (Extended Data Fig. 2a and 2b). In total, there were 49,676 differentially methylated CpG sites (absolute $\Delta\beta > 0.2$, FDR < 0.05), of which 92.5% were hypermethylated in IDH^{mut} compared with IDH^{wt} glioma samples (Extended Data Fig. 2c). The distribution per functional genomic region revealed a high proportion of hypermethylated CpGs located in regulatory regions. These regions encompass promoters, defined as constant genomic regions within a distance of -1.5 kb to +0.5 kb respect to transcription start site (TSS), and enhancers,

defined as distal regulatory elements associated with FANTOM robust promoters within a range of up to 500 kb (FDR < 1e-5; Pearson's correlation), as outlined by the FANTOM5 consortium³⁴. Our analysis confirms that enhancers are particularly sensitive to hypermethylation in IDH^{mut} glioma cells³⁵ (Extended Data Fig. 2c and 2d).

We then looked for methylome changes in the fraction of CD11B+ myeloid cells isolated from gliomas (n=26) and from normal brain tissues (n=6) (Supplementary Table 1). Principal component analysis (PCA) revealed a distinct segregation of myeloid cells based on both tissue origin and IDH mutation status in component 1, which accounted for 48% of the variance (Fig. 1b). Despite the substantial heterogeneity of methylome data in CD11B+ samples from IDH^{mut} tumors, we found 37,198 differentially methylated CpG sites (absolute $\Delta\beta > 0.2$, FDR < 0.05) when compared with CD11B+ cells from IDH^{wt} gliomas (Fig. 1c). Strikingly, similar to what was observed in glioma cells, CD11B+ samples from corresponding IDH^{mut} tumors exhibited a bias towards hypermethylation, particularly in regulatory regions (Fig. 1c). It is known that IDH^{wt} glioblastomas are enriched in MDMs, whereas the TME of IDH^{mut} tumors is dominated by tissue-resident microglia^{17,18}. However, the asymmetric distribution of the methylation changes we observed indicates that this was not simply an effect of differences in cell composition. Indeed, global hypermethylation was also observed when comparing the DNA methylome of CD11B+ cells isolated from IDH^{mut} tumors with CD11B+ cells isolated from normal brain tissues, both predominantly composed of microglial cells (Fig. 1c). While in this comparison the number of differentially methylated CpG sites and genomic region was higher, there is a notable overlap between regulatory regions that exhibited hypermethylation in both comparisons (Fig. 1d). Of these, the number and methylation level of affected enhancers, along with their overlap between the two comparisons, were greater than those observed for promoters (Fig. 1d). Functional enrichment analyses of genes regulated by hypermethylated regulatory regions intersected in the two comparisons indicated roles in inflammatory responses such as TNF- α , IFN- γ and IL2/IL6 signaling, as well as in complement and hypoxia pathways (Fig. 1e and Supplementary Table 2).

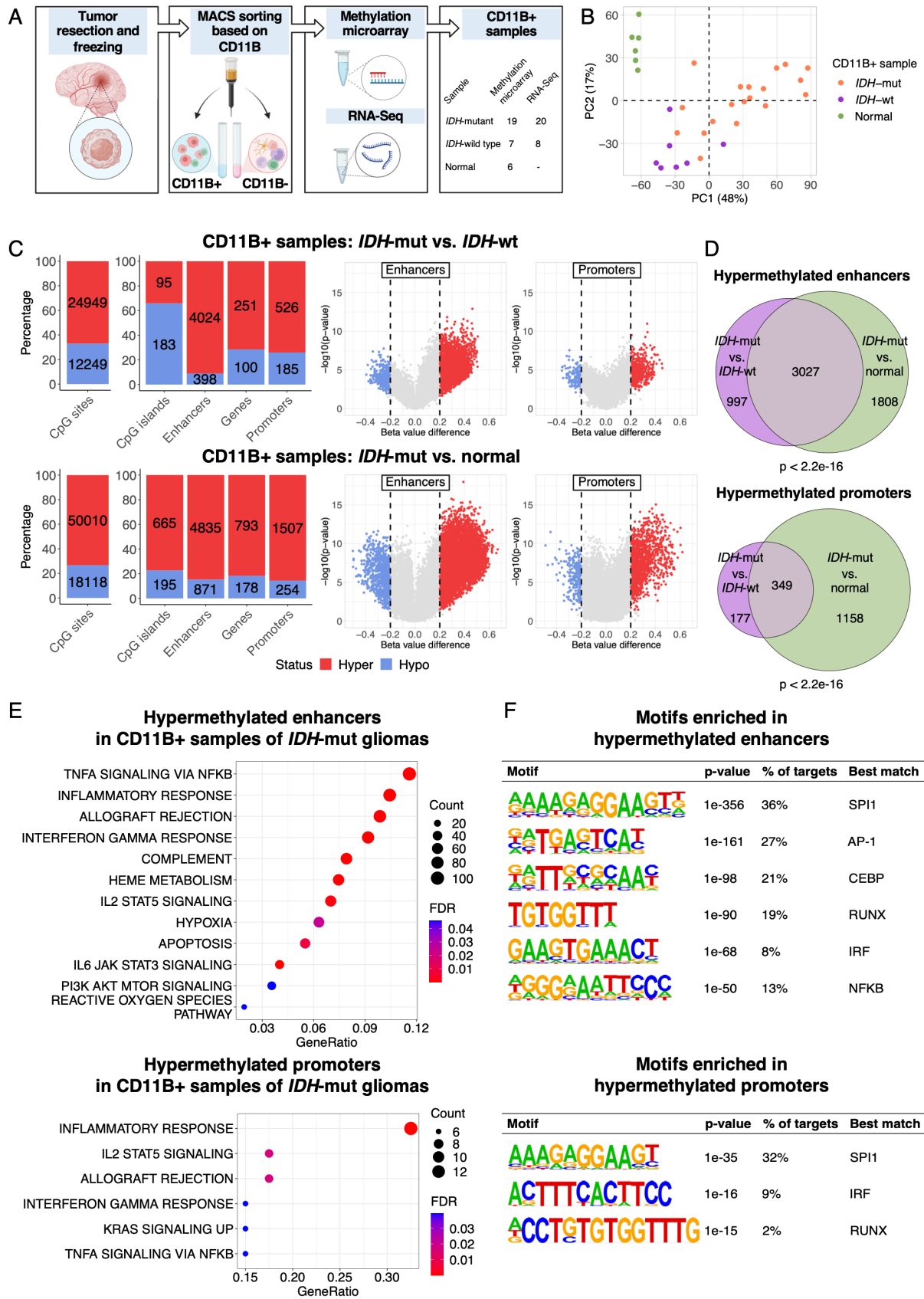


Figure 1. DNA methylome profiling of CD11B+ cells underscores hypermethylation in the myeloid compartment of IDH^{mut} gliomas. **(A)** Overview of the *ex vivo* study workflow. Tumor samples (n=36) underwent enzymatic dissociation, followed by CD11B-based magnetic sorting. DNA and/or RNA extraction was performed on both CD11B+ and CD11B- fractions for downstream analyses. Available methylome data of CD11B+ cells from six normal brains were included as controls for comparisons. Clinical, pathological, and genetic annotations of the study cohort are detailed in Supplementary Table 1. **(B)** Principal component analysis performed using methylome data from around 600,000 CpG sites across the genome in CD11B+ samples from the study cohort. **(C)** Stacked bar charts (left) show absolute numbers and relative percentages of CpG sites and of four genomic regions with respect to the methylation status (absolute $\Delta\beta > 0.2$, FDR < 0.05) for the indicated comparisons. Volcano plots (right), colored by methylation status, depict the magnitude and extent of differentially methylated enhancers and promoters for the indicated comparisons. **(D)** Venn diagrams illustrate significant overlaps between hypermethylated enhancers (upper panel) or promoters (bottom panel) in CD11B+ cells from IDH^{mut} gliomas, compared to IDH^{wt} gliomas or normal brain tissues. P-values were computed using over-representation analysis (ORA). **(E)** Bubble plots indicate the hallmark gene sets enriched in the lists of genes exhibiting hypermethylated enhancers (n=3027) and promoters (n=349) in CD11B+ samples from IDH^{mut} gliomas in comparison to CD11B+ samples from IDH^{wt} gliomas and normal brain tissues (Fig. 1D). The size and color code of each dot indicate the number of genes with significant enrichment for the indicated categories (FDR < 0.05). **(F)** Significant sequence motifs (ranked by p-value) enriched in hypermethylated enhancers and promoters in CD11B+ samples from IDH^{mut} gliomas, in comparison to CD11B+ samples from IDH^{wt} gliomas and normal brain tissues (Fig. 1D), were determined using HOMER.

Transcription factors (TFs) bind to specific DNA motifs on promoters and enhancers to control cell-type specific transcriptional programs, and the affinity can be modulated by the methylation status³⁶⁻³⁸. Since a substantial proportion of hypermethylation observed in CD11B+ cells from IDH^{mut} tumors involved regulatory elements in both comparisons (Fig. 1c), we sought to examine enriched TF binding motifs located within hypermethylated regulatory regions. This analysis revealed an overrepresentation of 21 motifs at 349 hypermethylated promoters and 24 motifs at 3027 hypermethylated enhancers (p-value < 10⁻¹²) (Fig. 1f). We found SPI1 (PU.1) as the most significantly enriched motif in both hypermethylated regulatory regions (36% of enhancers and 32% of promoters). Interestingly, the other top enriched motifs were bound by key TFs controlling an environment-dependent transcriptional network in microglial cells such as members of C/EBP, AP-1, RUNX, and IRF³⁹, alongside NF- κ B. Collectively, these results reveal extensive differences in the DNA methylome of TAMs as a function of the IDH mutational status.

Hypermethylation correlates with reduced expression of inflammatory regulons in CD11B+ cells from human IDH^{mut} gliomas

To investigate the transcriptome landscape of TAMs in gliomas, we performed RNA-seq on CD11B+ fractions (n=28, Supplementary Table 1). PCA indicated a good separation between samples derived from IDH^{wt} and IDH^{mut} cases (Extended Data Fig. 3a). Differential expression analysis identified 2714 genes upregulated and 1404 genes downregulated ($\log_2FC > 1$ or < -1 , respectively; $FDR < 0.05$) in TAMs from IDH^{mut} compared with those from IDH^{wt} (Supplementary Table 3). We found significant overlaps between the list of downregulated genes in our CD11B+ sample series and those reported by Klemm et al., who further discriminated the expression changes displayed by microglia and MDMs (Extended Data Fig. 3b). Noteworthy, the largest overlap occurred in downregulated genes within microglial cells from IDH^{mut} tumors, with 156 out of the 357 genes falling into this category. Furthermore, significant proportions of genes defining normal microglial signatures also intersected with the list of downregulated genes from our series of CD11B+ fractions in IDH^{mut} gliomas (Extended Data Fig. 3c). Enrichment analysis revealed that these downregulated genes are involved in proinflammatory pathways such as INF- γ/α response and IL6/JAK/STAT3 signaling, cell cycle/proliferation, hypoxia, glycolysis and the acquisition of mesenchymal-like traits (Extended Data Fig. 3d).

DNA methylation is an important mechanism of gene expression regulation. To evaluate the impact of methylation on the observed transcriptional changes in CD11B+ cells isolated from IDH^{mut} gliomas, we intersected the lists of differentially expressed genes with the lists of differentially methylated promoters or enhancers. This analysis involved 36 CD11B+ samples, with 18 of them having both data available (Supplementary Table 1). Contrary to IDH^{mut} glioma cells, where methylation and expression changes have been shown to be uncoupled^{35,40}, myeloid cells from these tumors displayed confident overlaps in the expected direction: for instance, reduced gene expression was strongly associated with hypermethylation at promoters and enhancers ($p\text{-value}=2.5e-14$ and $p\text{-value}=7.7e-18$, respectively, over-representation analysis (ORA) (quadrant IV, Fig. 2a), while the occurrence

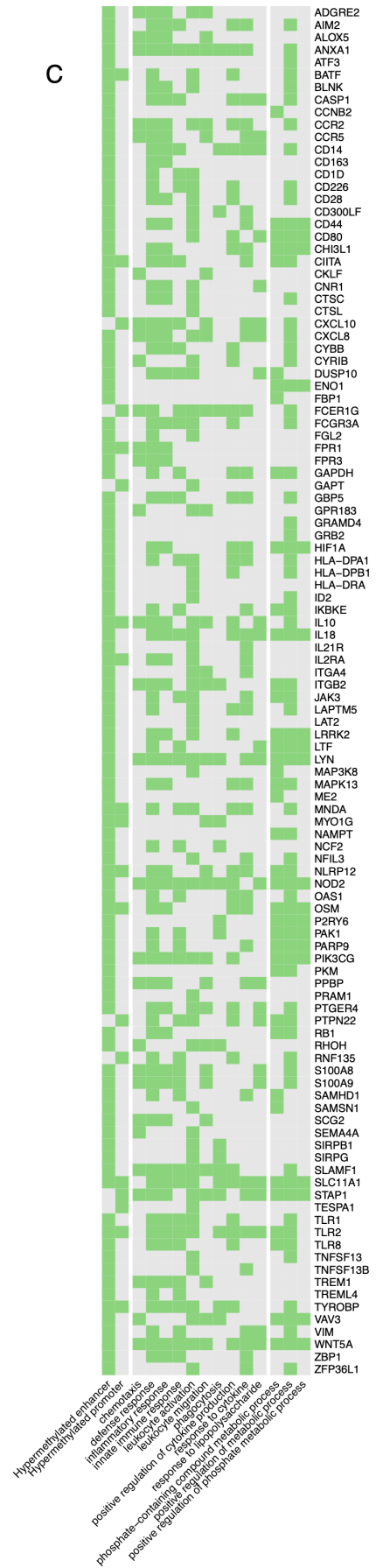
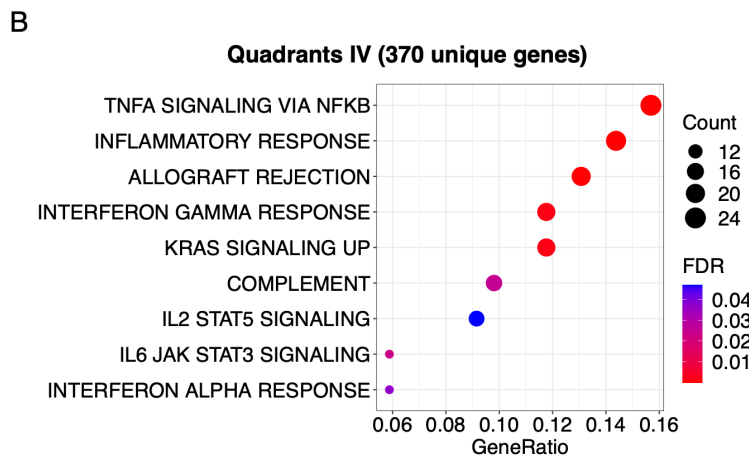
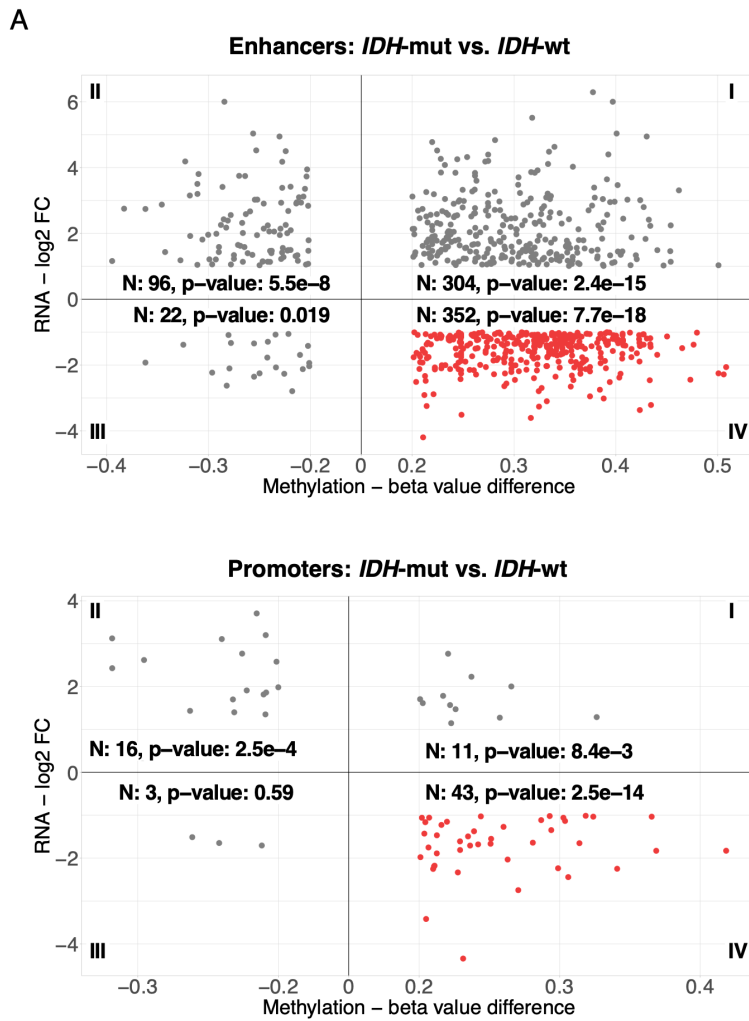


Figure 2. Integration of significant changes in the transcriptome and methylome displayed by CD11B+ myeloid cells in IDH^{mut} gliomas. (A) Cartesian diagrams represent genes (dots) exhibiting significant changes in both expression (Y-axis) and methylation (X-axis) at promoters or enhancers in CD11B+ cells from IDH^{mut} vs. IDH^{wt} gliomas. The total number of genes displaying differential methylation and expression changes is indicated for each quadrant. Over-representation of canonical methylation/expression associations (quadrants II and IV) and under-representation of non-canonical associations (quadrants I and III) were evaluated using ORA and URA, respectively. Quadrants IV (highlighted in red) indicate genes of interest exhibiting downregulation and hypermethylation at either promoters or enhancers (B) Bubble plot indicates the “hallmark gene sets” enriched in the integrative gene list (n=370) obtained by combining quadrants IV from both promoters and enhancers analyses. The size and color code of each dot indicate the number of genes with significant enrichment in the corresponding categories (FDR < 0.05). (C) The plot illustrates a subset of genes (n=110) from the integrative list that are enriched (FDR < 0.05) in Gene Ontology biological processes related to immune response and metabolism. The hypermethylation status at promoter and enhancer regions is also indicated. Positive or negative hits are represented in green or gray, respectively.

of genes showing non-canonical associations such as overexpression coupled with hypermethylation at promoters and enhancers, was lower than expected (quadrants I, Fig. 2a) (p-value=8.4e-3 and 2.4e-15, under-representation analysis (URA). This integrative analysis of methylome and transcriptome changes revealed 370 unique genes with a hypermethylated enhancer and/or promoter linked to downregulated expression in CD11B+ cells from IDH^{mut} tumors (Supplementary Table 4).

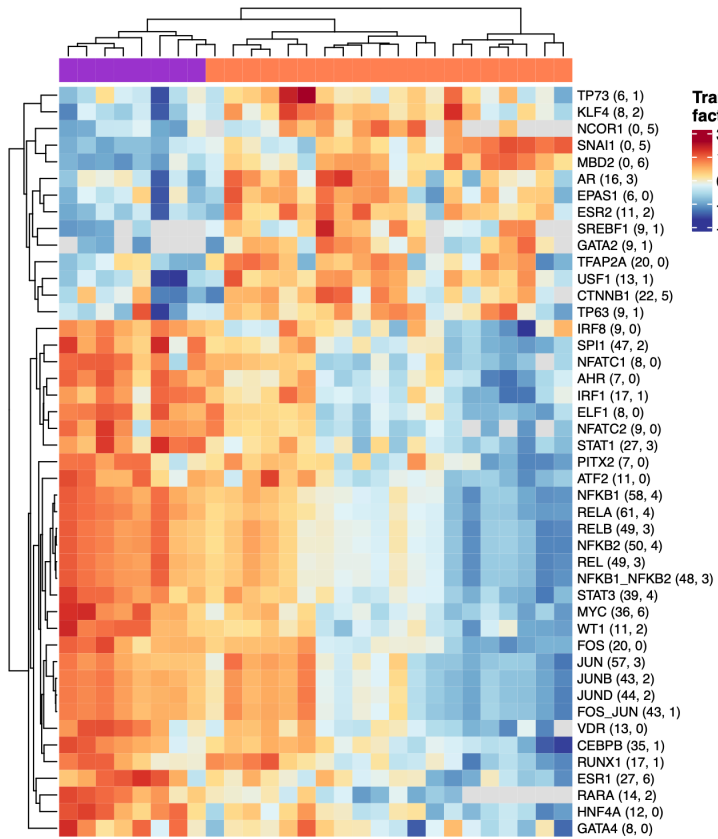
The integrative gene list contained key factors involved in TNF- α signaling via NF- κ B, IL6/JAK/STAT3 signaling, and response to IFN- γ / α (Fig. 2b and Supplementary Table 4). Biological processes such as chemotaxis, leukocyte activation, and positive regulation of metabolism also appeared enriched in this gene list (Fig. 2c). Among the genes whose downregulation was associated to hypermethylation at both regulatory regions, we found CIITA, the most important transactivator of MHC class II, the cytokine oncostatin M (OSM), and myeloid receptors such as formyl peptide receptor 1 (FPR1), and Toll-like receptor 2 (TLR2) (Fig. 2c). Hypermethylation at either promoter or enhancer together with reduced expression was observed for HLA genes, proinflammatory cytokines CXCL10, IL18, and CXCL8, chemokine receptors CCR2/5, FPR3 and TLR1/8, master regulators of glycolysis/hypoxia HIF1A, PKM, ENO1, CD44, and signaling components or enzymes

involved in cytokine production and NAD biosynthesis, such as TYROBP and NAMPT, respectively (Fig. 2c). Therefore, hypermethylation appears to affect various levels of signaling regulation within inflammatory pathways and, possibly, the activation of myeloid cells.

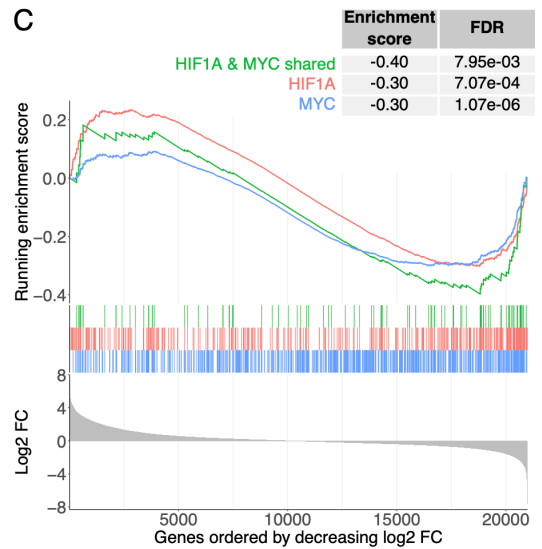
To assess the influence of DNA hypermethylation on TF binding at the enhancers highlighted in quadrants I and IV (Fig. 2a), we estimated TF activity by examining high-confidence TF-gene interactions ($n=1,209$ human TFs)^{41,42} in our RNA-seq data of CD11B+ samples. Analysis of regulons identified 45 TFs having differential activity (FDR <0.05; Wilcoxon's test) according to the IDH mutation status of corresponding tumors, with the majority of TFs showing a decreased activity in IDH^{mut} gliomas (Fig. 3a). Consistent with the binding motifs enriched in the entire repertoire of hypermethylated enhancers (Fig. 1f), this analysis emphasizes that lineage-determining and stimulus-related microglial TFs are repressed from DNA binding by methylated CpGs in CD11B+ cells from IDH^{mut} gliomas. Among these, SPI1 (PU.1), AP-1 complex (ATF2, FOS and JUN), and CEBPB, have previously been shown to be sensitive to methylation⁴³⁻⁴⁵, while NFATC2, RELA and STAT3 have been associated with microglial super-enhancers³⁹. Similar results were observed when using the whole set of hypermethylated promoters (Extended Data Fig. 4). In addition, these analyses revealed low activity of MYC and HIF1A (Fig. 3a and Extended Data Fig. 4).

On the other hand, a few TFs appeared activated in these cells, including TP63, TP73, SNAI1, CTNNB1, EPAS1/HIF2A and KLF4. In these cases, methylated CpGs could promote TF binding⁴⁶. Upon closer examination of specific TFs inactivated in CD11B+ cells from IDH^{mut} gliomas, a network inference analysis also suggests that TF-target genes implicated in inflammation and antigen presentation are effectively downregulated as a result of disrupted cooperative effects of core microglial TFs (Fig. 3b). Similarly, targets that are commonly regulated in a positive manner by both MYC and HIF1A, which play roles in the response to hypoxia and glycolysis, were more enriched than the targets regulated by each individual TF in the list of downregulated genes in CD11B+ cells from IDH^{mut} vs. IDH^{wt} tumors (Fig. 3c).

A



C



B

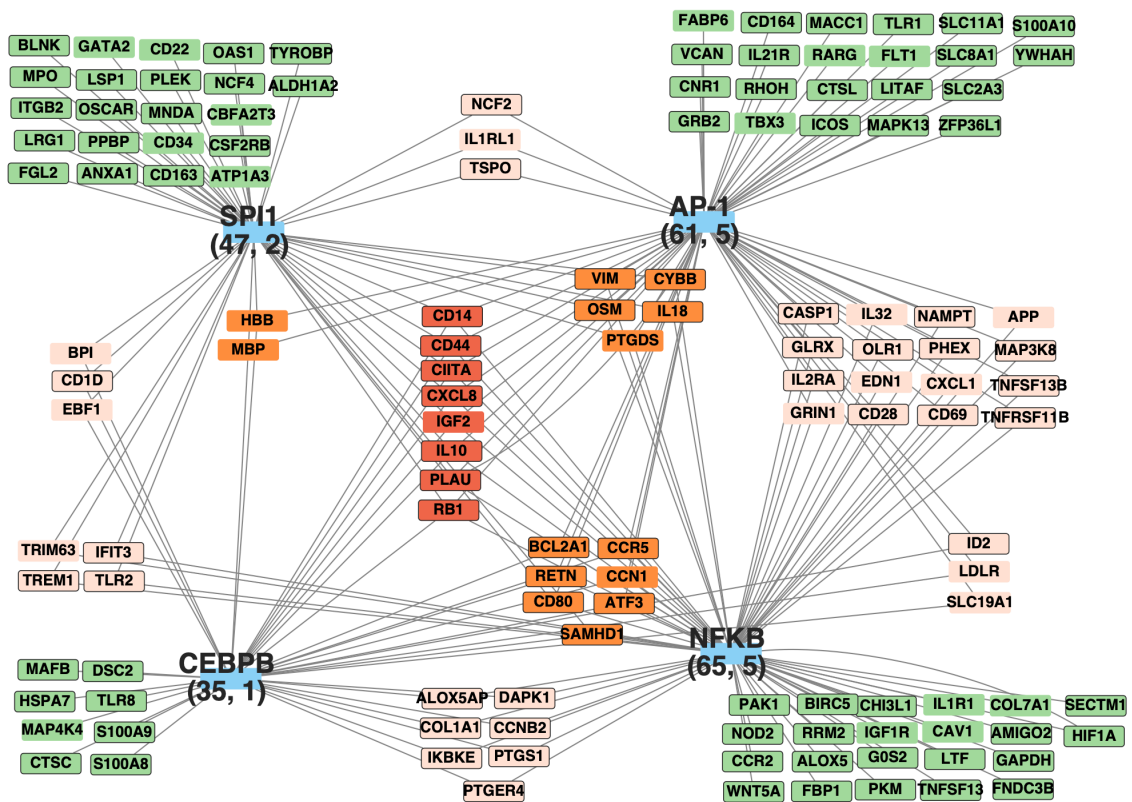


Figure 3. Gene regulatory network analysis reveals lower activity of core microglial TFs linked to hypermethylated enhancers in CD11B+ cells from IDH^{mut} gliomas. (A) The heatmap depicts TFs (n=45) exhibiting differential activity (FDR <0.05; Wilcoxon's test) in CD11B+ cells according to the IDH mutation status of corresponding tumors. The TFs targets used for this analysis, retrieved from the CollecTRI database were searched among the genes displaying upregulated/downregulated expression and hypermethylation at enhancers in myeloid cells from IDH^{mut} gliomas (quadrants I and IV, Fig. 2A). The number of targets regulated positively and negatively by each TF is indicated in brackets. Unsupervised clustering was performed using the z-scores of TF activity, where red and blue colors indicate high and low activity, respectively, and non-significant activity is colored in gray. (B) Gene regulatory network of four representative TFs (blue background) having lower activity in CD11B+ cells from IDH^{mut} compared to IDH^{wt} gliomas. TFs targets have a red, orange, pink or green background if they are controlled by four, three, two or one TF, respectively. Targets with or without black box come from quadrant I (hypermethylated enhancers and upregulated expression) or quadrant IV (hypermethylated enhancers and downregulated expression) of Fig. 2A, respectively. (C) Gene set enrichment analysis of positive gene targets of HIF1A, MYC (retrieved from CollecTRI database) and those in common between these TFs. Genes are ranked using log₂ fold change from differential expression analysis of CD11B+ samples in human gliomas (IDH^{mut}, n=14 vs. IDH^{wt}, n=8).

Of note, shared targets of these TFs involved in glycolysis (CD44, ENO1, GAPDH, HIF1A, ID2), and targets of HIF1A involved in NADH regeneration and mitochondrial function (ENO2, NAMPT, PKM, PFKFB4, SDHB) also appear in the integrative gene list (Fig. 2c). These findings were validated in published RNA-seq data of microglia and MDMs from IDH^{mut} vs. IDH^{wt} gliomas, with the most marked differences being displayed by microglia respect to MDMs (Extended Data Fig. 5). Overall, these results highlight enhancers as main targets of microenvironmental perturbations affecting microglial activation in IDH^{mut} gliomas and raise questions about the underlying mechanisms driving hypermethylation.

D-2HG inhibits TET-mediated 5mC oxidation and promotes DNA hypermethylation at lineage-specific enhancers in human microglia

We hypothesized that D-2HG, the oncometabolite produced by the IDH^{mut} glioma cells and released into the TME, could impact the DNA methylome of CD11B+ cells. Ten-eleven translocation (TET) enzymes are α -KG-dependent dioxygenases that mediate the first step of active DNA demethylation by catalyzing the conversion of 5-methylcytosine (5mC) into 5-hydroxymethylcytosine (5hmC)⁴⁷ (Extended Data Fig. 6a). Inhibition of TET-mediated DNA demethylation by D-2HG results in decreased levels of 5hmC along with increased levels of 5mC after several rounds of cell replications, ultimately establishing the G-CIMP-

high phenotype of IDH^{mut} gliomas^{27,48}. To explore whether this mechanism is at play in the myeloid cells of these tumors, we analyzed global levels of 5hmC and 5mC, as well as the cumulative cell replication history, in an independent series of CD11B+ and CD11B- fractions isolated from human gliomas, and from normal tissues used as controls (Extended Data Fig. 6b and 6c). We confirmed a higher 5mC/5hmC ratio in CD11B- cells of IDH^{mut} gliomas compared to non-tumor tissues (Extended Data Fig. 6b). Remarkably, a significant increase in 5mC/5hmC ratio was also observed in corresponding myeloid cells along with a higher cumulative number of cell divisions as indicated by epigenetic clock analysis (Extended Data Fig. 6c). These results suggest that TET inhibition contributes to the global DNA hypermethylation observed in myeloid cells (most likely microglia) from IDH^{mut} gliomas.

To ascertain the effect of D-2HG on TET-mediated DNA demethylation in human microglia, we set up primary cultures obtained from tissue aspirates of patients who underwent surgery for glioma or drug-resistant epilepsy (Fig. 4a). Microglial cells, maintained in a serum-free defined culture medium⁴⁹, are viable for up to 15 days. Over 95% of these cells express the markers ionized calcium-binding adapter molecule 1 (IBA1) and transmembrane protein 119 (TMEM119) (Fig. 4b), whereas less than 5% of cells were proliferating (KI67+) (not shown). Furthermore, these cells maintain a stable RNA-seq microglial signature over time (Extended Data Fig. 7a) and are functional, as evidenced by the proinflammatory response upon lipopolysaccharide (LPS) stimulation at 48 hours or 14 days (Extended Data Fig. 7b and 7c). To evaluate the uptake of D-2HG by human microglial cells, we measured intracellular levels after 48 hours of treatment at a concentration estimated to occur in the TME^{4,5}, which does not affect cell viability. We found that the levels of D-2HG reached by microglial cells were comparable to those observed in *bona fide* IDH^{mut} cells (Extended Data Fig. 8a and 8b, and Fig. 4c) and were sufficient to induce a significant decrease in TET enzymatic activity (Fig. 4d and Extended Data Fig. 8c). We then exposed primary microglia cultures to D-2HG for a prolonged period and observed that global levels of 5hmC in treated and control microglia have opposite trends over time, leading to a significant decrease of 5hmC levels in treated cells at 14 days (Fig. 4e and Extended Data Fig. 8d).

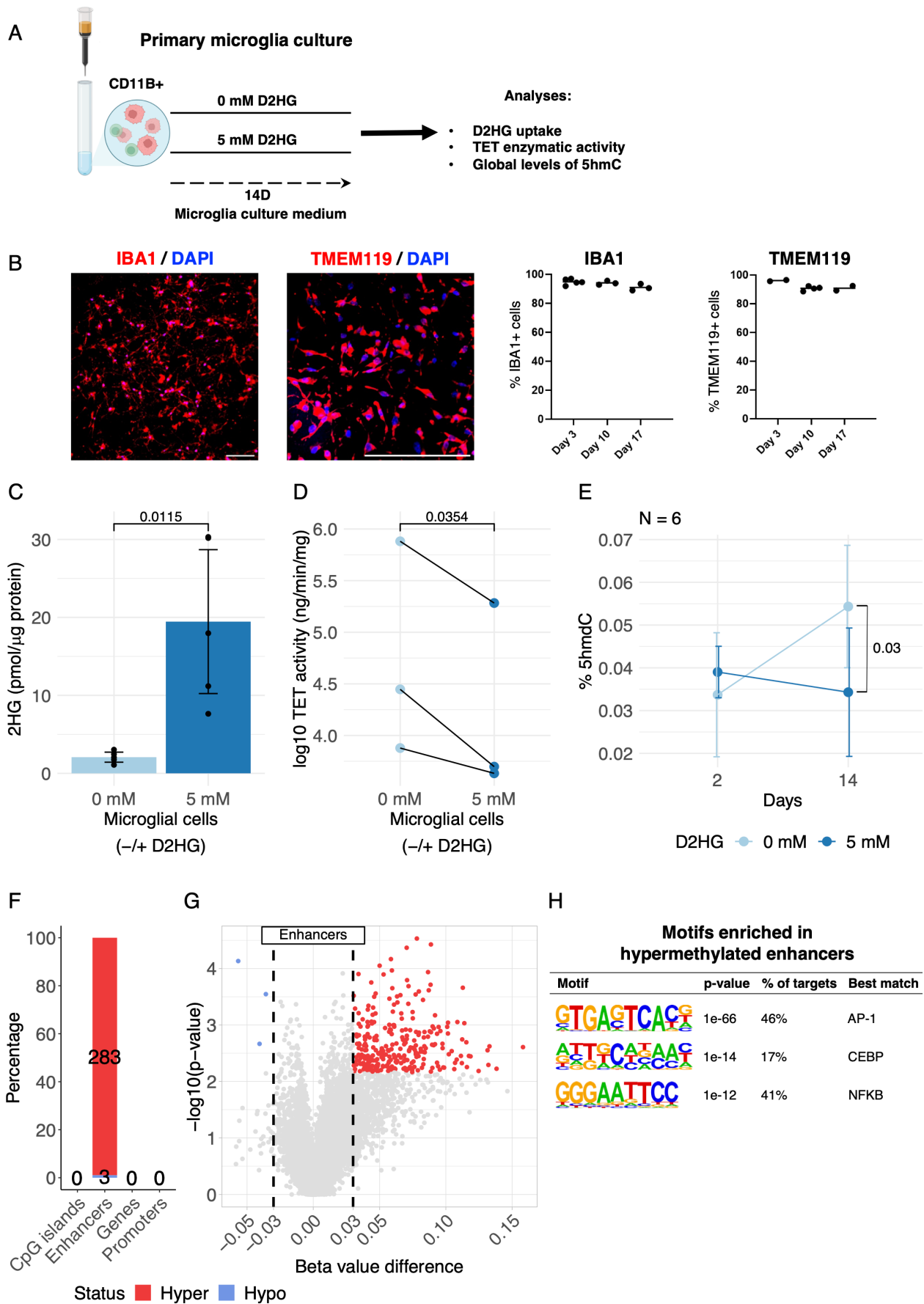


Figure 4. D-2HG uptake by human primary microglial cells inhibits TET function. **(A)** Overview of the experimental workflow for establishing primary microglia cultures treated with D-2HG, and analyses assessing the inhibition of TET-mediated DNA demethylation. The tissue collection procedures and culture conditions are thoroughly detailed in the Methods section. **(B)** Representative immunofluorescence images show the preserved expression of microglial markers TMEM119 (confocal microscopy) and IBA1 (Apotome) in primary cells at 12 days in culture (scale bars: 100 μ m). Estimated percentages of TMEM119+ and IBA1+ cells in primary cultures at different time points are indicated on the right. **(C)** The quantification of intracellular levels of 2HG was determined using LC/MS in primary human microglia obtained from five surgical aspirates with IDH^{wt} (n=2) or IDH^{mut} (n=3) status. Data are represented as the mean with a 95% CI; p-value was calculated using a one-sided paired t-test. **(D)** TET enzymatic activity measured as detection of hydroxymethylated product (ng) after 1-hour incubation of the substrate with protein extracts from microglia untreated and treated with 5 mM D-2HG over 48 hours. Primary cultures were generated from surgical aspirates with IDH^{wt} status (n=3). The p-value was calculated using one-sided paired t-test. **(E)** Assessment of global levels of 5hmC, determined by LC-MS/MS, in primary human microglia obtained from six surgical aspirates with IDH^{wt} (n=5) or IDH^{mut} (n=1) status after 48 hours and 14 days of treatment with 5 mM D-2HG (added every 2-3 days). Data are represented as the mean with a 95% CI; p-value was calculated using a one-sided paired t-test. **(F)** DNA methylation profiling of primary microglia was conducted with EPIC array. Stacked bar chart shows absolute numbers and relative percentages of functional genomic regions respect to the methylation status (absolute $\Delta\beta > 0.03$, FDR < 0.25) in D-2HG treated vs. untreated primary microglia cultured for 14 days. Samples were obtained from eight surgical aspirates with IDH^{wt} (n=5) or IDH^{mut} (n=3) status. **(G)** Volcano plot illustrates the magnitude and extent of differentially methylated enhancers in D-2HG treated vs. untreated primary microglia. **(H)** Motif enrichment analysis of hypermethylated enhancers in D-2HG-treated primary microglia. Significant sequence motifs (ranked by p-value) were determined using HOMER.

No concomitant changes in 5mC levels were observed in D-2HG-treated microglia (data not shown). These results suggest that TET-mediated demethylation in non-dividing human microglia is inhibited by D-2HG. However, contrary to the *ex vivo* situation (Extended Data Fig. 6b and 6c), the low proliferation rate of cultured microglia and the reduced time window (only 2 weeks) precluded our ability to demonstrate D-2HG-induced global hypermethylation. Nonetheless, further analysis of DNA methylome in microglial cells treated with D-2HG for 14 days, using the same EPIC array for the analysis of *ex vivo* CD11B+ cells in gliomas, revealed subtle yet reproducible hypermethylation at 283 enhancers (absolute $\Delta\beta > 0.03$, FDR < 0.25) (Fig. 4f and 4g). Importantly, these enhancers showed significant enrichment for motifs of lineage-determining and stimulus-responsive TFs as in the *ex vivo* study, including AP-1, C/EBP and NF- κ B, but not SPI1 (PU.1) (Fig. 4h).

While EPIC arrays offer sufficient coverage of enhancers, only a single probe captures methylation changes across an enhancer region⁵⁰. Moreover, this profiling method does not discriminate 5hmC from 5mC, which could provide valuable insights into impaired TET function. Considering the high turnover of DNA methylation at enhancers, which relies on TET activity rather than replicative passive dilution of 5mC⁵¹, we wondered whether D-2HG affects TET-mediated demethylation at enhancers genome-wide. To investigate this possibility, we performed a DNA methylome and hydroxymethylome profiling of microglial cells treated with D-2HG for 48 hours or 14 days. For this experiment, we used microglial preparations from normal brain tissues of three individuals with drug-resistant epilepsy to exclude tumor influences other than released D-2HG, and we applied a reduced representation and non-bisulfite sequencing approach⁵². The extensive coverage enables a more confident assessment of 5mCG and 5hmCG levels in enhancers, yet only across 20% of the enhancers analyzed with EPIC arrays, which cover ~58% of FANTOM annotated enhancers⁵⁰. Changes of 5mCG and 5hmCG levels in the entire enhancer regions were most evident at 14 days of treatment respect to 48 hours, with a marked difference for 5hmCG, reflecting its accumulation over time in D-2HG-treated cells (Fig. 5a). This result indicates that D-2HG-related changes in genomic 5hmC content, initially detected by LC-MS/MS, mostly occur in non-CpG contexts, and shows that TET function is not affected in the entire enhancers regions, at least *in vitro*. Moreover, while EPIC arrays revealed some lineage-specific enhancers that underwent hypermethylation following D-2HG treatment (Fig. 4f-4h), only a few of them were covered by the reduced representation sequencing approach.

To ascertain whether inhibition of TET-mediated demethylation by D-2HG affects a subset of lineage-specific enhancers, we pursued the following analytical strategy with our sequencing data (Fig. 5b). We aimed to use as ground truth the enhancers in CD11B+ cells from normal brain tissues, which eventually become hypermethylated in myeloid cells from IDH^{mut} gliomas, likely corresponding to microglia (Fig. 1c). Considering that the highest level of TET activity occurs around TFs binding motifs located in enhancers^{51,53}, we then focused our analysis on TFs binding motifs within hypermethylated enhancers found in both CD11B+

cells from IDH^{mut} gliomas (Fig. 1f) and D-2HG-treated microglia (Fig. 4h), potentially impacting TF occupancy (Fig. 3a and 3b).

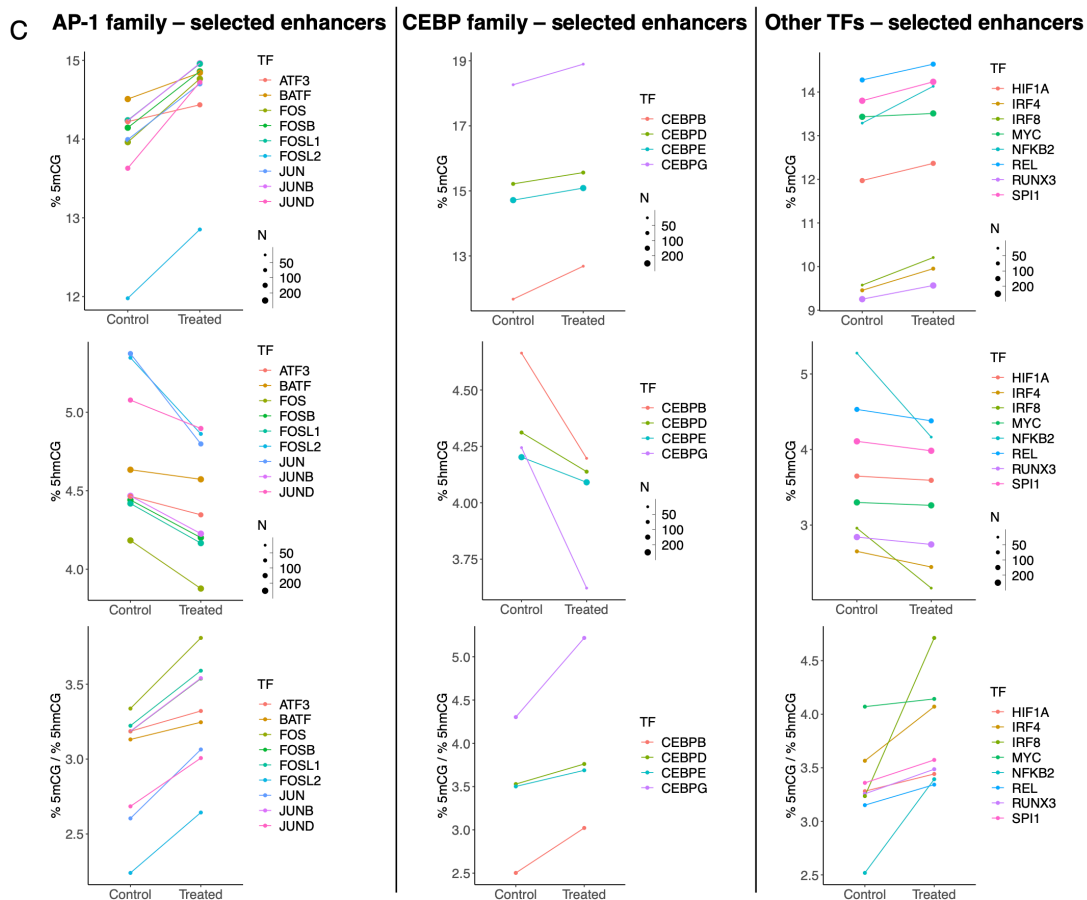
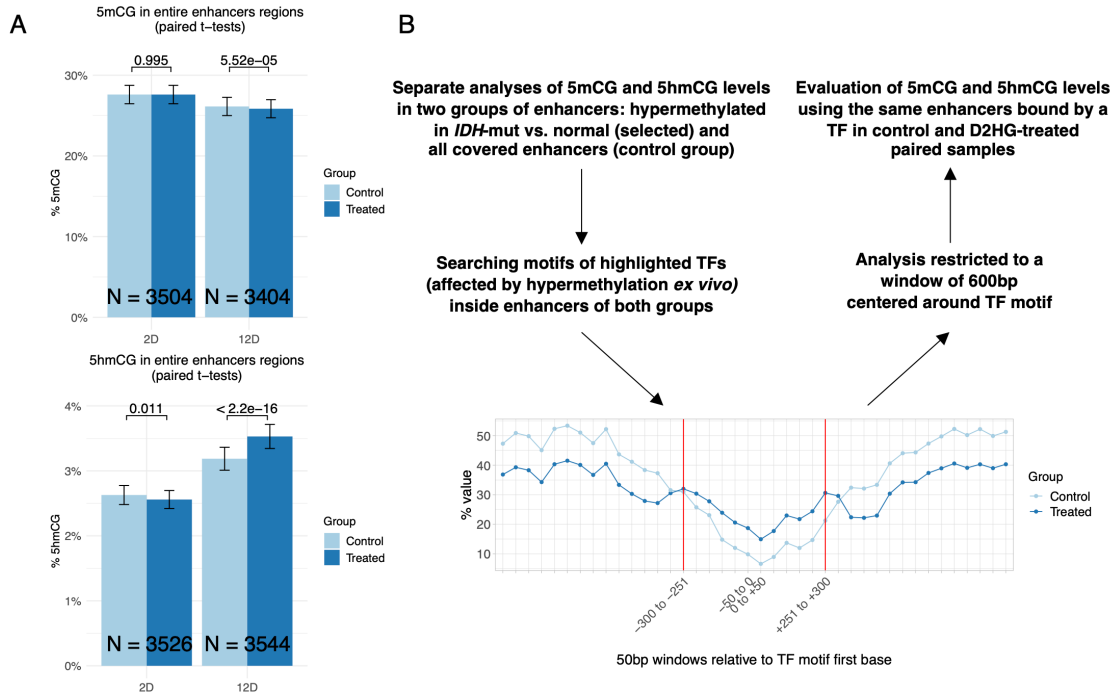


Figure 5. Reduced representation non-bisulfite sequencing reveals high 5mCG/5hmCG ratios at lineage-specific enhancers in D-2HG-treated primary microglia. (A) Bar plots show the percentages of 5mCG and 5hmCG at the whole set of covered enhancers (full-length regions) in primary human microglia treated with D-2HG for 48 hours or 14 days and in paired untreated controls. The number of paired enhancers for each comparison is indicated. Only common enhancers across patients were analyzed. **(B)** Workflow analysis of 5mCG and 5hmCG levels quantification in defined windows around TFs binding motifs, located in lineage-specific enhancers, in D-2HG-treated microglia for 14 days and in paired untreated controls. **(C)** Plots showing a separate analysis of 5mCG and 5hmC percentages (upper) around TFs binding motifs for the indicated TFs in D-2HG-treated microglia and paired untreated controls. Only common enhancers across patients were analyzed. The size of each dot indicates the number of enhancers analyzed in a paired manner between conditions. The 5mCG/5hmCG ratios (bottom), which are higher in D-2HG-treated microglia than in paired controls, are also shown. The TFs binding motifs for this analysis are located in enhancers exhibiting hypermethylation in CD11B+ cells from IDH^{mut} gliomas vs. normal brain tissues in the *ex vivo* study (Fig 1C).

Notably, higher 5mCG/5hmCG ratios were detected around binding motifs of members of the AP-1, C/EBP and NF- κ B TFs families in D-2HG-treated primary microglia compared to paired untreated controls with these motifs being located in hypermethylated enhancers of CD11B+ cells from IDH^{mut} gliomas vs. normal brain tissue (Fig. 5c). Similar results were obtained when this analysis was extended to motifs of SPI1 (PU.1), IRF4/8, RUNX3, HIF1A and MYC, which also appeared to be relevant in the *ex vivo* situation (Fig. 5c). In sharp contrast, 5mCG and 5hmCG levels in the proximity of binding motifs located in the whole set of covered enhancers, exhibit opposite trends (Extended Data Fig. 9a). Notably, the genes regulated by the selected enhancers bound by key TFs (Fig 5c), that exhibited hypermethylation/hypohydroxymethylation, were enriched among the downregulated genes, indicating a direct impact of D-2HG-induced hypermethylation on gene expression (Extended Data Fig. 9b and Supplementary Table 5). Taken together, these results strongly support that D-2HG has the potential to impede TET-mediated DNA demethylation selectively at lineage-specific enhancers, leading to a blunted microglial cell response.

D-2HG dampens the LPS-induced inflammatory response and increases basal oxidative metabolism in human microglial cells

Lineage-specific enhancers that were affected by D-2HG treatments in our *in vitro* experiments have been shown to be transcribed upon macrophage stimulation⁵⁴. Thus, we

hypothesized that the methylome primed by D-2HG could hinder the activation of enhancers governing the proinflammatory capacity of human microglia. To address this issue, we evaluated transcriptional changes in cells pre-treated with D-2HG for 14 days and subsequently challenged with LPS for 6 hours (Fig. 6a).

Gene set enrichment analysis (GSEA) indicated that treatment with D-2HG attenuates LPS-induced microglial activation (Fig. 6b). Specifically, these cells exhibit an M2-like phenotype characterized by enhanced OXPHOS and fatty acid metabolism alongside marked suppression of the inflammatory response pathways including TNF- α signaling via NF- κ B (Fig. 6b). Additionally, in RNA-seq data from the *ex vivo* study, we find reduced expression of proinflammatory cytokines in CD11B+ cells from IDH^{mut} compared to IDH^{wt} gliomas (Extended Data Fig. 10a). We then prompted to evaluate the effect of D-2HG on the expression of LPS-induced cytokines using RT-qPCR in an independent series of primary microglia preparations. We confirmed that the expression of TNFA and IL6 was abrogated by D-2HG in LPS-challenged cells compared to paired controls (p -value=0.02 and 0.07, respectively) (Extended Data Fig. 10b). Similarly, assessment of mitochondrial respiration parameters demonstrated that D-2HG-treated microglia exhibit an increase in basal and maximal respiration even after LPS stimulation (Extended Data Fig. 10c). This observation suggests that this oncometabolite impedes the glycolytic shift that accompanies cellular activation and instead favors OXPHOS metabolism. All in all, these results indicate that D-2HG dampens microglia proinflammatory response to LPS, likely through direct effects on TET-mediated demethylation at enhancers governing microglial activation.

Lastly, to determine whether suppressed microglial cell signaling linked to D-2HG-driven enhancer hypermethylation can be restored upon targeted therapy, we analyzed microglial cells from single-nucleus RNA-seq (snRNA-seq) data obtained from one oligodendroglioma patient treated with ivosidenib, an inhibitor of the IDH1 mutant enzyme that reduces D-2HG levels in tumor bulk (Fig 6c and Supplementary Table 1)⁵⁵.

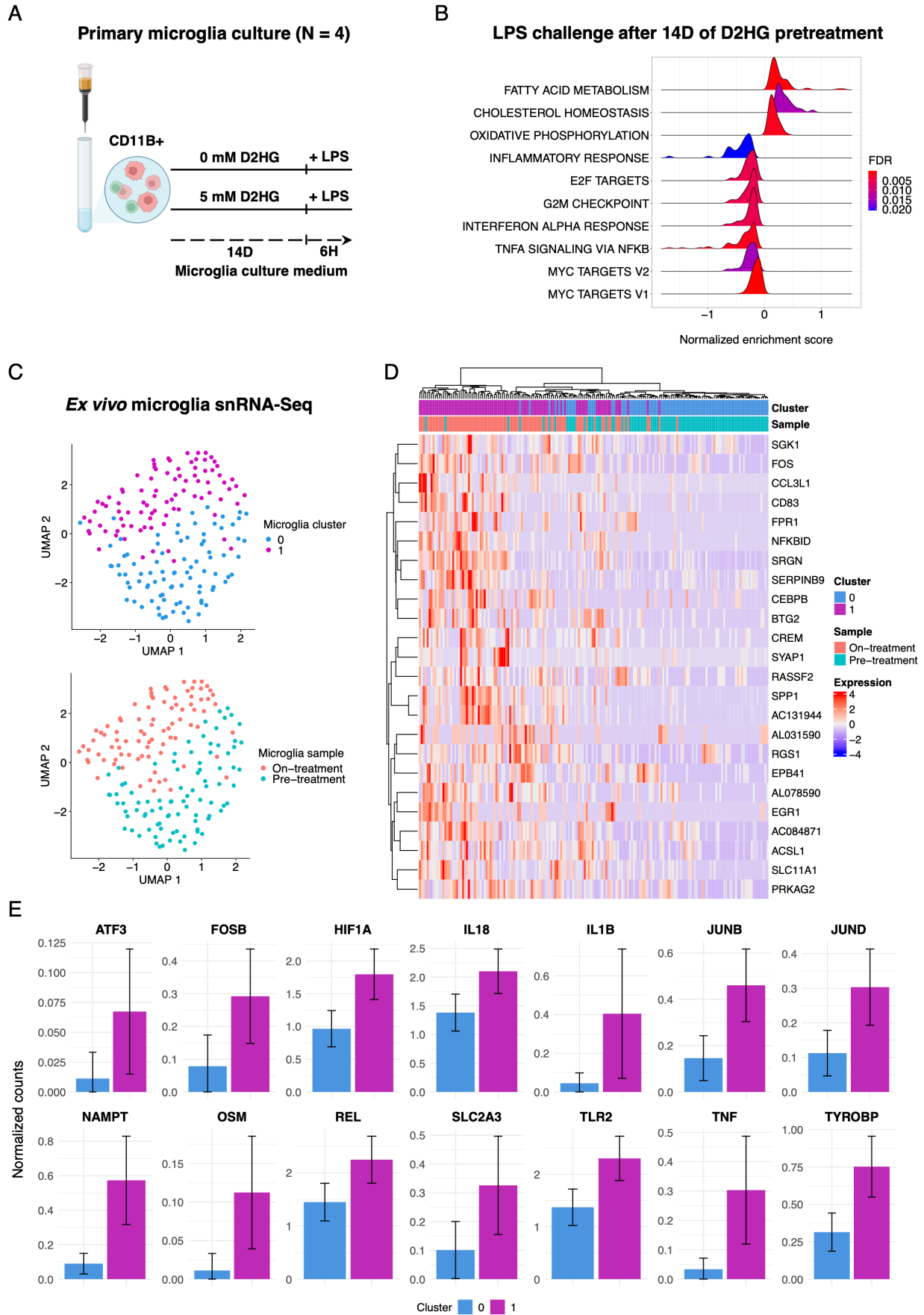


Figure 6. D-2HG impairs microglial activation. (A) Experimental workflow for the LPS challenge experiment in primary microglia pre-treated with D-2HG for 14 days. RNA-seq data was generated from human primary microglia obtained from four surgical aspirates with IDH^{wt} (n=3) or IDH^{mut} (n=1) status. Patient-paired approach was adopted for RNA-seq data analysis. **(B)** GSEA ridge plot illustrates “hallmark gene sets” in D-2HG-treated microglia for 14 days, 6 hours after LPS stimulation. Gene sets with positive or negative normalized enrichment score are associated with up or down regulated genes, respectively (FDR < 0.05). **(C)** Uniform Manifold Approximation and Projection (UMAP) plots depict microglial cells analyzed with snRNA-seq from one oligodendroglioma patient pre- and on-treatment with the mutant IDH inhibitor ivosidenib. **(D)** The heatmap illustrates the significantly upregulated genes (log₂FC > 1, Bonferroni-adjusted p-value < 0.05) in microglia upon ivosidenib treatment. **(E)** Normalized counts of selected genes in microglia pre and on-treatment. Data are represented as the mean with a 95% CI.

After removing low quality cells, 178 microglial cells remained, as determined by the high expression of markers TAL1 and SLC2A5, and the low/absence of expression of MDMs markers CD163 and TGFBI. These cells encompassed two well-defined clusters corresponding almost entirely to on- (n=87) and pre-treatment (n=91) microglia, on which the analysis was focused (Fig 6c). We noticed a transcriptional shift towards gene upregulation in cluster 1 (on-treatment) compared to cluster 2 (pre-treatment) (1683 genes with log₂FC >1, 501 genes with log₂FC < -1, respectively). Furthermore, we found 24 upregulated (including the master regulators TFs FOS and CEBPB) (Fig 6d) and 3 downregulated genes (Bonferroni-adjusted p-value < 0.05, log₂FC > 1 or < -1, respectively) with a strong enrichment of the upregulated genes in the TNF- α signaling via NF- κ B gene set (FDR=1.5e-4; ORA). Additionally, microglial cells in cluster 1 displayed overexpression of other TFs governing activation, including AP-1 family members (FOSB, ATF3, JUNB, and JUND), REL, and HIF1A, as well as related target genes highlighted in the *ex vivo* and *in vitro* analyses, such as OSM, IL18, IL1B, FPR1, TLR2, NAMPT, TNF, TYROBP, and SLC2A3 (GLUT-3) (Fig 6d and 6e). This result suggested that decreased levels of D-2HG in the TME may reverse the hypermethylation phenotype observed in microglia from IDH^{mut} gliomas, thereby enabling their activation program. Supporting this hypothesis, a significant proportion of genes upregulated following ivosidenib treatment are regulated by enhancers that were found to be hypermethylated in CD11B+ cells from IDH^{mut} gliomas (p-value = 0.0012, ORA).

Discussion

The development of new therapeutic options to cure glioma requires a deep understanding of the epigenetic mechanisms governing transcriptional programs, cell states, and proinflammatory capacities in TAMs. Differences in the transcriptome and chromatin landscapes have been associated with the IDH^{mut} status^{17,18,21}, but the extent and the role of DNA methylation in TAMs have remained uncharacterized. Herein, through genome-wide profiling of the DNA methylome, we uncovered global and differential distribution of 5mC and 5hmC changes in TAMs according to the IDH^{mut} status of gliomas. Our findings revealed how this differential methylation affects microglial enhancers involved in the regulation of proinflammatory and metabolic pathways.

We found that CD11B⁺ cells residing in an IDH^{mut} environment display a striking bias towards DNA hypermethylation. TAMs comprise MDMs and microglia in proportions and states of activation that differ according to glioma IDH^{mut} status, subtype, and grade¹⁷⁻²³. Previous studies reported that most of the TAMs in IDH^{mut} tumors are microglia, whereas IDH^{wt} gliomas are marked by an influx of MDMs¹⁷⁻²⁰. In this regard, we do not rule out the possibility that differentially methylated changes observed in CD11B⁺ cells partly reflect a decreased recruitment of MDMs in IDH^{mut} compared to IDH^{wt} tumors. However, the hypermethylation we observed holds true even when comparing CD11B⁺ cells from IDH^{mut} glioma to non-tumor brain tissues, both of which are highly enriched in microglia. In addition, a recent study indicated that immunomodulatory activity programs are expressed across myeloid cell types, and demonstrated convergent phenotypes of resident microglia and infiltrating MDMs, with the latter acquiring a microglia-like phenotype in tumors²³. Moreover, mouse studies indicate that MDMs can adopt a DNA methylation profile very similar to that of microglia after colonizing the central nervous system niche⁵⁶. Therefore, our bulk profiling of CD11B⁺ cells strongly suggests that microglia undergo a hypermethylated state in IDH^{mut} tumors. This assumption is further substantiated by our analyses of methylation across gene regulatory regions, revealing functional implications related to proinflammatory activation and metabolism in microglia.

We highlighted that the occurrence and extent of differentially methylated changes were more prominent in distal enhancers. DNA methylation at CpG sites within or flanking motifs may prevent TF binding at regulatory regions by inducing steric hindrance, altering DNA shape and rigidity, or influencing nucleosome positioning, thereby affecting the formation of active chromatin^{36,38,43,57-59}. A recent study showed that only a minority of enhancers in a given cell type are sensitive to DNA methylation⁶⁰. In line with this, our integrative analysis of methylome and transcriptome changes demonstrates that, among the hypermethylated enhancers displayed by CD11B+ cells from IDH^{mut} vs. IDH^{wt} comparison, 23% may account for the downregulated expression of target genes. We also observed that hypermethylated enhancers were enriched for motifs of lineage-determining TFs, including SPI1 (PU.1) and members of the C/EBP and RUNX families, as well as motifs for stimulus-induced TFs, such as AP-1, IRF, and NF- κ B. These TFs are known to regulate the functional properties of myeloid cells. Our interrogation of gene regulatory networks further supports the hypothesis that hypermethylated enhancers are responsible for the reduced activity of core TFs that govern the identity and activation program in human microglial cells³⁹. Specifically, hypermethylation seems to disrupt cooperative regulatory functions involving lineage-determining TFs SPI1 (PU.1) and C/EBP, and stimulus-responsive TFs AP-1 and NF- κ B, which in turn affect the expression of key genes involved in inflammatory responses. Hypermethylated enhancers also appear to influence the expression of activating receptors, as well as of genes involved in antigen presentation, an observation previously reported in bulk methylome analysis of IDH^{mut} gliomas⁶¹. These findings indicate that microglia in these tumors undergo a profound alteration of promoter-enhancer interactions that characterize these cells⁶².

In addition to microglial TFs, our data revealed the inactivation of HIF1A and MYC, which possibly reinforces the silencing of shared targets essential for the glycolytic shift of stimulated macrophages⁶³⁻⁶⁶. Along with a marked downregulation of several target genes, there was low expression of HIF1A, accompanied by hypermethylation at regulatory regions

of HIF1A and some of its targets. In particular, reduced expression of HIF1A targets such as LDHA, ENO1, HK2, PKM, VIM, ITGB2, and PGK1 has also been reported in bulk IDH^{mut} tumors and/or cells⁶⁷, which may be attributable to hypermethylation driving the silencing of these genes in addition to the effect of D-2HG on HIF-1 α protein destabilization⁶⁸. Collectively, our findings provide evidence that DNA hypermethylation may contribute to a reduced proinflammatory microglial response by targeting enhancers that orchestrate synergistic responses to environmental stimuli driving myeloid cell activation⁶⁹⁻⁷¹. This assumption is supported by our experiments, which demonstrate how oncometabolite signaling modulates the methylome and subsequently affects the activation of human microglia.

Our analysis of single-nucleus RNA sequencing data of two paired oligodendroglioma samples revealed that treatment with an inhibitor of the IDH1 mutant enzyme could unleash the signaling that suppresses microglia activation. This observation supports the notion that D-2HG production plays a major role in the suppressive signaling that affects microglia function and highlights the prognostic and therapeutic value of microglial activation in IDH^{mut} glioma. By establishing primary cultures of human microglia, we have shown that D-2HG is taken up by these cells, inhibits TET-mediated DNA demethylation, and hampers the accumulation of 5hmC genomic content after a 14 days treatment. Although D-2HG-driven global hypermethylation is challenging to reproduce in our microglial cultures, our analysis of methylome and hydroxymethylome at nucleotide resolution clearly demonstrates higher 5mCG/5hmCG ratios at lineage-specific enhancers that were also hypermethylated in *ex vivo* CD11B⁺ cells from IDH^{mut} gliomas. This result is consistent with the previous demonstration that the highest TET activity is localized to enhancer elements^{51,53}. Our observation that the 5hmC turnover is limited in cultures of non-proliferating microglial cells points to a passive demethylation mechanism that could unfold under successive rounds of replication. Nevertheless, a comprehensive characterization of other TET-mediated oxidized derivatives, such as 5fC and 5caC, and an assessment of the activity and the role of thymidine DNA glycosylase⁴⁷, will be required to determine the relative contribution of active vs. passive demethylation mechanisms in human microglia.

Regardless of the demethylation mechanism, we speculate that inhibition of TET2 in slowly proliferating microglial cells of IDH^{mut} gliomas, which are exposed to D-2HG over several years, may lead to full-blown hypermethylation, as opposed to the limited changes observed in our non-proliferating microglial cultures exposed to this oncometabolite for no more than two weeks. It is also possible that additional mechanisms contribute to the hypermethylation highlighted in the *ex vivo* context. Nevertheless, our *in vitro* system was instrumental in demonstrating that D-2HG readily affects TET-mediated demethylation at specific enhancers, leading to suppressed expression of targeted genes. A high turnover of DNA methylation at enhancers is crucial for cellular plasticity, differentiation, and responsiveness to environmental changes, for instance, during macrophage activation^{72,73}. Thus, the significant overlap of enhancer elements impacted by D-2HG *in vitro* with those exhibiting hypermethylation in myeloid cells from IDH^{mut} gliomas strongly suggests that the methylome of microglial cells primed by D-2HG negatively affects the transcriptional response to inflammatory stimuli.

Consistent with this hypothesis, we observed that D-2HG-treated microglia, when challenged with LPS, display attenuation of the inflammatory response while favoring an OXPHOS metabolism that marks anti-inflammatory M2-like macrophage phenotypes^{74,75}. While the hypermethylation we observed may affect the glycolytic shift—a metabolic response documented in iPSC-derived human microglia treated with LPS⁷⁶—our data indicate that hypermethylation could also impact genes involved in cytokine production. Considering the time-dependent effects of D-2HG on the microglia methylome, we propose that an epigenetic drift—involving the selection of hypermethylated enhancers over time—underlies the silencing of master regulators, which impedes not only the proinflammatory response but also the glycolytic reprogramming, both of which are essential for microglial cell activation. This does not exclude the possibility of contributions from chromatin remodeling and non-epigenetic mechanisms to the LPS hyporesponsiveness of D-2HG-treated microglia, including signaling pathways targeted by D-2HG in other cell types^{6,9,10,77}.

In particular, it has been reported that acute octyl-D-2HG treatment can dampen LPS-triggered cytokine expression in the immortalized mouse BV2 microglial cell line through a mechanism involving AMP-activated protein kinase (AMPK)-mTOR-mediated reduction of NF- κ B activity⁷⁷. Whether this mechanism also applies to human primary microglia remains undetermined.

In conclusion, we provide evidence that D-2HG reshapes the enhancer landscape of resident microglia in IDH^{mut} gliomas, thus impairing the regulatory function of core TFs. This priming mechanism precludes the capacity of these cells to mount the inflammatory response and possibly the shift towards a glycolytic metabolism. We speculate that D-2HG effects on myeloid cells promote a cold immune TME that favors tumor progression. Given that the reduced concentration of D-2HG in bulk tumors, induced by inhibitors of the IDH mutant enzyme, is associated with inflammatory and metabolic changes⁷⁸, it is important to evaluate the extent of these effects in myeloid cells and to correlate them with the clinical response to this therapeutic option.

Limitations of the study

We acknowledge certain limitations in our study that should be taken into consideration. Our comparative analyses of CD11B+ myeloid fractions from gliomas and non-tumor tissues remained at the bulk level. Moreover, the methylome profiling is limited to CpG residues in the EPIC array and to global levels assessed by LC-MS/MS, whereas no exhaustive analysis of 5hmC at nucleotide resolution was conducted *ex vivo*. While our results indicate that hypermethylation affects the dominant population of resident microglia cells in IDH^{mut} gliomas, employing single-cell multimodal approaches will be necessary to better associate enhancer landscapes with their regulatory roles in specific myeloid cell subsets/states. Lastly, we did not analyze the potential effects of D-2HG on the local chromatin environment, which could also influence enhancer function.

Acknowledgements

The authors express their deepest gratitude to the memory of Prof. Dr. Laurent Capelle for his insightful feedback and invaluable contribution to the collection of neurosurgical specimens for research purposes, including the present study. The authors also thank the personnel working at the ICM platforms iGenSeq (sequencing), Celis (cell culture), and Histomics (histology) for their technical support, and Julie Jardon, Coralie Gimonnet and Giovanni Scala for their assistance in experiments and bioinformatics. This work is supported by the Ligue Nationale contre le Cancer (Équipe Labellisée), as well as by the following grants: INCa-DGOS-Inserm 12560, Site de Recherche Intégré sur le Cancer (SiRIC CURAMUS), French National Cancer Institute (INCa-PLBIO22-243), Fondation Bristol Myers Squibb pour la Recherche en Immuno-Oncologie (BMS 2104009NA), French National Cancer Institute (INCa), Fondation ARC and Ligue National contre le cancer (LNCC) grant (PAIR TUMC21-001, INCa-16280), and Entreprises contre le Cancer Paris-Île-de-France (GEFLUC R20202DD). A.L. is supported by a Fondation Recherche Médicale (FRM) scholarship, Q.R. is supported by a French Ministry of Education and Research scholarship, and Y.H. is supported by a La Ligue Nationale contre le Cancer scholarship.

Author contributions

A.L.: Conceptualization, optimization of primary microglial cultures, designed and performed *in vitro* experiments, data collection, analysis and interpretation of results, draft editing. P.P.: Conceptualization, data curation, computational and statistical analyses, interpretation of results, data visualization, draft editing. B.M.: Provided surgical resection specimens, optimization of primary microglial cultures, draft editing. Q.R., S.J.: Performed *ex vivo* experiments and data visualization. Y.H., S.S.: Conducted validation experiments, data analysis and interpretation, data visualization, draft editing. P.M.: Provided surgical resection specimens. K.L., A.A.: Bioinformatics assistance, draft editing. M.V., A.I., C.B., E.H., N.P., K.M., S.T., M.L.S., M.T., F.B.: Provided material, data curation. A.D., I.F.: Performed LC/MS analysis of 2HG. G.A.K., P.J.K., L.J.M.: Performed LC-MS/MS and data analysis of global 5mC and 5hmC levels. E.D., E.E-H.: Performed Seahorse experiments and data analysis. L.A.S.: analysis of

epigenetic clocks and draft editing. A.I: Data analysis and interpretation, draft editing. M.C: Computational analyses, draft editing. M.M: Conceptualization, experimental design, data analysis and interpretation, draft editing. M.S: Conceptualization, experimental design, data analysis and interpretation, draft editing, funding acquisition, supervision. L.J.C-V: Conceptualization, experimental design, data analysis and interpretation, data visualization, writing—original draft, funding acquisition, project administration and supervision. All authors listed revised the manuscript critically for important intellectual content and approved it for publication.

Conflict statement

L.A.S. is a scientific advisor and co-founder of Cellintec L.L.C., which had no role in this research. M.L.S. is equity holder, scientific co-founder, and advisory board member of Immunitas Therapeutics. The other authors declare no competing or financial interests.

STAR Methods

Tumor samples and CD11B sorting

Human brain tissues were obtained with informed consent approved by the institutional ethical committee board in accordance with the Declaration of Helsinki. Samples for analyses were selected from the Pitié-Salpêtrière tumor bank Onconeurotek based on clinical information and validation by expert neuropathologists (K.M., S.T., F.B) of both histological features, and molecular diagnosis as previously described⁷⁹. Cryopreservation was as follows: tumors taken from the neurosurgery room were immediately transported on ice in HBSS (Gibco), cut into 2-5 mm diameter pieces, and submerged in cryotubes containing 1 mL of DMEM/F-12 (Gibco), 20% FBS, and 10% DMSO (Sigma-Aldrich). The cryotubes were placed at -80°C in alcohol-free freezing containers (Corning® CoolCell®). The cryopreserved samples were then stored in liquid nitrogen until they were used. On the day of analysis, tumor pieces were thawed and rinsed in DMEM/F-12. Next, the tissue was enzymatically and mechanically digested for 5-10 minutes at 37°C in an HBSS-papain-based lysis buffer

(Worthington) containing DNase (0.01%, Worthington) and L-Cysteine (124 µg/mL, Sigma). Enzymatic digestion was stopped with ovomucoid (700 µg/mL, Worthington). The homogenates were sequentially filtered using 100 µm, 70 µm, and 30 µm SmartStrainers (Miltenyi) to remove residual clumps. HBSS was added, and samples were then centrifuged at 300 g for 10 minutes at 4°C. Cell pellets were resuspended in an appropriate volume of cold MACS debris removal solution following the manufacturer's instructions (Miltenyi). The suspension was gently mixed by pipetting 10-12 times, and ice-cold DPBS without calcium and magnesium was added very slowly above the cell suspension to create a transparent gradient. The suspension was centrifuged at 4 °C and 3000 g for 10 min. After centrifugation, the top liquid and solid interphases were discarded, and cell suspensions were resuspended with cold MACS Buffer (0,5% BSA and 2 mM EDTA in PBS). Tubes were gently inverted 3-5 times and then centrifuged at 1000 g for 10 min at 4°C. After centrifugation, the supernatant was completely removed, and red blood cells lysis was performed with ACK buffer (Gibco) for 5 min at room temperature. Next, cells were centrifuged at 4°C and pellets were washed with cold DPBS. After centrifugation, cells were resuspended in MACS buffer and counted. Next, cell pellets were labeled with an appropriate volume of CD11B MicroBeads (Miltenyi) in MACS buffer and incubated for 15 min at 4°C. Subsequently, cells were resuspended in cold MACS buffer and centrifuged at 300 g for 10 min at 4°C. The supernatant was aspirated, and cells were resuspended in cold MACS buffer. LS MACS Separation Columns were placed in the magnetic field of a suitable MACS Separator, and the cell suspension was applied onto the columns. CD11B+ and CD11B- fractions were separately collected on ice. The dry pellets were stored at -80°C until nucleic acid extraction.

Nucleic acids extractions

RNA and DNA of CD11B+ and CD11B- samples were co-eluted using the AllPrep DNA/RNA Micro Kit (Qiagen, 80284) or AllPrep DNA/RNA Mini Kit (Qiagen, 80204) following the manufacturer's instructions. In some cases, nucleic acids were purified separately using the Maxwell RSC simplyRNA Cells Kit (Promega, AS 1390) and the Maxwell RSC Blood DNA Kit

(Promega, AS 1400), following the manufacturer's instructions. The yield and quality of total RNA was assessed using the TapeStation 2200 (Agilent) instrument.

Digital droplet PCR

IDH1 R132H, TERT C228T, and TERT C250T mutations were analyzed in CD11B⁺ and CD11B⁻ fractions from human gliomas using ddPCR. Droplet generation and partition was performed using the Bio-Rad system QX200. Primer sets, probes, and ddPCR™ Supermix for Probes (No dUTP) were used for quantification of absolute copy number in 3 ng of input DNA following the manufacturer's instructions. All primers and probes were obtained from Bio-Rad. Sequence information is available at www.bio-rad.com using the ID numbers: IDH1 p.R132H Hsa, Human (Ref: 10031246 UniqueAssayID: dHsaCP2000055), IDH1 WT for p.R132H Hsa, Human (Ref: 10031249 UniqueAssayID: dHsaCP2000056), TERT C228T_113 Hsa, Human (Ref: 12009308 UniqueAssayID: dHsaEXD72405942), TERT C250T_113 Hsa, Human (Ref: 12003908 UniqueAssayID: dHsaEXD46675715). The data were then analyzed using Poisson statistics to determine the target DNA template concentration in the original sample. Positive controls consisted of tumor DNA from the CD11B⁻ fractions and negative controls contained water instead of DNA.

DNA methylation profiling

Genomic DNA was quantified by Quant-iT dsDNA Broad range Assay (Thermo Fisher Scientific, Waltham, MA, USA) in a Tecan SPARK microplate Reader (TECAN, Switzerland). Total DNA (500 ng) from each sample was sodium bisulfite converted using Zymo EZ-96 DNA Methylation kit and following the manufacturer's recommendations for Infinium assay (Zymo Research, catalog number: D5004). After conversion, DNA concentration of each sample was adjusted to 50 ng/μL with M-elution Buffer or concentrated using speed vacuum. In total 300 ng of converted DNA for each sample was used as a template on the Infinium MethylationEPIC BeadChip following the manufacturer's recommendations. Briefly, bisulfite-converted DNA is whole genome amplified, fragmented and hybridized to the array. After hybridization, unhybridized and non specifically hybridized DNA is washed away, and the

captured product is extended with fluorescent labels coupled to nucleotides. Finally, the arrays are scanned with a high-resolution Illumina scanner (iScan), which acquires light images emitted from fluorophores. The intensities are measured and the methylation signals are extracted and recorded as raw data (IDAT). These assays were performed at the P3S platform (Sorbonne University). DNA methylation data were analyzed using the RnBeads package. In short, after the removal of bad quality samples, data were aligned to the hg19 assembly using the beta Mixture Quantile dilation (BMIQ) method for normalization and adjusted for sex as a covariate. Sex chromosomes were included and sites having a standard deviation below 0.01 across all samples were filtered out. Together with default annotations, we included the enhancers coordinates (entire enhancers regions) as defined in the FANTOM5 enhancer-robust promoter associations. Briefly, using Pearson's correlation, enhancers having and $FDR < 1e-5$ in an enhancer-promoter pair within 500 kb over cell types and organs were retained. The enhancer-promoter associations are computed between enhancers and all FANTOM robust promoters. Epigenetic clock analysis of CD11B+ cells from the *ex vivo study* was conducted using "epiTOC2" (Epigenetic Timer Of Cancer), which calculates the mitotic age of the cells using the updated total number of divisions per stem cell⁸⁰. This new method approximates age as a weighted estimate based on 163 CpG sites interrogated with EPIC arrays.

RNA sequencing

Library preparations were performed with Kapa mRNA Hyper prep (Roche) following the manufacturer's instructions and sequenced (paired end) with the Illumina Novaseq 6000 Sequencing system with 200 cycles cartridge, to obtain 2*60 million reads 100bases/RNA. Sequencing was performed at the iGenseq platform of the ICM – Paris Brain Institute. For the *in vitro* experiments, we combined Illumina Stranded Total RNA Prep and Ribo-Zero Plus. The quality of raw data was evaluated with FastQC. Sequences were trimmed or removed with Fastp software to retain only good quality paired reads. Star v2.5.3a was used to align reads on the GRCh38 reference genome using default parameters except for the maximum number of multiple alignments allowed for a read which was set to 1. Gene level transcript

quantification was done with rsem 1.2.28. Differential expression analysis was conducted using the quasi-likelihood F-test from the edgeR package. Normalized data were computed using the cpm function. Multiple hypothesis testing was corrected using the False Discovery Rate Benjamini-Hochberg method. Samples from all the *in vitro* experiments were analyzed in a paired manner per individual.

Sequence motif enrichment analysis

Motif enrichment was performed using Hypergeometric Optimization of Motif EnRichment (HOMER) v4.11⁸¹, enabling masking repeats, setting the parameter size to “given” and searching for motifs with a length within the range of 7-14 bp. We used HOCOMOCO v12 CORE as the reference dataset (matrix with threshold level corresponding to a p-value of 0.001)⁸².

Transcription factor activity

We used CollecTRI database⁴¹ to infer TF activity, which contains regulons comprising signed TF-target gene interactions. To estimate TF activity at hypermethylated enhancers, we took into account genes with associated overexpression or downregulation (falling in quadrants I and IV, respectively, Fig. 2a). These genes were then interrogated among the targets of each TF of the database. We retained the TFs having at least 5 total targets regulated in a positive or negative manner. Then, we computed the TF activity using the Normalized Enrichment Score (NES) of the Mann-Whitney-Wilcoxon genes set test (MWW-GST)⁴². We applied MWW-GST to each sample normalized data and retained TFs having an FDR < 0.05 for the NES in at least 18 samples and an FDR < 0.05 in the comparison of the activity between groups (Wilcoxon’s test). For promoters, we took into account all genes associated with hypermethylation in the IDH^{mut} vs. IDH^{wt} comparison without testing for differential activity between TFs. Heatmaps depicting TF activity at hypermethylated enhancers and promoters were generated using a z-score of the activity.

Primary cultures of human microglia

Primary microglial cultures were prepared using surgical aspirates obtained from patients with either brain tumors or drug-resistant epilepsy, following established surgical protocols. For gliomas, tissue collection involved the removal of both the adjacent "entry cortex" (the tissue surrounding the surgical access point) and the tumor core, whereas in cases of epilepsy surgery, only the normal tissue at the entry point was collected. Upon receipt (averaging 2 hours), tissues were promptly processed following the protocol specified for human tumor samples. After enzymatic digestion and MACS purification, CD11B⁺ cells were counted and directly seeded in non-coated 12-well plates at a density of 750-1000 K cells/well in DMEM/F12, GlutaMAX medium (Gibco Ref# 10565018) supplemented with N-acetyl-cysteine and insulin [5 µg/mL], apo-Transferrin [100 µg/mL], sodium selenite [100 ng/mL], human TGFβ₂ [2 ng/mL], CSF-1 [20 ng/mL], ovine wool cholesterol [1.5 µg/mL], ascorbic acid [75 µM] and penicillin/streptomycin⁴⁹. All reagents were purchased from Sigma and growth factors from Preprotech. Non-permeable D-2HG acid disodium salt (Sigma) was used at a final concentration of 5 mM for all the experiments, with treatments starting at 48 hours culture. Half of the culture medium was renewed every 2-3 days. For the 6 hours LPS challenge experiments, 1% FBS was added to all conditions.

IDH^{mut} and IDH^{wt} cell lines

Human glioma cell lines IDH^{wt} were established by the GlioTEX team (Glioblastoma and Experimental Therapeutics) in the Paris Brain Institute (ICM) laboratory. Cultured cells were maintained at 37 °C, 5% CO₂ under neurosphere growth conditions using DMEM/F12 medium (Gibco) supplemented with 1% penicillin/streptomycin, B27 diluted 1:50 (Gibco), EGF (20 ng/mL), and FGF (20 ng/mL) (Preprotech). Human glioma cell lines IDH^{mut} BT88, BT54 were kindly provided by Artee Luchman and Sam Weiss (University of Calgary); BT237, BT138 were kindly provided by Keith Ligon (Dana-Farber Cancer Institute). Cells were grown using DMEM/F12 medium (Gibco) supplemented with B27 (1/100; Gibco), 20ng/ml EGF and FGF (Peprotech). IDH^{wt} and IDH^{mut} cell lines were used as negative and positive controls, respectively, in assays applied to quantify intracellular D-2HG levels. The Idh1 R132H

conditional knock-in (cKI) mouse line (Bardella et al., 2016) crossed with *Rosa26^{LSL-YFP}* (Srinivas et al., 2001) was used to generate postnatal (P0-P1) neural progenitor cells. Cells were grown in DMEM/F-12 with GlutaMAX™ Supplement (61965-026, ThermoFisher), Penicillin-Streptomycin 1X (15140122, Life Technologies), B27 supplement 1X (17502048, ThermoFisher), N2 supplement 1X (17502048, ThermoFisher), 0.6% w/v D-glucose (G8769, Sigma), 5mM HEPES (15630056, Life Technologies) and 20µg/ mL insulin (I5500, Sigma). Growth factors (20 ng/ mL EGF GMP100-15, Peprotech, and 10 ng/ mL bFGF GMP100-18B, Peprotech) were added to the cultures and replaced every 2-3 days. Cells were maintained in a humidified incubator at 37 °C with 5% CO₂. Cultures were infected with a Cre expressing adenovirus (Ad:cre, VB180308-1398jmt, VectorBuilder) after 1 passage, enabling recombination at the *Idh1* and *Rosa26LSL-YFP* locus leading to expression of *Idh1* R132H and YFP. Efficient DNA recombination was assessed through YFP visualization in NSC. Cells were cultured for 3-6 passages and assayed for D-2HG levels using a fluorimetric test, TET enzymatic activity, and 5mC/5hmC genomic content using LC-MS/MS.

Immunofluorescence staining

Sterile coverslips were placed in 12 multiple wells and the surface was covered with poly-D-lysine and laminin (Sigma). The plate was incubated at room temperature (RT) for 2 hours and the solution was aspirated; then, it was rinsed with sterile water and allowed to dry. Cells were seeded at a density of 750K cells/well and maintained as described for 3, 10 and 17 days. Cells were washed with PBS (Gibco) and fixed with 4% paraformaldehyde (Electron Microscopy Sciences) in PBS for 10 min at RT. Next, cells were washed with PBS and permeabilized with 0,1% Triton X-100 in 1x PBS for 5 min at RT. Cells were quickly washed with PBS and blocked for non-specific binding sites with Human Fc Block (#564219, BD Pharmingen) for 10 min at RT, and subsequently with 5% donkey in PBS for 30-60 min at RT. Incubation with primary antibodies was overnight at 4°C using anti-Iba1 (#19-19741, Wako; diluted 1/800), Tmem119 (#A16075D, BioLegend; diluted 1/100), or Ki-67 (#AB16667-1001, Abcam; diluted 1/250) in a humidified and light protected chamber. Coverslips were washed with PBS and incubated with secondary antibodies (anti-rabbit #A21206 or anti-mouse

#A21203; diluted 1/1000) in blocking solution for 30 min at RT and protected from light. Subsequently, the coverslips were washed with PBS and mounted with Fluoroshield-DAPI solution (Sigma) and read under an Apotome inverted microscope (ZEISS Apotome 3) and a confocal microscope (A1R HD25 Nikon Inverted). Negative controls (background fluorescence) were obtained omitting primary antibodies. The percentages of TMEM119+ and IBA1+ cells were determined in primary cultures grown in uncoated wells by counting 3 to 5 fields, covering 0.22% of the well surface, at different time points over a two-week period. The fields were randomly selected in the area where the cell density, as assessed by DAPI, was adequate.

Intracellular quantifications of D-2HG

Cultured cells were pelleted by centrifugation to remove the media, followed by two washes with ice-cold DPBS to ensure complete removal of all D-2HG-containing media. Microglial cells were collected by trypsinization (0.25% for 5 min), whereas glioma cells and neurospheres were collected using accutase. Corresponding culture medium supplemented with 10% FBS was added for inactivation. After centrifugation (300 g at 4°C for 5 min) the resulting pellet was washed with cold DPBS. Cell pellets were then preserved at -80°C until used. The concentration of D-2HG in cell lysates was determined using the D-2-Hydroxyglutarate (D-2HG) Assay Kit (Ref MAK320, Sigma) and with LC/MS for validation. For the fluorometric assay, cellular extracts were prepared by adding 75 µl of CellLytic MT Cell Lysis Reagent (Sigma) with Protease Inhibitor Cocktail (Sigma). An aliquot was kept for protein quantification with the Pierce™ BCA Protein Assay Kit (Thermo Fisher Scientific). The collected supernatants were deproteinized by perchloric acid precipitation and neutralized with KOH. A standard curve was prepared with serial dilutions of D-2HG. The equivalent of 5000 pmol was added to a cell extract and used as spike-in internal control. The plate is incubated at 37°C for 30–60 minutes. This assay is based on the oxidation of D-2HG to α -ketoglutarate (α KG) by the enzyme (D)-2-hydroxyglutarate dehydrogenase (HGDH), coupled with the reduction of NAD⁺ to NADH⁸³. The amount of NADH formed is then quantitated by the diaphorase-mediated reduction of resazurin to the fluorescent dye resorufin (λ_{ex} =

540 nm/ λ_{em} = 590 nm) using Spectramax i3x microplate reader. The concentration of D-2HG for each sample is estimated as pmol/ μ g of protein. For the quantification of 2HG using LC-MS, dry cell pellets were lysed in water and the solution was divided in half for 2-HG measurement and protein quantification. NaCl was added and samples were acidified using HCl. A liquid-liquid extraction of organic acids with ethylacetate was performed. Three extractions were performed, organic phases were pooled, dried under nitrogen stream at 30 °C. Then samples were derivated by a standard silylation protocol N,O-Bis [trimethylsilyl] trifluoroacetamide and 1% TMCS (Trimethylchlorosilane) under anhydrous conditions using pyridine. Chromatographic separation was performed with a TR-5MS (30m x 0.25 mm x 0.25 mm) column from Thermo Scientific (Waltham, Massachusetts, USA). Spectral data acquisitions were performed using XCalibur software (Thermo Electron Corporation, Austin, TX, USA). Samples were placed 30 min at 80°C, and then injected into the GC system. Quantifications were performed using internal standard 2-hydroxyglutaric acid-D3 from Cambridge isotope laboratories (Tewksbury, Massachusetts, USA).

LC-MS/MS assessment of genomic 5mC and 5hmC content

Genomic DNA (gDNA) was isolated as indicated and concentrated by ethanol precipitation. Samples were then digested at 37°C for 12 h in 25 μ L reactions containing 1-4 μ g of gDNA, 7.5 U of DNA Degradase Plus (Zymo Research), reaction buffer and isotope labeled internal standards [700 pmol 2'-deoxycytidine-15N3 (Cambridge Isotope Laboratories, Inc.); 1.75 pmol 5-methyl-2'-deoxy cytidine-d3 (Toronto Research Chemicals); 1 pmol 5-hydroxymethyl-2'-deoxycytidine-d3 (Toronto Research Chemicals)] for quantification. Prior to LC/MS analysis, samples were diluted 1:1 in mobile phase component A (see below). The LC-MS system consisted of a Shimadzu Nexera UPLC system in-line with a SCIEX 6500 QTrap mass spectrometer equipped with a TurboV Ion spray source and operated in positive ion mode. The analytes were chromatographed on a gradient elution system where mobile phase A was water with 10 mM ammonium formate and 0.05% trifluoroacetic acid (TFA) (Sigma Aldrich); and mobile phase B was 7:1 methanol:acetonitrile (ThermoFisher Scientific), with 10 mM ammonium formate and 0.05% TFA. The column was a Phenomenex Curosil-

PPF column (10 x 0.2 cm 1.7 μ m) (Phenomenex Inc) held at 42°C. The flow rate was 300 μ L/min and the gradient started at % B = 1.0% (held for 30 s) and was then increased to 19% over 5 min. All analytes were detected using selected reaction monitoring (SRM). Analyst software (version 1.6.2) was used to acquire and process the data. Supplementary Table 6 gives the Q1 and Q3 m/z values, collision energy (CE) and declustering potential (DP) for all analytes and their internal standards. Analytes were quantified by stable isotope dilution against their stably labeled internal standard. Data represents a percentage for each analyte relative to the total cytosine pool (dC+5mC+5hmC) in the same sample.

Reduced Representation Enzymatic Methyl sequencing (RREM-seq)

Library preparation was performed using 100 ng of genomic DNA is spiked with 0.95 ng of unmethylated Lambda DNA and 0.05 ng of CpG methylated pUC19. The mixture is digested with 400 units of MspI (New England Biolabs) in NEB ultra II buffer (New England Biolabs) in a final volume of 57 μ L for 2 hours at 37°C. After enzymatic DNA digestion, fragments are repaired and A-tailed using 15 units of Klenow 3'-5' exo- (New England Biolabs). After End-repair and A-tailing, Illumina universal methylated adapters are ligated to DNA fragments using the NEB ultra II ligation module, following the provider's recommendations. After ligation step, DNA fragments are purified and size-selected with a two steps SPRI beads purification in order to select fragments from 40bp to 400bp. Clean-up ligated DNA is eluted in 10 mM Tris pH 8. Purification product is then converted using the Enzymatic methyl-seq module (New England Biolabs) following the provider's recommendations. Briefly, 5mC are converted to 5hmC with TET2, then 5hmC are specifically protected from APOBEC deamination with a T4-BGT glycosylation. After 5hmC/5mC glycosylation, libraries are denatured during 10min at 85°C in 20% Formamide. Then unmodified cytosines are deaminated during APOBEC reaction. The converted product is amplified by PCR using indexing primers and polymerase KAPA HiFi Hotstart U+ Ready Mix 2X in a final volume of 50 μ L for 13 cycles. PCR products are finally purified with a 1.2X SPRI ratio, then controlled by capillary electrophoresis on Fragment Analyzer. After quantification by qPCR libraries are sequenced on an Illumina Novaseq 6000 as paired-end 100b reads.

Reduced Representation hydroxyMethyl sequencing (RREhM-seq)

We used the RREhM-seq protocol published by Sun, Zhiyi et al⁵². with slight modifications. Library preparation was performed using an input of 200 ng with a spike of 1.9 ng of unmethylated Lambda DNA and 0.1 ng of CpG methylated pUC19. Following MspI digestion and reparation with Klenow 3'-5' exo-, pyrrolo-dC Illumina adapters are used instead of 5mC adapters during the ligation step. For the TET2 step during the conversion, TET2 enzyme and Fe²⁺ are replaced by H₂O to avoid 5mC protection. The product is deaminated, amplified, qualified and sequenced in the same conditions as RREM-seq libraries. RREM-seq and RREhM-seq were performed by Integragen SA (Evry, France).

RREM-seq & RREhM-seq data analysis

FastQ files were aligned using BSseeker2 (<https://github.com/BSSeeker/BSseeker2>) on hg19 genome with bowtie2. The hg19 index was built with the rrbs option on and selected fragments size between 40bp and 400 bp. The adapters sequence and CCGG motif were removed during the alignment steps. After alignment, methylation calling is performed in order to obtain methylation level and covering for each cytosine positions from the library. Options to remove overlap and bad quality sequences were enabled. For RREM-seq libraries, methylation signal corresponds to 5mC and 5hmC, whereas the methylation signal only concerns 5hmC for RREhM-seq libraries⁸⁴. Levels of total 5mC (methylation and hydroxymethylation) or 5hmC were defined as percentage of the number of reads having the corresponding modification on a specific cytosine divided by the number of reads covering that cytosine (modified or not modified). Methylation-only level was obtained subtracting 5hmC level from the total 5mC level. CpG sites were analyzed with methylKit package⁸⁵ using a minimum coverage of 10 reads per base. For the defined window analysis, TFs motifs were retrieved from HOCOMOCO v12 CORE and searched inside entire enhancers regions using Biostrings package⁸⁶ with a maximum mismatch of 1 base. The region of interest was defined as a window of 600 bp centered around the first base of the motif. For each patient, only common enhancers windows between treated and control samples were analyzed. Microglia samples used for analyses of 5mC and 5hmC at 2 days (2D) and 14 days

(14D) were obtained from the aspirates of normal tissue from three patients with epilepsy who underwent surgery. One technical outlier from the 5hmC analysis at 14D was excluded from the study. 5mC-only and 5hmC levels are reported as the mean across patients for each time point/condition, using only the common enhancer regions or defined windows shared among patients.

TET enzymatic assay

Nuclei isolation was performed using the nuclear extraction kit (cat. Ab113474, Abcam, Cambridge, MA, USA). Cells were collected by trypsinization (0.25% for 5 min) and counted. Then, cells were resuspended in an appropriate volume of pre-extraction buffer containing dithiothreitol and protease inhibitor cocktail, and incubated on ice for 2 minutes. After centrifugation at 12,000 rpm for 3 minutes, the cytoplasmic extract (supernatant) was carefully removed, leaving behind the nuclear pellet. Two volumes of extraction buffer containing dithiothreitol and protease inhibitor cocktail were added to the nuclear pellet. The extract was incubated on ice for 15 minutes with vortexing for 5 seconds every 3 minutes. After incubation, the suspension was centrifuged for 10 minutes at 14,000 rpm at 4°C, and the resulting supernatant was transferred to a new microcentrifuge vial. Protein quantification from the nuclear extract was performed using a Pierce™ BCA Protein Assay Kit (Thermo Fisher Scientific) following the manufacturer's instructions. Technical triplicates for this assay were performed using 12 µg of protein from nuclear extracts of microglial cells (untreated and treated with D-2HG), as well as from external controls (neurospheres obtained from the cKI Idh R132H mouse model). To determine TET enzymatic activity, we employed the TET Hydroxylase Activity kit from Abcam (ab156913). In this fluorimetric assay, a methylated substrate is stably coated onto microplate wells. Active TET enzymes bind to the substrate and convert the methylated substrate into hydroxymethylated products. The hydroxymethylated products generated by TET activity can be recognized with a specific antibody. The ratio or amount of hydroxymethylated products, which is proportional to the enzyme activity, was measured fluorometrically using a fluorescent microplate reader with

excitation at 530 nm and emission at 590 nm. The TET enzyme activity is proportional to the relative fluorescent units measured.

RT-qPCR

Total RNA from cultured microglia was purified using the Maxwell RSC simplyRNA Cells Kit (Promega). Next, 300 ng of RNA was reverse transcribed to complementary DNA using the Maxima First Strand cDNA Synthesis Kit (Thermo Fisher Scientific). Assays were run in triplicate on a Light Cycler 480 instrument (Roche) using the LightCycler 480 SYBR Green Master 2X (Roche). Primer sequences were as follow: TNFA, forward: 5'-GAGCCAGCTCCCTCTATTTA-3', reverse: 5'-GGGAACAGCCTATTGTTTCAG-3'; IL-6, forward: 5'-CCTTCCAAAGATGGCTGAAA-3', reverse: 5'-TGGCTTGTTCTCACTACT-3'; PPIA, forward: 5'-ATGCTGGACCCAACACAAAT-3', reverse: 5'-TCTTTCACCTTGCCAAACACC-3'; ACTB, forward: 5'-CCAACCGCGAGAAGATGA-3', reverse: 5'-CCAGAGGCGTACAGGGATAG-3'. Linearity and efficiency, as well as specific amplifications were verified for all primer sets. Relative quantifications of cytokine expression were normalized to the mean of the two control genes (PPIA and ACTB) and expressed as fold change⁸⁷.

Mitochondrial respiration measurement

Real-time measurement of oxygen consumption rate (OCR) was performed using XFe extracellular flux analyzer (Seahorse Bioscience, Billerica, MA) following the manufacturer's instructions. Primary isolated microglia (as detailed in materials and methods) were plated at a density of 1,000,000 cells/well in XFe24 cell culture microplates pre-coated with poly-L-lysine (Sigma). Cells were maintained in 200 μ l DMEM/F-12 medium supplemented as previously indicated and treated with 5 mM D-2HG for a period of 12 days. Half of the culture medium was renewed every 2-3 days. The day of the experiment, cells were stimulated with LPS (1 μ g/mL) for 6 hours. FBS 1% was also added to all experimental conditions. Next, the medium was replaced by Seahorse XF base medium (Agilent, 102353-100) supplemented with 17.5 mM D-Glucose (Dextrose), 0.5 mM sodium pyruvate and 2.5 mM L-Glutamine and incubated for 1 h in CO₂ free incubator at 37 °C. The utility plate was hydrated with XF calibrant solution (pH 7.4) (Agilent, 100840-000; 1 mL/well) and incubated overnight (37°C,

CO₂-free). The day after, the utility plate with the cartridge containing injector ports and sensors was run on the Seahorse for calibration. The assay medium (Seahorse XF DMEM assay medium, pH 7.4) was prepared immediately before assay. OCR was measured under basal conditions and after sequential injection of the following inhibitors: Oligomycin (1 μ M) to stop ATP-synthase, FCCP (1 μ M) to dissipate proton gradient, and Rotenone/Antimycin A (0.5 μ M each to block electron transport chain (ETC). All the following measurements were carried out with 2 min mix, 2 min delay, and 3 min measure. Three baseline OCR measurements were recorded, followed by assessment of mitochondrial metabolism by injection of oligomycin, FCCP, and a combination of rotenone and antimycin A. The following parameters were deduced: basal respiration (OCR values, used to provide ATP under baseline conditions), ATP-linked respiration (following oligomycin injection, a reduction in OCR values represents the part of basal respiration used to produce ATP), and maximal respiration (the maximal OCR values following FCCP injection). Basal respiration was calculated from the subtraction between the last rate measurement before oligomycin injection and the non-mitochondrial respiration rate (NMRT) determined as the minimum rate measurement after rotenone/antimycin A injection. Maximal respiration was calculated by subtracting the maximum measurement after FCCP injection and the NMRT. ATP-linked respiration was calculated by subtracting the last rate measurement before oligomycin injection and the minimum rate measurement after oligomycin injection. OCR data were normalized by the number of viable cells estimated at the end of the experiment. To do this, the cells were fixed with paraformaldehyde 4%, followed by washes with PBS and DAPI [10 μ g/mL] staining. Nuclei were automatically counted in a CellInsight NXT platform.

Single-nucleus RNA sequencing analysis

We downloaded raw data of oligodendroglioma (patient BWH445) from Spitzer et al. study on IDH1⁵⁵ GSE260928 and used Seurat (version 5.0.3)⁸⁸ to perform data analysis. First, we performed data quality control excluding cells having less than 1500 or more than 3400 genes expressed and less than 2200 or more than 12000 unique molecular identifiers. These stringent thresholds allowed us to have high-quality nuclei also avoiding doublets.

Subsequently, we normalized the entire raw gene count matrix by regularized negative binomial regression using the `sctransform` function version 2 and clustering cells using 30 principal components. We selected the microglia cluster based on the expression of *TAL1*, *P2RY12*, *SLC2A5* and the absence of the infiltrating myeloid marker *CD163*. Selected microglial cells were then analyzed using the raw expression matrix and normalized with the `sctransform` function version 2 and clustered using 20 principal components. Differential expression analysis was performed using the function `FindMarkers`.

Statistical analysis and plots generation

Sample sizes and statistical tests are provided in the figure legends. Analyses were performed with R. Normal distribution of data was verified with Shapiro-Wilk's normality test ($p\text{-value} > 0.05$). Plots and analyses were generated using `ggplot2`⁸⁹, the extension `ggsignif`⁹⁰, `ComplexHeatmap`⁹¹, `Cytoscape`⁹², `clusterProfiler`⁹³ and `eulerr`⁹⁴. Hallmark gene set collection (v2023.1.Hs) for GSEA analyses⁹⁵ was downloaded from the Molecular Signatures Database (MSigDB)⁹⁶.

Data and code availability

Data and code are available upon request.

Supplementary Tables

Supplementary Table 1: Clinical, pathological and genetic features of the study cohort.

Supplementary Table 2: Genes regulated by hypermethylated enhancers and promoters in CD11B+ cells from IDH^{mut} gliomas.

Supplementary Table 3: Differentially expressed genes in CD11B+ cells from IDH^{mut} vs. IDH^{wt} gliomas.

Supplementary Table 4: Genes regulated by hypermethylated enhancers and/or promoters linked to downregulated expression in CD11B+ cells from IDH^{mut} vs. IDH^{wt} gliomas.

Supplementary Table 5: Genes regulated by the selected enhancers bound by TFs of Fig 5c exhibiting hypermethylation/hypohydroxymethylation in D-2HG-treated microglia.

Supplementary Table 6: Analyte and internal standard Q1 and Q3 m/z values, collision energy (CE), and declustering potential (DP) for LC-MS/MS quantifications.

References

1. van den Bent, M. J., Geurts, M., French, P. J., Smits, M., Capper, D., Bromberg, J. E. C., & Chang, S. M. (2023). Primary brain tumours in adults. *The Lancet*, 402(10412), 1564–1579. [https://doi.org/10.1016/S0140-6736\(23\)01054-1](https://doi.org/10.1016/S0140-6736(23)01054-1).
2. Dang, L., White, D. W., Gross, S., Bennett, B. D., Bittinger, M. A., Driggers, E. M., Fantin, V. R., Jang, H. G., Jin, S., Keenan, M. C., Marks, K. M., Prins, R. M., Ward, P. S., Yen, K. E., Liao, L. M., Rabinowitz, J. D., Cantley, L. C., Thompson, C. B., vander Heiden, M. G., & Su, S. M. (2009). Cancer-associated IDH1 mutations produce 2-hydroxyglutarate. *Nature*, 462(7274), 739–744. <https://doi.org/10.1038/nature08617>.
3. Richard, Q., Laurence, A., Mallat, M., Sanson, M., & Castro-Vega, L. J. (2022). New insights into the Immune TME of adult-type diffuse gliomas. *Current Opinion in Neurology*, 35(6), 794–802. <https://doi.org/10.1097/WCO.0000000000001112>.
4. Linninger, A., Hartung, G. A., Liu, B. P., Mirkov, S., Tangen, K., Lukas, R. v, Unruh, D., James, C. D., Sarkaria, J. N., & Horbinski, C. (2018). Modeling the diffusion of D-2-hydroxyglutarate from IDH1 mutant gliomas in the central nervous system. *Neuro-Oncology*, 20(9), 1197–1206. <https://doi.org/10.1093/neuonc/noy051>.
5. Pickard, A. J., Sohn, A. S. W., Bartenstein, T. F., He, S., Zhang, Y., & Gallo, J. M. (2016). Intracerebral Distribution of the Oncometabolite d-2-Hydroxyglutarate in Mice Bearing Mutant Isocitrate Dehydrogenase Brain Tumors: Implications for Tumorigenesis. *Frontiers in Oncology*, 6. <https://doi.org/10.3389/fonc.2016.00211>.
6. Bunse, L., Pusch, S., Bunse, T., Sahm, F., Sanghvi, K., Friedrich, M., Alansary, D., Sonner, J. K., Green, E., Deumelandt, K., Kilian, M., Neftel, C., Uhlig, S., Kessler, T., von Landenberg, A., Berghoff, A. S., Marsh, K., Steadman, M., Zhu, D., ... Platten, M. (2018). Suppression of antitumor T cell immunity by the oncometabolite (R)-2-hydroxyglutarate. *Nature Medicine*, 24(8), 1192–1203. <https://doi.org/10.1038/s41591-018-0095-6>.

7. Böttcher, M., Renner, K., Berger, R., Mentz, K., Thomas, S., Cardenas-Conejo, Z. E., Dettmer, K., Oefner, P. J., Mackensen, A., Kreutz, M., & Mougiakakos, D. (2018). D-2-hydroxyglutarate interferes with HIF-1 α stability skewing T-cell metabolism towards oxidative phosphorylation and impairing Th17 polarization. *Oncot Immunology*, 7(7), e1445454. <https://doi.org/10.1080/2162402X.2018.1445454>.
8. Ugele, I., Cárdenas-Conejo, Z., Hammon, K., Wehrstein, M., Bruss, C., Peter, K., Singer, K., Gottfried, E., Boesch, J., Oefner, P., Dettmer, K., Renner, K., & Kreutz, M. (2019). D-2-Hydroxyglutarate and L-2-Hydroxyglutarate Inhibit IL-12 Secretion by Human Monocyte-Derived Dendritic Cells. *International Journal of Molecular Sciences*, 20(3), 742. <https://doi.org/10.3390/ijms20030742>.
9. Friedrich, M., Sankowski, R., Bunse, L., Kilian, M., Green, E., Ramallo Guevara, C., Pusch, S., Poschet, G., Sanghvi, K., Hahn, M., Bunse, T., Münch, P., Gegner, H. M., Sonner, J. K., von Landenberg, A., Cichon, F., Aslan, K., Trobisch, T., Schirmer, L., ... Platten, M. (2021). Tryptophan metabolism drives dynamic immunosuppressive myeloid states in IDH-mutant gliomas. *Nature Cancer*, 2(7), 723–740. <https://doi.org/10.1038/s43018-021-00201-z>.
10. Notarangelo, G., Spinelli, J. B., Perez, E. M., Baker, G. J., Kurmi, K., Elia, I., Stopka, S. A., Baquer, G., Lin, J.-R., Golby, A. J., Joshi, S., Baron, H. F., Drijvers, J. M., Georgiev, P., Ringel, A. E., Zaganjor, E., McBrayer, S. K., Sorger, P. K., Sharpe, A. H., ... Haigis, M. C. (2022). Oncometabolite R-2HG alters T cell metabolism to impair CD8 + T cell function. *Science*, 377(6614), 1519–1529. <https://doi.org/10.1126/science.abj5104>.
11. Ruiz-Moreno, C., Marco Salas, S., Samuelsson, E., Brandner, S., Kranendonk, M.E., Nilsson, M., Stunnenberg, H.G. Harmonized single-cell landscape, intercellular crosstalk and tumor architecture of glioblastoma. doi: <https://doi.org/10.1101/2022.08.27.505439>.
12. Müller, S., Kohanbash, G., Liu, S. J., Alvarado, B., Carrera, D., Bhaduri, A., Watchmaker, P. B., Yagnik, G., di Lullo, E., Malatesta, M., Amankulor, N. M., Kriegstein, A. R., Lim, D. A., Aghi, M., Okada, H., & Diaz, A. (2017). Single-cell profiling of human gliomas reveals macrophage ontogeny as a basis for regional differences in macrophage

- activation in the tumor microenvironment. *Genome Biology*, 18(1), 234.
<https://doi.org/10.1186/s13059-017-1362-4>.
13. Mantovani, A., Allavena, P., Marchesi, F., & Garlanda, C. (2022). Macrophages as tools and targets in cancer therapy. *Nature Reviews Drug Discovery*, 21(11), 799–820. <https://doi.org/10.1038/s41573-022-00520-5>.
 14. Park, M. D., Silvin, A., Ginhoux, F., & Merad, M. (2022). Macrophages in health and disease. *Cell*, 185(23), 4259–4279. <https://doi.org/10.1016/j.cell.2022.10.007>.
 15. Amit, I., Winter, D. R., & Jung, S. (2016). The role of the local environment and epigenetics in shaping macrophage identity and their effect on tissue homeostasis. *Nature Immunology*, 17(1), 18–25. <https://doi.org/10.1038/ni.3325>.
 16. Bowman, R. L., Klemm, F., Akkari, L., Pyonteck, S. M., Sevenich, L., Quail, D. F., Dhara, S., Simpson, K., Gardner, E. E., Iacobuzio-Donahue, C. A., Brennan, C. W., Tabar, V., Gutin, P. H., & Joyce, J. A. (2016). Macrophage Ontogeny Underlies Differences in Tumor-Specific Education in Brain Malignancies. *Cell Reports*, 17(9), 2445–2459. <https://doi.org/10.1016/j.celrep.2016.10.052>.
 17. Klemm, F., Maas, R. R., Bowman, R. L., Kornete, M., Soukup, K., Nassiri, S., Brouland, J.-P., Iacobuzio-Donahue, C. A., Brennan, C., Tabar, V., Gutin, P. H., Daniel, R. T., Hegi, M. E., & Joyce, J. A. (2020). Interrogation of the Microenvironmental Landscape in Brain Tumors Reveals Disease-Specific Alterations of Immune Cells. *Cell*, 181(7), 1643–1660.e17. <https://doi.org/10.1016/j.cell.2020.05.007>.
 18. Friebel, E., Kapolou, K., Unger, S., Núñez, N. G., Utz, S., Rushing, E. J., Regli, L., Weller, M., Greter, M., Tugues, S., Neidert, M. C., & Becher, B. (2020). Single-Cell Mapping of Human Brain Cancer Reveals Tumor-Specific Instruction of Tissue-Invading Leukocytes. *Cell*, 181(7), 1626–1642.e20. <https://doi.org/10.1016/j.cell.2020.04.055>.
 19. Venteicher, A. S., Tirosh, I., Hebert, C., Yizhak, K., Neftel, C., Filbin, M. G., Hovestadt, V., Escalante, L. E., Shaw, M. L., Rodman, C., Gillespie, S. M., Dionne, D., Luo, C. C., Ravichandran, H., Mylvaganam, R., Mount, C., Onozato, M. L., Nahed, B. v., Wakimoto, H., ... Suvà, M. L. (2017). Decoupling genetics, lineages, and

- microenvironment in IDH-mutant gliomas by single-cell RNA-seq. *Science*, 355(6332). <https://doi.org/10.1126/science.aai8478>.
20. Hara, T., Chanoch-Myers, R., Mathewson, N. D., Myskiw, C., Atta, L., Bussema, L., Eichhorn, S. W., Greenwald, A. C., Kinker, G. S., Rodman, C., Gonzalez Castro, L. N., Wakimoto, H., Rozenblatt-Rosen, O., Zhuang, X., Fan, J., Hunter, T., Verma, I. M., Wucherpennig, K. W., Regev, A., ... Tirosh, I. (2021). Interactions between cancer cells and immune cells drive transitions to mesenchymal-like states in glioblastoma. *Cancer Cell*, 39(6), 779-792.e11. <https://doi.org/10.1016/j.ccell.2021.05.002>.
21. Blanco-Carmona, E., Narayanan, A., Hernandez, I., Nieto, J. C., Elosua-Bayes, M., Sun, X., Schmidt, C., Pamir, N., Özduman, K., Herold-Mende, C., Pagani, F., Cominelli, M., Taranda, J., Wick, W., von Deimling, A., Poliani, P. L., Rehli, M., Schlesner, M., Heyn, H., & Turcan, Ş. (2023). Tumor heterogeneity and tumor-microglia interactions in primary and recurrent IDH1-mutant gliomas. *Cell Reports Medicine*, 4(11), 101249. <https://doi.org/10.1016/j.xcrm.2023.101249>.
22. Gupta, P., Dang, M., Oberai, S., Migliozzi, S., Trivedi, R., Kumar, G., ... & Bhat, K. P. (2024). Immune landscape of isocitrate dehydrogenase-stratified primary and recurrent human gliomas. *Neuro-Oncology*, noae139. doi: <https://doi.org/10.1093/neuonc/noae139>.
23. Miller, E., El Farran, C.A., Couturier, C.P., Chen, Z., D'Antonio, J.P., Verga, J., Villanueva, M.A., Gonzalez Castro, L.N., Tong, Y.E., Saadi, T.A., Chiocca, A.N., Fischer, D.S., Heiland, D.H., Guerriero, J.L., Petrecca, K., Suva, M.L., Shalek, A.K., Bernstein, B.E. (2023). Programs, Origins, and Niches of Immunomodulatory Myeloid Cells in Gliomas. doi: <https://doi.org/10.1101/2023.10.24.563466>.
24. Pombo Antunes, A. R., Scheyltjens, I., Lodi, F., Messiaen, J., Antoranz, A., Duerinck, J., Kancheva, D., Martens, L., de Vlaminck, K., van Hove, H., Kjølner Hansen, S. S., Bosisio, F. M., van der Borght, K., de Vleeschouwer, S., Sciote, R., Bouwens, L., Verfaillie, M., Vandamme, N., Vandenbroucke, R. E., ... Movahedi, K. (2021). Single-cell profiling of myeloid cells in glioblastoma across species and disease stage

- reveals macrophage competition and specialization. *Nature Neuroscience*, 24(4), 595–610. <https://doi.org/10.1038/s41593-020-00789-y>.
25. Yeo, A. T., Rawal, S., Delcuze, B., Christofides, A., Atayde, A., Strauss, L., Balaj, L., Rogers, V. A., Uhlmann, E. J., Varma, H., Carter, B. S., Boussiotis, V. A., & Charest, A. (2022). Single-cell RNA sequencing reveals evolution of immune landscape during glioblastoma progression. *Nature Immunology*, 23(6), 971–984. <https://doi.org/10.1038/s41590-022-01215-0>.
26. Abdelfattah, N., Kumar, P., Wang, C., Leu, J.-S., Flynn, W. F., Gao, R., Baskin, D. S., Pichumani, K., Ijare, O. B., Wood, S. L., Powell, S. Z., Haviland, D. L., Parker Kerrigan, B. C., Lang, F. F., Prabhu, S. S., Huntoon, K. M., Jiang, W., Kim, B. Y. S., George, J., & Yun, K. (2022). Single-cell analysis of human glioma and immune cells identifies S100A4 as an immunotherapy target. *Nature Communications*, 13(1), 767. <https://doi.org/10.1038/s41467-022-28372-y>.
27. Noushmehr, H., Weisenberger, D. J., Diefes, K., Phillips, H. S., Pujara, K., Berman, B. P., Pan, F., Pelloski, C. E., Sulman, E. P., Bhat, K. P., Verhaak, R. G. W., Hoadley, K. A., Hayes, D. N., Perou, C. M., Schmidt, H. K., Ding, L., Wilson, R. K., van den Berg, D., Shen, H., ... Aldape, K. (2010). Identification of a CpG Island Methylator Phenotype that Defines a Distinct Subgroup of Glioma. *Cancer Cell*, 17(5), 510–522. <https://doi.org/10.1016/j.ccr.2010.03.017>.
28. Chuntova, P., Yamamichi, A., Chen, T., Narayanaswamy, R., Ronseaux, S., Hudson, C., Tron, A. E., Hyer, M. L., Montoya, M., Mende, A. L., Nejo, T., Downey, K. M., Diebold, D., Lu, M., Nicolay, B., & Okada, H. (2022). Inhibition of D-2HG leads to upregulation of a proinflammatory gene signature in a novel HLA-A2/HLA-DR1 transgenic mouse model of IDH1R132H-expressing glioma. *Journal for ImmunoTherapy of Cancer*, 10(5), e004644. <https://doi.org/10.1136/jitc-2022-004644>.
29. de Witte, L. D., Wang, Z., Snijders, G. L. J. L., Mendelev, N., Liu, Q., Sneeboer, M. A. M., Boks, M. P. M., Ge, Y., & Haghighi, F. (2022). Contribution of Age, Brain Region, Mood Disorder Pathology, and Interindividual Factors on the Methylome of Human

- Microglia. *Biological Psychiatry*, 91(6), 572–581.
<https://doi.org/10.1016/j.biopsych.2021.10.020>.
30. Zheng, P.-P., van der Weiden, M., van der Spek, P. J., Vincent, A. J. P. E., & Kros, J. M. (2012). Isocitrate dehydrogenase 1R132H mutation in microglia/macrophages in gliomas. *Cancer Biology & Therapy*, 13(10), 836–839.
<https://doi.org/10.4161/cbt.20836>.
31. Ceccarelli, M., Barthel, F. P., Malta, T. M., Sabedot, T. S., Salama, S. R., Murray, B. A., Morozova, O., Newton, Y., Radenbaugh, A., Pagnotta, S. M., Anjum, S., Wang, J., Manyam, G., Zoppoli, P., Ling, S., Rao, A. A., Grifford, M., Cherniack, A. D., Zhang, H., ... Zmuda, E. (2016). Molecular Profiling Reveals Biologically Discrete Subsets and Pathways of Progression in Diffuse Glioma. *Cell*, 164(3), 550–563.
<https://doi.org/10.1016/j.cell.2015.12.028>.
32. Klughammer, J., Kiesel, B., Roetzer, T., Fortelny, N., Nemc, A., Nenning, K.-H., Furtner, J., Sheffield, N. C., Datlinger, P., Peter, N., Nowosielski, M., Augustin, M., Mischkulnig, M., Ströbel, T., Alpar, D., Ergüner, B., Senekowitsch, M., Moser, P., Freyschlag, C. F., ... Bock, C. (2018). The DNA methylation landscape of glioblastoma disease progression shows extensive heterogeneity in time and space. *Nature Medicine*, 24(10), 1611–1624. <https://doi.org/10.1038/s41591-018-0156-x>.
33. Binder, H., Willscher, E., Loeffler-Wirth, H., Hopp, L., Jones, D. T. W., Pfister, S. M., Kreuz, M., Gramatzki, D., Fortenbacher, E., Hentschel, B., Tatagiba, M., Herrlinger, U., Vatter, H., Matschke, J., Westphal, M., Krex, D., Schackert, G., Tonn, J. C., Schlegel, U., ... Loeffler, M. (2019). DNA methylation, transcriptome and genetic copy number signatures of diffuse cerebral WHO grade II/III gliomas resolve cancer heterogeneity and development. *Acta Neuropathologica Communications*, 7(1), 59.
<https://doi.org/10.1186/s40478-019-0704-8>.
34. Andersson, R., Gebhard, C., Miguel-Escalada, I., Hoof, I., Bornholdt, J., Boyd, M., Chen, Y., Zhao, X., Schmidl, C., Suzuki, T., Ntini, E., Arner, E., Valen, E., Li, K., Schwarzfischer, L., Glatz, D., Raithel, J., Lilje, B., Rapin, N., ... Sandelin, A. (2014). An

- atlas of active enhancers across human cell types and tissues. *Nature*, 507(7493), 455–461. <https://doi.org/10.1038/nature12787>.
35. Chaligne, R., Gaiti, F., Silverbush, D., Schiffman, J. S., Weisman, H. R., Kluegel, L., Gritsch, S., Deochand, S. D., Gonzalez Castro, L. N., Richman, A. R., Klughammer, J., Biancalani, T., Muus, C., Sheridan, C., Alonso, A., Izzo, F., Park, J., Rozenblatt-Rosen, O., Regev, A., ... Landau, D. A. (2021). Epigenetic encoding, heritability and plasticity of glioma transcriptional cell states. *Nature Genetics*, 53(10), 1469–1479. <https://doi.org/10.1038/s41588-021-00927-7>.
36. Stadler, M. B., Murr, R., Burger, L., Ivanek, R., Lienert, F., Schöler, A., Nimwegen, E. van, Wirbelauer, C., Oakeley, E. J., Gaidatzis, D., Tiwari, V. K., & Schübeler, D. (2011). DNA-binding factors shape the mouse methylome at distal regulatory regions. *Nature*, 480(7378), 490–495. <https://doi.org/10.1038/nature10716>.
37. Aran, D., Sabato, S., & Hellman, A. (2013). DNA methylation of distal regulatory sites characterizes dysregulation of cancer genes. *Genome Biology*, 14(3), R21. <https://doi.org/10.1186/gb-2013-14-3-r21>.
38. Blattler, A., & Farnham, P. J. (2013). Cross-talk between Site-specific Transcription Factors and DNA Methylation States. *Journal of Biological Chemistry*, 288(48), 34287–34294. <https://doi.org/10.1074/jbc.R113.512517>.
39. Gosselin, D., Skola, D., Coufal, N. G., Holtman, I. R., Schlachetzki, J. C. M., Sajti, E., Jaeger, B. N., O'Connor, C., Fitzpatrick, C., Pasillas, M. P., Pena, M., Adair, A., Gonda, D. D., Levy, M. L., Ransohoff, R. M., Gage, F. H., & Glass, C. K. (2017). An environment-dependent transcriptional network specifies human microglia identity. *Science*, 356(6344). <https://doi.org/10.1126/science.aal3222>.
40. Court, F., le Boiteux, E., Fogli, A., Müller-Barthélémy, M., Vaurs-Barrière, C., Chautard, E., Pereira, B., Biau, J., Kemeny, J.-L., Khalil, T., Karayan-Tapon, L., Verrelle, P., & Arnaud, P. (2019). Transcriptional alterations in glioma result primarily from DNA methylation-independent mechanisms. *Genome Research*, 29(10), 1605–1621. <https://doi.org/10.1101/gr.249219.119>.

41. Müller-Dott, S., Tsirvouli, E., Vazquez, M., Ramirez Flores, R. O., Badia-i-Mompel, P., Fallegger, R., Türei, D., Læg Reid, A., & Saez-Rodriguez, J. (2023). Expanding the coverage of regulons from high-confidence prior knowledge for accurate estimation of transcription factor activities. *Nucleic Acids Research*, 51(20), 10934–10949. <https://doi.org/10.1093/nar/gkad841>.
42. Frattini, V., Pagnotta, S. M., Tala, Fan, J. J., Russo, M. v., Lee, S. B., Garofano, L., Zhang, J., Shi, P., Lewis, G., Sanson, H., Frederick, V., Castano, A. M., Cerulo, L., Rolland, D. C. M., Mall, R., Mokhtari, K., Elenitoba-Johnson, K. S. J., Sanson, M., ... Iavarone, A. (2018). A metabolic function of FGFR3-TACC3 gene fusions in cancer. *Nature*, 553(7687), 222–227. <https://doi.org/10.1038/nature25171>.
43. Yin, Y., Morgunova, E., Jolma, A., Kaasinen, E., Sahu, B., Khund-Sayeed, S., Das, P. K., Kivioja, T., Dave, K., Zhong, F., Nitta, K. R., Taipale, M., Popov, A., Ginno, P. A., Domcke, S., Yan, J., Schübeler, D., Vinson, C., & Taipale, J. (2017). Impact of cytosine methylation on DNA binding specificities of human transcription factors. *Science*, 356(6337). <https://doi.org/10.1126/science.aaj2239>.
44. Suzuki, T., Maeda, S., Furuhashi, E., Shimizu, Y., Nishimura, H., Kishima, M., & Suzuki, H. (2017). A screening system to identify transcription factors that induce binding site-directed DNA demethylation. *Epigenetics & Chromatin*, 10(1), 60. <https://doi.org/10.1186/s13072-017-0169-6>.
45. Yang, J., Zhang, X., Blumenthal, R. M., & Cheng, X. (2020). Detection of DNA Modifications by Sequence-Specific Transcription Factors. *Journal of Molecular Biology*, 432(6), 1661–1673. <https://doi.org/10.1016/j.jmb.2019.09.013>.
46. Spruijt, C. G., Gnerlich, F., Smits, A. H., Pfaffeneder, T., Jansen, P. W. T. C., Bauer, C., Münzel, M., Wagner, M., Müller, M., Khan, F., Eberl, H. C., Mensinga, A., Brinkman, A. B., Lephikov, K., Müller, U., Walter, J., Boelens, R., van Ingen, H., Leonhardt, H., ... Vermeulen, M. (2013). Dynamic Readers for 5-(Hydroxy)Methylcytosine and Its Oxidized Derivatives. *Cell*, 152(5), 1146–1159. <https://doi.org/10.1016/j.cell.2013.02.004>

47. Wu, X., & Zhang, Y. (2017). TET-mediated active DNA demethylation: mechanism, function and beyond. *Nature Reviews Genetics*, 18(9), 517–534.
<https://doi.org/10.1038/nrg.2017.33>.
48. Turcan, S., Rohle, D., Goenka, A., Walsh, L. A., Fang, F., Yilmaz, E., Campos, C., Fabius, A. W. M., Lu, C., Ward, P. S., Thompson, C. B., Kaufman, A., Guryanova, O., Levine, R., Heguy, A., Viale, A., Morris, L. G. T., Huse, J. T., Mellinghoff, I. K., & Chan, T. A. (2012). IDH1 mutation is sufficient to establish the glioma hypermethylator phenotype. *Nature*, 483(7390), 479–483. <https://doi.org/10.1038/nature10866>.
49. Tewari, M., Khan, M., Verma, M., Coppens, J., Kemp, J. M., Bucholz, R., Mercier, P., & Egan, T. M. (2021). Physiology of Cultured Human Microglia Maintained in a Defined Culture Medium. *ImmunoHorizons*, 5(4), 257–272.
<https://doi.org/10.4049/immunohorizons.2000101>.
50. Pidsley, R., Zotenko, E., Peters, T. J., Lawrence, M. G., Risbridger, G. P., Molloy, P., van Dijk, S., Muhlhausler, B., Stirzaker, C., & Clark, S. J. (2016). Critical evaluation of the Illumina MethylationEPIC BeadChip microarray for whole-genome DNA methylation profiling. *Genome Biology*, 17(1), 208. <https://doi.org/10.1186/s13059-016-1066-1>.
51. Ginno, P. A., Gaidatzis, D., Feldmann, A., Hoerner, L., Imanci, D., Burger, L., Zilbermann, F., Peters, A. H. F. M., Edenhofer, F., Smallwood, S. A., Krebs, A. R., & Schübeler, D. (2020). A genome-scale map of DNA methylation turnover identifies site-specific dependencies of DNMT and TET activity. *Nature Communications*, 11(1), 2680. <https://doi.org/10.1038/s41467-020-16354-x>.
52. Sun, Z., Vaisvila, R., Hussong, L.-M., Yan, B., Baum, C., Saleh, L., Samaranayake, M., Guan, S., Dai, N., Corrêa, I. R., Pradhan, S., Davis, T. B., Evans, T. C., & Ettwiller, L. M. (2021). Nondestructive enzymatic deamination enables single-molecule long-read amplicon sequencing for the determination of 5-methylcytosine and 5-hydroxymethylcytosine at single-base resolution. *Genome Research*, 31(2), 291–300.
<https://doi.org/10.1101/gr.265306.120>.
53. Yu, M., Hon, G. C., Szulwach, K. E., Song, C.-X., Zhang, L., Kim, A., Li, X., Dai, Q., Shen, Y., Park, B., Min, J.-H., Jin, P., Ren, B., & He, C. (2012). Base-Resolution Analysis of 5-

- Hydroxymethylcytosine in the Mammalian Genome. *Cell*, 149(6), 1368–1380.
<https://doi.org/10.1016/j.cell.2012.04.027>.
54. Kaikkonen, M. U., Spann, N. J., Heinz, S., Romanoski, C. E., Allison, K. A., Stender, J. D., Chun, H. B., Tough, D. F., Prinjha, R. K., Benner, C., & Glass, C. K. (2013). Remodeling of the Enhancer Landscape during Macrophage Activation Is Coupled to Enhancer Transcription. *Molecular Cell*, 51(3), 310–325.
<https://doi.org/10.1016/j.molcel.2013.07.010>.
55. Spitzer, A., Gritsch, S., Nomura, M., Jucht, A., Fortin, J., Raviram, R., Weisman, H. R., Gonzalez Castro, L. N., Druck, N., Chanoch-Myers, R., Lee, J. J. Y., Mylvaganam, R., Lee Servis, R., Fung, J. M., Lee, C. K., Nagashima, H., Miller, J. J., Arrillaga-Romany, I., Louis, D. N., ... Tirosh, I. (2024). Mutant IDH inhibitors induce lineage differentiation in IDH-mutant oligodendroglioma. *Cancer Cell*, 42(5), 904-914.e9.
<https://doi.org/10.1016/j.ccell.2024.03.008>.
56. Lund, H., Pieber, M., Parsa, R., Han, J., Grommisch, D., Ewing, E., Kular, L., Needhamsen, M., Espinosa, A., Nilsson, E., Överby, A. K., Butovsky, O., Jagodic, M., Zhang, X.-M., & Harris, R. A. (2018). Competitive repopulation of an empty microglial niche yields functionally distinct subsets of microglia-like cells. *Nature Communications*, 9(1), 4845. <https://doi.org/10.1038/s41467-018-07295-7>.
57. Keshet, I., Lieman-Hurwitz, J., & Cedar, H. (1986). DNA methylation affects the formation of active chromatin. *Cell*, 44(4), 535–543. [https://doi.org/10.1016/0092-8674\(86\)90263-1](https://doi.org/10.1016/0092-8674(86)90263-1).
58. Lee, J. Y., & Lee, T.-H. (2012). Effects of DNA Methylation on the Structure of Nucleosomes. *Journal of the American Chemical Society*, 134(1), 173–175.
<https://doi.org/10.1021/ja210273w>.
59. Rao, S., Chiu, T.-P., Kribelbauer, J. F., Mann, R. S., Bussemaker, H. J., & Rohs, R. (2018). Systematic prediction of DNA shape changes due to CpG methylation explains epigenetic effects on protein–DNA binding. *Epigenetics & Chromatin*, 11(1), 6.
<https://doi.org/10.1186/s13072-018-0174-4>.

60. Kreibich, E., Kleinendorst, R., Barzaghi, G., Kaspar, S., & Krebs, A. R. (2023). Single-molecule footprinting identifies context-dependent regulation of enhancers by DNA methylation. *Molecular Cell*, 83(5), 787–802.e9.
<https://doi.org/10.1016/j.molcel.2023.01.017>.
61. Luoto, S., Hermelo, I., Vuorinen, E. M., Hannus, P., Kesseli, J., Nykter, M., & Granberg, K. J. (2018). Computational Characterization of Suppressive Immune Microenvironments in Glioblastoma. *Cancer Research*, 78(19), 5574–5585.
<https://doi.org/10.1158/0008-5472.CAN-17-3714>.
62. Nott, A., Holtman, I. R., Coufal, N. G., Schlachetzki, J. C. M., Yu, M., Hu, R., Han, C. Z., Pena, M., Xiao, J., Wu, Y., Keulen, Z., Pasillas, M. P., O'Connor, C., Nickl, C. K., Schafer, S. T., Shen, Z., Rissman, R. A., Brewer, J. B., Gosselin, D., ... Glass, C. K. (2019). Brain cell type-specific enhancer-promoter interactome maps and disease - risk association. *Science*, 366(6469), 1134–1139.
<https://doi.org/10.1126/science.aay0793>.
63. Cheng, S.-C., Quintin, J., Cramer, R. A., Shepardson, K. M., Saeed, S., Kumar, V., Giamarellos-Bourboulis, E. J., Martens, J. H. A., Rao, N. A., Aghajani-refah, A., Manjeri, G. R., Li, Y., Ifrim, D. C., Arts, R. J. W., van der Veer, B. M. J. W., Deen, P. M. T., Logie, C., O'Neill, L. A., Willems, P., ... Netea, M. G. (2014). mTOR- and HIF-1 α -mediated aerobic glycolysis as metabolic basis for trained immunity. *Science*, 345(6204).
<https://doi.org/10.1126/science.1250684>.
64. Palsson-McDermott, E. M., Curtis, A. M., Goel, G., Lauterbach, M. A. R., Sheedy, F. J., Gleeson, L. E., van den Bosch, M. W. M., Quinn, S. R., Domingo-Fernandez, R., Johnston, D. G. W., Jiang, J., Israelsen, W. J., Keane, J., Thomas, C., Clish, C., Vander Heiden, M., Xavier, R. J., & O'Neill, L. A. J. (2015). Pyruvate Kinase M2 Regulates Hif-1 α Activity and IL-1 β Induction and Is a Critical Determinant of the Warburg Effect in LPS-Activated Macrophages. *Cell Metabolism*, 21(1), 65–80.
<https://doi.org/10.1016/j.cmet.2014.12.005>.

65. Corcoran, S. E., & O'Neill, L. A. J. (2016). HIF1 α and metabolic reprogramming in inflammation. *Journal of Clinical Investigation*, 126(10), 3699–3707.
<https://doi.org/10.1172/JCI84431>.
66. Sangineto, M., Ciarnelli, M., Cassano, T., Radesco, A., Moola, A., Bukke, V. N., Romano, A., Villani, R., Kanwal, H., Capitano, N., Duda, L., Avolio, C., & Serviddio, G. (2023). Metabolic reprogramming in inflammatory microglia indicates a potential way of targeting inflammation in Alzheimer's disease. *Redox Biology*, 66, 102846.
<https://doi.org/10.1016/j.redox.2023.102846>.
67. Chesnelong, C., Chaumeil, M. M., Blough, M. D., Al-Najjar, M., Stechishin, O. D., Chan, J. A., Pieper, R. O., Ronen, S. M., Weiss, S., Luchman, H. A., & Cairncross, J. G. (2014). Lactate dehydrogenase A silencing in IDH mutant gliomas. *Neuro-Oncology*, 16(5), 686–695. <https://doi.org/10.1093/neuonc/not243>.
68. Koivunen, P., Lee, S., Duncan, C. G., Lopez, G., Lu, G., Ramkissoon, S., Losman, J. A., Joensuu, P., Bergmann, U., Gross, S., Travins, J., Weiss, S., Looper, R., Ligon, K. L., Verhaak, R. G. W., Yan, H., & Kaelin Jr, W. G. (2012). Transformation by the (R)-enantiomer of 2-hydroxyglutarate linked to EGLN activation. *Nature*, 483(7390), 484–488. <https://doi.org/10.1038/nature10898>
69. Lavin, Y., Winter, D., Blecher-Gonen, R., David, E., Keren-Shaul, H., Merad, M., Jung, S., & Amit, I. (2014). Tissue-Resident Macrophage Enhancer Landscapes Are Shaped by the Local Microenvironment. *Cell*, 159(6), 1312–1326.
<https://doi.org/10.1016/j.cell.2014.11.018>.
70. Gosselin, D., Link, V. M., Romanoski, C. E., Fonseca, G. J., Eichenfield, D. Z., Spann, N. J., Stender, J. D., Chun, H. B., Garner, H., Geissmann, F., & Glass, C. K. (2014). Environment Drives Selection and Function of Enhancers Controlling Tissue-Specific Macrophage Identities. *Cell*, 159(6), 1327–1340.
<https://doi.org/10.1016/j.cell.2014.11.023>.
71. Troutman, T. D., Kofman, E., & Glass, C. K. (2021). Exploiting dynamic enhancer landscapes to decode macrophage and microglia phenotypes in health and disease. *Molecular Cell*, 81(19), 3888–3903. <https://doi.org/10.1016/j.molcel.2021.08.004>.

72. Parry, A., Rulands, S., & Reik, W. (2021). Active turnover of DNA methylation during cell fate decisions. *Nature Reviews Genetics*, 22(1), 59–66.
<https://doi.org/10.1038/s41576-020-00287-8>.
73. Onodera, A., González-Avalos, E., Lio, C.-W. J., Georges, R. O., Bellacosa, A., Nakayama, T., & Rao, A. (2021). Roles of TET and TDG in DNA demethylation in proliferating and non-proliferating immune cells. *Genome Biology*, 22(1), 186.
<https://doi.org/10.1186/s13059-021-02384-1>.
74. Vats, D., Mukundan, L., Odegaard, J. I., Zhang, L., Smith, K. L., Morel, C. R., Greaves, D. R., Murray, P. J., & Chawla, A. (2006). Oxidative metabolism and PGC-1 β attenuate macrophage-mediated inflammation. *Cell Metabolism*, 4(1), 13–24.
<https://doi.org/10.1016/j.cmet.2006.05.011>.
75. Huang, S. C.-C., Everts, B., Ivanova, Y., O’Sullivan, D., Nascimento, M., Smith, A. M., Beatty, W., Love-Gregory, L., Lam, W. Y., O’Neill, C. M., Yan, C., Du, H., Abumrad, N. A., Urban, J. F., Artyomov, M. N., Pearce, E. L., & Pearce, E. J. (2014). Cell-intrinsic lysosomal lipolysis is essential for alternative activation of macrophages. *Nature Immunology*, 15(9), 846–855. <https://doi.org/10.1038/ni.2956>.
76. Sabogal-Guáqueta, A. M., Marmolejo-Garza, A., Trombetta-Lima, M., Oun, A., Hunneman, J., Chen, T., Koistinaho, J., Lehtonen, S., Kortholt, A., Wolters, J. C., Bakker, B. M., Eggen, B. J. L., Boddeke, E., & Dolga, A. (2023). Species-specific metabolic reprogramming in human and mouse microglia during inflammatory pathway induction. *Nature Communications*, 14(1), 6454. <https://doi.org/10.1038/s41467-023-42096-7>.
77. Han, C., Zheng, J., Sun, L., Yang, H., Cao, Z., Zhang, X., Zheng, L., & Zhen, X. (2019). The oncometabolite 2-hydroxyglutarate inhibits microglial activation via the AMPK/mTOR/NF- κ B pathway. *Acta Pharmacologica Sinica*, 40(10), 1292–1302.
<https://doi.org/10.1038/s41401-019-0225-9>.
78. Mellinghoff, I. K., Lu, M., Wen, P. Y., Taylor, J. W., Maher, E. A., Arrillaga-Romany, I., Peters, K. B., Ellingson, B. M., Rosenblum, M. K., Chun, S., Le, K., Tassinari, A., Choe, S., Toubouti, Y., Schoenfeld, S., Pandya, S. S., Hassan, I., Steelman, L., Clarke, J. L., &

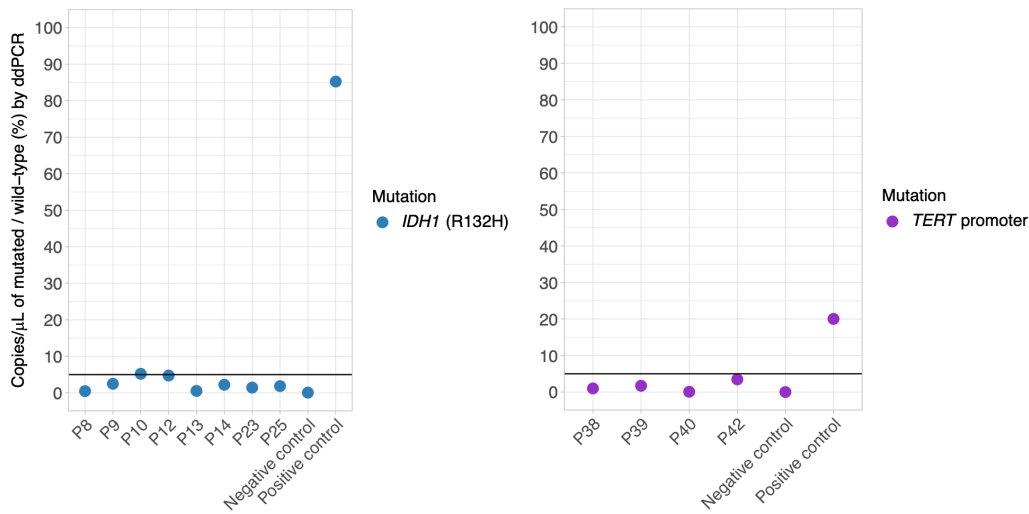
- Cloughesy, T. F. (2023). Vorasidenib and ivosidenib in IDH1-mutant low-grade glioma: a randomized, perioperative phase 1 trial. *Nature Medicine*, 29(3), 615–622. <https://doi.org/10.1038/s41591-022-02141-2>.
79. di Stefano, A. L., Picca, A., Saragoussi, E., Bielle, F., Ducray, F., Villa, C., Eoli, M., Paterra, R., Bellu, L., Mathon, B., Capelle, L., Bourg, V., Gloaguen, A., Philippe, C., Frouin, V., Schmitt, Y., Lerond, J., Leclerc, J., Lasorella, A., ... Sanson, M. (2020). Clinical, molecular, and radiomic profile of gliomas with FGFR3-TACC3 fusions. *Neuro-Oncology*, 22(11), 1614–1624. <https://doi.org/10.1093/neuonc/noaa121>.
80. Teschendorff, A. E. (2020). A comparison of epigenetic mitotic-like clocks for cancer risk prediction. *Genome Medicine*, 12(1), 56. <https://doi.org/10.1186/s13073-020-00752-3>.
81. Heinz, S., Benner, C., Spann, N., Bertolino, E., Lin, Y. C., Laslo, P., Cheng, J. X., Murre, C., Singh, H., & Glass, C. K. (2010). Simple Combinations of Lineage-Determining Transcription Factors Prime cis-Regulatory Elements Required for Macrophage and B Cell Identities. *Molecular Cell*, 38(4), 576–589. <https://doi.org/10.1016/j.molcel.2010.05.004>.
82. Vorontsov, I. E., Eliseeva, I. A., Zinkevich, A., Nikonov, M., Abramov, S., Boytsov, A., Kamenets, V., Kasianova, A., Kolmykov, S., Yevshin, I. S., Favorov, A., Medvedeva, Y. A., Jolma, A., Kolpakov, F., Makeev, V. J., & Kulakovskiy, I. V. (2024). HOCOMOCO in 2024: a rebuild of the curated collection of binding models for human and mouse transcription factors. *Nucleic Acids Research*, 52(D1), D154–D163. <https://doi.org/10.1093/nar/gkad1077>.
83. Balss, J., Pusch, S., Beck, A.-C., Herold-Mende, C., Krämer, A., Thiede, C., Buckel, W., Langhans, C.-D., Okun, J. G., & von Deimling, A. (2012). Enzymatic assay for quantitative analysis of (d)-2-hydroxyglutarate. *Acta Neuropathologica*, 124(6), 883–891. <https://doi.org/10.1007/s00401-012-1060-y>.
84. Ewing, A. D., Smits, N., Sanchez-Luque, F. J., Faivre, J., Brennan, P. M., Richardson, S. R., Cheetham, S. W., & Faulkner, G. J. (2020). Nanopore Sequencing Enables

- Comprehensive Transposable Element Epigenomic Profiling. *Molecular Cell*, 80(5), 915-928.e5. <https://doi.org/10.1016/j.molcel.2020.10.024>.
85. Akalin, A., Kormaksson, M., Li, S., Garrett-Bakelman, F. E., Figueroa, M. E., Melnick, A., & Mason, C. E. (2012). methylKit: a comprehensive R package for the analysis of genome-wide DNA methylation profiles. *Genome Biology*, 13(10), R87. <https://doi.org/10.1186/gb-2012-13-10-r87>
86. Pagès H, Aboyou P, Gentleman R, DebRoy S (2024). Biostrings: Efficient manipulation of biological strings. R package version 2.72.0, <https://bioconductor.org/packages/Biostrings>
87. Schmittgen, T. D., & Livak, K. J. (2008). Analyzing real-time PCR data by the comparative CT method. *Nature Protocols*, 3(6), 1101–1108. <https://doi.org/10.1038/nprot.2008.73>.
88. Hao, Y., Stuart, T., Kowalski, M. H., Choudhary, S., Hoffman, P., Hartman, A., Srivastava, A., Molla, G., Madad, S., Fernandez-Granda, C., & Satija, R. (2024). Dictionary learning for integrative, multimodal and scalable single-cell analysis. *Nature Biotechnology*, 42(2), 293–304. <https://doi.org/10.1038/s41587-023-01767-y>.
89. Wickham, H., & Wickham, H. (2016). Data analysis (pp. 189-201). Springer International Publishing. doi.org/10.1007/978-3-319-24277-4_9.
90. Ahlmann-Eltze, C., & Patil, I. (2021). ggsignif: R Package for Displaying Significance Brackets for 'ggplot2'. *PsyArxiv*. doi.org/10.31234/osf.io/7awm6.
91. Gu, Z. (2022). Complex Heatmap Visualization, *iMeta*. doi.org/10.1002/imt2.43.
92. Shannon, P., Markiel, A., Ozier, O., Baliga, N. S., Wang, J. T., Ramage, D., ... & Ideker, T. (2003). Cytoscape: a software environment for integrated models of biomolecular interaction networks. *Genome research*, 13(11), 2498-2504. doi.org/10.1101/gr.1239303.
93. Wu, T., Hu, E., Xu, S., Chen, M., Guo, P., Dai, Z., ... & Yu, G. (2021). clusterProfiler 4.0: A universal enrichment tool for interpreting omics data. *The innovation*, 2(3). doi.org/10.1016/j.xinn.2021.100141.

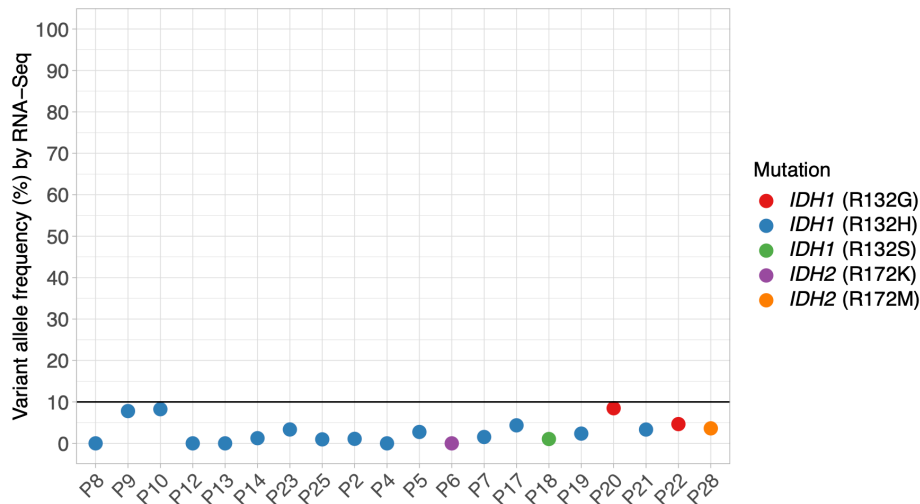
94. Larsson J. (2024). eulerr: Area-Proportional Euler and Venn Diagrams with Ellipses. R package version 7.0.0, <https://CRAN.R-project.org/package=eulerr>.
95. Subramanian, A., Tamayo, P., Mootha, V. K., Mukherjee, S., Ebert, B. L., Gillette, M. A., ... & Mesirov, J. P. (2005). Gene set enrichment analysis: a knowledge-based approach for interpreting genome-wide expression profiles. *Proceedings of the National Academy of Sciences*, 102(43), 15545-15550. doi.org/10.1073/pnas.0506580102.
96. Liberzon, A., Birger, C., Thorvaldsdóttir, H., Ghandi, M., Mesirov, J. P., & Tamayo, P. (2015). The molecular signatures database hallmark gene set collection. *Cell systems*, 1(6), 417-425. doi.org/10.1016/j.cels.2015.12.004.
97. Khanna, A., Larson, D., Srivatsan, S., Mosior, M., Abbott, T., Kiwala, S., ... & Miller, C. (2022). Bam-readcount - rapid generation of basepair-resolution sequence metrics. *The Journal of Open Source Software*, 7(69), 3722. doi.org/10.21105/joss.03722.
98. Aaronson, J., Beaumont, V., Blevins, R. A., Andreeva, V., Murasheva, I., Shneyderman, A., ... & Vogt, T. F. (2021). HDinHD: A rich data portal for Huntington's disease research. *Journal of Huntington's Disease*, 10(3), 405-412. doi.org/10.3233/JHD-210491.

Extended data

A

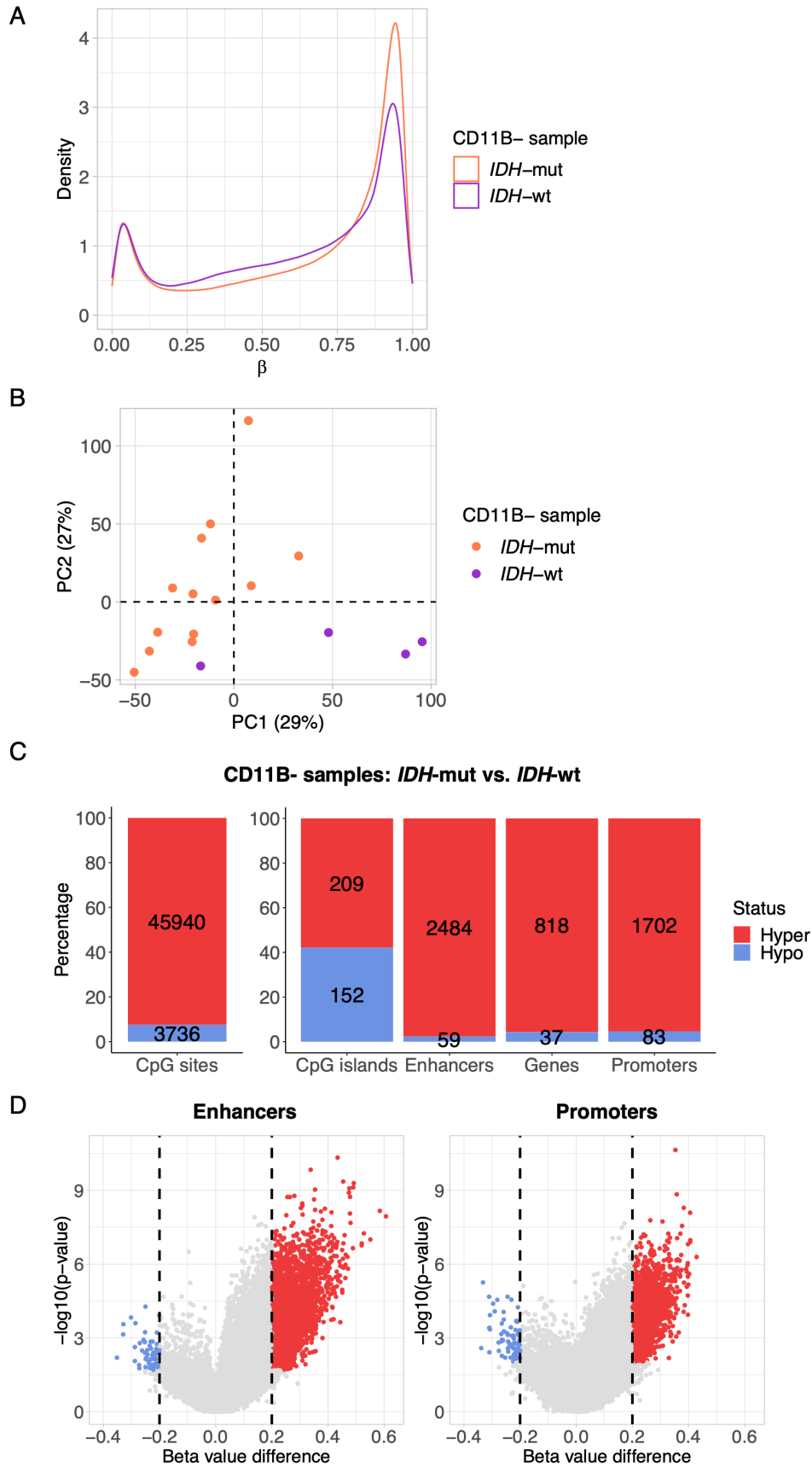


B

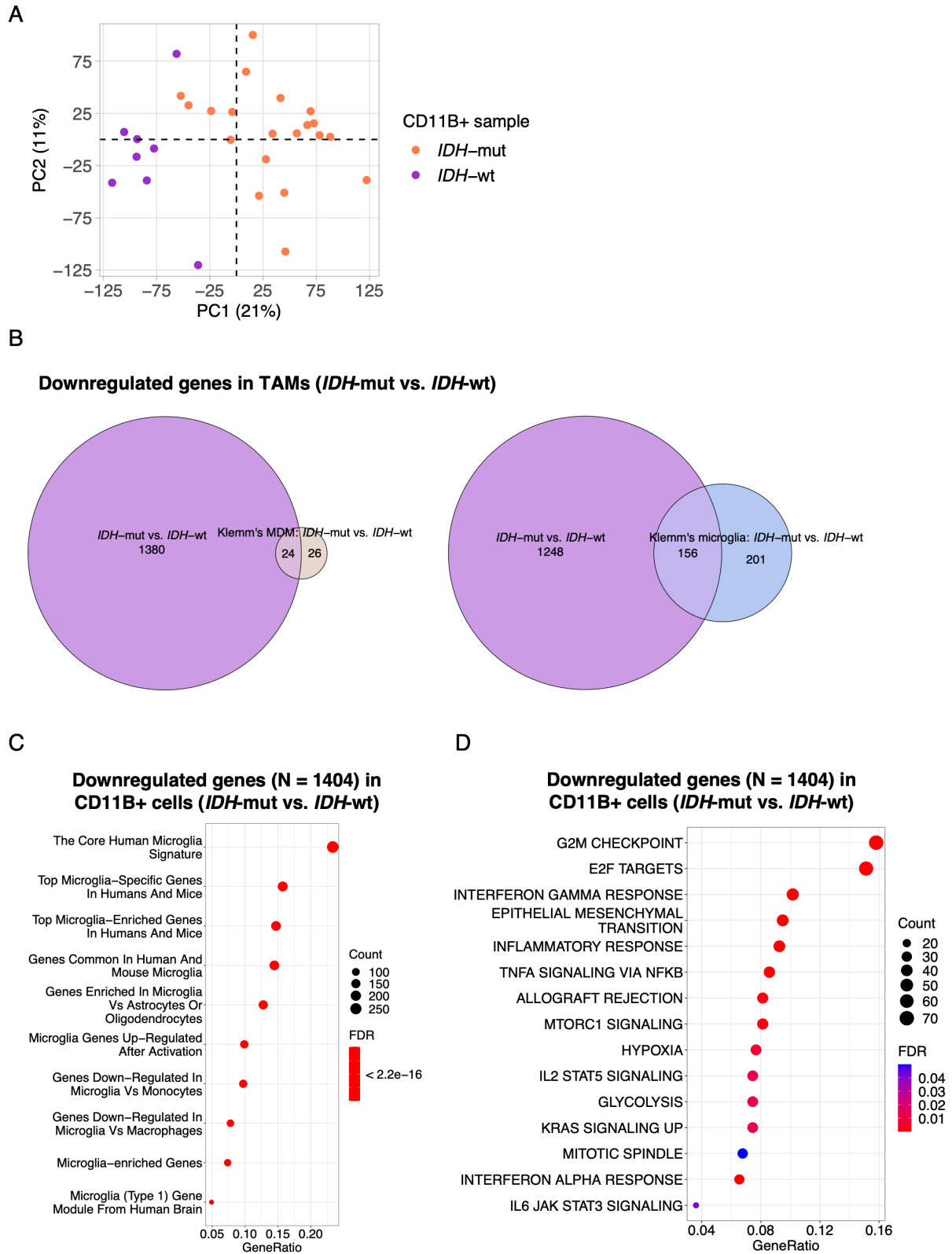


Extended Data Fig. 1. Purity of CD11B+ myeloid fractions isolated from human gliomas. (A) Digital droplet PCR (ddPCR) performed with specific assays to evaluate IDH1 R132H, TERT promoter mutations C228T/C250T, and corresponding wildtype alleles in available DNAs from CD11B+ samples (n=12) isolated from human gliomas with known

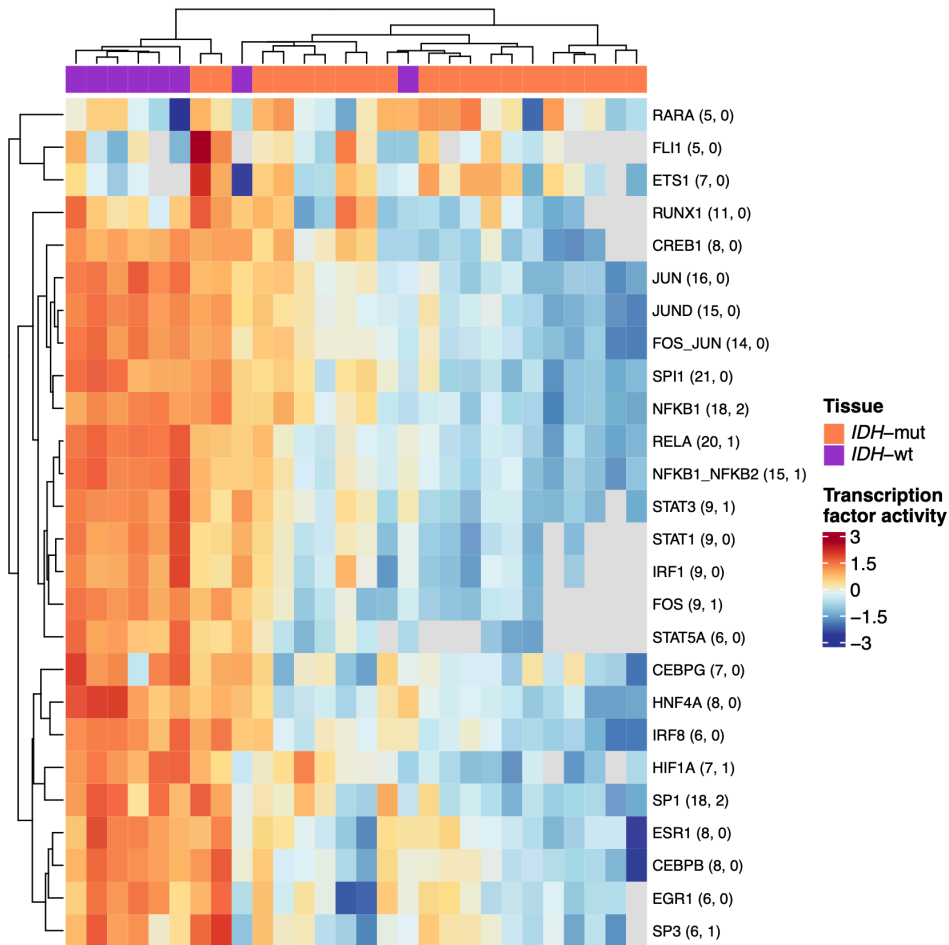
mutation status. Less than 5% copies/ μL of the indicated mutations relative to their corresponding wildtype alleles were detected in the same reaction for each analyzed sample. Positive and negative controls from bulk tumors for each assay are also shown. The detection of IDHmut and TERT mutations in positive controls differs, possibly reflecting regional clonal heterogeneity. **(B)** Expression frequency of IDH mutated alleles was assessed in RNA-seq data from CD11B+ samples (n=20) isolated from human gliomas with known mutation status using bam-readcount⁹⁷. Compared to ddPCR, this analysis slightly overestimated the contamination in samples P9 and P10.



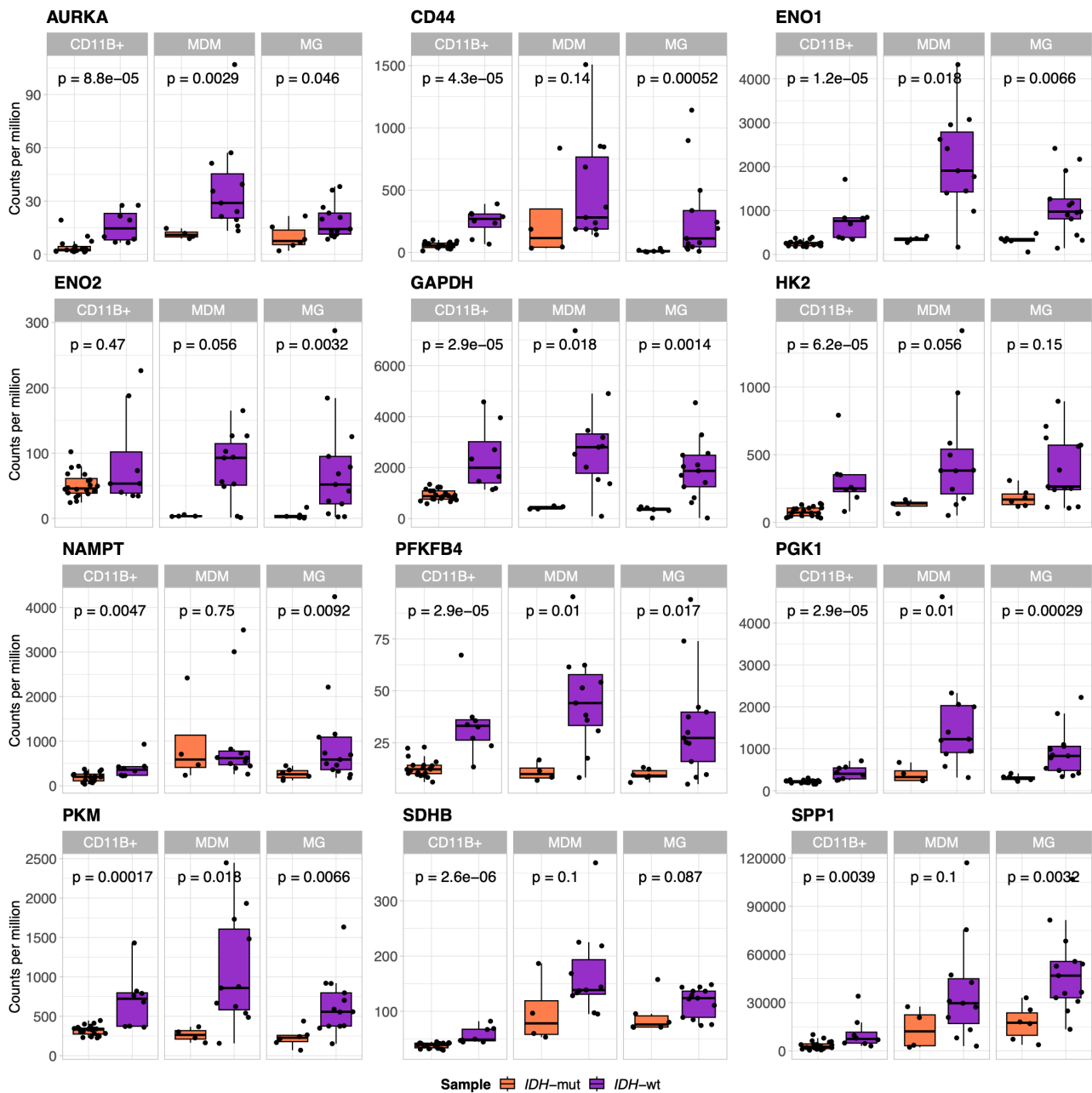
Extended Data Fig. 2. CD11B- fractions enriched of glioma cells display global DNA hypermethylation in IDH^{mut} gliomas. (A) Density plot of DNA methylation levels (β -values) in glioma cells-enriched CD11B- fractions isolated from IDH^{mut} (n=13) and IDH^{wt} (n=4) tumors. **(B)** Principal component analysis performed using methylome data from around 600,000 CpG sites across the genome in CD11B- samples from the study cohort. **(C)** Stacked bar charts show absolute numbers and relative percentages of CpG sites and of four functional genomic regions respect to the methylation status in the CD11B- samples from IDH^{mut} vs. IDH^{wt} tumors. **(D)** Volcano plots depict the magnitude and extent of differentially methylated changes (colored red and blue) located at enhancers and promoters in CD11B- samples from IDH^{mut} vs. IDH^{wt} tumors.



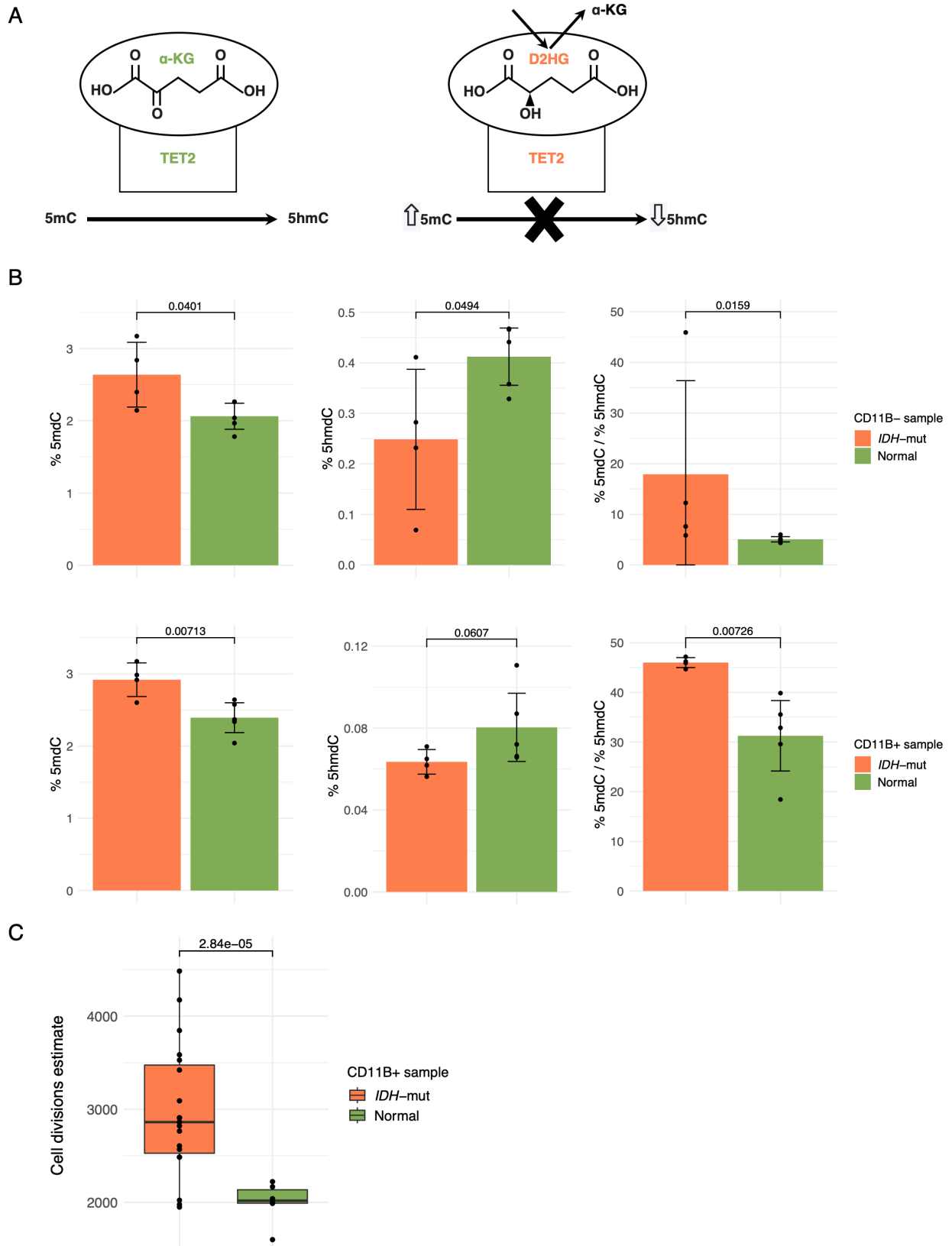
Extended Data Fig. 3. Genes with reduced expression in CD11B+ cells from IDH^{mut} human gliomas belong to microglial signatures. **(A)** Principal component analysis performed using RNA-seq data from *ex vivo* CD11B+ myeloid cells isolated from IDH^{mut} (n=20) and IDH^{wt} (n=8) tumors. **(B)** Venn diagrams illustrate significant overlaps between downregulated genes displayed by CD11B+ cells fraction from IDH^{mut} gliomas (this study), and downregulated genes displayed by MDMs (left) or microglial cells (right) in Klemm et al. study. P-values were computed using overrepresentation analysis (ORA). **(C)** Enrichment analysis of the downregulated genes in CD11B+ cells fraction from IDH^{mut} gliomas in the present study using HDinHD microglia signatures dataset⁹⁸. **(D)** Enrichment analysis of the downregulated genes in CD11B+ cells fraction from IDH^{mut} gliomas (this study) using hallmark signatures dataset.



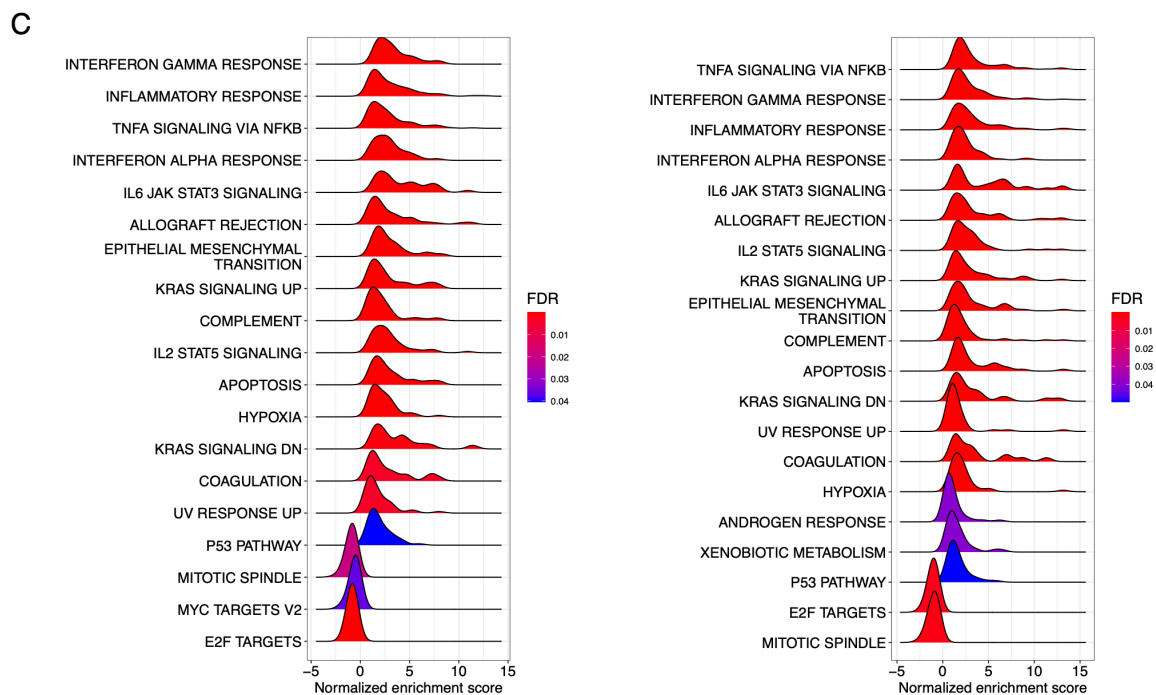
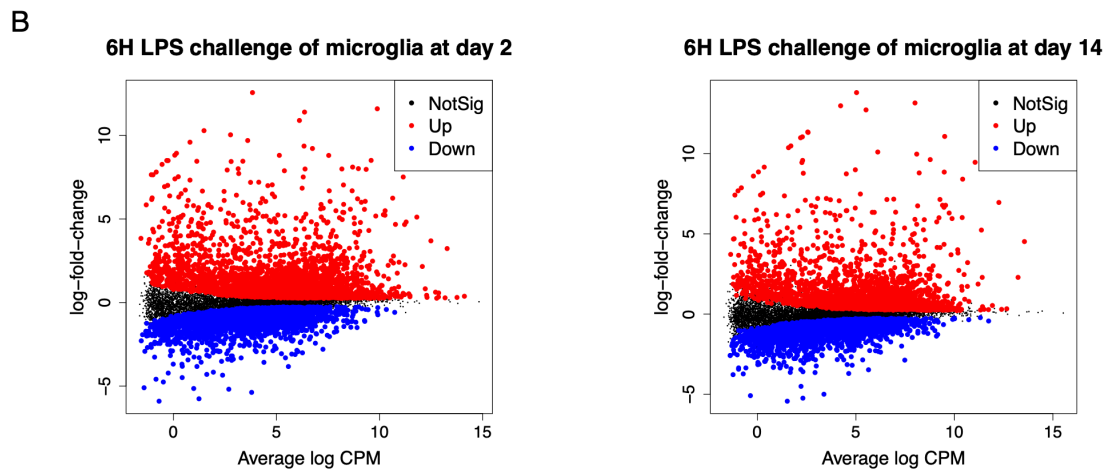
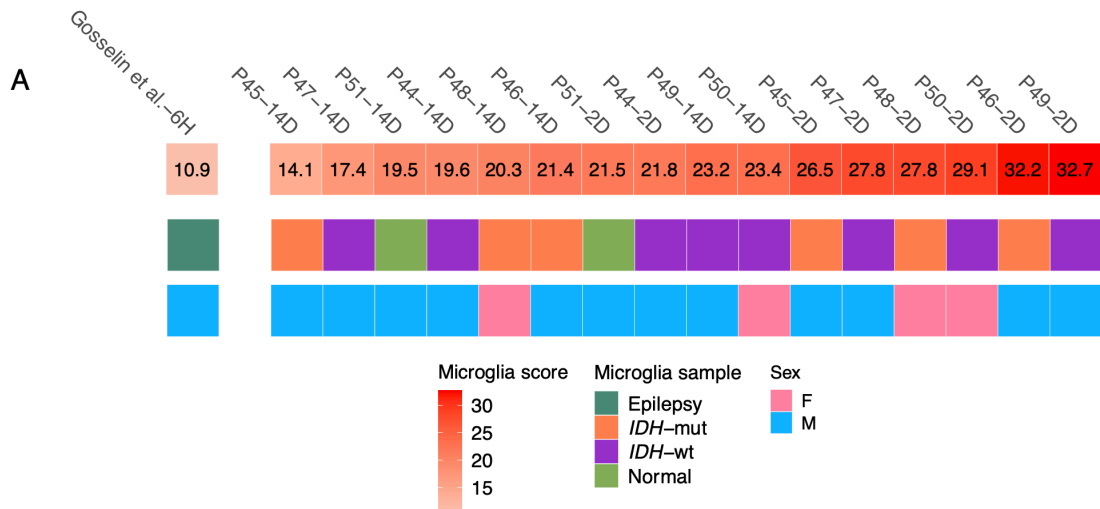
Extended Data Fig. 4. Transcription factors activity controlling genes with hypermethylated promoter in CD11B+ cells from human gliomas. The heatmap depicts TFs (n=26) exhibiting differential activity (FDR <0.05; Wilcoxon's test) in CD11B+ cells according with the IDH mutation status of corresponding tumors. The TF targets used for this analysis, retrieved from the CollecTRI database, were searched among the genes displaying hypermethylation at promoters in CD11B+ cells fraction from IDH^{mut} vs. IDH^{wt} comparison (Fig. 1D). The number of targets regulated positively and negatively by each TF is shown in brackets. Unsupervised clustering was performed using the z-scores of TF activity, where red and blue colors indicate high and low activity, respectively. Non-significant activity is shown in gray.



Extended Data Fig. 5. Positive targets of HIF1A/MYC display low expression in microglia and MDMs from IDH^{mut} gliomas. Box plots showing normalized RNA-seq expression data for representative targets of HIF1A/MYC in CD11B⁺ myeloid cells from the present study cohort (IDH^{mut}, n=20 vs. IDH^{wt}, n=8), as well as in myeloid cells from the Klemm et al. study comprising MDMs (IDH^{mut}, n=4 vs. IDH^{wt}, n=11) and microglia (IDH^{mut}, n=6 vs. IDH^{wt}, n=13) used as validation set. P-values were computed using Wilcoxon's test.



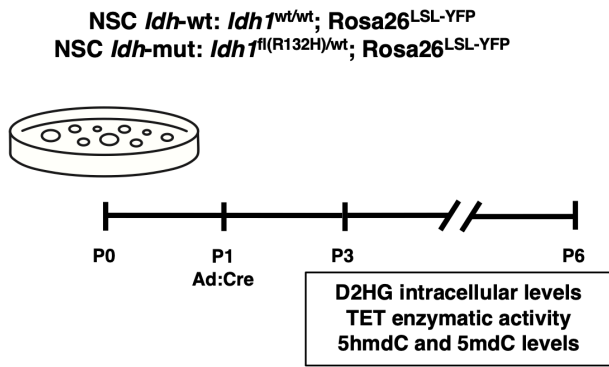
Extended Data Fig. 6. LC-MS/MS analysis of 5mC and 5hmC genomic content and cell divisions estimate in CD11B+ myeloid cells from IDH^{mut} gliomas and normal brain tissues. **(A)** Schematic representation of α -KG-dependent enzymatic oxidation of 5mC by TET2 and effect of competitive inhibition of TET2 by D-2HG over time in bulk IDH^{mut} gliomas. **(B)** Global levels of 5mC and 5hmC (left) and 5mC/5hmC ratios (right) were measured in CD11B- (upper) and CD11B+ (bottom) fractions from IDH^{mut} gliomas (n=4) and from normal tissues collected during epilepsy surgery (n=5), which served as controls for comparisons. Data are represented as the mean with a 95% CI; p-values were calculated using one-sided Welch's test except for comparison of ratios in CD11B- (one-sided Wilcoxon's test). **(C)** Epigenetic mitotic clock analysis was conducted by applying the epiTOC2⁸⁰ model to methylome data (EPIC arrays) of CD11B+ fractions from IDH^{mut} gliomas (n=19) and from normal brain tissues (n=6). The model (adjusted by age) estimates the cumulative number of stem cell divisions in the myeloid compartment. The p-value was calculated using Welch's test.



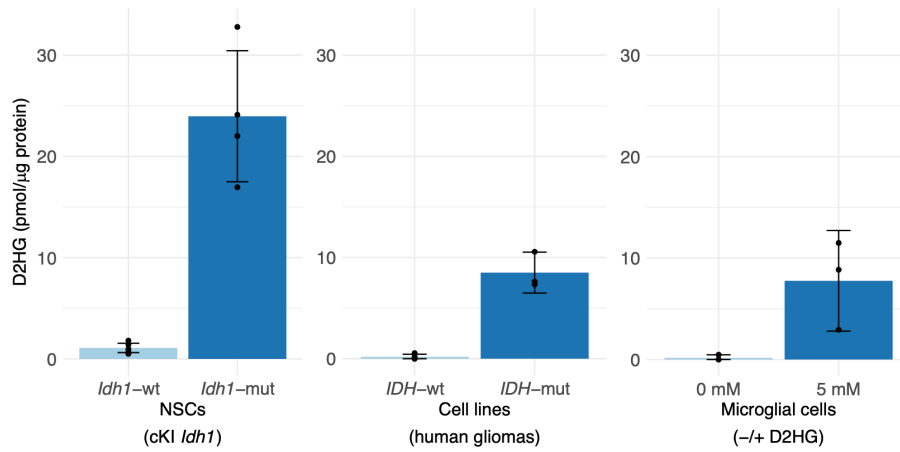
Extended Data Fig. 7. Assessment of the functionality of primary microglial cultures.

(A) Analysis of a human microglia signature at 2 days (2D) and 14 days (14D) using RNA-seq data from eight independent primary cultures. A microglial score was determined as follows: we took the microglia signature genes and the raw gene expression matrix from Gosselin et al³⁹. Subsequently, after normalizing the expression data, we calculated the median of the differences of each gene from the microglia signature in our samples with respect to the five negative samples used as controls in Gosselin et al. study. Microglia score was defined as the average of these five medians. The plot (upper), showing such microglia score per sample, demonstrates that the signature is nearly twice as high, even at 14 days of culture, when using defined culture conditions (as in our study), in comparison to the study by Gosselin et al. study (culture shock at 6 hours), irrespective of tissue origin and sex (as indicated at the bottom). **(B)** The plots illustrate expression changes using four primary microglial cultures analyzed with RNA-seq in a paired manner, 6 hours after LPS stimulation at 2 days (left) and 14 days (right). Red and blue colors indicate upregulation and downregulation, respectively, with FDR <0.05, in LPS-stimulated microglia vs. control. **(C)** Ridge plots illustrate hallmark gene sets GSEA analyses in LPS-stimulated microglia at 2 days (left) and 14 days (right) of culture. Activated (>0) and inactivated (<0) gene sets with FDR < 0.05 are shown.

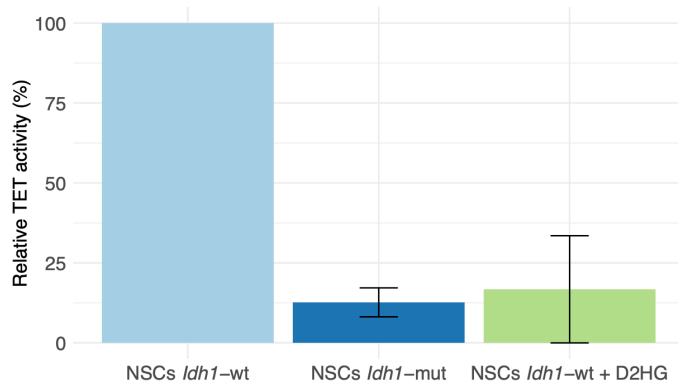
A



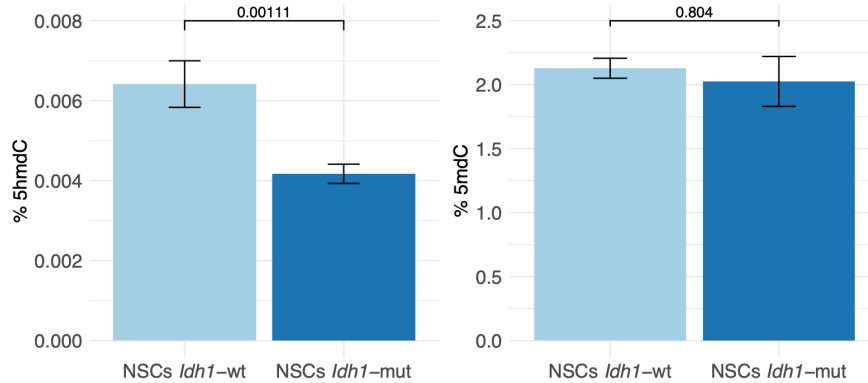
B



C

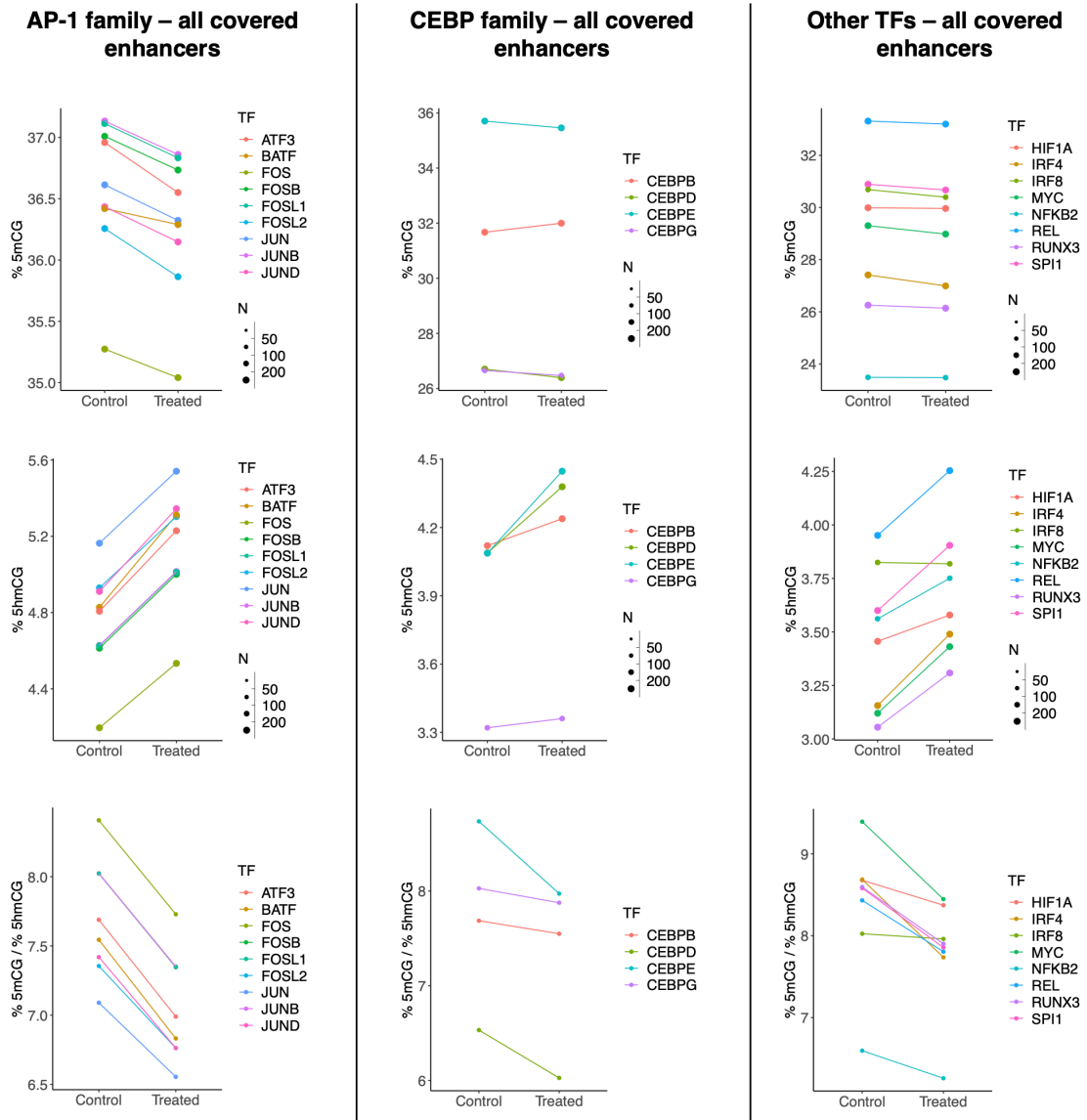


D

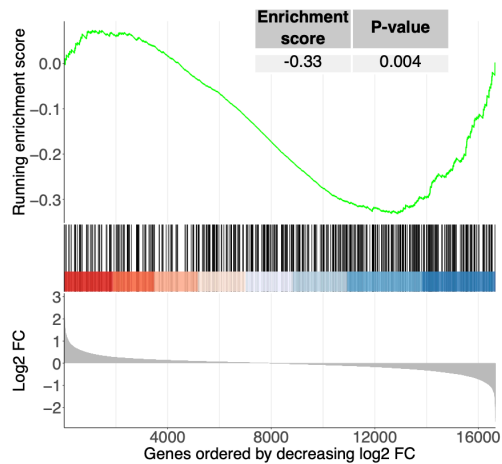


Extended Data Fig. 8. Assessment of D-2HG levels and TET function in external controls. **(A)** Workflow procedure for inducing the *in vitro* expression of Idh1 R132H in neural progenitor cells (NSCs) obtained from a conditional knock-in IDH^{mut} mouse model (cKI Idh1), used as external isogenic controls in three assays. Cells collected at day 14 for analyses underwent 3-6 passages. **(B)** Intracellular levels of D-2HG were determined using a fluorimetric assay in primary microglia treated with D-2HG [5 mM] for 48 hours. Microglia were obtained from samples with IDH^{wt} status (n=3). External controls for comparison (cKI model Idhwt n=5; Idhmut n=4, and patient-derived glioma cells IDH^{wt} n=4; IDH^{mut} n=3) are also shown. The levels of D-2HG in each sample were normalized to the corresponding micrograms of protein to enable comparisons among cell types. Data are represented as the mean with a 95% CI. **(C)** TET enzymatic activity assessed in nuclei extracts from NSCs after 14 days in culture. The plot shows a dramatic reduction of TET activity in IDH^{mut} cells with respect to the IDH^{wt} control. Data are represented as the mean with a 95% CI from technical replicates (n=2). A negative internal control, consisting of D-2HG with a final concentration of 400 μ M, added to the IDH^{wt} extract during the assay, is also indicated (green color). **(D)** Quantification of 5hmC and 5mC global levels determined by LC-MS/MS in IDH^{mut} and IDH^{wt} NSCs controls after 14 days in culture. Data are represented as the mean with a 95% CI from technical replicates (n=4). P-values were calculated using one-sided Welch's test.

A



B



Extended Data Fig. 9. Single-base resolution analysis of 5mCG and 5hmCG in the proximity of TFs motifs in all covered enhancers of D-2HG-treated primary microglia.

(A) Plots showing separate analysis of 5mCG and 5hmCG percentages (upper) in the proximity of binding motifs, residing in all covered enhancers, for the indicated TFs in D-2HG-treated microglia and paired untreated controls. The size of each dot indicates the number of motifs analyzed in a paired manner between conditions. The 5mCG/5hmCG ratios at analyzed regions are also shown. The whole set of covered enhancers (used as controls) comprises the selected enhancers of Fig. 5c. **(B)** GSEA analysis using ranked genes by decreasing log₂FC of D-2HG-treated vs. control samples of RNA-seq. The plot shows a significant bias towards decreased expression of genes regulated by D-2HG-driven hypermethylated/hypohydroxymethylated enhancers bound by TFs depicted in Fig 5c. Both methylome/hydroxymethylome and RNA-seq analyses were conducted using the same samples and in a paired manner.

Extended Data Fig. 10. Validation experiments on primary microglia treated with D-2HG for 14 days and challenged with LPS. (A) Heatmap depicting the expression of proinflammatory cytokines in CD11B+ cells from IDH^{mut} (n=20) and IDH^{wt} (n=8) human gliomas using RNA-seq data. **(B)** The plots indicate the expression of TNFA and IL6 (relative to housekeeping controls) in paired D-2HG-treated and control samples as determined by RT-qPCR. Primary microglia were obtained from surgical aspirates with IDH^{mut} status (n=4). P-values were calculated using one-sided paired t-tests. **(C)** Assessment of oxygen consumption rate (OCR) in paired D-2HG-treated and control samples as determined by XFe extracellular flux analyzer. Basal respiration (BR), maximal respiration (MR) and ATP-linked respiration (ALR) parameters are indicated for the comparisons control vs. D-2HG, and LPS vs. LPS+D-2HG. Primary microglia were obtained from surgical aspirate of one IDH^{wt} meningioma. Cells were maintained, treated, and collected under the same conditions as previously shown (Fig. 6a).

Chapter 4

Discussion and Perspectives

4.1 *Ex vivo* study

Our *ex vivo* study revealed that the myeloid compartment in IDH-m gliomas exhibits DNA hypermethylation. Using EPIC arrays, a DNA methylation platform with extensive coverage of regulatory regions (Pidsley et al. 2016), we found that this hypermethylation predominantly affects enhancer elements. Integrative analysis of methylome and transcriptome changes suggested that this hypermethylation is linked with down-regulation of genes involved in inflammatory responses and glycolytic metabolism. Motif enrichment analysis of hypermethylated regions, along with gene regulatory network assessments, indicated reduced activity of core transcription factors involved in regulating microglial activation. Taken together, these results point to hypermethylation as a potential mechanism underlying the hyporesponsive state of microglia in IDH-m gliomas.

4.1.1 Heterogeneity of CD11B+ cell populations

For this *ex vivo* study, we initially obtained highly purified fractions of CD11B+ cells from a well-characterized series of IDH-m and IDH-wt human gliomas for comparison. CD11B+ fractions comprise a variety of myeloid cell populations, including NK cells, neutrophils, dendritic cells, myeloid-derived suppressor cells, monocytes, BAMs, MDMs, and resident microglia. Among these, TAMs are the most abundant cells in human diffuse gliomas (Klemm et al. 2020; Friebel et al. 2020), the relative proportions of TAM-MDMs and TAM-MGs varying according to the IDH mutation status, and tumor grade (Klemm et al. 2020; Friebel et al. 2020; Venteicher et al. 2017; Hara et al. 2021; Miller et al. 2023; Gupta et al. 2024). ScRNA-seq data revealed further subsets of TAM-MDMs and TAM-MGs in human gliomas. In this context, our initial observation of DNA methylome differences between CD11B+ cells from IDH-m vs IDH-wt gliomas may, at least in part, reflect differences in cell composition.

We further used another comparator by analyzing public methylome data of CD11B+ cells – isolated and profiled similarly – from non-tumor age-matched samples. Indeed, microglial cells are a majority among CD11B+ cells in normal brain tissue and to IDH-m gliomas alike. We also observed DNA hypermethylation in CD11B+ cells from IDH-m gliomas using this comparator, with significant overlap between both comparisons. While we cannot exclude the possibility that methylation changes partly reflect a reduced recruitment of TAM-MDMs in IDH-m tumors, this suggests that resident microglia undergo a true hypermethylation in IDH-m gliomas.

Future studies employing single-cell methylome profiling will be required to further elucidate whether those changes are restricted to specific microglial subsets (Lee et al. 2019).

4.1.2 TAM patterning by the TME

The microenvironment contributes to dynamic patterning myeloid cells. Irrespective of the cancer context, the epigenetic regulation of macrophages – at the level of DNA methylation, histone modifications or chromatin structure – relies on tissue-specific transcription factors that are modulated by the tissue environment (Amit, Winter, and Jung 2016). Recent scRNA-seq studies of human gliomas showed that immunomodulatory programs can be expressed across myeloid cells, regardless of their ontological origin (Miller et al. 2023). Moreover, relative proportions of TAM-MDMs and TAM-MGs depend on tumor grade and disease stage regardless of the IDH-m status (Miller et al. 2023; Gupta et al. 2024). Indeed, experimental evidence has demonstrated that during glioma progression, infiltrating TAM-MDMs take over the niche previously occupied by resident microglia (Pombo Antunes et al. 2021; Yeo et al. 2022). Notably, infiltrating macrophages may adopt microglia-like characteristics (Miller et al. 2023; Bouzid et al. 2023), including microglial DNA methylation signatures, upon colonization of the central nervous system microenvironment (Lund et al. 2018). This observation might in part explain the subset of TAMs displaying mixed features of MDMs and microglia observed in various scRNA-seq studies (Pombo Antunes et al. 2021; Abdelfattah et al. 2022; Haley et al. 2024). Additionally, epigenetic rewiring via chromatin modifications has also emerged as a mechanism underlying the modulation of TAMs properties both in IDH-wt and IDH-m gliomas (Kloosterman et al. 2024; Blanco-Carmona et al. 2023). Altogether, these observations, along with our findings on DNA hypermethylation of TAM-MGs in IDH-m gliomas, reinforce the concept of TAM education by the TME (Lavin et al. 2014; Amit, Winter, and Jung 2016), highlighting the specific underlying epigenetic mechanisms at play in gliomas.

4.1.3 Link between DNA hypermethylation and transcription factor binding

Different studies suggest that DNA hypermethylation may impact transcription factor binding by altering the accessibility of specific genomic regions (Yin et al. 2017; Kribelbauer et al. 2017; Kaluscha et al. 2022). We observed that DNA hypermethylation in CD11B⁺ cells from IDH-m gliomas occurs primarily at enhancer regions, which could inhibit the binding of transcription factors known to regulate microglial identity and responsiveness to inflammatory stimuli (Gosselin, Skola, et al. 2017). It has been postulated that during development and responses to internal and external signals, an open chromatin configuration is defined by a set of lineage-determining transcription factors to enable enhancer activity (Glass and Natoli 2016; Holtman, Skola, and Glass 2017; Balak, C. Z. Han, and Glass 2024). These distal regulatory regions thus integrate environmental information with cell fate programs to initiate cell-type-specific transcriptional responses (Lavin et al. 2014). Unlike promoters, enhancers have a comparable CpG density to the genomic average (Hwang et al. 2015). In contrast, enhancers are enriched in 5hmC reflecting high turnover and active regulation by TET enzymes (Lister et al. 2013; Wen et al. 2014; F. Lu et

al. 2014). This enrichment maintains a flexible chromatin state that allows transcription factors to bind and activate gene expression. Therefore, minor changes in TET-mediated methylation at enhancers could result in a greater impact on the expression of target genes.

Notably, although IDH-m cells also undergo prominent hypermethylation in enhancer elements (Chaligne et al. 2021, and our results), it has been demonstrated that changes in promoters and enhancers methylation are not coupled with gene expression in glioma IDH-m cells (Turcan, Makarov, et al. 2018; Núñez et al. 2019; Court et al. 2019). In contrast, nearly a quarter of the hypermethylated changes observed in CD11B+ cells from these tumors were significantly correlated with the downregulation of genes involved in microglial activation. This observation is consistent with recent studies showing that only a fraction of enhancers in a given cell are sensitive to DNA methylation (Kreibich et al. 2023). Whether hypermethylation at lineage-specific enhancers further affects the recruitment of TET demethylase, local chromatin remodeling or histone modification induced by some pioneer transcription factors such as PU.1 and C/EBP warrants further investigation. A more thorough characterization of enhancers affected by hypermethylation in CD11B+ cells from IDH-m gliomas should also involve indirect interrogation of their activated/inactivated, latent or poised states using maps of chromatin marks, or a direct verification of long non-coding RNAs (lncRNAs) expressed at enhancers (the so-called eRNAs). Furthermore, although our integrative methylome/transcriptome analysis proved informative, it remains correlative. RNA-seq data primarily reflects transcript abundance rather than measuring gene transcription specifically. Additionally, the binding of transcription factors to methyl-sensitive enhancers suggested in our study requires further biochemical confirmation. In this regard, using CUT&Tag assays will be instrumental in examining the occupancy of lineage-specific TFs at hypermethylated enhancers across the genome in CD11B+ cells from IDH-m gliomas (Bartosovic, Kabbe, and Castelo-Branco 2021).

4.1.4 Inhibition of TET-mediated demethylation

It is well known that D-2HG drives DNA hypermethylation in IDH-m cells by inhibiting TET demethylases. Since this oncometabolite accumulates in the TME at concentrations sufficient to inhibit TET enzymatic activity (Losman, Koivunen, and Kaelin 2020), and it is taken up by myeloid cells (Friedrich, Sankowski, et al. 2021), we advanced the hypothesis that such a mechanism could explain the hypermethylation observed in CD11B+ cells from IDH-m gliomas. To address this question, it was necessary to examine not only 5mC but also 5hmC levels, the first intermediate in the TET-mediated demethylation pathway (X. Wu and Yi Zhang 2017). Prior studies have shown that 5hmC levels in *bulk* tumors correlate negatively with proliferation and tumor grade, irrespective of 5mC levels and IDH-m status (S.-G. Jin et al. 2011; Kraus et al. 2012). In fact, low 5hmC levels at enhancer elements were linked to poor prognosis in glioblastomas (Johnson et al. 2016). While low 5hmC levels are primarily indicative of TET inhibition, they may also reflect accelerated replication dynamics, resulting in passive demethylation in highly proliferating cells. This passive demethylation further complicates the interpretation of 5hmC dynamics in proliferating cancer cells, underscoring the need to compare these observations to non-tumoral cells.

Herein, I confirmed high 5mC/5hmC ratios in both CD11B- (predominantly

glioma cells) and corresponding CD11B⁺ (predominantly myeloid cells) fractions from an independent series of IDH-m gliomas compared to non-tumor brain tissues by applying a sensitive LC/MS approach.

Together, our analyses using EPIC arrays and LC/MS support the hypothesis that D-2HG-driven hypermethylation is at play not only in glioma cells but also in myeloid cells from IDH-m gliomas. However, a more comprehensive characterization of 5mC and 5hmC at nucleotide resolution is needed to determine whether TET-mediated demethylation is impaired at specific enhancers.

4.2 *In vitro* study

In this study, we provide experimental evidence that D-2HG induces changes in the DNA methylome and function of human microglia, partially recapitulating the *ex vivo* observations made in CD11B⁺ cells from IDH-m gliomas. To test the hypothesis that D-2HG impairs TET-mediated demethylation at specific enhancers in human microglia, I developed an *in vitro* culture system.

4.2.1 *In vitro* model

Before discussing the results, I will highlight key characteristics of the model we used:

1. We chose to focus exclusively on **human cells**, making our results more directly applicable than murine studies. Although murine models capture many aspects of immune responses, human specificities from biochemical, genomic, or pharmacological points of view are well documented (Masopust, Sivula, and Jameson 2017; Mestas and Hughes 2004; Seok et al. 2013). Notably, substantial divergence of transcription factor binding sites and enhancer elements have also been reported (Yokoyama, Yang Zhang, and J. Ma 2014; Reilly et al. 2015). These differences are particularly pronounced in microglia (Masuda et al. 2020). Discrepancies between human and murine microglia have been observed with regards to gene expression, proliferation, heterogeneity, cytokine production, and immunometabolic pathways (Smith and Dragunow 2014; Wolf, Boddeke, and Kettenmann 2017; Sabogal-Guáqueta et al. 2023). Mancuso et al. further emphasized that mouse microglia lack orthologues for key microglial genes (Mancuso et al. 2019). Additionally, Geirsdottir et al. conducted a comparative scRNA-seq analysis across species, showing that while microglia express a conserved core gene program, human microglia display significantly greater heterogeneity. They also identified notable differences in gene modules, including complement pathways and phagocytosis (Geirsdottir et al. 2019).

2. I used **primary cultures** of microglia, instead of immortalized human microglial cell lines (HMO6, HμGlia, HMC3, C13NJ). Although these immortalized cell lines replicate certain key features of *in situ* microglia and are easy to maintain in culture, they fail to accurately replicate microglial activation responses (Nagai et al. 2001; Horvath et al. 2008; Das et al. 2016). Furthermore, we observed that D-2HG does not

penetrate the immortalized microglia cell line HMC3, whereas it readily enters primary microglial cells (unpublished data). Therefore, primary microglia offer a more suitable model for addressing the questions posed in this study.

I set up primary microglial cultures from surgical aspirates obtained from patients with either brain tumors or drug-resistant epilepsy, following established surgical protocols. For gliomas, tissue collection involved the removal of both the adjacent “entry cortex” (the tissue surrounding the surgical access point) and the tumor core, whereas in cases of epilepsy surgery, only the normal tissue at the entry point was collected. To control for the large inter-individual variability, I analyzed the samples in a paired manner. Each experiment was carried out using multiple biological replicates to ensure reproducibility. It is worth mentioning that, while our microglial cultures were instrumental in performing the experiments, those obtained from epilepsy surgery were found to be more suitable, as they are not primed by a tumor microenvironment.

3. We developed a human microglia culture model grown in **serum free medium**, following the protocol of Bohlen et al. (Bohlen et al. 2017), adapted to human cells by Tewari et al. (Tewari et al. 2021). While primary microglial cultures are often maintained in medium containing calf serum, this method can lead to abnormal proliferation, diminished production of proinflammatory cytokines, and altered phagocytic profile (Timmerman, Burm, and Bajramovic 2018; Bohlen et al. 2017). In contrast, Tewari et al. demonstrated that microglia cultured in serum-free conditions exhibit improved response to pro-inflammatory signals, including enhanced cytokines and ROS release, while maintaining their phagocytic capacity (Tewari et al. 2021). Importantly, I confirmed that our cultures remained functional and retained the expression of markers and microglial signatures even at 14 days in culture. This contrasts with its decreased expression, including core transcription factors, observed when grown in 5% fetal bovine serum (Gosselin, Skola, et al. 2017).

4. The serum-free medium used in our model preserve a **low replicative** rate of microglia. Tewari et al. reported the percentage of proliferating microglia grown in serum-free conditions is minimal ($1.37\% \pm 0.3\%$ of Ki-67 positive cells) (Tewari et al. 2021), closely mirroring the rate of proliferating microglia in the intact adult human brain (Askew et al. 2017). In contrast, microglia cultured with 10% of calf serum show significantly higher proliferation rates, with Ki-67 expression around 6% (Tewari et al. 2021). This low replicative rate in serum-free conditions is crucial for studying DNA demethylation, as it allows active mechanisms to be distinguished from passive demethylation caused by dilution of methylation marks during cell division.

Importantly, the defined medium we used contained not only CSF-1, TGF- β 2, and cholesterol to enhance cell survival, but also glutamine to maintain adequate levels of 2OG (via glutaminolysis), and ascorbic acid to ensure the proper functioning of TET enzymes (Tarhonskaya et al. 2014).

5. We used **non-cell-permeable D-2HG** for all *in vitro* experiments, as opposed to most studies that used the cell-permeable octyl-D-2HG, a precursor esterified molecule that must be cleaved upon uptake (Chowdhury et al. 2011; W. Xu et al. 2011; C.-J. Han et al. 2019). While the use of cell-permeable D-2HG is relevant for

studying cancer cells and modelling cell-intrinsic effects, it is more questionable to use such compound for studying effects on cells residing in the TME, where D-2HG must enter the cell to have an effect. Wang et al. established that a D-2HG treatment at concentrations of 3 to 30 mM elevated intracellular D-2HG/2-OG ratios, but to a much lesser extent than an octyl-D-2HG treatment at a lower dose (1 mM) (Xiaomin Wang et al. 2022). They showed that octyl-D-2HG led to time-dependent D-2HG accumulation in treated cells, with continuous conversion of octyl-D-2HG to D-2HG in the intracellular compartment, allowing the preservation of the concentration gradient of octyl-D-2HG across the plasma membrane (ibid.). We decided to use a concentration of 5mM of D-2HG, which mimics what is observed in the TME (Linninger et al. 2018), and is significantly lower than in other studies that used concentrations of 10-30 mM (Bunse, Pusch, et al. 2018; L. Zhang et al. 2018; Friedrich, Sankowski, et al. 2021; Notarangelo et al. 2022; Afsari and McIntyre 2023; Hammon et al. 2024). We confirmed that the molecule was taken up by primary microglia and reached concentrations (comparable to *bona fide* IDH-m cells) sufficient to inhibit TET activity. Furthermore, we ensured that this concentration was maintained by renewing the medium every 2–3 days.

4.2.2 D-2HG selectively affects lineage-specific enhancers

Consistent with an active demethylation mechanism in low-proliferating cells, we observed that D-2HG hinders the accumulation of genomic levels of 5hmC after 14 days of treatment in both primary microglia and control neural stem cells expressing IDH-m, without any concomitant changes in 5mC levels, as determined by LC/MS. However, analysis of methylation using EPIC arrays, similar to the *ex vivo* study, revealed a tendency toward hypermethylation affecting a few lineage-specific enhancers in D-2HG treated microglia. Although the methylation differences observed *in vitro* were less pronounced compared to those in CD11B+ cells from IDH-m tumors, this effect was consistently replicated across microglia derived from unrelated donors. Next, we aimed to discriminate between 5mC and 5hmC levels at CpGs within enhancers using a reduced representation sequencing approach. However, in contrast to the low genomic content of 5hmC detected by LC/MS in D-2HG-treated microglia, higher 5hmC levels were observed when analyzing the full-length sequences of enhancers. We attributed this discrepancy to differences in methodology, with LC/MS capturing changes in both CpG and non-CpG contexts on a global scale, not limited to enhancers.

Considering that 5hmC levels are relatively low at the proximity of transcription factor binding sites (± 100 bp) but high at flanking regions in embryonic stem cells (ESCs) (M. Yu et al. 2012), we next focused our analysis on the vicinity of motifs identified as hypermethylated in our *ex vivo* study. Remarkably, we found high 5mC/5hmC ratios in enhancers bound by transcription factors governing microglial function, but not in the remaining set of genome-wide enhancers. This finding strongly suggests that active demethylation by TET at lineage-specific enhancers is affected by D-2HG treatments in primary microglia.

It should be noted that the effects of D-2HG on methylation that we observed were less significant than those reported in the context of TET deletion (Rasmussen et al. 2015). This can be explained by two main factors: i) D-2HG is a weak inhibitor of TET2 (Losman, Koivunen, and Kaelin 2020), and ii) the increase in 5mC levels after TET knockdown may result from the loss of both catalytic and non-catalytic activi-

ties of TET. Indeed, the physical presence of TET proteins at methylation-free sites impedes 5mC deposition by DNA methyltransferases (DNMTs) (X. Wu and Yi Zhang 2017). Supporting this hypothesis, Lu et al. reported that a triple knockout of TET1, TET2 and TET3 in mouse ESCs leads to the accumulation of 5mC at active promoters where TET binds strongly, while oxidized forms of 5mC are present at low levels (F. Lu et al. 2014). Moreover, it has been shown that overexpressing catalytically inactive TET mutants can rescue the phenotype of TET knockout or knockdown (Y. Xu et al. 2012; Kaas et al. 2013; Tsai et al. 2014; C. Jin et al. 2014; Montagner et al. 2016). Thus, the catalytic-independent actions of TET should not be affected by D-2HG inhibition.

Furthermore, TET deficiency leads not only to hypermethylation at enhancers but also to hypomethylation at gene desertic regions including repeated sequences (López-Moyado et al. 2019), an aspect we did not explore. Recent research showed that TET2 regulates oxidation of chromatin-associated retrotransposon RNA (car-RNA) 5mC to maintain a chromatin compaction state at repeated sequences, such as long interspersed nuclear elements (LINEs) (Zou et al. 2024), which could play a role in the hypomethylation reported in these sequences.

A particular role of TET at enhancers is supported by various studies. The genomic distribution of oxidized forms of 5mC has been extensively studied in ESCs (X. Wu and Yi Zhang 2017). In these cells, 5hmC is enriched at distal regulatory elements such as enhancers and transcription-factor-bound regions (Sun et al. 2015; M. Yu et al. 2012; Pastor et al. 2011; Stroud et al. 2011; Szulwach et al. 2011; Feldmann et al. 2013). Neurons, as post-mitotic cells, do not experience replication-dependent dilution of methylation marks, resulting in differences in 5hmC content in promoters and gene bodies compared to ESCs (X. Wu and Yi Zhang 2017). However, in both cell types, 5hmC is found around enhancer regions, suggesting that active DNA demethylation via TET enzymes is involved in these distal regulatory regions (Wen et al. 2014; Lister et al. 2013). In line with this hypothesis, Hon et al. reported that deletion of Tet2 in ESCs leads to a significant loss of 5hmC at enhancers, accompanied by hypermethylation of these enhancers and delayed gene induction during the early stages of differentiation (Hon et al. 2014). Ginno et al. established a genome-scale map of DNA methylation kinetics, comparing methylation levels in the absence of TET enzymes, demonstrating that TET activity particularly contributes to the demethylation of enhancer elements (Ginno et al. 2020). Among TET enzymes, TET2 appears to play a crucial role at enhancers. Comparisons between TET1-depleted and TET2-depleted ESCs revealed distinct target preferences: TET1 is more active at promoters and TET2 is predominant at gene bodies of highly expressed genes and enhancers (Hon et al. 2014; Huang et al. 2014). Overall, our observations on DNA methylation modifications, predominantly at enhancers, in both *ex vivo* and *in vitro* studies, are consistent with the inhibition of TET2.

4.2.3 Effects of D-2HG beyond the methylome

D-2HG is a more potent inhibitor of histone demethylases (IC₅₀ around 150 μmol/l) than TET demethylases (IC₅₀ around 5 mmol/l) (C. Lu et al. 2012; Kernytsky et al. 2015; Sasaki, Knobbe, Munger, et al. 2012; Turcan, Makarov, et al. 2018; Laukka et al. 2018; Losman, Koivunen, and Kaelin 2020). An increase of the repressive histone methylation marks such as H3K9me₃ or the activating histone mark H3K4me₃ is observed in IDH-m gliomas compared to IDH-wt gliomas, as well as in IDH-m im-

mortalized human astrocytes (C. Lu et al. 2012; Turcan, Makarov, et al. 2018). Thus, we anticipate that D-2HG will also affect chromatin states in our cultures, warranting further investigation.

It has been shown that the inhibition of the histone demethylase KDM4B by D-2HG results in hypermethylation of chromatin at sites of DNA damage, thereby impeding the recruitment of DNA repair machinery (Sulkowski, Oeck, et al. 2020). D-2HG also inhibits ALKBH2/3 (IC₅₀ around 500 $\mu\text{mol/l}$) which are involved in both DNA repair (Pu Wang et al. 2015) and the oxidation of 5mC to 5hmC during DNA replication (Bian et al. 2019). The interplay between the DNA damage response (DDR) and DNA methylation has also recently gained attention. Studies demonstrated a potential role of DNA methylation/demethylation in mediating DDR. For instance, 5hmC marks sites of DNA damage to help preserve genome stability (Kafer et al. 2016; Nakatani et al. 2015), while Tet-deficient cells exhibit accumulation of damaged DNA and impaired DDR (An et al. 2015). In contrast however, TET-mediated demethylation at neuronal enhancers has been shown to promote DNA damage (D. Wang et al. 2022). In addition to TET inhibition at methyl-sensitive enhancers, we hypothesize that D-2HG in *in vitro* microglia may also involve the relocation of TET activity at sites of DNA damage, potentially including non-active enhancers, to safeguard cell viability.

Altogether, the potential effects of D-2HG on the local chromatin environment and the DNA damage response in microglia merit further investigation.

4.2.4 Impact of D-2HG on microglial function

The turnover of methylation marks by TET activity at enhancers is crucial for fine-tuning gene expression, especially during development, differentiation, and environmental responses (Parry, Rulands, and Reik 2021). Given that lineage-specific enhancers hypermethylated in CD11B⁺ cells from IDH-m gliomas were associated with decreased expression of genes involved in inflammatory and metabolic responses, we hypothesized that enhancers primed by D-2HG-induced hypermethylation could have a direct impact on microglial function.

In a physiological context, both TET2 and D-2HG have been implicated in the inflammatory response and the associated metabolic shift in activated macrophages. Upon macrophage stimulation, transcription factors such as NF- κ B and/or C/EBPA bind to a TET2 regulatory region to induce its expression (Cull et al. 2017; Carrillo-Jimenez et al. 2019; Kallin et al. 2012). Additionally, protein-protein interactions between TET2 and myeloid transcription factors including PU.1 (Rica et al. 2013), C/EBPA (Sardina et al. 2018), RUNX1 (Suzuki et al. 2017), KLF4 (Sardina et al. 2018), enable its recruitment to specific enhancers required for cell activation, triggering TET-mediated demethylation.

Our transcriptome analyses demonstrated that D-2HG-treated microglia exhibit a hyporesponsive phenotype after LPS stimulation, yet further validations at the protein level (e.g. cytokines in the supernatants) are needed to confirm these observations. Nonetheless, our results align with prior studies in LPS stimulated macrophages pre-treated with cell-permeable octyl-D-2HG (1 h at 0.5 mM) (Goede et al. 2022). RNA-seq of these cells after 5 h of LPS treatment showed impairment of pathways related to myeloid cell activation, cytokine production, and the innate immune response, suggesting that D-2HG dampens the inflammatory activation of macrophages after LPS stimulation (ibid.). The authors reported a diminution of

LPS-induced secretion of the inflammatory mediators IL-6, and TNF α at the protein level. Of note, TNF α expression was rescued after supplementation with 2-OG, indicating that at least some effects of D-2HG involve inhibition of 2-OG-dependent enzymes (ibid.).

Additionally, studies demonstrated that, during acute LPS stimulation, myeloid enhancers are primed in a C/EBP β -dependent manner to increase chromatin accessibility, thereby amplifying the inflammatory response upon secondary stimulation (Laval et al. 2020). Consequently, it is plausible that D-2HG-induced hypermethylation at enhancers targeted by C/EBP β could disrupt this mechanism, rendering microglial cells in a state that shares some similarities with an “M2”-like state, as supported by enhanced expression of fatty acid oxidation and OXPHOS signatures in our cultures.

Other studies established a link between TET2 activity and the response to inflammatory stimuli. Carrillo-Jimenez et al. showed that TLR activation after LPS stimulation leads to an early (2h) and sustained (24h) upregulation of TET2 in immortalized murine microglia, through a NF- κ B-dependent pathway (Carrillo-Jimenez et al. 2019). Using TET2 knockdown cells, they observed a downregulation of genes implicated in the immune response after LPS stimulation, including type I IFN response. However, there were no significant changes in 5mC and 5hmC levels in the promoters of target genes whose expression was altered by TET2 knockdown. Consequently, the authors concluded that the effect of TET2 does not involve its catalytic activity. Nevertheless, it should be noted that this study did not assess 5mC and 5hmC levels at enhancers across the genome. Subsequently, Onodera et al. showed that non-dividing macrophages treated by LPS accumulate 5hmC at enhancers enriched in NF- κ B motif, where TET is recruited (Onodera et al. 2021). They hypothesized that the transcription factor NF- κ B participates to its recruitment. These results support our hypothesis regarding the impairment of inflammatory response upon TET inhibition.

Other mechanisms, not mutually exclusive, likely contribute to the establishment of a hyporeactive state following inflammatory stimuli. D-2HG competitively inhibits other 2OG-dependant enzymes, with a lower IC50, potentially influencing the response to inflammatory stimuli via inhibition of these enzymes. For instance, exposure to oxidized low density lipoprotein, which triggers the inflammatory polarization of macrophages (characterized by iNOS expression and production of inflammatory cytokines as TNF- α , or interleukin-1 β), has been shown to increase KDM4A expression in macrophages (Xue Wang et al. 2017). Knockdown of *KDM4A* significantly impaired M1 polarization and expression of inflammatory cytokines induced by oxidized low density lipoprotein (ibid.). Similarly, knockdown or overexpression of *KDM5C/KDM6A* in microglial cultures has been shown to affect the production of inflammatory cytokines (Qi et al. 2021). Liu et al. reported that ratios of 2OG/succinate modulate the activity of KDM6B enzymes which in turn reprogram M2 genes expression via demethylation of H3K27 (Liu et al. 2017). While further investigation is required to understand the impact of D-2HG on the function of KDMs histone demethylases in microglial cells, our findings regarding the hyporeactive state of D-2HG-treated microglia align with the potential impairment of the activity of transcription factors that regulate the inflammatory response.

In addition to mechanisms involving 2OG-dependent enzyme inhibition, other pathways could coexist. For example, Friedrich et al. reported that D-2HG induces L-tryptophan uptake in macrophages and its conversion into L-kynurenine, which

acts as an endogenous ligand for the aryl-hydrocarbon receptor. Activation of this receptor leads to increased secretion of the anti-inflammatory cytokines interleukin-10 and transforming growth factor- β (Friedrich, Sankowski, et al. 2021). It has also been reported that treatment of murine immortalized microglia with octyl-D-2HG dampens LPS-induced cytokine expression through a mechanism involving AMPK-mTOR-mediated reduction of NF- κ B activity (C.-J. Han et al. 2019).

A major limitation of our *in vitro* study is the lack of a direct causal link between the hyporeactive state of D-2HG-treated microglia and the hypermethylation observed at specific enhancers. Given the mild effects of D-2HG on the methylome of primary microglia, it is possible that the disruption of convergent mechanisms, such as those involving the NF- κ B signaling pathway, is also at play *in vitro*, whereas DNA hypermethylation at lineage-specific enhancers becomes more relevant for establishing gene silencing upon more prolonged exposure to D-2HG, suggested by our *ex vivo* study. Our single-base resolution methylome and hydroxymethylome analysis was indeed instrumental in demonstrating a direct impact of D-2HG on those enhancers – an effect not previously reported in human microglia. Supporting these findings, snRNA-seq analysis of microglia from tumor samples revealed that treatment with an IDH-m inhibitor, which depletes D-2HG levels in the TME, restores the expression of genes involved in activation. Notably, these genes are regulated by microglial enhancers that were found to be hypermethylated in our *ex vivo* study. In this context, Friedrich et al. previously reported that a treatment of mice bearing intracranial IDH-m glioma with IDHi led to the partial reversal of an IDH-m-associated attenuated antigen presentation signature in macrophages (Friedrich, Sankowski, et al. 2021). Altogether, these observations support the idea that D-2HG contributes to suppressive signaling that impairs microglial function. This provides additional rationale for combining IDHi with immunotherapies.

To further validate our observations, it will be interesting to test whether knocking-down TET2 with siRNAs phenocopies the effects of D-2HG, and whether TET2 overexpression can rescue the activation state of D-2HG-treated microglia. However, as discussed in previous sections, these approaches will not discriminate enzymatic from non-enzymatic effects of TET2. To address this, we plan to use itaconate, a metabolite that selectively inhibits TET2 enzymatic activity without affecting 2-OG-dependent histone demethylases (L.-L. Chen et al. 2022). In fact, itaconate has been shown to readily impact inflammatory and metabolic responses in macrophages (O'Neill and Artyomov 2019; L.-L. Chen et al. 2022). Additionally, to determine whether chronic treatment with D-2HG or itaconate leads to progressive significant accumulation of DNA hypermethylation (as presumably occurred in CD11B+ cells from IDH-m gliomas), we will use proliferating immortalized HMC3 cells treated by the cell-permeable octyl-D-2HG.

4.3 Conclusion

In IDH-m gliomas, chronic exposure of microglia to D-2HG promotes hypermethylation at lineage-specific enhancers by inhibiting TET-mediated demethylation. We postulate that this epigenetic priming mechanism disrupts the regulatory function of core transcription factors, impairing the capacity of these cells to mount an inflammatory response, and possibly impairing the shift towards a glycolytic metabolism. We speculate that these and other documented non-epigenetic effects of D-2HG in TME cells contributes to the immune evasion by blocking the

amplification of the inflammatory response. Given that reduced levels of D-2HG induced by IDH-m inhibitors lead to an IFN- γ enriched environment (Mellinghoff, M. Lu, et al. 2023), it is crucial to evaluate the extent to which the effects of D-2HG on the epigenome of myeloid cells can be reversed by this therapeutic option. Furthermore, understanding how hypermethylation affects interactions between microglia and other tumor-infiltrating immune cells will be also important for therapeutic development. Lastly, our findings suggest significant D-2HG-driven epigenomic modifications in tissue-resident microglia, in contrast to the non-epigenetic effects reported in infiltrating immune cells in IDH-m gliomas. Since resident cells are exposed to D-2HG from the earliest stages of gliomagenesis, our study underscores the importance of investigating the effects of this oncometabolite on astrocytes and even neuronal functions. Furthermore, elevated levels of D-2HG have been reported in other cancers through mechanisms independent of IDH-m, suggesting that our results may have broader implications for understanding microenvironmental dysregulations in these cancers.

Appendix A

Abstract presented to the EANO 2024 conference

Control/Tracking Number: 2024-A-129-EANO

Activity: Abstracts

Current Date/Time: 5/22/2024 2:48:35 PM

The oncometabolite D-2-hydroxyglutarate promotes DNA hypermethylation at lineage-specific enhancers controlling microglial activation in IDH-mutated gliomas

Author Block: A. Laurence^{1,2}, P. Pugliese¹, B. Mathon^{1,2}, Q. Richard¹, S. Jouannet², Y. Hayat¹, S. Scuderi¹, P. Marijon^{1,2}, K. Labreche¹, A. Alentorn^{1,2}, M. Verreault¹, A. Idbah^{1,2}, C. Birzu^{1,2}, E. Huillard¹, N. Pottier¹, A. Desmons³, I. Fayache³, G. A. Kaas⁴, P. J. Kingsley⁴, L. J. Marnett⁴, E. Duplus⁵, E. El-Habr⁵, L. A. Salas⁶, K. Mokhtari^{1,2}, S. Tran^{1,2}, M. L. Suvà⁷, A. Iavarone⁸, M. Ceccarelli⁸, M. Touat^{1,2}, F. Bielle^{1,2}, M. Mallat¹, M. Sanson^{1,2}, L. Castro-Vega¹;
¹ICM - Paris Brain Institute, Paris, France, ²APHP - Hôpital Pitié Salpêtrière, Paris, France, ³APHP - Hôpital Saint-Antoine, Paris, France, ⁴Vanderbilt University, Nashville, TN, United States, ⁵Institut de biologie Paris Seine, Paris, France, ⁶Geisel School of Medicine at Dartmouth, Lebanon, NH, United States, ⁷Massachusetts General Hospital and Harvard Medical School, Boston, MA, United States, ⁸Sylvester Comprehensive Cancer Center, Miami, FL, United States.

Abstract:

Background: Resident microglia are highly plastic myeloid cells. Their phenotype and immune response are determined by the microenvironment composition. Although microglial cells are highly abundant in IDH-mutated (IDHm) gliomas, how this particular environment modulates the transcriptional programs and cell states of these cells remain largely uncharacterized. Herein we investigated whether and how D-2HG, the oncometabolite produced by the IDH mutation and released into the tumor microenvironment, impinges upon the phenotypic and functional properties of resident microglia.

Material and Methods: We analyzed bulk DNA methylome (Methylation EPIC array) and transcriptome of CD11b+magnetic-purified fractions from IDHm (n= 25) and IDH-wildtype (n=11) gliomas, as well from normal brain tissues (n=6). To determine direct effects of D-2-hydroxyglutarate (D-2HG), the oncometabolite produced by IDHm glioma cells, we optimized human primary microglial cultures obtained from glioma or drug-resistant epilepsy surgery. Microglia exposed to 5mM D-2HG or vehicle for 14 days were analyzed with DNA methylome (LC-MS/MS, EPIC arrays and single-base resolution approaches) and transcriptome (RNA-seq). Using snRNA-seq, we analyzed microglial transcriptome from a paired sample of one IDHm glioma patient before and after treatment with the IDH-inhibitor vorasidenib, which is known to deplete tumor D-2HG levels.

Results: We uncovered that CD11b+ myeloid cells in human IDHm gliomas exhibit DNA hypermethylation predominantly at enhancer elements. Hypermethylation was linked to decreased expression of genes involved in inflammatory responses and glycolytic metabolism, as well as inactivation of transcription factors that regulate microglial responses to environmental stimuli. Prolonged exposure of human primary microglia to D-2HG inhibited TET-mediated 5mC oxidation, resulting in a reduced accumulation of global 5hmC levels. We observed high 5mC/5hmC ratios particularly at lineage-specific enhancers. Consistent with the remodeled enhancer landscape, D-2HG-treated microglia showed reduced proinflammatory capacity and enhanced oxidative phosphorylation. Conversely, depletion of D-2HG levels following vorasidenib treatment in an IDHm glioma patient was associated with overexpression of genes related to microglial activation.

Conclusion: Our findings provide a mechanistic rationale for the hyporesponsive state of microglia in IDHm gliomas and support the hypothesis that oncometabolites such as D-2HG may disrupt the function of immune cells residing in the tumor microenvironment.

Author Disclosure Information:

A. Laurence: None. **P. Pugliese:** None. **B. Mathon:** None. **Q. Richard:** None. **S. Jouannet:** None. **Y. Hayat:** None. **S. Scuderi:** None. **P. Marijon:** None. **K. Labreche:** None. **A. Alentorn:** None. **M. Verreault:** None. **A. Idbah:** A. Employment (full or part-time); Significant; Transgene, Sanofi, Air Liquide and Nutriheragene. **C. Other Research Support** (supplies, equipment, receipt of drugs or other in-kind support); Modest; Carthera, Leo Pharma. **F. Consultant/Advisory Board;** Modest; Novocure, Novartis, Polytone Laser, Leo Pharma, Boehringer Ingelheim. **C. Birzu:** None. **E. Huillard:** None. **N. Pottier:** None. **A. Desmons:** None. **I. Fayache:** None. **G.A. Kaas:** None. **P.J. Kingsley:** None. **L.J. Marnett:** None. **E. El-Habr:** None. **L.A. Salas:** None. **K. Mokhtari:** None. **S. Tran:** None. **M.L. Suvà:** None. **A. Iavarone:** None. **M. Ceccarelli:** None. **M. Touat:** B. Research Grant (principal investigator, collaborator or consultant and pending grants as well as grants already received); Modest; Sanofi. **D. Speakers Bureau/Honoraria** (speakers bureau, symposia, and expert witness); Modest; Servier, Novocure, Ono, Resilience. **F. Consultant/Advisory Board;** Modest; Servier, Novocure, NH TherAguix. **F. Bielle:** A. Employment (full or part-time); Significant; next-of-kin employed by Bristol Myers-Squibb. **M. Mallat:** None. **M. Sanson:** None. **L. Castro-Vega:** None.

Affirmation / Allocation (Complete):

*I confirm the acknowledgement of the above. : True

*I am submitting: a regular abstract

Topic (Complete): 02. Tumor microenvironment

Keyword (Complete): D-2HG ; TAMs ; IDH mutation

Presentation Preference (Complete): Oral preferred

More Information (Complete):

- 1.) I am an EANO Allied Health Professional or Nurse member and want to apply for the Investigator Travel Scholarship. : No
- 2.) I am an EANO member and a young investigator (graduate student/resident/fellow) within my first five years of my initial clinical or academic appointment and want to apply for the Young Investigator Travel Scholarship.: Yes
- 3.) I am an EANO member (all member categories) and want to apply for the EANO-SNO Travel Scholarship to attend SNO 2024 – please note that if selected for the EANO-SNO scholarship, your abstract will be selected for an oral presentation at both: No
- 4.) I am an abstract submitter from low-, middle-low and upper-middle income countries and would like to apply for travel support through the EANO International Outreach Scholarship.: No

*Date of Doctorate - dd.mm.yyyy - REQUIRED for number 2! : 13/09/2024

*Date of Birth - dd.mm.yyyy - REQUIRED for number 2! : 18/05/1989

Status: Complete

Appendix B

Articles and reviews related to this PhD

B.1 Classification OMS 2021 des tumeurs du système nerveux central

A. Laurence, S. Tran, M. Peyre, and A. Idbaih (Feb. 15, 2023). *Classification OMS 2021 des tumeurs du système nerveux central*. In: *EM-Consulte*. URL: <https://www.em-consulte.com/article/1573026/classification-oms-2021-des-tumeurs-du-systeme-ner>

Article under copyright, see A. Laurence et al. (2023), page 1.

Article under copyright, see A. Laurence et al. (2023), page 2.

Article under copyright, see A. Laurence et al. (2023), page 3.

Article under copyright, see A. Laurence et al. (2023), page 4.

Article under copyright, see A. Laurence et al. (2023), page 5.

Article under copyright, see A. Laurence et al. (2023), page 6.

Article under copyright, see A. Laurence et al. (2023), page 7.

Article under copyright, see A. Laurence et al. (2023), page 8.

Article under copyright, see A. Laurence et al. (2023), page 9.

Article under copyright, see A. Laurence et al. (2023), page 10.

Article under copyright, see A. Laurence et al. (2023), page 11.

Article under copyright, see A. Laurence et al. (2023), page 12.

Article under copyright, see A. Laurence et al. (2023), page 13.

Article under copyright, see A. Laurence et al. (2023), page 14.

Article under copyright, see A. Laurence et al. (2023), page 15.

Article under copyright, see A. Laurence et al. (2023), page 16.

Article under copyright, see A. Laurence et al. (2023), page 17.

B.2 Advances in the treatment of IDH-mutant gliomas

Chooyoung Baek, Alice Laurence, and Mehdi Touat (Sept. 12, 2024). "Advances in the treatment of IDH-mutant gliomas". In: *Current Opinion in Neurology*. ISSN: 1473-6551. DOI: 10.1097/WCO.0000000000001316

Article under copyright, see Baek, Alice Laurence, and Mehdi Touat (2024), page 1.

Article under copyright, see Baek, Alice Laurence, and Mehdi Touat (2024), page 2.

Article under copyright, see Baek, Alice Laurence, and Mehdi Touat (2024), page 3.

Article under copyright, see Baek, Alice Laurence, and Mehdi Touat (2024), page 4.

Article under copyright, see Baek, Alice Laurence, and Mehdi Touat (2024), page 5.

Article under copyright, see Baek, Alice Laurence, and Mehdi Touat (2024), page 6.

Article under copyright, see Baek, Alice Laurence, and Mehdi Touat (2024), page 7.

Article under copyright, see Baek, Alice Laurence, and Mehdi Touat (2024), page 8.

Article under copyright, see Baek, Alice Laurence, and Mehdi Touat (2024), page 9.

B.3 New insights into the Immune TME of adult-type diffuse gliomas

Quentin Richard, Alice Laurence, Michel Mallat, Marc Sanson, and Luis Jaime Castro-Vega (Dec. 1, 2022). "New insights into the Immune TME of adult-type diffuse gliomas". In: *Current Opinion in Neurology* 35.6, pp. 794–802. ISSN: 1473-6551. DOI: 10.1097/WCO.0000000000001112



New insights into the Immune TME of adult-type diffuse gliomas

Quentin Richard^a, Alice Laurence^a, Michel Mallat^a, Marc Sanson^{a,b,c} and Luis Jaime Castro-Vega^a

Purpose of review

Adult-type diffuse gliomas are highly heterogeneous tumors. Bulk transcriptome analyses suggested that the composition of the tumor microenvironment (TME) corresponds to genetic and clinical features. In this review, we highlight novel findings on the intratumoral heterogeneity of IDH-wildtype and IDH-mutant gliomas characterized at single-cell resolution, and emphasize the mechanisms shaping the immune TME and therapeutic implications.

Recent findings

Emergent evidence indicates that in addition to genetic drivers, epigenetic mechanisms and microenvironmental factors influence the glioma subtypes. Interactions between glioma and immune cells contribute to immune evasion, particularly in aggressive tumors. Spatial and temporal heterogeneity of malignant and immune cell subpopulations is high in recurrent gliomas. IDH-wildtype and IDH-mutant tumors display distinctive changes in their myeloid and lymphoid compartments, and D-2HG produced by IDH-mutant cells impacts the immune TME.

Summary

The comprehensive dissection of the intratumoral ecosystem of human gliomas using single-cell and spatial transcriptomic approaches advances our understanding of the mechanisms underlying the immunosuppressed state of the TME, supports the prognostic value of tumor-associated macrophages and microglial cells, and sheds light on novel therapeutic options.

Keywords

adult-type diffuse gliomas, D-2-hydroxyglutarate, IDH mutation, immune tumor microenvironment, intratumoral heterogeneity, single-cell and spatial transcriptomics

INTRODUCTION

Adult-type diffuse gliomas are brain tumors with aggressive behavior characterized by cell migration into the brain parenchyma, thereby precluding curative surgical resection. Survival and quality of life of patients remain dismal with current standard of care consisting of surgery followed by adjuvant radiation and chemotherapy. In the current classification (WHO CNS5), isocitrate dehydrogenase (IDH1/2) mutations and 1p/19q codeletion along with histology define three major categories of adult diffuse gliomas: glioblastoma grade IV (IDH-wildtype); astrocytoma grade 2–4 (IDH-mutant without 1p/19q-codeletion); and oligodendroglioma grade 2–3 (IDH-mutant and 1p/19q-codeleted) [1] (Fig. 1). Of these, glioblastomas are the most aggressive tumors with patients having a median overall survival of 15 months. Patients with low-grade IDH-mutant gliomas have a more favourable prognosis, but these tumors invariably progress, recur as higher grades, and become resistant to therapy. It is increasingly recognized that the tumor

microenvironment (TME) is a key factor of tumor progression and response to immunotherapies. Here we discuss the latest findings regarding the intratumoral heterogeneity of gliomas, with focus on the composition of the immune TME, highlight therapeutic implications, and provide research perspectives.

^aParis Brain Institute (ICM), Hôpital Pitié-Salpêtrière, Inserm U 1127, CNRS UMR 7225, Sorbonne Université, Genetics and Development of Brain Tumors Team, ^bDepartment of Neurology 2, Pitié-Salpêtrière Hospital and ^cOnconeurotek Tumor Bank, Paris, France

Correspondence to Luis Jaime Castro-Vega, MD, PhD, Genetics & Development of Brain Tumors, ICM - Paris Brain Institute, Hôpital Pitié, 47 Bd de l'Hôpital, 75013 Paris, France. Tel: +33 (0)1 57 27 40 99; e-mail: luis.castrovega@icm-institute.org

Curr Opin Neurol 2022, 35:794–802

DOI:10.1097/WCO.0000000000001112

This is an open access article distributed under the terms of the Creative Commons Attribution-Non Commercial-No Derivatives License 4.0 (CCBY-NC-ND), where it is permissible to download and share the work provided it is properly cited. The work cannot be changed in any way or used commercially without permission from the journal.

KEY POINTS

- High intratumoral heterogeneity and environmental stimuli define aggressive and recurrent gliomas.
- Dynamic competition of resident and infiltrating macrophages occurs during glioma progression.
- Distinctive changes in the immune TME are linked to the IDH mutation status.
- Cell-extrinsic D-2HG impinges upon the function of immune cells.

INTRATUMORAL HETEROGENEITY OF IDH-WILDTYPE GLIOMAS

Bulk transcriptome profiling of The Cancer Genome Atlas (TCGA) glioma cohort suggested four tumor subtypes: proneural, neural, classical, and mesenchymal, characterized by defined genetic drivers [2]. Deconvolution analyses of the immune cell composition of these tumors, revealed that the mesenchymal subtype, which exhibits the worst prognosis, is enriched in neutrophils and tumor-associated macrophages (TAMs) [3]. This enrichment involves NF1 deficiency in malignant cells, which promotes chemoattraction of TAMs [3]. Longitudinal analyses showed that recurrent tumors increase the TAM population whereas temozolomide-related hypermutation correlates with enrichment of CD8+ T cells [3]. However,

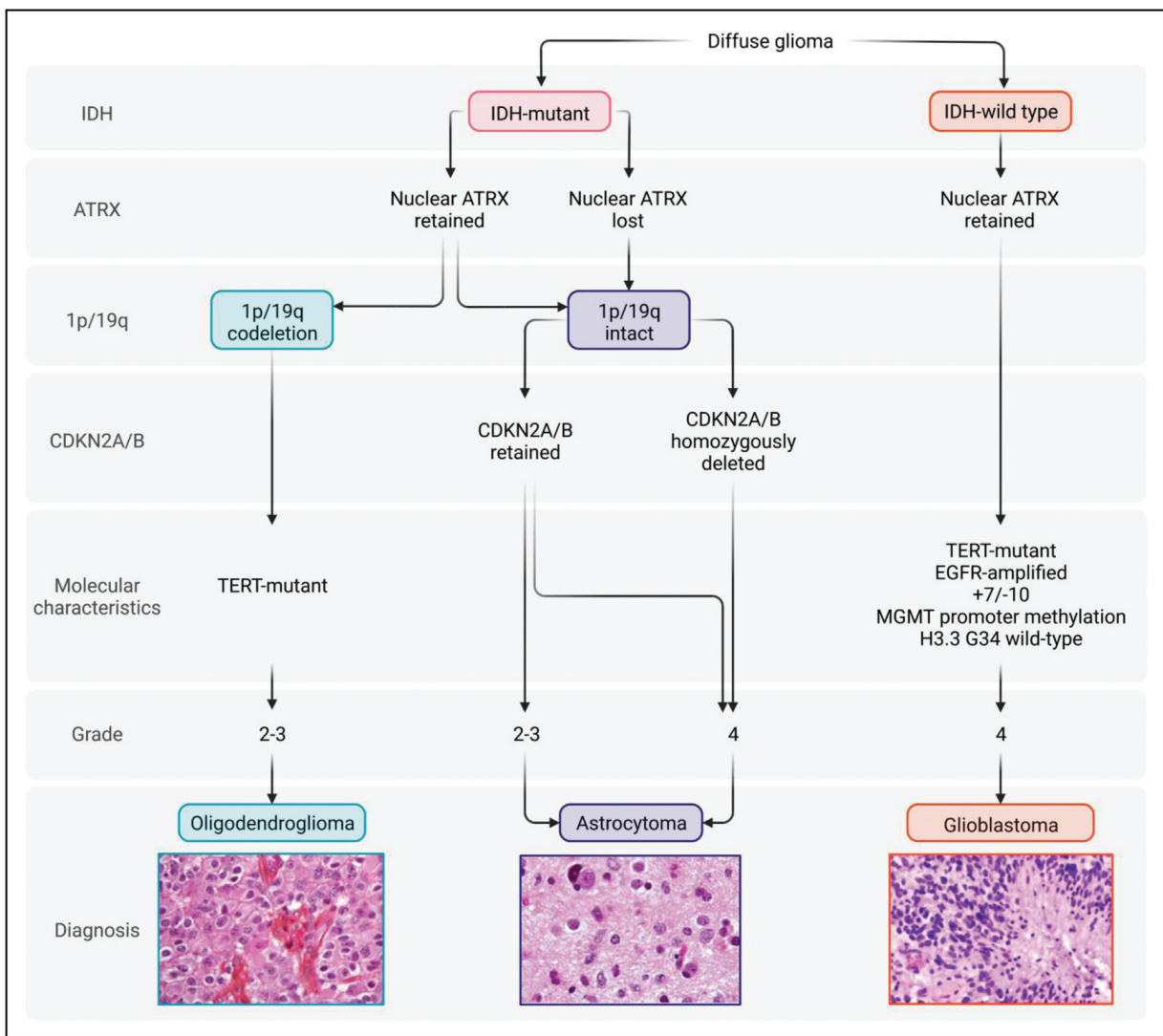


FIGURE 1. Adult-type diffuse glioma classification (WHO CNS5). The main genetic alterations of IDH-wildtype and IDH-mutant tumors and their corresponding histological appearance are indicated. IDH, isocitrate dehydrogenase.

these findings await confirmation, as it is possible that hypermutation might correlate with enrichment of CD8+ T cells in specific subpopulations (e.g. pediatric patients with CMMRD) rather than in temozolomide-related contexts. Previous bulk RNA-seq studies suggested that transition from proneural to mesenchymal subtype occurs with disease recurrence and resistance to treatment. However, it was not until the advent of powerful single-cell RNA sequencing (scRNA-seq) that a more accurate assessment of the intratumoral heterogeneity of gliomas, including malignant and immune cells, has been enabled.

It turned out that four cellular malignant states coexist in a given tumor: neural, progenitor-like (NPC-like) oligodendrocyte progenitor-like (OPC-like), astrocyte-like (AC-like), and mesenchymal-like (MES-like) [4] (Fig. 2a). These states, with the exception of MES-like are reminiscent of neurodevelopmental programs as they express astrocytic, oligodendroglial, and stem progenitor cell signatures to some extent. Importantly, it was shown that in addition to genetic drivers, the predominance of one state over the others defines the tumor subtype [4]. Evidence supporting dynamic interconversion between these states was provided in lineage-tracing experiments using a genetic mouse model and patient-derived xenografts, in which one single cell gives rise to the four archetypal subtypes [4].

This switching model argues for a dynamic plasticity of four different cell states, and contrasts with two other scRNA-seq studies supporting the cancer stem cell (CSC) hypothesis, in which a cellular hierarchy prevails [5,6[¶],7[¶]]. Indeed, a signature of quiescent (nonproliferative) CSCs was identified, which differs from the transcriptional signatures of the four archetypal cellular states [6[¶]]. Importantly, chemotherapy exerts selection pressure on CSCs, and may account for therapy resistance to antimetabolic drugs and temozolomide [6[¶],7[¶]], thus emphasizing the need to target the right cells. Regardless of the cell of origin and the defined genetic drivers, the question remains about the factors that influence the plasticity and outcomes of glioblastoma cells.

Multiomics analyses of glioma cells at single-cell resolution revealed that intratumoral epigenetic diversity (but not genomic alterations alone) accounts for adaptive changes to environmental stimuli such as hypoxia and irradiation, leading to cell-state transitions [8[¶],9[¶]]. Additional characterization of glioblastomas by spatially resolved transcriptomics showed that inflammation and hypoxia, as well as changes in metabolic activity and the neural environment contribute to the transcriptional heterogeneity that characterizes the four cellular archetypes [11[¶]]. In particular, expression of potassium channels and metabotropic glutamate receptors are important for the transition between

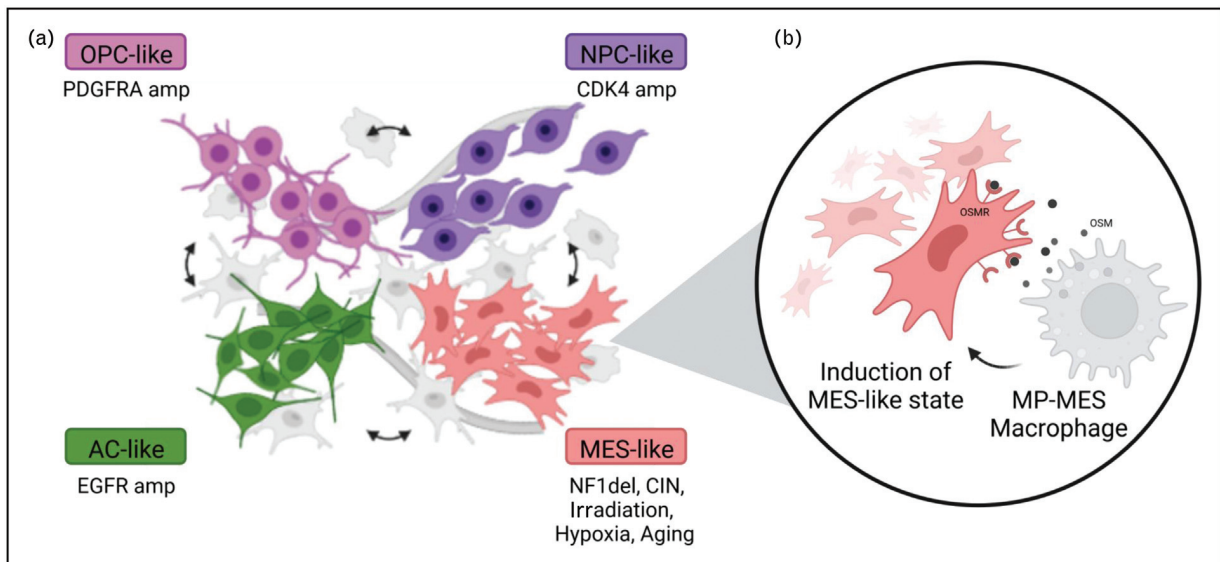


FIGURE 2. Intratumoral heterogeneity of glioma cells and immune-evasion mechanisms in the mesenchymal-like subtype. (a) The four cellular archetypes present in a given glioma, and their corresponding genetic drivers are indicated. Additional factors influencing the proportion of the MES-like state such as chromosome instability (CIN), hypoxia, irradiation, and a senescent environment are also indicated. (b) Induction of MES-like glioma cells by MES-like macrophages. MES, mesenchymal-like.

OPC-like and NPC-like tumors, whereas hypoxia leads to genomic instability in MES-like subtype [10¹¹]. Moreover, age-related changes in the neural environment promote enrichment in the MES-like subtype [10¹¹], a finding consistent with the fact that age is the main risk factor for glioblastoma development. Senescence in malignant cells also contributes to the development and heterogeneity of these tumors [11¹²]. Of note, a transcriptional signature of senescence correlated with poor prognosis in human patients, whereas treatments with a senolytic agent improved the survival of mice bearing gliomas [11¹²], and efficiently eliminated preirradiated tumors [12¹³]. Therefore, targeting of senescent cells appears as a novel therapeutic option.

ROLES OF TAMs IN IMMUNE EVASION AND TUMOR PROGRESSION

In addition to the microenvironment and the genetic drivers, reciprocal crosstalks between malignant cells and TAMs contribute to the aggressive phenotype of MES-like tumors [13¹⁴]. Serial transplantation experiments of CSCs from MES-like tumors showed that these cells are endowed with immune-evasive properties via demethylation of IRF8, CD73, and PD-L1 [13¹⁴]. This epigenetic immunoeediting process leads to the establishment of a myeloid-enriched TME deemed to play immunosuppressive roles. In coculture experiments, TAMs were found to stimulate transcriptional changes responsible for immune-evasiveness cells in CSCs, whereas in glioma-bearing mice, pharmacological elimination of TAMs resulted in increased survival and clearance of immune-evading tumors [13¹⁴]. TAMs can directly induce the MES-like state of glioblastoma cells through a mechanism involving macrophage-secreted oncostatin M (OSM), a well known epithelial-to-mesenchymal transition inducer, which binds the cognate receptor (OSMR) expressed by malignant cells to activate STAT3 signaling [14¹⁵]. Intriguingly, TAMs from MES-like tumors also display a mesenchymal-like phenotype probably induced by ligands produced by MES-like cancer cells that bind cognate receptors expressed by TAMs [14¹⁵] (Fig. 2Bb).

TAM's phenotype and function are determined by ontogeny and environmental cues. Functional specificity or heterogeneity in TAMs has been addressed through scRNA-seq analyses of CD45+ or CD11b+ cells from GL261 tumors and human glioblastomas, which enabled an in-depth characterization of the myeloid compartment [15¹⁶]. New subsets of dendritic cells, monocyte-derived macrophages (MDMs), and border-associated macrophages (BAMs) were uncovered for the first time. Analysis of newly diagnosed and recurrent tumors

showed that the myeloid compartment is highly dynamic [15¹⁶]. Elegant experiments of GL261 tumors growing in Cx3cr1CreER:R26-YFP mice (to fate-map microglia) and in Ccr2 knockout mice (MDMs recruitment is prevented) demonstrated that brain resident macrophages such as microglia, are outnumbered by MDMs upon recurrence [15¹⁶]. Enrichment in pro-inflammatory and proliferative microglial cells has also been reported in high-grade glioblastomas in the contexts of the SETD2 mutation and EGFR overexpression [17,18]. The largest scRNA-seq study to date to characterize myeloid cells in human gliomas confirmed the MES-like phenotype of TAMs and hypoxia subtypes [19²⁰]. Signatures of TAMs were used to interrogate TCGA and scRNA-seq data, and indicated that immunosuppressive MDMs and inflammatory microglial cells correlate with worse and better prognosis, respectively [19²⁰]. This study highlighted the S100A4 protein in myeloid cells as a novel immunotherapy target [19²⁰].

IDENTIFICATION OF KEY LIGAND-RECEPTOR PAIRS

With regard to the composition of infiltrating T cells in IDH-wildtype gliomas, a combined scRNA-seq and T-cell receptor-sequencing analysis identified a subpopulation of CD8+ T cells expressing the inhibitory receptor CD161, which binds to CLEC2D expressed by malignant and myeloid cells to inhibit antitumoral activity [20²¹]. Indeed, genetic inactivation of KLRB1 (the gene-encoding CD161) or blockade of CD161 resulted in enhanced killing activity by T cells *in vitro* and improved survival *in vivo* [20²¹]. Thus, the authors suggest that targeting the CLEC2D-CD161 axis may synergize PD-1 blockade to enhance the antitumor function of distinct T-cell populations. Further analyses of spatially distinct regions revealed high regional heterogeneity of malignant and immune cells, and highlighted ligand-receptor interactions among glioma, myeloid cells, and T cells [19²⁰]. Similarly, a longitudinal study showed high heterogeneity of genomic alterations, neoantigens, and T-cell clones in recurrent tumors [21²²]. The spatiotemporal heterogeneity of the immune infiltrates emphasizes dynamic changes over time and the presence of tumor niches where the proximity (intercellular distances) is critical for immune cell activation/repression.

THE IMMUNE TME IN IDH-MUTANT GLIOMAS

The IDH enzyme catalyses the conversion of isocitrate to α -ketoglutarate (α -KG), whereas IDH1/2

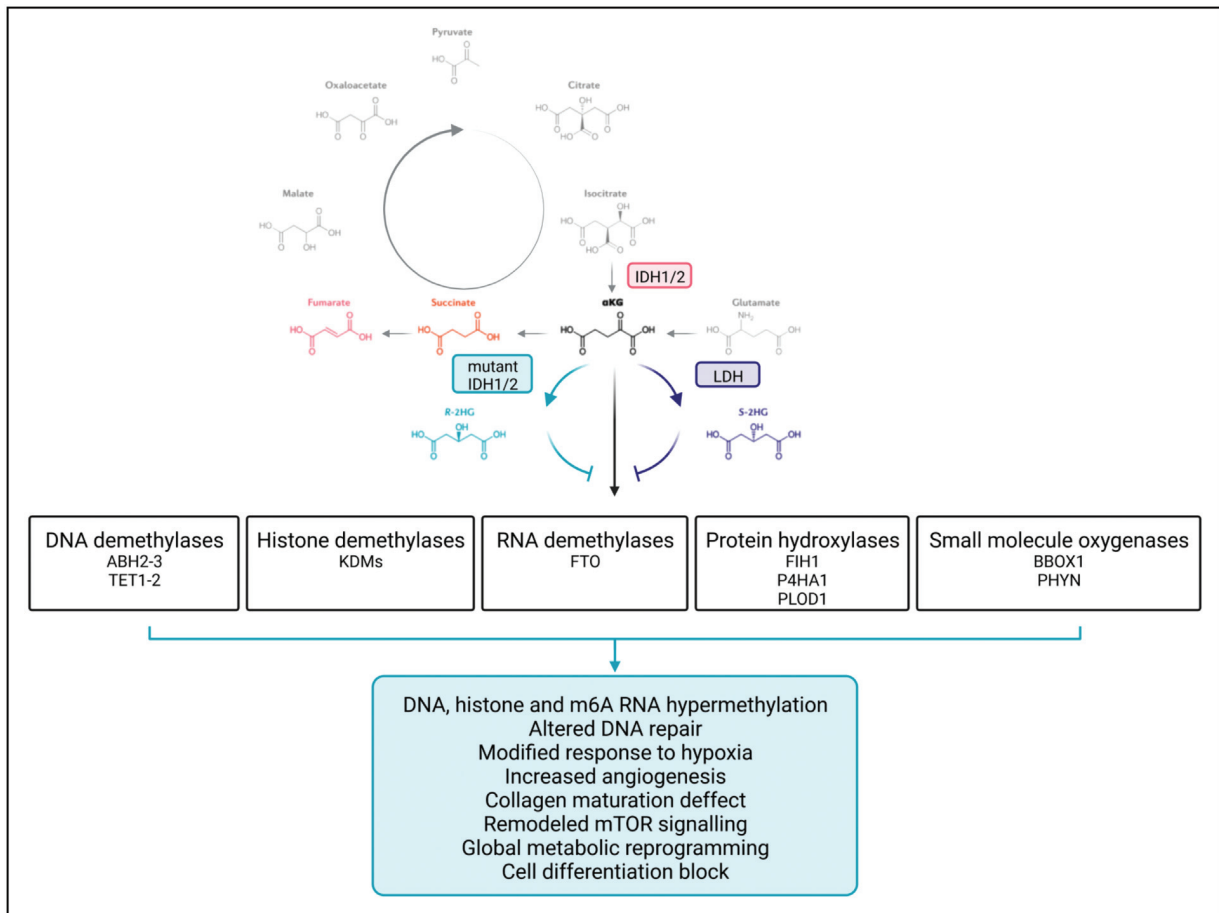


FIGURE 3. Effects of the IDH1/2 mutation. Enzymatic activity of IDH-wildtype produces α -ketoglutarate, whereas neomorphic IDH1/2 mutations produce D-2-hydroxyglutarate [D-2HG]. Canonical examples of α -ketoglutarate-dependent enzymes and consequences of their inhibition by high levels of D-2HG are also indicated. IDH, isocitrate dehydrogenase.

mutations, which are frequent in diffuse gliomas, convert α -KG to D-2-hydroxyglutarate (D-2HG) [22] (Fig. 3a). It is believed that such accumulation drives cellular transformation by inhibiting α -KG-dependent dioxygenases [23], ultimately leading to widespread hypermethylation, blocking of cell differentiation and defective collagen maturation [24–28] (Fig. 3b). Moreover, IDH-mutant cells present dysregulation of the metabolic profile and redox state promoting glycolysis and enhancing the production of reactive oxygen species [29]. Strikingly, IDH-mutant, SDH-mutant, and FH-mutant tumors, which accumulate the oncometabolites D-2HG, succinate, and fumarate, respectively, do not only display epigenomic reprogramming but also exhibit a cold immune microenvironment [30].

Seminal studies using scRNA-seq of bulk tumors uncovered essential differences in the tumor architecture of IDH-wildtype and IDH-mutant gliomas [9[–],31,32]. On one hand, malignant cells from IDH-mutant tumors follow a hierarchical organization with cycling stem-like cells giving rise to noncycling

astrocyte-like and oligodendrocyte-like lineages [9[–],31]. On the other hand, high-grade tumors undergo changes in the myeloid compartment with increased abundance of macrophages over microglia [32]. Initial analyses of the immune cell composition using TCGA bulk RNA-seq data, as well as experiments in syngeneic glioma models demonstrated a downregulation of immune-related signaling pathways and chemotaxis factors in IDH-mutant compared with IDH-wildtype gliomas [33,34]. Recent analyses of TCGA and immunohistochemical validations, confirmed a low expression of T-cell markers in IDH-mutant glioma, and revealed significant enrichment of CD4⁺ naive T cells and a reduction of memory T cells [35]. Low numbers of dendritic cells and immunosuppressive cells, including Tregs (Foxp3⁺) and TAMs (CD163⁺) were also shown, particularly in oligodendrogliomas [36]. Additional evaluation of the Chinese Glioma Genome Atlas (CGGA) cohort revealed higher infiltration of natural killer (NK) cells [37]. Moreover, IDH-mutant gliomas exhibit DNA

hypermethylation of the CD274 promoter leading to low expression of the immune ligand PD-L1 [36,38,39].

Two important studies using fluorescence-activated cell sorting followed by RNA-seq or CyTOF analyses of immune cells further confirmed that IDH-wildtype gliomas are more infiltrated by CD8+ and CD4+ T-cell subsets (including Tregs), as well as by MDMs, whereas IDH-mutant tumors display a high proportion of microglial cells and a high monocyte/MDM ratio. NK cells display immature and cytotoxic phenotypes in IDH-wildtype and IDH-mutant gliomas, respectively [40²²,41²²]. Establishing the differences in the abundance and functionality of the immune cell populations between these tumor types is crucial for the designing of efficient immunotherapeutic strategies.

Although, the IDH-mutated status was suggested to shape the TME, IDH-mutant astrocytomas and oligodendrogliomas differ in some genetic alterations, and exhibit different prognoses. In this regard, evaluation of TCGA and CGGA data indicated that immune infiltration is higher in astrocytomas than oligodendrogliomas [42]. Further analysis of bulk tumors using a combination of scRNA-seq and scATAC-seq approaches revealed a significant overexpression of chemotaxis factors CSF1 and FLT3LG in ATRX-mutated astrocytomas, and upregulation of CD163, a marker of immunosuppressive myeloid cells [43²²]. The causal role of the ATRX loss-of-function in shaping the myeloid compartment was confirmed in the SB28 mouse glioma model [43²²]. Thus, the effect of this genetic driver is reminiscent of the impact of NF1 deficiency in MES-like glioblastomas and raises the question whether genes affected by the codeletion 1p/19q that characterize IDH-mutant oligodendrogliomas (e.g. CSF1 encoded in 1p and TGFβ in 19q) account for TME changes.

Preclinical studies also explored how D-2HG acting in glioma cells could affect the TME [44,45]. Using a sleeping beauty transposon system to model IDH-mutant astrocytoma, it was shown that ATRX loss enhances DNA damage response via up-regulation of the ATM signaling pathway, which in turn was explained by D-2HG-induced hypermethylation of histone 3 (H3) [44]. The IDH mutation was also associated with hypermethylation of the activating mark H3K4me3 in the promoter region of the gene encoding granulocyte-colony stimulating factor (G-CSF) in CSCs [45]. Hence, CSC production of G-CSF was responsible for an expansion of immature granulocytic myeloid cells infiltrating the TME [45]. These results suggest that compared with IDH-wild type glioma, the overall low level of immune infiltrates in IDH-mutant gliomas involves altered expression of effectors acting on the recruitment or

the differentiation of infiltrating immune cells via D-2HG-driven epigenetic alterations in malignant cells. Nevertheless, as this oncometabolite accumulates to millimolar levels in the TME [46,47], it may also affect the phenotypic and functional properties of immune cells.

CELL-EXTRINSIC ROLES OF D-2HG

Recent in-vitro studies provided evidence for the uptake of D-2HG by cells typically residing in the TME, via the sodium-dependent dicarboxylate transporter 3 (SLC13A3) [35] or the glutamate transporter SLC1A1 [48²²] (Fig. 4). Increased D-2HG levels were also found in T cells isolated from acute myeloid leukaemia (AML) patients harbouring IDH2 mutations [49], and in CD11b+ cells from an IDH-mutant mouse model [50²²]. Treatments with D-2HG used at nontoxic albeit high concentrations (>5 mmol/l) reduce IL-12 secretion and preclude LPS-induced glycolysis in dendritic cells [51], and prevent LPS-induced activation in murine microglia by affecting the AMPK/mTOR/NF-κB-signaling pathway [52]. In endothelial cells, D-2HG fuels mitochondrial respiration and angiogenesis [48²²].

With respect to cultured T cells, D-2HG promotes a metabolic switch from aerobic glycolysis towards oxidative phosphorylation in activated T cells and favors the growth or differentiation of Tregs [49]. In contrast, in-vivo studies using GL261 cells overexpressing IDH wildtype or IDH mutant showed decreased numbers of Tregs in IDH-mutant gliomas [53] and impaired T-cell activation by reducing proliferation and cytokine production [35]. Because the functional response of immune cells depends on environmental signals and cell–cell interactions, which may be prevented *in vitro*, there is a need to characterize the effects of D-2HG *in vivo*. In this regard, inhibition of the enzymatic function of the IDH mutation increased the CD4+ population and restored the antitumor activity of T cells [35]. Moreover, this therapeutic approach combined with PD-1 inhibition increased overall survival [35,54²²].

In addition, recent evidence demonstrated that D-2HG drives an immunosuppressive myeloid state by altering the tryptophan metabolism in MDMs via activation of AHR [55²²]. Pseudotime inference analyses using scRNA-seq data of flow cytometry-purified CD45+ cells from IDH-mutant and IDH-wildtype GL261 gliomas confirmed the high monocyte/MDM ratio previously observed in IDH-mutant human tumors [40²²] and further revealed a high monocyte/dendritic cell ratio [56²²]. The authors suggested an immature phenotype of monocyte-derived cells upon D-2HG exposure. However, in-vitro

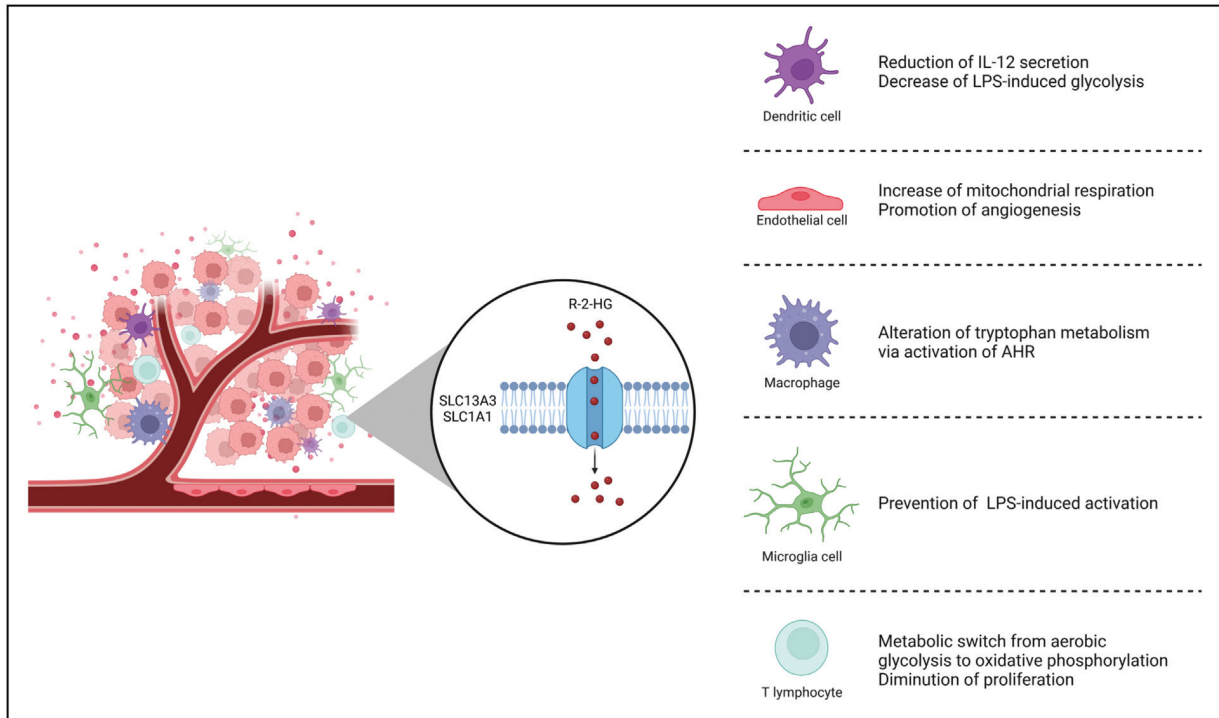


FIGURE 4. Cellular uptake of D-2-hydroxyglutarate. Cell types able to take up D-2HG according to in-vitro studies as well as two of the transporters so far reported are indicated. D-2HG, D-2-hydroxyglutarate.

experiments revealed conflicting results with a previous study showing that neither differentiation, nor antigen presentation of dendritic cells is affected by D-2HG [57]. This further emphasizes the challenges to characterize the effects of D-2HG on immune cell function *in vitro*.

Collectively, these data argue against a simple reduction of immune cell recruitment by chemotactic factors. More investigation is required to specify the roles of D-2HG as immunomodulator of the TME in IDH-mutant gliomas.

CONCLUSION

Although immunotherapy targeting the PD-L1/PD-1 axis has achieved advances in various cancers, phase III clinical trials failed to show efficacy in newly diagnosed and recurrent glioblastomas. The presence of dysfunctional T cells [58,59], as well as suppressive cells such as Tregs and TAMs in the TME may account for this lack of response. The comprehensive characterization of the immune TME at single-cell resolution and experimental evidence in mouse models point to prominent roles of TAMs and their interactions with malignant and T cells during tumor progression. Hence, focus on the myeloid compartment, and the immune checkpoints expressed by these cells is highly encouraged in order to uncover specific mechanisms leading to the immunosuppressive TME.

TAMs do not only offer a prognostic value but also are potential targets for therapies aimed at depleting/repolarizing these cells to a pro-inflammatory state thereby allowing effector T-cell infiltration and activation [60–63]. Nevertheless, targeting the myeloid population should be more specific as MDMs are more abundant in IDH wild-type gliomas and recurrent tumors (regardless of the IDH status) whereas microglial cells are the major population in IDH-mutant gliomas. Moreover, the pro-tumorigenic role of nonparenchymal macrophages, which are located in meninges, perivascular niches, and even within the cerebrospinal fluid, remains unexplored [64,65]. So far, a relatively small number of human gliomas have been profiled for scRNA-seq analysis of the TME. As more data will be generated, a more complete atlas of myeloid cells could help to identify novel subsets that correlate with clinical outcomes. Efforts are currently underway to better characterize TAM subtypes, ligand–receptor pairs, and immune checkpoints expressed by these cells [66]. It is becoming clear that glioblastoma progression requires not only genetic drivers but also microenvironment interactions [9^{–11},67]. While most of the work on immunoevading mechanisms and myeloid interactions has been done in MES-like gliomas [13^{–14},18,67], the immunomodulatory mechanisms operating in low-grade and IDH-mutant gliomas remain largely unknown.

Differences in the TME of astrocytomas and oligodendrogliomas suggested by bulk RNA-seq studies [36,42,68,69] may be linked to their distinct prognosis and need to be ascertained using scRNA-seq. IDH-mutant tumors are infiltrated by a low number of immune cells. Although results from clinical trials with IDH mutation inhibitors are promising [70], preclinical studies suggest that this approach may be more effective if combined with immunotherapies (checkpoint blockade or IDH1R132H vaccines) [35,54^{***}]. Although cell-extrinsic effects of D-2HG mediate some changes in the TME, the impact of this oncometabolite on the epigenome of immune cells remains unexplored. Hence, these are exciting times to discover additional roles of D-2HG in the TME of IDH-mutant gliomas.

Acknowledgements

We thank all members of the laboratory, as well as the guest speakers of the seminar series on the TME of gliomas held at the ICM – Paris Brain Institute for insightful discussions. We apologize to all colleagues whose contributions could not be cited because of space limitations. Figures were created with BioRender's web-based software, and pictures were kindly provided by Dr. Karima Mokhtari, Hôpital de la Pitié Salpêtrière, Paris, France.

Financial support and sponsorship

Work in the Genetics & Development of Brain Tumors Lab is supported by the grants Fondation Bristol Myers Squibb pour la Recherche en Immuno-Oncologie (BMS 2104009NA), French National Cancer Institute (INCA-PLBIO22-243), and Entreprises contre le Cancer Paris-Île-de-France (GEFLUC R20202DD). The group is supported by La Ligue Nationale contre le Cancer (Équipe Labellisée) and by the Site de Recherche Intégré sur le Cancer (SiRIC CURAMUS). A.L.-L. is supported by Fondation Recherche Médicale (FRM) scholarship, and Q.R. is supported by the French Ministry of Education and Research scholarship.

Conflicts of interest

There are no conflicts of interest.

REFERENCES AND RECOMMENDED READING

Papers of particular interest, published within the annual period of review, have been highlighted as:

- of special interest
- ■ of outstanding interest

1. Louis DN, Perry A, Wesseling P, *et al.* The 2021 WHO Classification of Tumors of the Central Nervous System: a summary. *Neuro Oncol* 2021; 23:1231–1251.
 2. Verhaak RGW, Hoadley KA, Purdom E, *et al.* Integrated genomic analysis identifies clinically relevant subtypes of glioblastoma characterized by abnormalities in PDGFRA, IDH1, EGFR, and NF1. *Cancer Cell* 2010; 17:98–110.
 3. Wang Q, Hu B, Hu X, *et al.* Tumor evolution of glioma-intrinsic gene expression subtypes associates with immunological changes in the micro-environment. *Cancer Cell* 2018; 33:152.
 4. Neftel C, Laffy J, Filbin MG, *et al.* An integrative model of cellular states, plasticity, and genetics for glioblastoma. *Cell* 2019; 178:835.e21–849.e21.
 5. Gimple RC, Yang K, Halbert ME, *et al.* Brain cancer stem cells: resilience through adaptive plasticity and hierarchical heterogeneity. *Nat Rev Cancer* 2022; 22:497–514.
 6. Xie XP, Laks DR, Sun D, *et al.* Quiescent human glioblastoma cancer stem cells drive tumor initiation, expansion, and recurrence following chemotherapy. *Dev Cell* 2022; 57:32.e8–46.e8.
- This study identifies an expression signature of quiescent glioblastoma CSCs in mouse gliomas that is retrieved in humans independently of the glioma tumor subtypes, and accounts for tumor resistance to antimetabolic drugs.
7. Couturier CP, Ayyadury S, Le PU, *et al.* Single-cell RNA-seq reveals that glioblastoma recapitulates a normal neurodevelopmental hierarchy. *Nat Commun* 2020; 11:3406.
- scRNA-seq comparative analysis using the neurodevelopmental hierarchy as a roadmap reveals cycling progenitor glioblastoma stem cells resistant to temozolomide.
8. Chaligne R, Gaiti F, Silverbush D, *et al.* Epigenetic encoding, heritability and plasticity of glioma transcriptional cell states. *Nat Genet* 2021; 53:1469–1479.
- Multomics single cell analysis, and in particular DNA methylation, confirms a hierarchical organization of IDH-mutant gliomas and further argues for plastic cellular states of IDH-wildtype tumors.
9. Johnson KC, Anderson KJ, Courtois ET, *et al.* Single-cell multimodal glioma analyses identify epigenetic regulators of cellular plasticity and environmental stress response. *Nat Genet* 2021; 53:1456–1468.
- Multomics single cell analysis identifies high epigenetic diversity in aggressive glioblastomas underlying adaptive changes to environmental stimuli.
10. Ravi VM, Will P, Kueckelhaus J, *et al.* Spatially resolved multiomics deciphers bidirectional tumor-host interdependence in glioblastoma. *Cancer Cell* 2022; 40:639.e13–655.e13.
- Spatial transcriptomic analysis highlights the environmental factors that influence the archetypal cell state transitions in glioblastomas.
11. Salam R, Saliou A, Bielle F, *et al.* Cellular senescence in malignant cells promotes tumor progression in mouse and patient glioblastoma. *bioRxiv* 2022. doi: <https://doi.org/10.1101/2022.05.18.492465>.
- This study identifies senescent glioblastoma cells whose expression signature correlates with poor prognosis in human patients. A preclinical proof-of-concept of a senolytic therapy is provided.
12. Fletcher-Sananikone E, Kanji S, Tomimatsu N, *et al.* Elimination of radiation-induced senescence in the brain tumor microenvironment attenuates glioblastoma recurrence. *Cancer Res* 2021; 81:5935–5947.
- This study shows noncancer senescent cells, particularly astrocytes, are generated after irradiation and favor tumor progression. A preclinical proof-of-concept of a senolytic therapy is provided.
13. Gangoso E, Southgate B, Bradley L, *et al.* Glioblastomas acquire myeloid-affiliated transcriptional programs via epigenetic immunoevasion to elicit immune evasion. *Cell* 2021; 184:2454.e26–2470.e26.
- This study reveals epigenetic mechanisms in glioblastoma stem cells that underlie immune evasion and the establishment of a TME enriched on TAMs.
14. Hara T, Chanoch-Myers R, Mathewson ND, Myskiw C, *et al.* Interactions between cancer cells and immune cells drive transitions to mesenchymal-like states in glioblastoma. *Cancer Cell* 2021; 39:779.e11–792.e11.
- TAMs induce the MES-like phenotype of glioma cells via OSM.
15. Pombo Antunes AR, Scheyltjens I, Lodi F, *et al.* Single-cell profiling of myeloid cells in glioblastoma across species and disease stage reveals macrophage competition and specialization. *Nat Neurosci* 2021; 24:595–610.
- Characterization of the myeloid compartment of human and mouse glioblastomas at single-cell resolution and experimental evidence of a dynamic competition of resident and infiltrating macrophages during tumor progression.
16. Ochocka N, Segit P, Walentyowicz KA, *et al.* Single-cell RNA sequencing reveals functional heterogeneity of glioma-associated brain macrophages. *Nat Commun* 2021; 12:1151.
- scRNA-seq analysis of TAMs heterogeneity in a mouse glioblastoma model.
17. Liu H, Sun Y, Zhang Q, *et al.* Pro-inflammatory and proliferative microglia drive progression of glioblastoma. *Cell Rep* 2021; 36:109718.
 18. Yeo AT, Rawal S, Delcuze B, *et al.* Single-cell RNA sequencing reveals evolution of immune landscape during glioblastoma progression. *Nat Immunol* 2022; 23:971–984.
 19. Abdelfattah N, Kumar P, Wang C, *et al.* Single-cell analysis of human glioma and immune cells identifies S100A4 as an immunotherapy target. *Nat Commun* 2022; 13:767.
- scRNA-seq analysis of the myeloid compartment of a large series of human gliomas supports a prognostic value of subsets of TAMs and microglia cells.
20. Mathewson ND, Ashenberg O, Tirosh I, *et al.* Inhibitory CD161 receptor identified in glioma-infiltrating T cells by single-cell analysis. *Cell* 2021; 184:1281.e26–1298.e26.
- scRNA-seq analysis of the lymphocytic infiltrate of gliomas identifies the inhibitory signal CLEC2D-CD161.

21. Schaeffler MO, Richters MM, Wang AZ, *et al.* Characterization of the genomic and immunologic diversity of malignant brain tumors through multisector analysis. *Cancer Discov* 2022; 12:154–171.
- Comprehensive multiregional analysis of immunologic diversity of gliomas reveals high spatial heterogeneity and ligand–receptor interactions, particularly with myeloid cells.
22. Dang L, White DW, Gross S, *et al.* Cancer-associated IDH1 mutations produce 2-hydroxyglutarate. *Nature* 2010; 465:966.
23. Xu W, Yang H, Liu Y, *et al.* Oncometabolite 2-hydroxyglutarate is a competitive inhibitor of α -ketoglutarate-dependent dioxygenases. *Cancer Cell* 2011; 19:17–30.
24. Noushmehr H, Weisenberger DJ, Diefes K, *et al.* Identification of a CpG island methylator phenotype that defines a distinct subgroup of glioma. *Cancer Cell* 2010; 17:510–522.
25. Turcan S, Rohle D, Goenka A, *et al.* IDH1 mutation is sufficient to establish the glioma hypermethylator phenotype. *Nature* 2012; 483:479–483.
26. Markolovic S, Wilkins SE, Schofield CJ. Protein hydroxylation catalyzed by 2-oxoglutarate-dependent oxygenases. *J Biol Chem* 2015; 290:20712–20722.
27. Lu C, Ward PS, Kapoor GS, *et al.* IDH mutation impairs histone demethylation and results in a block to cell differentiation. *Nature* 2012; 483:474–478.
28. Sasaki M, Knobbe CB, Itsumi M, *et al.* D-2-hydroxyglutarate produced by mutant IDH1 perturbs collagen maturation and basement membrane function. *Genes Dev* 2012; 26:2038–2049.
29. Fack F, Tardito S, Hochart G, *et al.* Altered metabolic landscape in IDH-mutant gliomas affects phospholipid, energy, and oxidative stress pathways. *EMBO Mol Med* 2017; 9:1681–1695.
30. Thorsson V, Gibbs DL, Brown SD, *et al.* The immune landscape of cancer. *Immunity* 2018; 48:812.e14–830.e14.
31. Tirosh I, Venteicher AS, Hebert C, *et al.* Single-cell RNA-seq supports a developmental hierarchy in human oligodendroglioma. *Nature* 2016; 539:309–313.
32. Venteicher AS, Tirosh I, Hebert C, *et al.* Decoupling genetics, lineages, and microenvironment in IDH-mutant gliomas by single-cell RNA-seq. *Science (New York, NY)* 2017; 355:eaai8478.
33. Amankulor NM, Kim Y, Arora S, *et al.* Mutant IDH1 regulates the tumor-associated immune system in gliomas. *Genes Dev* 2017; 31:774–786.
34. Kohanbash G, Carrera DA, Shrivastav S, *et al.* Isocitrate dehydrogenase mutations suppress STAT1 and CD8+ T cell accumulation in gliomas. *J Clin Invest* 2017; 127:1425–1437.
35. Bunse L, Pusch S, Bunse T, *et al.* Suppression of antitumor T cell immunity by the oncometabolite (R)-2-hydroxyglutarate. *Nat Med* 2018; 24:1192–1203.
36. Mu L, Long Y, Yang C, *et al.* The IDH1 mutation-induced oncometabolite, 2-hydroxyglutarate, may affect DNA methylation and expression of PD-L1 in gliomas. *Front Mol Neurosci* 2018; 11:82.
37. Ren F, Zhao Q, Huang L, *et al.* The R132H mutation in IDH1 promotes the recruitment of NK cells through CX3CL1/CX3CR1 chemotaxis and is correlated with a better prognosis in gliomas. *Immunol Cell Biol* 2019; 97:457–469.
38. Berghoff AS, Kiesel B, Widhalm G, *et al.* Correlation of immune phenotype with IDH mutation in diffuse glioma. *Neuro Oncol* 2017; 19:1460–1468.
39. Röver LK, Gevensleben H, Dietrich J, *et al.* PD-1 (PDCD1) promoter methylation is a prognostic factor in patients with diffuse lower-grade gliomas harboring isocitrate dehydrogenase (IDH) mutations. *EBioMedicine* 2018; 28:97–104.
40. Klemm F, Maas RR, Bowman RL, *et al.* Interrogation of the microenvironmental landscape in brain tumors reveals disease-specific alterations of immune cells. *Cell* 2020; 181:1643.e17–1660.e17.
- First comprehensive characterization of the immune landscape of human gliomas suggesting an influence of IDH mutation status.
41. Friebel E, Kapolou K, Unger S, *et al.* Single-cell mapping of human brain cancer reveals tumor-specific instruction of tissue-invading leukocytes. *Cell* 2020; 181:1626.e20–1642.e20.
- First comprehensive characterization of the immune landscape of human gliomas suggesting an influence of IDH mutation status.
42. Zhao B, Xia Y, Yang F, *et al.* Molecular landscape of IDH-mutant astrocytoma and oligodendroglioma grade 2 indicate tumor purity as an underlying genomic factor. *Mol Med* 2022; 28:34.
43. Babikir H, Wang L, Shamardani K, *et al.* ATRX regulates glial identity and the tumor microenvironment in IDH-mutant glioma. *Genome Biol* 2021; 22:311. scRNA-seq study showing differences in the TME between astrocytomas and oligodendrogliomas, and a causal role of ATRX loss.
44. Núñez FJ, Mendez FM, Kadiyala P, *et al.* IDH1-R132H acts as a tumor suppressor in glioma via epigenetic up-regulation of the DNA damage response. *Sci Transl Med* 2019; 11:eaq1427.
45. Alghamri MS, McClellan BL, Avvari RP, *et al.* G-CSF secreted by mutant IDH1 glioma stem cells abolishes myeloid cell immunosuppression and enhances the efficacy of immunotherapy. *Sci Adv* 2021; 7:eabh3243.
46. Linninger A, Hartung GA, Liu BP, *et al.* Modeling the diffusion of D-2-hydroxyglutarate from IDH1 mutant gliomas in the central nervous system. *Neuro Oncol* 2018; 20:1197–1206.
47. Pickard AJ, Sohn ASW, Bartenstein TF, *et al.* Intracerebral distribution of the oncometabolite d-2-hydroxyglutarate in mice bearing mutant isocitrate dehydrogenase brain tumors: implications for tumorigenesis. *Front Oncol* 2016; 6:211.
48. Wang X, Chen Z, Xu J, *et al.* SLC1A1-mediated cellular and mitochondrial influx of R-2-hydroxyglutarate in vascular endothelial cells promotes tumor angiogenesis in IDH1-mutant solid tumors. *Cell Res* 2022; 32:638–658.
- First evidence for the role of D-2HG on endothelial cells.
49. Böttcher M, Renner K, Berger R, *et al.* D-2-hydroxyglutarate interferes with HIF-1 α stability skewing T-cell metabolism towards oxidative phosphorylation and impairing Th17 polarization. *Oncoimmunology* 2018; 7:e1445454.
50. Chuntova P, Yamamichi A, Chen T, *et al.* Inhibition of D-2HG leads to upregulation of a proinflammatory gene signature in a novel HLA-A2/HLA-DR1 transgenic mouse model of IDH1R132H-expressing glioma. *J Immunother Cancer* 2022; 10:e004644.
- This study shows the effects of inhibiting the enzymatic function of the IDH mutation on immune cell compartments in a mouse glioma model.
51. Ugele I, Cárdenas-Conejo ZE, Hammon K, *et al.* D-2-hydroxyglutarate and L-2-hydroxyglutarate inhibit IL-12 secretion by human monocyte-derived dendritic cells. *Int J Mol Sci* 2019; 20:742.
52. Han C-J, Zheng J-Y, Sun L, *et al.* The oncometabolite 2-hydroxyglutarate inhibits microglial activation via the AMPK/mTOR/NF- κ B pathway. *Acta Pharmacol Sin* 2019; 40:1292–1302.
53. Richardson LG, Nieman LT, Stemmer-Rachamimov AO, *et al.* IDH-mutant gliomas harbor fewer regulatory T cells in humans and mice. *Oncoimmunology* 2020; 9:1806662.
54. Kadiyala P, Carney Sv, Gauss JC, *et al.* Inhibition of 2-hydroxyglutarate elicits metabolic reprogramming and mutant IDH1 glioma immunity in mice. *J Clin Invest* 2021; 131:e139542.
- This study demonstrates the efficacy of combined D-2HG inhibition/IR/TMZ with anti-PDL1 immune checkpoint blockade in a mouse astrocytoma model.
55. Friedrich M, Sankowski R, Bunse L, *et al.* Tryptophan metabolism drives dynamic immunosuppressive myeloid states in IDH-mutant gliomas. *Nat Cancer* 2021; 2:723–740.
- First evidence for the role of D-2HG on macrophages.
56. Friedrich M, Hahn M, Michel J, *et al.* Dysfunctional dendritic cells limit antigen-specific T cell response in glioma. *Neuro Oncol* 2022; noac138. doi: 10.1093/neuonc/noac138.
- First evidence indicating that D-2HG affects dendritic cell differentiation and antigen presentation.
57. Zhang L, Sorensen MD, Kristensen BW, *et al.* D-2-hydroxyglutarate is an intercellular mediator in IDH-mutant gliomas inhibiting complement and T cells. *Clin Cancer Res* 2018; 24:5381–5391.
58. Woroniecka K, Chongsathidkiet P, Rhodin K, *et al.* T-cell exhaustion signatures vary with tumor type and are severe in glioblastoma. *Clin Cancer Res* 2018; 24:4175–4186.
59. Davidson TB, Lee A, Hsu M, *et al.* Expression of PD-1 by T cells in malignant glioma patients reflects exhaustion and activation. *Clin Cancer Res* 2019; 25:1913–1922.
60. Müller S, Kohanbash G, Liu SJ, *et al.* Single-cell profiling of human gliomas reveals macrophage ontogeny as a basis for regional differences in macrophage activation in the tumor microenvironment. *Genome Biol* 2017; 18:234.
61. Pyonteck SM, Akkari L, Schuhmacher AJ, *et al.* CSF-1R inhibition alters macrophage polarization and blocks glioma progression. *Nat Med* 2013; 19:1264–1272.
62. Goswami S, Anandhan S, Raychaudhuri D, Sharma P. Myeloid cell-targeted therapies for solid tumours. *Nat Rev Immunol* 2022. doi: 10.1038/s41577-022-00737-w.
63. Pittet MJ, Michielin O, Migliorini D. Clinical relevance of tumour-associated macrophages. *Nat Rev Clin Oncol* 2022; 19:402–421.
64. van Hove H, Martens L, Scheyltjens I, *et al.* A single-cell atlas of mouse brain macrophages reveals unique transcriptional identities shaped by ontogeny and tissue environment. *Nat Neurosci* 2019; 22:1021–1035.
65. Munro DAD, Movahedi K, Priller J. Macrophage compartmentalization in the brain and cerebrospinal fluid system. *Sci Immunol* 2022; 7:eabk0391.
66. Gupta P, Dang M, Bojja K, *et al.* Transcriptionally defined immune contexture in human gliomas at single-cell resolution. *Neuro-oncology* 2020; 22(Suppl 2):ii112–ii112.
67. Varn FS, Johnson KC, Martinek J, *et al.* Glioma progression is shaped by genetic evolution and microenvironment interactions. *Cell* 2022; 185:2184.e16–2199.e16.
- This study provides evidence for genetic alterations influencing glioma progression and emphasizes interactions with myeloid cells.
68. Zhang Y, Xie Y, He L, *et al.* 1p/19q co-deletion status is associated with distinct tumor-associated macrophage infiltration in IDH mutated lower-grade gliomas. *Cell Oncol* 2021; 44:193–204.
69. Lin W, Qiu X, Sun P, *et al.* Association of IDH mutation and 1p19q co-deletion with tumor immune microenvironment in lower-grade glioma. *Mol Ther Oncolytics* 2021; 21:288–302.
70. Mellinghoff IK, Ellingson BM, Touat M, *et al.* Ivosidenib in isocitrate dehydrogenase 1-mutated advanced glioma. *J Clin Oncol* 2020; 38:3398–3406.

B.4 Reciprocal interactions between glioma and tissue-resident cells fueling tumor progression

To appear as Chapter 11 in *Handbook of Clinical Neurology: HCN Volume 210, Neuroglia in Neurologic and Psychiatric Disorders*.

Chapter under copyright, to appear as Chapter 11 in *Handbook of Clinical Neurology: HCN Volume 210, Neuroglia in Neurologic and Psychiatric Disorders*.

Chapter under copyright, to appear as Chapter 11 in *Handbook of Clinical Neurology: HCN Volume 210, Neuroglia in Neurologic and Psychiatric Disorders*.

Chapter under copyright, to appear as Chapter 11 in *Handbook of Clinical Neurology: HCN Volume 210, Neuroglia in Neurologic and Psychiatric Disorders*.

Chapter under copyright, to appear as Chapter 11 in *Handbook of Clinical Neurology: HCN Volume 210, Neuroglia in Neurologic and Psychiatric Disorders*.

Chapter under copyright, to appear as Chapter 11 in *Handbook of Clinical Neurology: HCN Volume 210, Neuroglia in Neurologic and Psychiatric Disorders*.

Chapter under copyright, to appear as Chapter 11 in *Handbook of Clinical Neurology: HCN Volume 210, Neuroglia in Neurologic and Psychiatric Disorders*.

Chapter under copyright, to appear as Chapter 11 in *Handbook of Clinical Neurology: HCN Volume 210, Neuroglia in Neurologic and Psychiatric Disorders*.

Chapter under copyright, to appear as Chapter 11 in *Handbook of Clinical Neurology: HCN Volume 210, Neuroglia in Neurologic and Psychiatric Disorders*.

Chapter under copyright, to appear as Chapter 11 in *Handbook of Clinical Neurology: HCN Volume 210, Neuroglia in Neurologic and Psychiatric Disorders*.

Chapter under copyright, to appear as Chapter 11 in *Handbook of Clinical Neurology: HCN Volume 210, Neuroglia in Neurologic and Psychiatric Disorders*.

Chapter under copyright, to appear as Chapter 11 in *Handbook of Clinical Neurology: HCN Volume 210, Neuroglia in Neurologic and Psychiatric Disorders*.

Chapter under copyright, to appear as Chapter 11 in *Handbook of Clinical Neurology: HCN Volume 210, Neuroglia in Neurologic and Psychiatric Disorders*.

Chapter under copyright, to appear as Chapter 11 in *Handbook of Clinical Neurology: HCN Volume 210, Neuroglia in Neurologic and Psychiatric Disorders*.

Chapter under copyright, to appear as Chapter 11 in *Handbook of Clinical Neurology: HCN Volume 210, Neuroglia in Neurologic and Psychiatric Disorders*.

Chapter under copyright, to appear as Chapter 11 in *Handbook of Clinical Neurology: HCN Volume 210, Neuroglia in Neurologic and Psychiatric Disorders*.

Chapter under copyright, to appear as Chapter 11 in *Handbook of Clinical Neurology: HCN Volume 210, Neuroglia in Neurologic and Psychiatric Disorders*.

Chapter under copyright, to appear as Chapter 11 in *Handbook of Clinical Neurology: HCN Volume 210, Neuroglia in Neurologic and Psychiatric Disorders*.

Chapter under copyright, to appear as Chapter 11 in *Handbook of Clinical Neurology: HCN Volume 210, Neuroglia in Neurologic and Psychiatric Disorders*.

Chapter under copyright, to appear as Chapter 11 in *Handbook of Clinical Neurology: HCN Volume 210, Neuroglia in Neurologic and Psychiatric Disorders*.

Chapter under copyright, to appear as Chapter 11 in *Handbook of Clinical Neurology: HCN Volume 210, Neuroglia in Neurologic and Psychiatric Disorders*.

Chapter under copyright, to appear as Chapter 11 in *Handbook of Clinical Neurology: HCN Volume 210, Neuroglia in Neurologic and Psychiatric Disorders*.

Chapter under copyright, to appear as Chapter 11 in *Handbook of Clinical Neurology: HCN Volume 210, Neuroglia in Neurologic and Psychiatric Disorders*.

Chapter under copyright, to appear as Chapter 11 in *Handbook of Clinical Neurology: HCN Volume 210, Neuroglia in Neurologic and Psychiatric Disorders*.

Chapter under copyright, to appear as Chapter 11 in *Handbook of Clinical Neurology: HCN Volume 210, Neuroglia in Neurologic and Psychiatric Disorders*.

Chapter under copyright, to appear as Chapter 11 in *Handbook of Clinical Neurology: HCN Volume 210, Neuroglia in Neurologic and Psychiatric Disorders*.

Chapter under copyright, to appear as Chapter 11 in *Handbook of Clinical Neurology: HCN Volume 210, Neuroglia in Neurologic and Psychiatric Disorders*.

Appendix C

Research articles and reviews not directly related to this PhD that I co-authored

C.1 Cell of Origin of Brain and Spinal Cord Tumors

Alice Laurence, Emmanuelle Huillard, Franck Bielle, and Ahmed Idbah (2023). "Cell of Origin of Brain and Spinal Cord Tumors". In: *Advances in Experimental Medicine and Biology* 1394, pp. 85–101. ISSN: 0065-2598. DOI: 10.1007/978-3-031-14732-6_6

Abstract

A better understanding of cellular and molecular biology of primary central nervous system (CNS) tumors is a critical step toward the design of innovative treatments. In addition to improving knowledge, identification of the cell of origin in tumors allows for sharp and efficient targeting of specific tumor cells promoting and driving oncogenic processes. The World Health Organization identifies approximately 150 primary brain tumor subtypes with various ontogeny and clinical outcomes. Identification of the cell of origin of each tumor type with its lineage and differentiation level is challenging. In the current chapter, we report the suspected cell of origin of various CNS primary tumors including gliomas, glioneuronal tumors, medulloblastoma, meningioma, atypical teratoid rhabdoid tumor, germinomas, and lymphoma. Most of them have been pinpointed through transgenic mouse models and analysis of molecular signatures of tumors. Identification of the cell or cells of origin in primary brain tumors will undoubtedly open new therapeutic avenues, including the reactivation of differentiation programs for therapeutic perspectives.

C.2 Integrated proteogenomic characterization of glioblastoma evolution

Kyung-Hee Kim, Simona Migliozi, Harim Koo, Jun-Hee Hong, Seung Min Park, Sooheon Kim, Hyung Joon Kwon, Seokjun Ha, Luciano Garofano, Young Taek Oh, Fulvio D'Angelo, Chan Il Kim, Seongsoo Kim, Ji Yoon Lee, Jiwon Kim, Jisoo Hong, Eun-Hae Jang, Bertrand Mathon, Anna-Luisa Di Stefano, Franck Bielle, Alice Laurence, Alexey I. Nesvizhskii, Eun-Mi Hur, Jinlong Yin, Bingyang Shi, Youngwook Kim, Kyung-Sub Moon, Jeong Taik Kwon, Shin Heon Lee, Seung Hoon Lee, Ho Shin Gwak, Anna Lasorella, Heon Yoo, Marc Sanson, Jason K. Sa, Chul-Kee Park, Do-Hyun Nam, Antonio Iavarone, and Jong Bae Park (Mar. 11, 2024). "Integrated proteogenomic characterization of glioblastoma evolution". In: *Cancer Cell* 42.3, 358–377.e8. ISSN: 1878-3686. DOI: 10.1016/j.cccell.2023.12.015

Abstract

The evolutionary trajectory of glioblastoma (GBM) is a multifaceted biological process that extends beyond genetic alterations alone. Here, we perform an integrative proteogenomic analysis of 123 longitudinal glioblastoma pairs and identify a highly proliferative cellular state at diagnosis and replacement by activation of neuronal transition and synaptogenic pathways in recurrent tumors. Proteomic and phosphoproteomic analyses reveal that the molecular transition to neuronal state at recurrence is marked by post-translational activation of the wingless-related integration site (WNT)/ planar cell polarity (PCP) signaling pathway and BRAF protein kinase. Consistently, multi-omic analysis of patient-derived xenograft (PDX) models mirror similar patterns of evolutionary trajectory. Inhibition of B-raf proto-oncogene (BRAF) kinase impairs both neuronal transition and migration capability of recurrent tumor cells, phenotypic hallmarks of post-therapy progression. Combinatorial treatment of temozolomide (TMZ) with BRAF inhibitor, vemurafenib, significantly extends the survival of PDX models. This study provides comprehensive insights into the biological mechanisms of glioblastoma evolution and treatment resistance, highlighting promising therapeutic strategies for clinical intervention.

Appendix D

Clinical articles not directly related to this PhD that I co-authored

D.1 Articles on lymphomas

D.1.1 SARS-CoV-2 infection in patients with primary central nervous system lymphoma

Alice Laurence, Renata Ursu, Caroline Houillier, Basma Abdi, Gianpiero Tebano, Cyril Quemeneur, Sylvain Choquet, Roberta Di Blasi, Fernando Lozano, Andrea Morales, Alberto Durán-Peña, Lila Sirven-Villaros, Bertrand Mathon, Karima Mokhtari, Franck Bielle, Nadine Martin-Duverneuil, Jean-Yves Delattre, Anne-Geneviève Marcelin, Valérie Pourcher, Agusti Alentorn, Ahmed Idbaih, Antoine F. Carpentier, Véronique Leblond, Khê Hoang-Xuan, and Mehdi Touat (Sept. 2021). "SARS-CoV-2 infection in patients with primary central nervous system lymphoma". In: *Journal of Neurology* 268.9, pp. 3072–3080. ISSN: 0340-5354, 1432-1459. DOI: 10.1007/s00415-020-10311-w. URL: <https://link.springer.com/10.1007/s00415-020-10311-w> (visited on 03/03/2022)

Abstract

Background Cancer patients may be at higher risk for severe coronavirus infectious disease-19 (COVID-19); however, the outcome of Primary Central Nervous System Lymphoma (PCNSL) patients with SARS-CoV-2 infection has not been described yet. **Methods** We conducted a retrospective study within the Lymphomes Oculo-Cérébraux national network (LOC) to assess the clinical characteristics and outcome of SARS-CoV-2 infection in PCNSL patients (positive real-time polymerase chain reaction of nasopharyngeal swab or evocative lung computed tomography scan). We compared clinical characteristics between patients with severe (death and/or intensive care unit admission) and mild disease. **Results** Between March and May 2020, 13 PCNSL patients were diagnosed with SARS-CoV-2 infection, 11 (85%) of whom were undergoing chemotherapy at the time of infection. The mortality rate was 23% (3/13), and two additional patients (15%) required mechanical ventilation. Two patients (15%) had no COVID-19 symptoms. History of diabetes mellitus was more common in severe patients (3/5 vs 0/8, $p = 0.03$). Two patients recovered from

COVID-19 after mechanical ventilation during more than two weeks and resumed chemotherapy. In all, chemotherapy was resumed after COVID-19 recovery in nine patients (69%) after a median delay of 16 days (range 3–32), none of whom developed unusual chemotherapy complication nor SARS-Cov2 reactivation. **Conclusion** This preliminary analysis suggests that, while being at higher risk be for severe illness, PCNSL patients with COVID-19 might be treated maximally especially if they achieved oncological response at the time of SARS-CoV-2 infection. Chemotherapy might be resumed without prolonged delay in PCNSL patients with COVID-19.

D.1.2 SARS-CoV-2 infection in patients with primary central nervous system lymphoma in the vaccination era

Alice Laurence, Renata Ursu, Emeline Tabouret, Vincent Harlay, Guido Ahle, Sylvain Choquet, Carole Soussain, Cécile Moluçon-Chabrot, Bertrand Mathon, Karima Mokhtari, Valérie Pourcher, Lucia Nichelli, Stéphane Marot, Mehdi Touat, Khê Hoang-Xuan, and Caroline Houillier (Jan. 2023). "SARS-CoV-2 infection in patients with primary central nervous system lymphoma in the vaccination era". In: *Leukemia & Lymphoma* 64.1, pp. 221–224. ISSN: 1029-2403. DOI: 10.1080/10428194.2022.2131420

D.1.3 Impact of severe acute respiratory syndrome coronavirus-2 infection on the outcome of primary central nervous system lymphoma treatment: A study of the International PCNSL Collaborative Group

Sara Steffanoni, Teresa Calimeri, Alice Laurence, Christopher P. Fox, Carole Sous-sain, Christian Grommes, Maria Chiara Tisi, Jesca Boot, Nicola Crosbie, Carlo Visco, Luca Arcaini, Sridhar Chaganti, Marianna C. Sassone, Alvaro Alencar, Daniele Armiento, Ilaria Romano, Jorg Dietrich, Gilad Itchaki, Riccardo Bruna, Nicola S. Fracchiolla, Laura Arletti, Adriano Venditti, Stephen Booth, Pellegrino Musto, Khê Hoang Xuan, Tracy T. Batchelor, Kate Cwynarski, and Andrés J. M. Ferreri (Nov. 2022). "Impact of severe acute respiratory syndrome coronavirus-2 infection on the outcome of primary central nervous system lymphoma treatment: A study of the International PCNSL Collaborative Group". In: *British Journal of Haematology* 199.4, pp. 507–519. ISSN: 1365-2141. DOI: 10.1111/bjh.18396

Abstract

To optimise management of severe acute respiratory syndrome coronavirus-2 (SARS-CoV-2) infection identifying high-risk patients and maintaining treatment dose intensity is an important issue in patients with aggressive lymphomas. In the present study, we report on the presentation, management, and outcome of an international series of 91 patients with primary central nervous system lymphoma and SARS-CoV-2 infection. SARS-CoV-2 was diagnosed before/during first-line treatment in 64 patients, during follow-up in 21, and during salvage therapy in six. Among the 64 patients infected before/during first-line chemotherapy, 38 (59%) developed pneumonia and 26 (41%) did not clear the virus. Prolonged exposure to steroids before viral infection and/or treatment with high-dose cytarabine favoured pneumonia development and virus persistence and were associated with poorer survival; 81% of patients who did not clear virus died early from coronavirus disease 2019 (COVID-19). Vaccination was associated with lower pneumonia incidence and in-hospital mortality. Chemotherapy was initiated/resumed in 43 (67%) patients, more commonly among patients who did not develop pneumonia, cleared the virus, or did not receive steroids during infection. Chemotherapy resumption in patients with viral persistence should be indicated cautiously as it was associated with a poorer survival (6-month, 70% and 87%, $p = 0.07$). None of the 21 patients infected during follow-up died from COVID-19, requiring similar measures as infected subjects in the general population.

D.1.4 Inflammatory demyelinating polyneuropathies and lymphoma: clues to diagnosis and therapy

Nicolas Noel, Guillemette Beaudonnet, Cécile Cauquil, Alice Laurence, Mathilde De Menthon, Céline Labeyrie, Pascale Chrétien, Clovis Adam, Salima Hacein-Bey-Abina, Cécile Goujard, Olivier Lambotte, and David Adams (Aug. 2021). "Inflammatory demyelinating polyneuropathies and lymphoma: clues to diagnosis and therapy". In: *Leukemia & Lymphoma* 62.8, pp. 2000–2004. ISSN: 1029-2403. DOI: 10.1080/10428194.2021.1889535

D.1.5 Prognostic Value of CSF IL-10 at Early Assessment of Induction Chemotherapy in Primary CNS Lymphomas: A LOC Network Study

Dora Herzi, Magali Le Garff-Tavernier, Elise Sourdeau, Sylvain Choquet, Carole Soussain, Lucia Nichelli, Bertrand Mathon, Karima Mokhtari, Alice Laurence, Agusti Alentorn, Ines Boussen, Marion Alcantara, Khê Hoang-Xuan, and Caroline Houillier (June 25, 2024). "Prognostic Value of CSF IL-10 at Early Assessment of Induction Chemotherapy in Primary CNS Lymphomas: A LOC Network Study". In: *Neurology* 102.12, e209527. ISSN: 1526-632X. DOI: 10.1212/WNL.000000000209527

Abstract

OBJECTIVES: Despite a high response rate at the first evaluation during induction chemotherapy, the risk of early relapse remains high and unpredictable in primary CNS lymphomas (PCSNLs). We aimed to assess the prognostic value of early IL-10 levels in CSF (e-IL-10) after 2 months of induction chemotherapy. **METHODS:** We retrospectively selected from the LOC (Lymphomes Oculo-Cérébraux) network database patients with PCSNLs who had complete or partial response at the 2-month evaluation of a high-dose methotrexate-based first-line chemotherapy for whom e-IL-10 was available. **RESULTS:** Thirty patients (median age: 62 years, brain involvement in 30/30, CSF involvement in 10/30, median baseline CSF IL-10: 27.5 pg/mL) met the selection criteria. e-IL-10 was undetectable in 22 patients and detectable in 8 patients. At the end of induction treatment, 7 of 8 and 4 of 22 of the patients with detectable and undetectable e-IL-10 had experienced progressive disease, respectively ($p = 0.001$, OR: 26.8, 95% CI 2-1,478). The median progression-free survival times were 5.8 months (95% CI 2.8-8.8) and 28.7 months (95% CI 13.4-43.9) in the groups with detectable and undetectable e-IL-10, respectively ($p < 0.001$). **DISCUSSION:** Our results suggest that despite an objective response, the persistence of detectable e-IL-10 is associated with a high risk of early relapse in PCSNL. A closer follow-up of such patients is warranted.

D.2 Articles on gliomas

D.2.1 Brain metastasis of a urothelial neuroendocrine carcinoma: A double pitfall for neuropathologists and DNA-methylation profiling

Arnault Tauziède-Espariat, Julien Masliah-Planchon, Suzanne Tran, Mathilde Filser, Raphaël Saffroy, Dorian Bochaton, Lauren Hasty, Suhan Senova, Paul Kouv, Karima Mokhtari, Clovis Adam, Nicolas Poté, Fabrice Chrétien, Alice Métais, Pascale Varlet, Franck Bielle, and Alice Laurence (Feb. 2024). "Brain metastasis of a urothelial neuroendocrine carcinoma: A double pitfall for neuropathologists and DNA-methylation profiling". In: *Neuropathology and Applied Neurobiology* 50.1, e12951. ISSN: 1365-2990. DOI: 10.1111/nan.12951

D.2.2 Prognosis of glioblastoma patients improves significantly over time interrogating historical controls

A. Thomas-Joulié, S. Tran, L. El Houari, A. Seyve, F. Bielle, C. Birzu, F. Lozano-Sanchez, K. Mokhtari, M. Giry, Y. Marie, F. Laigle-Donadey, C. Dehais, C. Houillier, D. Psimaras, A. Alentorn, A. Laurence, M. Touat, M. Sanson, K. Hoang-Xuan, A. Kas, L. Rozenblum, M.-O. Habert, L. Nichelli, D. Leclercq, D. Galanaud, J. Jacob, C. Karachi, L. Capelle, A. Carpentier, B. Mathon, L. Belin, and A. Idbaih (May 2024). "Prognosis of glioblastoma patients improves significantly over time interrogating historical controls". In: *European Journal of Cancer (Oxford, England: 1990)* 202, p. 114004. ISSN: 1879-0852. DOI: 10.1016/j.ejca.2024.114004

Abstract

BACKGROUND: Glioblastoma (GBM) is the most common devastating primary brain cancer in adults. In our clinical practice, median overall survival (mOS) of GBM patients seems increasing over time. **METHODS:** To address this observation, we have retrospectively analyzed the prognosis of 722 newly diagnosed GBM patients, aged below 70, in good clinical conditions (i.e. Karnofsky Performance Status -KPS- above 70%) and treated in our department according to the standard of care (SOC) between 2005 and 2018. Patients were divided into two groups according to the year of diagnosis (group 1: from 2005 to 2012; group 2: from 2013 to 2018). **RESULTS:** Characteristics of patients and tumors of both groups were very similar regarding confounding factors (age, KPS, MGMT promoter methylation status and treatments). Follow-up time was fixed at 24 months to ensure comparable survival times between both groups. Group 1 patients had a mOS of 19 months ([17.3-21.3]) while mOS of group 2 patients was not reached. The recent period of diagnosis was significantly associated with a longer mOS in univariate analysis (HR=0.64, 95% CI [0.51 - 0.81]), $p < 0.001$). Multivariate Cox analysis showed that the period of diagnosis remained significantly prognostic after adjustment on confounding factors (adjusted Hazard Ratio (aHR) 0.49, 95% CI [0.36-0.67], $p < 0.001$). **CONCLUSION:** This increase of mOS over time in newly diagnosed GBM patients could be explained by better management of potentially associated non-neurological diseases, optimization of validated SOC, better management of treatments side effects, supportive care and participation in clinical trials.

D.2.3 IDH-wildtype lower-grade diffuse gliomas: the importance of histological grade and molecular assessment for prognostic stratification

Giulia Berzero, Anna Luisa Di Stefano, Susanna Ronchi, Franck Bielle, Chiara Villa, Erell Guillerm, Laurent Capelle, Bertrand Mathon, Alice Laurence, Marine Giry, Yohann Schmitt, Yannick Marie, Ahmed Idbaih, Khe Hoang-Xuan, Jean-Yves Delatre, Karima Mokhtari, and Marc Sanson (June 1, 2021). "IDH-wildtype lower-grade diffuse gliomas: the importance of histological grade and molecular assessment for prognostic stratification". In: *Neuro-Oncology* 23.6, pp. 955–966. ISSN: 1523-5866. DOI: 10.1093/neuonc/noaa258

Abstract

BACKGROUND: Isocitrate dehydrogenase (IDH) wildtype (wt) grade II gliomas are a rare and heterogeneous entity. Survival and prognostic factors are poorly defined. **METHODS:** We searched retrospectively all patients diagnosed with diffuse World Health Organization (WHO) grades II and III gliomas at our center (1989-2020). **RESULTS:** Out of 517 grade II gliomas, 47 were "diffuse astrocytomas, IDHwt." Tumors frequently had fronto-temporo-insular location (28/47, 60%) and infiltrative behavior. We found telomerase reverse transcriptase (TERT) promoter mutations (23/45, 51%), whole chromosome 7 gains (10/37, 27%), whole chromosome 10 losses (10/41, 24%), and EGFR amplifications (4/43, 9%), but no TP53 mutations (0/22, 0%). Median overall survival (OS) was 59 months (vs 19 mo for IDHwt grade III gliomas) ($P < 0.0001$). Twenty-nine patients (29/43, 67%) met the definition of molecular glioblastoma according to cIMPACT-NOW update 3. Median OS in this subset was 42 months, which was shorter compared with patients with IDHwt grade II gliomas not meeting this definition (median OS: 57 mo), but substantially longer compared with IDHwt grade III gliomas meeting the definition for molecular glioblastoma (median OS: 17 mo, $P < 0.0001$). Most patients with IDHwt grade II gliomas met cIMPACT criteria because of isolated TERT promoter mutations (16/26, 62%), which were not predictive of poor outcome (median OS: 88 mo). Actionable targets, including 5 gene fusions involving FGFR3, were found in 7 patients (24%). **CONCLUSIONS:** Our findings highlight the importance of histological grading and molecular profiling for the prognostic stratification of IDHwt gliomas and suggest some caution when assimilating IDHwt grade II gliomas to molecular glioblastomas, especially those with isolated TERT promoter mutation.

D.3 Other articles

D.3.1 Brain Metabolic Alterations in Seropositive Autoimmune Encephalitis: An 18F-FDG PET Study

Sébastien Bergeret, Cristina Birzu, Pierre Meneret, Alain Giron, Sophie Demeret, Clemence Marois, Louis Cousyn, Laura Rozenblum, Alice Laurenge, Agusti Alentorn, Vincent Navarro, Dimitri Psimaras, and Aurélie Kas (Feb. 9, 2023). "Brain Metabolic Alterations in Seropositive Autoimmune Encephalitis: An 18F-FDG PET Study". In: *Biomedicines* 11.2, p. 506. ISSN: 2227-9059. DOI: 10.3390/biomedicines11020506

Abstract

INTRODUCTION: Autoimmune encephalitis (AE) diagnosis and follow-up remain challenging. Brain 18F-fluoro-deoxy-glucose positron emission tomography (FDG PET) has shown promising results in AE. Our aim was to investigate FDG PET alterations in AE, according to antibody subtype. **METHODS:** We retrospectively included patients with available FDG PET and seropositive AE diagnosed in our center between 2015 and 2020. Brain PET Z-score maps (relative to age matched controls) were analyzed, considering metabolic changes significant if $|Z\text{-score}| \geq 2$. **RESULTS:** Forty-six patients were included (49.4 yrs [18; 81]): 13 with GAD autoantibodies, 11 with anti-LGI1, 9 with NMDAR, 5 with CASPR2, and 8 with other antibodies. Brain PET was abnormal in 98% of patients versus 53% for MRI. The most frequent abnormalities were medial temporal lobe (MTL) and/or striatum hypermetabolism (52% and 43% respectively), cortical hypometabolism (78%), and cerebellum abnormalities (70%). LGI1 AE tended to have more frequent MTL hypermetabolism. NMDAR AE was prone to widespread cortical hypometabolism. Fewer abnormalities were observed in GAD AE. Striatum hypermetabolism was more frequent in patients treated for less than 1 month ($p = 0.014$), suggesting a relation to disease activity. **CONCLUSION:** FDG PET could serve as an imaging biomarker for early diagnosis and follow-up in AE.

Bibliography

- Abdelfattah, Nourhan et al. (Feb. 9, 2022). "Single-cell analysis of human glioma and immune cells identifies S100A4 as an immunotherapy target". In: *Nature Communications* 13.1, p. 767. ISSN: 2041-1723. DOI: 10.1038/s41467-022-28372-y.
- Afsari, Faezeh and Thomas M. McIntyre (Feb. 15, 2023). "D-2-Hydroxyglutarate Inhibits Calcineurin Phosphatase Activity to Abolish NF-AT Activation and IL-2 Induction in Stimulated Lymphocytes". In: *Journal of Immunology (Baltimore, Md.: 1950)* 210.4, pp. 504–514. ISSN: 1550-6606. DOI: 10.4049/jimmunol.2200050.
- Ajami, Bahareh, Jami L. Bennett, et al. (July 31, 2011). "Infiltrating monocytes trigger EAE progression, but do not contribute to the resident microglia pool". In: *Nature Neuroscience* 14.9, pp. 1142–1149. ISSN: 1546-1726. DOI: 10.1038/nn.2887.
- Ajami, Bahareh, Nikolay Samusik, et al. (Apr. 2018). "Single-cell mass cytometry reveals distinct populations of brain myeloid cells in mouse neuroinflammation and neurodegeneration models". In: *Nature Neuroscience* 21.4, pp. 541–551. ISSN: 1546-1726. DOI: 10.1038/s41593-018-0100-x.
- Alghamri, Mahmoud S. et al. (Oct. 2021). "G-CSF secreted by mutant IDH1 glioma stem cells abolishes myeloid cell immunosuppression and enhances the efficacy of immunotherapy". In: *Science Advances* 7.40, eabh3243. ISSN: 2375-2548. DOI: 10.1126/sciadv.abh3243.
- Alliot, F., I. Godin, and B. Pessac (Nov. 18, 1999). "Microglia derive from progenitors, originating from the yolk sac, and which proliferate in the brain". In: *Brain Research. Developmental Brain Research* 117.2, pp. 145–152. ISSN: 0165-3806. DOI: 10.1016/s0165-3806(99)00113-3.
- Amankulor, Nduka M. et al. (Apr. 15, 2017). "Mutant IDH1 regulates the tumor-associated immune system in gliomas". In: *Genes & Development* 31.8, pp. 774–786. ISSN: 1549-5477. DOI: 10.1101/gad.294991.116.
- Amit, Ido, Deborah R. Winter, and Steffen Jung (Jan. 2016). "The role of the local environment and epigenetics in shaping macrophage identity and their effect on tissue homeostasis". In: *Nature Immunology* 17.1, pp. 18–25. ISSN: 1529-2916. DOI: 10.1038/ni.3325.
- An, Jungeun et al. (Nov. 26, 2015). "Acute loss of TET function results in aggressive myeloid cancer in mice". In: *Nature Communications* 6, p. 10071. ISSN: 2041-1723. DOI: 10.1038/ncomms10071.
- Andersen, Brian M., Camilo Faust Akl, et al. (Dec. 2021). "Glial and myeloid heterogeneity in the brain tumour microenvironment". In: *Nature Reviews. Cancer* 21.12, pp. 786–802. ISSN: 1474-1768. DOI: 10.1038/s41568-021-00397-3.
- Andersen, Brian M. and David A. Reardon (Dec. 1, 2022). "Immunotherapy approaches for adult glioma: knowledge gained from recent clinical trials". In: *Current Opinion in Neurology* 35.6, pp. 803–813. ISSN: 1473-6551. DOI: 10.1097/WCO.0000000000001118.

- Arrieta, Víctor A. et al. (Jan. 17, 2023). "Immune checkpoint blockade in glioblastoma: from tumor heterogeneity to personalized treatment". In: *The Journal of Clinical Investigation* 133.2, e163447. ISSN: 1558-8238. DOI: 10.1172/JCI163447.
- Askew, Katharine et al. (Jan. 10, 2017). "Coupled Proliferation and Apoptosis Maintain the Rapid Turnover of Microglia in the Adult Brain". In: *Cell Reports* 18.2, pp. 391–405. ISSN: 2211-1247. DOI: 10.1016/j.celrep.2016.12.041.
- Autry, Adam W. et al. (Aug. 2022). "Spectroscopic imaging of D-2-hydroxyglutarate and other metabolites in pre-surgical patients with IDH-mutant lower-grade gliomas". In: *Journal of Neuro-Oncology* 159.1, pp. 43–52. ISSN: 1573-7373. DOI: 10.1007/s11060-022-04042-3.
- Baek, Chooyoung, Alice Laurence, and Mehdi Touat (Sept. 12, 2024). "Advances in the treatment of IDH-mutant gliomas". In: *Current Opinion in Neurology*. ISSN: 1473-6551. DOI: 10.1097/WCO.0000000000001316.
- Balak, Christopher D., Claudia Z. Han, and Christopher K. Glass (Feb. 2024). "Deciphering microglia phenotypes in health and disease". In: *Current Opinion in Genetics & Development* 84, p. 102146. ISSN: 1879-0380. DOI: 10.1016/j.gde.2023.102146.
- Bardella, Chiara et al. (2016). "Expression of Idh1R132H in the Murine Subventricular Zone Stem Cell Niche Recapitulates Features of Early Gliomagenesis". In: *Cancer Cell* 30.4, pp. 578–594. ISSN: 1878-3686. DOI: 10.1016/j.cccell.2016.08.017.
- Bartosovic, Marek, Mukund Kabbe, and Gonçalo Castelo-Branco (July 2021). "Single-cell CUT&Tag profiles histone modifications and transcription factors in complex tissues". In: *Nature Biotechnology* 39.7, pp. 825–835. ISSN: 1546-1696. DOI: 10.1038/s41587-021-00869-9.
- Bauchet, Luc and Quinn T. Ostrom (Jan. 2019). "Epidemiology and Molecular Epidemiology". In: *Neurosurgery Clinics of North America* 30.1, pp. 1–16. ISSN: 1558-1349. DOI: 10.1016/j.nec.2018.08.010.
- Bent, Martin J. van den, Alba A. Brandes, et al. (Jan. 20, 2013). "Adjuvant procarbazine, lomustine, and vincristine chemotherapy in newly diagnosed anaplastic oligodendroglioma: long-term follow-up of EORTC brain tumor group study 26951". In: *Journal of Clinical Oncology: Official Journal of the American Society of Clinical Oncology* 31.3, pp. 344–350. ISSN: 1527-7755. DOI: 10.1200/JCO.2012.43.2229.
- Bent, Martin J. van den, C. Mircea S. Tesileanu, et al. (June 2021). "Adjuvant and concurrent temozolomide for 1p/19q non-co-deleted anaplastic glioma (CATNON; EORTC study 26053-22054): second interim analysis of a randomised, open-label, phase 3 study". In: *The Lancet. Oncology* 22.6, pp. 813–823. ISSN: 1474-5488. DOI: 10.1016/S1470-2045(21)00090-5.
- Bergeret, Sébastien et al. (Feb. 9, 2023). "Brain Metabolic Alterations in Seropositive Autoimmune Encephalitis: An 18F-FDG PET Study". In: *Biomedicines* 11.2, p. 506. ISSN: 2227-9059. DOI: 10.3390/biomedicines11020506.
- Berzero, Giulia et al. (June 1, 2021). "IDH-wildtype lower-grade diffuse gliomas: the importance of histological grade and molecular assessment for prognostic stratification". In: *Neuro-Oncology* 23.6, pp. 955–966. ISSN: 1523-5866. DOI: 10.1093/neuonc/noaa258.
- Bian, Ke et al. (June 20, 2019). "DNA repair enzymes ALKBH2, ALKBH3, and AlkB oxidize 5-methylcytosine to 5-hydroxymethylcytosine, 5-formylcytosine and 5-carboxylcytosine in vitro". In: *Nucleic Acids Research* 47.11, pp. 5522–5529. ISSN:

- 1362-4962. DOI: 10.1093/nar/gkz395.
- Blanco-Carmona, Enrique et al. (Nov. 21, 2023). "Tumor heterogeneity and tumor-microglia interactions in primary and recurrent IDH1-mutant gliomas". In: *Cell Reports. Medicine* 4.11, p. 101249. ISSN: 2666-3791. DOI: 10.1016/j.xcrm.2023.101249.
- Bohlen, Christopher J. et al. (May 17, 2017). "Diverse requirements for microglial survival, specification, and function revealed by defined-medium cultures". In: *Neuron* 94.4, 759–773.e8. ISSN: 0896-6273. DOI: 10.1016/j.neuron.2017.04.043. URL: <https://www.ncbi.nlm.nih.gov/pmc/articles/PMC5523817/> (visited on 04/26/2021).
- Böttcher, Martin et al. (2018). "D-2-hydroxyglutarate interferes with HIF-1 α stability skewing T-cell metabolism towards oxidative phosphorylation and impairing Th17 polarization". In: *Oncoimmunology* 7.7, e1445454. ISSN: 2162-4011. DOI: 10.1080/2162402X.2018.1445454.
- Bouffet, Eric et al. (July 1, 2016). "Immune Checkpoint Inhibition for Hypermutant Glioblastoma Multiforme Resulting From Germline Biallelic Mismatch Repair Deficiency". In: *Journal of Clinical Oncology: Official Journal of the American Society of Clinical Oncology* 34.19, pp. 2206–2211. ISSN: 1527-7755. DOI: 10.1200/JCO.2016.66.6552.
- Bouزيد, Hind et al. (July 2023). "Clonal hematopoiesis is associated with protection from Alzheimer's disease". In: *Nature Medicine* 29.7, pp. 1662–1670. ISSN: 1546-170X. DOI: 10.1038/s41591-023-02397-2.
- Bowman, Robert L. et al. (2016). "Macrophage Ontogeny Underlies Differences in Tumor-Specific Education in Brain Malignancies". In: *Cell Reports* 17.9, pp. 2445–2459. ISSN: 2211-1247. DOI: 10.1016/j.celrep.2016.10.052.
- Bralten, Linda B. C. et al. (Mar. 2011). "IDH1 R132H decreases proliferation of glioma cell lines in vitro and in vivo". In: *Annals of Neurology* 69.3, pp. 455–463. ISSN: 1531-8249. DOI: 10.1002/ana.22390.
- Buckner, Jan C. et al. (Apr. 7, 2016). "Radiation plus Procarbazine, CCNU, and Vincristine in Low-Grade Glioma". In: *The New England Journal of Medicine* 374.14, pp. 1344–1355. ISSN: 1533-4406. DOI: 10.1056/NEJMoa1500925.
- Bunse, Lukas, Stefan Pusch, et al. (2018). "Suppression of antitumor T cell immunity by the oncometabolite (R)-2-hydroxyglutarate". In: *Nature Medicine* 24.8, pp. 1192–1203. ISSN: 1546-170X. DOI: 10.1038/s41591-018-0095-6.
- Bunse, Lukas, Anne-Kathleen Rupp, et al. (May 23, 2022). "AMPLIFY-NEOVAC: a randomized, 3-arm multicenter phase I trial to assess safety, tolerability and immunogenicity of IDH1-vac combined with an immune checkpoint inhibitor targeting programmed death-ligand 1 in isocitrate dehydrogenase 1 mutant gliomas". In: *Neurological Research and Practice* 4.1, p. 20. ISSN: 2524-3489. DOI: 10.1186/s42466-022-00184-x.
- Cairncross, Gregory et al. (Jan. 20, 2013). "Phase III trial of chemoradiotherapy for anaplastic oligodendroglioma: long-term results of RTOG 9402". In: *Journal of Clinical Oncology: Official Journal of the American Society of Clinical Oncology* 31.3, pp. 337–343. ISSN: 1527-7755. DOI: 10.1200/JCO.2012.43.2674.
- Cairns, Rob A. and Tak W. Mak (July 2013). "Oncogenic isocitrate dehydrogenase mutations: mechanisms, models, and clinical opportunities". In: *Cancer Discovery* 3.7, pp. 730–741. ISSN: 2159-8290. DOI: 10.1158/2159-8290.CD-13-0083.
- Cancer Genome Atlas Research Network et al. (June 25, 2015). "Comprehensive, Integrative Genomic Analysis of Diffuse Lower-Grade Gliomas". In: *The New*

- England Journal of Medicine* 372.26, pp. 2481–2498. ISSN: 1533-4406. DOI: 10.1056/NEJMoa1402121.
- Cao, Chuan et al. (Oct. 20, 2023). “D-2-hydroxyglutarate regulates human brain vascular endothelial cell proliferation and barrier function”. In: *Journal of Neuropathology and Experimental Neurology* 82.11, pp. 921–933. ISSN: 1554-6578. DOI: 10.1093/jnen/nlad072.
- Capper, David et al. (Feb. 2011). “Mutation-specific IDH1 antibody differentiates oligodendrogliomas and oligoastrocytomas from other brain tumors with oligodendroglioma-like morphology”. In: *Acta Neuropathologica* 121.2, pp. 241–252. ISSN: 1432-0533. DOI: 10.1007/s00401-010-0770-2.
- Carrillo-Jimenez, Alejandro et al. (Oct. 15, 2019). “TET2 Regulates the Neuroinflammatory Response in Microglia”. In: *Cell Reports* 29.3, 697–713.e8. ISSN: 2211-1247. DOI: 10.1016/j.celrep.2019.09.013.
- Chalighe, Ronan et al. (Oct. 2021). “Epigenetic encoding, heritability and plasticity of glioma transcriptional cell states”. In: *Nature Genetics* 53.10, pp. 1469–1479. ISSN: 1546-1718. DOI: 10.1038/s41588-021-00927-7.
- Chan, Steven M. et al. (Feb. 2015). “Isocitrate dehydrogenase 1 and 2 mutations induce BCL-2 dependence in acute myeloid leukemia”. In: *Nature Medicine* 21.2, pp. 178–184. ISSN: 1546-170X. DOI: 10.1038/nm.3788.
- Chen, Hao et al. (May 9, 2017). “Mutant IDH1 and seizures in patients with glioma”. In: *Neurology* 88.19, pp. 1805–1813. ISSN: 1526-632X. DOI: 10.1212/WNL.0000000000003911.
- Chen, Lei-Lei et al. (Mar. 2022). “Itaconate inhibits TET DNA dioxygenases to dampen inflammatory responses”. In: *Nature Cell Biology* 24.3, pp. 353–363. ISSN: 1476-4679. DOI: 10.1038/s41556-022-00853-8.
- Choi, Changho et al. (Jan. 26, 2012). “2-hydroxyglutarate detection by magnetic resonance spectroscopy in IDH-mutated patients with gliomas”. In: *Nature Medicine* 18.4, pp. 624–629. ISSN: 1546-170X. DOI: 10.1038/nm.2682.
- Chowdhury, Rasheduzzaman et al. (May 2011). “The oncometabolite 2-hydroxyglutarate inhibits histone lysine demethylases”. In: *EMBO reports* 12.5, pp. 463–469. ISSN: 1469-3178. DOI: 10.1038/embor.2011.43.
- Chuntova, Pavlina et al. (May 2022). “Inhibition of D-2HG leads to upregulation of a proinflammatory gene signature in a novel HLA-A2/HLA-DR1 transgenic mouse model of IDH1R132H-expressing glioma”. In: *Journal for Immunotherapy of Cancer* 10.5, e004644. ISSN: 2051-1426. DOI: 10.1136/jitc-2022-004644.
- Court, Franck et al. (Oct. 2019). “Transcriptional alterations in glioma result primarily from DNA methylation-independent mechanisms”. In: *Genome Research* 29.10, pp. 1605–1621. ISSN: 1549-5469. DOI: 10.1101/gr.249219.119.
- Cull, Alyssa H. et al. (Nov. 2017). “Tet2 restrains inflammatory gene expression in macrophages”. In: *Experimental Hematology* 55, 56–70.e13. ISSN: 1873-2399. DOI: 10.1016/j.exphem.2017.08.001.
- Dang, Lenny et al. (Dec. 10, 2009). “Cancer-associated IDH1 mutations produce 2-hydroxyglutarate”. In: *Nature* 462.7274, pp. 739–744. ISSN: 1476-4687. DOI: 10.1038/nature08617.
- Daniel, Paul et al. (2019). “Temozolomide Induced Hypermutation in Glioma: Evolutionary Mechanisms and Therapeutic Opportunities”. In: *Frontiers in Oncology* 9, p. 41. ISSN: 2234-943X. DOI: 10.3389/fonc.2019.00041.
- Darmanis, Spyros et al. (Oct. 31, 2017). “Single-Cell RNA-Seq Analysis of Infiltrating Neoplastic Cells at the Migrating Front of Human Glioblastoma”. In: *Cell reports*

- 21.5, pp. 1399–1410. ISSN: 2211-1247. DOI: 10.1016/j.celrep.2017.10.030. URL: <https://www.ncbi.nlm.nih.gov/pmc/articles/PMC5810554/> (visited on 06/10/2020).
- Das, Amitabh et al. (July 11, 2016). “Transcriptome sequencing reveals that LPS-triggered transcriptional responses in established microglia BV2 cell lines are poorly representative of primary microglia”. In: *Journal of Neuroinflammation* 13.1, p. 182. ISSN: 1742-2094. DOI: 10.1186/s12974-016-0644-1.
- Deczkowska, Aleksandra et al. (May 17, 2018). “Disease-Associated Microglia: A Universal Immune Sensor of Neurodegeneration”. In: *Cell* 173.5, pp. 1073–1081. ISSN: 1097-4172. DOI: 10.1016/j.cell.2018.05.003.
- Delhommeau, François et al. (May 28, 2009). “Mutation in TET2 in myeloid cancers”. In: *The New England Journal of Medicine* 360.22, pp. 2289–2301. ISSN: 1533-4406. DOI: 10.1056/NEJMoa0810069.
- Ehret, Felix et al. (Feb. 2023). “Loss of IDH mutation or secondary tumour manifestation? Evolution of an IDH-mutant and 1p/19q-codeleted oligodendroglioma after 15 years of continuous temozolomide treatment and radiotherapy: A case report”. In: *Neuropathology and Applied Neurobiology* 49.1, e12859. ISSN: 1365-2990. DOI: 10.1111/nan.12859.
- Esmaili, Morteza et al. (Sept. 1, 2014). “IDH1 R132H mutation generates a distinct phospholipid metabolite profile in glioma”. In: *Cancer Research* 74.17, pp. 4898–4907. ISSN: 1538-7445. DOI: 10.1158/0008-5472.CAN-14-0008.
- Evans, Katrina T. et al. (Dec. 2023). “Microglia promote anti-tumour immunity and suppress breast cancer brain metastasis”. In: *Nature Cell Biology* 25.12, pp. 1848–1859. ISSN: 1476-4679. DOI: 10.1038/s41556-023-01273-y.
- Fan, Jing et al. (Feb. 20, 2015). “Human phosphoglycerate dehydrogenase produces the oncometabolite D-2-hydroxyglutarate”. In: *ACS chemical biology* 10.2, pp. 510–516. ISSN: 1554-8937. DOI: 10.1021/cb500683c.
- Favero, F. et al. (May 2015). “Glioblastoma adaptation traced through decline of an IDH1 clonal driver and macro-evolution of a double-minute chromosome”. In: *Annals of Oncology: Official Journal of the European Society for Medical Oncology* 26.5, pp. 880–887. ISSN: 1569-8041. DOI: 10.1093/annonc/mdv127.
- Feldmann, Angelika et al. (2013). “Transcription factor occupancy can mediate active turnover of DNA methylation at regulatory regions”. In: *PLoS genetics* 9.12, e1003994. ISSN: 1553-7404. DOI: 10.1371/journal.pgen.1003994.
- Figuroa, Maria E. et al. (Dec. 14, 2010). “Leukemic IDH1 and IDH2 mutations result in a hypermethylation phenotype, disrupt TET2 function, and impair hematopoietic differentiation”. In: *Cancer Cell* 18.6, pp. 553–567. ISSN: 1878-3686. DOI: 10.1016/j.ccr.2010.11.015.
- Flavahan, William A. et al. (Jan. 7, 2016). “Insulator dysfunction and oncogene activation in IDH mutant gliomas”. In: *Nature* 529.7584, pp. 110–114. ISSN: 1476-4687. DOI: 10.1038/nature16490.
- Flowers, Antwoine et al. (May 3, 2017). “Proteomic analysis of aged microglia: shifts in transcription, bioenergetics, and nutrient response”. In: *Journal of Neuroinflammation* 14.1, p. 96. ISSN: 1742-2094. DOI: 10.1186/s12974-017-0840-7.
- Foskolou, Iosifina P., Lukas Bunse, and Jan Van den Bossche (Oct. 2023). “2-hydroxyglutarate rides the cancer-immunity cycle”. In: *Current Opinion in Biotechnology* 83, p. 102976. ISSN: 1879-0429. DOI: 10.1016/j.copbio.2023.102976.
- Friebel, Ekaterina et al. (May 22, 2020). “Single-Cell Mapping of Human Brain Cancer Reveals Tumor-Specific Instruction of Tissue-Invading Leukocytes”. In: *Cell*. ISSN:

- 1097-4172. DOI: 10.1016/j.cell.2020.04.055.
- Friedrich, Mirco, Markus Hahn, et al. (Feb. 14, 2023). "Dysfunctional dendritic cells limit antigen-specific T cell response in glioma". In: *Neuro-Oncology* 25.2, pp. 263–276. ISSN: 1523-5866. DOI: 10.1093/neuonc/noac138.
- Friedrich, Mirco, Roman Sankowski, et al. (May 24, 2021). "Tryptophan metabolism drives dynamic immunosuppressive myeloid states in IDH-mutant gliomas". In: *Nature Cancer*. ISSN: 2662-1347. DOI: 10.1038/s43018-021-00201-z. URL: <http://www.nature.com/articles/s43018-021-00201-z> (visited on 05/25/2021).
- Fuente, Macarena I. de la et al. (Jan. 5, 2023). "Olutasidenib (FT-2102) in patients with relapsed or refractory IDH1-mutant glioma: A multicenter, open-label, phase Ib/II trial". In: *Neuro-Oncology* 25.1, pp. 146–156. ISSN: 1523-5866. DOI: 10.1093/neuonc/noac139.
- Geirsdottir, Laufey et al. (Dec. 12, 2019). "Cross-Species Single-Cell Analysis Reveals Divergence of the Primate Microglia Program". In: *Cell* 179.7, 1609–1622.e16. ISSN: 1097-4172. DOI: 10.1016/j.cell.2019.11.010.
- Ginhoux, Florent et al. (Nov. 5, 2010). "Fate mapping analysis reveals that adult microglia derive from primitive macrophages". In: *Science (New York, N.Y.)* 330.6005, pp. 841–845. ISSN: 1095-9203. DOI: 10.1126/science.1194637.
- Ginno, Paul Adrian et al. (May 29, 2020). "A genome-scale map of DNA methylation turnover identifies site-specific dependencies of DNMT and TET activity". In: *Nature Communications* 11.1, p. 2680. ISSN: 2041-1723. DOI: 10.1038/s41467-020-16354-x.
- Glass, Christopher K. and Gioacchino Natoli (Jan. 2016). "Molecular control of activation and priming in macrophages". In: *Nature Immunology* 17.1, pp. 26–33. ISSN: 1529-2916. DOI: 10.1038/ni.3306.
- Goede, Kyra E. de et al. (May 6, 2022). "d-2-Hydroxyglutarate is an anti-inflammatory immunometabolite that accumulates in macrophages after TLR4 activation". In: *Biochimica Et Biophysica Acta. Molecular Basis of Disease* 1868.9, p. 166427. ISSN: 1879-260X. DOI: 10.1016/j.bbadis.2022.166427.
- Goldberg, Sarah B. et al. (July 2016). "Pembrolizumab for patients with melanoma or non-small-cell lung cancer and untreated brain metastases: early analysis of a non-randomised, open-label, phase 2 trial". In: *The Lancet. Oncology* 17.7, pp. 976–983. ISSN: 1474-5488. DOI: 10.1016/S1470-2045(16)30053-5.
- Gosselin, David, Verena M. Link, et al. (Dec. 4, 2014). "Environment drives selection and function of enhancers controlling tissue-specific macrophage identities". In: *Cell* 159.6, pp. 1327–1340. ISSN: 1097-4172. DOI: 10.1016/j.cell.2014.11.023.
- Gosselin, David, Dylan Skola, et al. (June 23, 2017). "An environment-dependent transcriptional network specifies human microglia identity". In: *Science (New York, N.Y.)* 356.6344, eaal3222. ISSN: 1095-9203. DOI: 10.1126/science.aa13222.
- Grabert, Kathleen et al. (Mar. 2016). "Microglial brain region-dependent diversity and selective regional sensitivities to aging". In: *Nature Neuroscience* 19.3, pp. 504–516. ISSN: 1546-1726. DOI: 10.1038/nn.4222.
- Grassian, Alexandra R. et al. (June 15, 2014). "IDH1 mutations alter citric acid cycle metabolism and increase dependence on oxidative mitochondrial metabolism". In: *Cancer Research* 74.12, pp. 3317–3331. ISSN: 1538-7445. DOI: 10.1158/0008-5472.CAN-14-0772-T.
- Greenwald, Alissa C. et al. (May 9, 2024). "Integrative spatial analysis reveals a multi-layered organization of glioblastoma". In: *Cell* 187.10, 2485–2501.e26. ISSN:

- 1097-4172. DOI: 10.1016/j.ccell.2024.03.029.
- Guilhamon, Paul et al. (2013). "Meta-analysis of IDH-mutant cancers identifies EBF1 as an interaction partner for TET2". In: *Nature Communications* 4, p. 2166. ISSN: 2041-1723. DOI: 10.1038/ncomms3166.
- Gunn, Kathryn et al. (June 2, 2023). "(R)-2-Hydroxyglutarate Inhibits KDM5 Histone Lysine Demethylases to Drive Transformation in IDH-Mutant Cancers". In: *Cancer Discovery* 13.6, pp. 1478–1497. ISSN: 2159-8290. DOI: 10.1158/2159-8290.CD-22-0825.
- Gupta, Pravesh et al. (Aug. 10, 2024). "Immune landscape of isocitrate dehydrogenase-stratified primary and recurrent human gliomas". In: *Neuro-Oncology*, noae139. ISSN: 1523-5866. DOI: 10.1093/neuonc/noae139.
- Hagemeyer, Nora et al. (Sept. 2017). "Microglia contribute to normal myelinogenesis and to oligodendrocyte progenitor maintenance during adulthood". In: *Acta Neuropathologica* 134.3, pp. 441–458. ISSN: 1432-0533. DOI: 10.1007/s00401-017-1747-1.
- Haley, Michael J. et al. (May 17, 2024). "Hypoxia coordinates the spatial landscape of myeloid cells within glioblastoma to affect survival". In: *Science Advances* 10.20, eadj3301. ISSN: 2375-2548. DOI: 10.1126/sciadv.adj3301.
- Hambardzumyan, Dolores, David H. Gutmann, and Helmut Kettenmann (Jan. 2016). "The role of microglia and macrophages in glioma maintenance and progression". In: *Nature Neuroscience* 19.1, pp. 20–27. ISSN: 1546-1726. DOI: 10.1038/nn.4185.
- Hammon, Kathrin et al. (Aug. 1, 2024). "D-2-hydroxyglutarate supports a tolerogenic phenotype with lowered major histocompatibility class II expression in non-malignant dendritic cells and acute myeloid leukemia cells". In: *Haematologica* 109.8, pp. 2500–2514. ISSN: 1592-8721. DOI: 10.3324/haematol.2023.283597.
- Hammond, Timothy R. et al. (Jan. 15, 2019). "Single-Cell RNA Sequencing of Microglia throughout the Mouse Lifespan and in the Injured Brain Reveals Complex Cell-State Changes". In: *Immunity* 50.1, 253–271.e6. ISSN: 1097-4180. DOI: 10.1016/j.immuni.2018.11.004.
- Han, Chao-Jun et al. (Oct. 2019). "The oncometabolite 2-hydroxyglutarate inhibits microglial activation via the AMPK/mTOR/NF-κB pathway". In: *Acta Pharmacologica Sinica* 40.10, pp. 1292–1302. ISSN: 1745-7254. DOI: 10.1038/s41401-019-0225-9.
- Hara, Toshiro et al. (June 14, 2021). "Interactions between cancer cells and immune cells drive transitions to mesenchymal-like states in glioblastoma". In: *Cancer Cell* 39.6, 779–792.e11. ISSN: 1878-3686. DOI: 10.1016/j.ccell.2021.05.002.
- Hermann, Andrea, Rachna Goyal, and Albert Jeltsch (Nov. 12, 2004). "The Dnmt1 DNA-(cytosine-C5)-methyltransferase methylates DNA processively with high preference for hemimethylated target sites". In: *The Journal of Biological Chemistry* 279.46, pp. 48350–48359. ISSN: 0021-9258. DOI: 10.1074/jbc.M403427200.
- Herzi, Dora et al. (June 25, 2024). "Prognostic Value of CSF IL-10 at Early Assessment of Induction Chemotherapy in Primary CNS Lymphomas: A LOC Network Study". In: *Neurology* 102.12, e209527. ISSN: 1526-632X. DOI: 10.1212/WNL.000000000209527.
- Holtman, Inge R., Dylan Skola, and Christopher K. Glass (Sept. 1, 2017). "Transcriptional control of microglia phenotypes in health and disease". In: *The Journal of Clinical Investigation* 127.9, pp. 3220–3229. ISSN: 1558-8238. DOI: 10.1172/JCI90604.

- Hon, Gary C. et al. (Oct. 23, 2014). "5mC oxidation by Tet2 modulates enhancer activity and timing of transcriptome reprogramming during differentiation". In: *Molecular Cell* 56.2, pp. 286–297. ISSN: 1097-4164. DOI: 10.1016/j.molcel.2014.08.026.
- Horvath, Ryan J. et al. (Oct. 2008). "Differential migration, LPS-induced cytokine, chemokine, and NO expression in immortalized BV-2 and HAPI cell lines and primary microglial cultures". In: *Journal of Neurochemistry* 107.2, pp. 557–569. ISSN: 1471-4159. DOI: 10.1111/j.1471-4159.2008.05633.x.
- Huang, Yun et al. (Jan. 28, 2014). "Distinct roles of the methylcytosine oxidases Tet1 and Tet2 in mouse embryonic stem cells". In: *Proceedings of the National Academy of Sciences of the United States of America* 111.4, pp. 1361–1366. ISSN: 1091-6490. DOI: 10.1073/pnas.1322921111.
- Hwang, Woochang et al. (2015). "Prediction of promoters and enhancers using multiple DNA methylation-associated features". In: *BMC genomics* 16 Suppl 7 (Suppl 7), S11. ISSN: 1471-2164. DOI: 10.1186/1471-2164-16-S7-S11.
- Inoue, Satoshi et al. (Aug. 8, 2016). "Mutant IDH1 Downregulates ATM and Alters DNA Repair and Sensitivity to DNA Damage Independent of TET2". In: *Cancer Cell* 30.2, pp. 337–348. ISSN: 1878-3686. DOI: 10.1016/j.cccell.2016.05.018.
- Ito, Shinsuke et al. (Aug. 26, 2010). "Role of Tet proteins in 5mC to 5hmC conversion, ES-cell self-renewal and inner cell mass specification". In: *Nature* 466.7310, pp. 1129–1133. ISSN: 1476-4687. DOI: 10.1038/nature09303.
- Jackson, Christopher M., John Choi, and Michael Lim (Sept. 2019). "Mechanisms of immunotherapy resistance: lessons from glioblastoma". In: *Nature Immunology* 20.9, pp. 1100–1109. ISSN: 1529-2916. DOI: 10.1038/s41590-019-0433-y.
- Jin, Chunlei et al. (June 2014). "TET1 is a maintenance DNA demethylase that prevents methylation spreading in differentiated cells". In: *Nucleic Acids Research* 42.11, pp. 6956–6971. ISSN: 1362-4962. DOI: 10.1093/nar/gku372.
- Jin, Seung-Gi et al. (Dec. 15, 2011). "5-Hydroxymethylcytosine is strongly depleted in human cancers but its levels do not correlate with IDH1 mutations". In: *Cancer Research* 71.24, pp. 7360–7365. ISSN: 1538-7445. DOI: 10.1158/0008-5472.CAN-11-2023.
- Johanns, Tanner M. et al. (Nov. 2016). "Immunogenomics of Hypermutated Glioblastoma: A Patient with Germline POLE Deficiency Treated with Checkpoint Blockade Immunotherapy". In: *Cancer Discovery* 6.11, pp. 1230–1236. ISSN: 2159-8290. DOI: 10.1158/2159-8290.CD-16-0575.
- Johnson, Kevin C. et al. (Nov. 25, 2016). "5-Hydroxymethylcytosine localizes to enhancer elements and is associated with survival in glioblastoma patients". In: *Nature Communications* 7, p. 13177. ISSN: 2041-1723. DOI: 10.1038/ncomms13177.
- Kaas, Garrett A. et al. (Sept. 18, 2013). "TET1 controls CNS 5-methylcytosine hydroxylation, active DNA demethylation, gene transcription, and memory formation". In: *Neuron* 79.6, pp. 1086–1093. ISSN: 1097-4199. DOI: 10.1016/j.neuron.2013.08.032.
- Kacimi, Salah Eddine O. et al. (Oct. 2, 2024). "Survival Outcomes Associated With First-Line Procarbazine, CCNU, and Vincristine or Temozolomide in Combination With Radiotherapy in IDH-Mutant 1p/19q-Codeleted Grade 3 Oligodendroglioma". In: *Journal of Clinical Oncology: Official Journal of the American Society of Clinical Oncology*, JCO2400049. ISSN: 1527-7755. DOI: 10.1200/JCO.24.00049.
- Kadiyala, Padma et al. (Feb. 15, 2021). "Inhibition of 2-hydroxyglutarate elicits metabolic reprogramming and mutant IDH1 glioma immunity in mice". In: *Jour-*

- nal of Clinical Investigation* 131.4, e139542. ISSN: 0021-9738, 1558-8238. DOI: 10.1172/JCI139542. URL: <https://www.jci.org/articles/view/139542> (visited on 06/17/2021).
- Kafer, Georgia Rose et al. (Feb. 16, 2016). "5-Hydroxymethylcytosine Marks Sites of DNA Damage and Promotes Genome Stability". In: *Cell Reports* 14.6, pp. 1283–1292. ISSN: 2211-1247. DOI: 10.1016/j.celrep.2016.01.035.
- Kalinina, Juliya et al. (Dec. 15, 2016). "Selective Detection of the D-enantiomer of 2-Hydroxyglutarate in the CSF of Glioma Patients with Mutated Isocitrate Dehydrogenase". In: *Clinical Cancer Research: An Official Journal of the American Association for Cancer Research* 22.24, pp. 6256–6265. ISSN: 1557-3265. DOI: 10.1158/1078-0432.CCR-15-2965.
- Kallin, Eric M. et al. (Oct. 26, 2012). "Tet2 facilitates the derepression of myeloid target genes during CEBP α -induced transdifferentiation of pre-B cells". In: *Molecular Cell* 48.2, pp. 266–276. ISSN: 1097-4164. DOI: 10.1016/j.molcel.2012.08.007.
- Kaluscha, Sebastian et al. (Dec. 2022). "Evidence that direct inhibition of transcription factor binding is the prevailing mode of gene and repeat repression by DNA methylation". In: *Nature Genetics* 54.12, pp. 1895–1906. ISSN: 1546-1718. DOI: 10.1038/s41588-022-01241-6.
- Keenan, Tanya E., Kelly P. Burke, and Eliezer M. Van Allen (Mar. 2019). "Genomic correlates of response to immune checkpoint blockade". In: *Nature Medicine* 25.3, pp. 389–402. ISSN: 1546-170X. DOI: 10.1038/s41591-019-0382-x.
- Keren-Shaul, Hadas et al. (June 15, 2017). "A Unique Microglia Type Associated with Restricting Development of Alzheimer's Disease". In: *Cell* 169.7, 1276–1290.e17. ISSN: 1097-4172. DOI: 10.1016/j.cell.2017.05.018.
- Kernytsky, Andrew et al. (Jan. 8, 2015). "IDH2 mutation-induced histone and DNA hypermethylation is progressively reversed by small-molecule inhibition". In: *Blood* 125.2, pp. 296–303. ISSN: 1528-0020. DOI: 10.1182/blood-2013-10-533604.
- Khan, Fatima et al. (Jan. 3, 2023). "Macrophages and microglia in glioblastoma: heterogeneity, plasticity, and therapy". In: *The Journal of Clinical Investigation* 133.1, e163446. ISSN: 1558-8238. DOI: 10.1172/JCI163446.
- Kickingreder, Philipp et al. (Nov. 5, 2015). "IDH mutation status is associated with a distinct hypoxia/angiogenesis transcriptome signature which is non-invasively predictable with rCBV imaging in human glioma". In: *Scientific Reports* 5, p. 16238. ISSN: 2045-2322. DOI: 10.1038/srep16238.
- Kim, Kyung-Hee et al. (Mar. 11, 2024). "Integrated proteogenomic characterization of glioblastoma evolution". In: *Cancer Cell* 42.3, 358–377.e8. ISSN: 1878-3686. DOI: 10.1016/j.ccell.2023.12.015.
- Klemm, Florian et al. (June 25, 2020). "Interrogation of the Microenvironmental Landscape in Brain Tumors Reveals Disease-Specific Alterations of Immune Cells". In: *Cell* 181.7, 1643–1660.e17. ISSN: 1097-4172. DOI: 10.1016/j.cell.2020.05.007.
- Kloosterman, Daan J. et al. (Sept. 19, 2024). "Macrophage-mediated myelin recycling fuels brain cancer malignancy". In: *Cell* 187.19, 5336–5356.e30. ISSN: 1097-4172. DOI: 10.1016/j.cell.2024.07.030.
- Klug, Maja et al. (May 26, 2013). "5-Hydroxymethylcytosine is an essential intermediate of active DNA demethylation processes in primary human monocytes". In: *Genome Biology* 14.5, R46. ISSN: 1474-760X. DOI: 10.1186/gb-2013-14-5-r46.
- Kluger, Harriet M. et al. (Jan. 1, 2019). "Long-Term Survival of Patients With

- Melanoma With Active Brain Metastases Treated With Pembrolizumab on a Phase II Trial". In: *Journal of Clinical Oncology: Official Journal of the American Society of Clinical Oncology* 37.1, pp. 52–60. ISSN: 1527-7755. DOI: 10.1200/JCO.18.00204.
- Kohanbash, Gary et al. (Apr. 3, 2017). "Isocitrate dehydrogenase mutations suppress STAT1 and CD8+ T cell accumulation in gliomas". In: *The Journal of Clinical Investigation* 127.4, pp. 1425–1437. ISSN: 1558-8238. DOI: 10.1172/JCI90644.
- Koivunen, Peppi et al. (Feb. 15, 2012). "Transformation by the (R)-enantiomer of 2-hydroxyglutarate linked to EGLN activation". In: *Nature* 483.7390, pp. 484–488. ISSN: 1476-4687. DOI: 10.1038/nature10898.
- Komori, Takashi (Feb. 2022). "Grading of adult diffuse gliomas according to the 2021 WHO Classification of Tumors of the Central Nervous System". In: *Laboratory Investigation; a Journal of Technical Methods and Pathology* 102.2, pp. 126–133. ISSN: 1530-0307. DOI: 10.1038/s41374-021-00667-6.
- Kranendijk, Martijn et al. (July 2012). "Progress in understanding 2-hydroxyglutaric acidurias". In: *Journal of Inherited Metabolic Disease* 35.4, pp. 571–587. ISSN: 1573-2665. DOI: 10.1007/s10545-012-9462-5.
- Kraus, Theo F. J. et al. (Oct. 1, 2012). "Low values of 5-hydroxymethylcytosine (5hmC), the "sixth base," are associated with anaplasia in human brain tumors". In: *International Journal of Cancer* 131.7, pp. 1577–1590. ISSN: 1097-0215. DOI: 10.1002/ijc.27429.
- Kreibich, Elisa et al. (Mar. 2, 2023). "Single-molecule footprinting identifies context-dependent regulation of enhancers by DNA methylation". In: *Molecular Cell* 83.5, 787–802.e9. ISSN: 1097-4164. DOI: 10.1016/j.molcel.2023.01.017.
- Kribelbauer, Judith F. et al. (June 13, 2017). "Quantitative Analysis of the DNA Methylation Sensitivity of Transcription Factor Complexes". In: *Cell Reports* 19.11, pp. 2383–2395. ISSN: 2211-1247. DOI: 10.1016/j.celrep.2017.05.069.
- Kusi, Meena et al. (Jan. 11, 2022). "2-Hydroxyglutarate destabilizes chromatin regulatory landscape and lineage fidelity to promote cellular heterogeneity". In: *Cell Reports* 38.2, p. 110220. ISSN: 2211-1247. DOI: 10.1016/j.celrep.2021.110220.
- Langemeijer, Saskia M. C. et al. (July 2009). "Acquired mutations in TET2 are common in myelodysplastic syndromes". In: *Nature Genetics* 41.7, pp. 838–842. ISSN: 1546-1718. DOI: 10.1038/ng.391.
- Lassman, Andrew B. et al. (Aug. 10, 2022). "Joint Final Report of EORTC 26951 and RTOG 9402: Phase III Trials With Procarbazine, Lomustine, and Vincristine Chemotherapy for Anaplastic Oligodendroglial Tumors". In: *Journal of Clinical Oncology: Official Journal of the American Society of Clinical Oncology* 40.23, pp. 2539–2545. ISSN: 1527-7755. DOI: 10.1200/JCO.21.02543.
- Laukka, Tuomas et al. (Sept. 14, 2018). "Cancer-associated 2-oxoglutarate analogues modify histone methylation by inhibiting histone lysine demethylases". In: *Journal of Molecular Biology* 430.18, pp. 3081–3092. ISSN: 1089-8638. DOI: 10.1016/j.jmb.2018.06.048.
- Laurence, A. et al. (Feb. 15, 2023). *Classification OMS 2021 des tumeurs du système nerveux central*. In: *EM-Consulte*. URL: <https://www.em-consulte.com/article/1573026/classification-oms-2021-des-tumeurs-du-systeme-ner>.
- Laurence, Alice, Emmanuelle Huillard, et al. (2023). "Cell of Origin of Brain and Spinal Cord Tumors". In: *Advances in Experimental Medicine and Biology* 1394, pp. 85–101. ISSN: 0065-2598. DOI: 10.1007/978-3-031-14732-6_6.
- Laurence, Alice, Renata Ursu, Caroline Houillier, et al. (Sept. 2021). "SARS-CoV-

- 2 infection in patients with primary central nervous system lymphoma". In: *Journal of Neurology* 268.9, pp. 3072–3080. ISSN: 0340-5354, 1432-1459. DOI: 10.1007/s00415-020-10311-w. URL: <https://link.springer.com/10.1007/s00415-020-10311-w> (visited on 03/03/2022).
- Laurenge, Alice, Renata Ursu, Emeline Tabouret, et al. (Jan. 2023). "SARS-CoV-2 infection in patients with primary central nervous system lymphoma in the vaccination era". In: *Leukemia & Lymphoma* 64.1, pp. 221–224. ISSN: 1029-2403. DOI: 10.1080/10428194.2022.2131420.
- Laval, Bérengère de et al. (May 7, 2020). "C/EBP β -Dependent Epigenetic Memory Induces Trained Immunity in Hematopoietic Stem Cells". In: *Cell Stem Cell* 26.5, 657–674.e8. ISSN: 1875-9777. DOI: 10.1016/j.stem.2020.01.017.
- Lavin, Yonit et al. (Dec. 4, 2014). "Tissue-resident macrophage enhancer landscapes are shaped by the local microenvironment". In: *Cell* 159.6, pp. 1312–1326. ISSN: 1097-4172. DOI: 10.1016/j.cell.2014.11.018.
- Lawson, L. J. et al. (1990). "Heterogeneity in the distribution and morphology of microglia in the normal adult mouse brain". In: *Neuroscience* 39.1, pp. 151–170. ISSN: 0306-4522. DOI: 10.1016/0306-4522(90)90229-w.
- Lee, Dong-Sung et al. (Oct. 2019). "Simultaneous profiling of 3D genome structure and DNA methylation in single human cells". In: *Nature Methods* 16.10, pp. 999–1006. ISSN: 1548-7105. DOI: 10.1038/s41592-019-0547-z.
- Leonardi, Roberta et al. (Apr. 27, 2012). "Cancer-associated isocitrate dehydrogenase mutations inactivate NADPH-dependent reductive carboxylation". In: *The Journal of Biological Chemistry* 287.18, pp. 14615–14620. ISSN: 1083-351X. DOI: 10.1074/jbc.C112.353946.
- Linninger, Andreas et al. (Aug. 2, 2018). "Modeling the diffusion of D-2-hydroxyglutarate from IDH1 mutant gliomas in the central nervous system". In: *Neuro-Oncology* 20.9, pp. 1197–1206. ISSN: 1523-5866. DOI: 10.1093/neuonc/ny051.
- Lister, Ryan et al. (Aug. 9, 2013). "Global epigenomic reconfiguration during mammalian brain development". In: *Science (New York, N.Y.)* 341.6146, p. 1237905. ISSN: 1095-9203. DOI: 10.1126/science.1237905.
- Liu, Pu-Ste et al. (Sept. 2017). " α -ketoglutarate orchestrates macrophage activation through metabolic and epigenetic reprogramming". In: *Nature Immunology* 18.9, pp. 985–994. ISSN: 1529-2916. DOI: 10.1038/ni.3796.
- López-Moyado, Isaac F. et al. (Aug. 20, 2019). "Paradoxical association of TET loss of function with genome-wide DNA hypomethylation". In: *Proceedings of the National Academy of Sciences of the United States of America* 116.34, pp. 16933–16942. ISSN: 1091-6490. DOI: 10.1073/pnas.1903059116.
- Losman, Julie-Aurore, Peppi Koivunen, and William G. Kaelin (Dec. 2020). "2-Oxoglutarate-dependent dioxygenases in cancer". In: *Nature Reviews. Cancer* 20.12, pp. 710–726. ISSN: 1474-1768. DOI: 10.1038/s41568-020-00303-3.
- Losman, Julie-Aurore, Ryan E. Looper, et al. (Mar. 29, 2013). "(R)-2-hydroxyglutarate is sufficient to promote leukemogenesis and its effects are reversible". In: *Science (New York, N.Y.)* 339.6127, pp. 1621–1625. ISSN: 1095-9203. DOI: 10.1126/science.1231677.
- Louis, David N. et al. (Aug. 2, 2021). "The 2021 WHO Classification of Tumors of the Central Nervous System: a summary". In: *Neuro-Oncology* 23.8, pp. 1231–1251. ISSN: 1523-5866. DOI: 10.1093/neuonc/noab106.
- Lu, Chao et al. (Feb. 15, 2012). "IDH mutation impairs histone demethylation and

- results in a block to cell differentiation". In: *Nature* 483.7390, pp. 474–478. ISSN: 1476-4687. DOI: 10.1038/nature10860.
- Lu, Falong et al. (Oct. 1, 2014). "Role of Tet proteins in enhancer activity and telomere elongation". In: *Genes & Development* 28.19, pp. 2103–2119. ISSN: 1549-5477. DOI: 10.1101/gad.248005.114.
- Luchman, H. Artee et al. (Feb. 2012). "An in vivo patient-derived model of endogenous IDH1-mutant glioma". In: *Neuro-Oncology* 14.2, pp. 184–191. ISSN: 1523-5866. DOI: 10.1093/neuonc/nor207.
- Lund, Harald et al. (Nov. 19, 2018). "Competitive repopulation of an empty microglial niche yields functionally distinct subsets of microglia-like cells". In: *Nature Communications* 9.1, p. 4845. ISSN: 2041-1723. DOI: 10.1038/s41467-018-07295-7.
- Luoto, Suvi et al. (Oct. 1, 2018). "Computational Characterization of Suppressive Immune Microenvironments in Glioblastoma". In: *Cancer Research* 78.19, pp. 5574–5585. ISSN: 1538-7445. DOI: 10.1158/0008-5472.CAN-17-3714.
- Ma, Shenghong et al. (Apr. 20, 2015). "D-2-hydroxyglutarate is essential for maintaining oncogenic property of mutant IDH-containing cancer cells but dispensable for cell growth". In: *Oncotarget* 6.11, pp. 8606–8620. ISSN: 1949-2553. DOI: 10.18632/oncotarget.3330.
- Mah, L.-J., A. El-Osta, and T. C. Karagiannis (Apr. 2010). "gammaH2AX: a sensitive molecular marker of DNA damage and repair". In: *Leukemia* 24.4, pp. 679–686. ISSN: 1476-5551. DOI: 10.1038/leu.2010.6.
- Mancuso, Renzo et al. (Dec. 2019). "Stem-cell-derived human microglia transplanted in mouse brain to study human disease". In: *Nature Neuroscience* 22.12, pp. 2111–2116. ISSN: 1546-1726. DOI: 10.1038/s41593-019-0525-x.
- Masopust, David, Christine P. Sivula, and Stephen C. Jameson (July 15, 2017). "Of Mice, Dirty Mice, and Men: Using Mice To Understand Human Immunology". In: *Journal of Immunology (Baltimore, Md.: 1950)* 199.2, pp. 383–388. ISSN: 1550-6606. DOI: 10.4049/jimmunol.1700453.
- Masuda, Takahiro et al. (July 2020). "Novel Hexb-based tools for studying microglia in the CNS". in: *Nature Immunology* 21.7, pp. 802–815. ISSN: 1529-2916. DOI: 10.1038/s41590-020-0707-4.
- Mellinghoff, Ingo K., Martin J. van den Bent, et al. (Aug. 17, 2023). "Vorasidenib in IDH1- or IDH2-Mutant Low-Grade Glioma". In: *The New England Journal of Medicine* 389.7, pp. 589–601. ISSN: 1533-4406. DOI: 10.1056/NEJMoa2304194.
- Mellinghoff, Ingo K., Benjamin M. Ellingson, et al. (Oct. 10, 2020). "Ivosidenib in Isocitrate Dehydrogenase 1 – Mutated Advanced Glioma". In: *Journal of Clinical Oncology* 38.29, pp. 3398–3406. ISSN: 0732-183X, 1527-7755. DOI: 10.1200/JCO.19.03327. URL: <https://ascopubs.org/doi/10.1200/JCO.19.03327> (visited on 06/01/2024).
- Mellinghoff, Ingo K., Min Lu, et al. (Mar. 2023). "Vorasidenib and ivosidenib in IDH1-mutant low-grade glioma: a randomized, perioperative phase 1 trial". In: *Nature Medicine* 29.3, pp. 615–622. ISSN: 1078-8956, 1546-170X. DOI: 10.1038/s41591-022-02141-2. URL: <https://www.nature.com/articles/s41591-022-02141-2> (visited on 06/01/2024).
- Mellinghoff, Ingo K., Marta Penas-Prado, et al. (Aug. 15, 2021). "Vorasidenib, a Dual Inhibitor of Mutant IDH1/2, in Recurrent or Progressive Glioma; Results of a First-in-Human Phase I Trial". In: *Clinical Cancer Research* 27.16, pp. 4491–4499. ISSN: 1078-0432, 1557-3265. DOI: 10.1158/1078-0432.CCR-21-0611. URL: <https://aacrjournals.org/clincancerres/article/27/>

- 16/4491/671595/Vorasidenib-a-Dual-Inhibitor-of-Mutant-IDH1-2-in (visited on 06/01/2024).
- Mestas, Javier and Christopher C. W. Hughes (Mar. 1, 2004). "Of mice and not men: differences between mouse and human immunology". In: *Journal of Immunology (Baltimore, Md.: 1950)* 172.5, pp. 2731–2738. ISSN: 0022-1767. DOI: 10.4049/jimmunol.172.5.2731.
- Miller, Tyler E. et al. (Oct. 27, 2023). *Programs, Origins, and Niches of Immunomodulatory Myeloid Cells in Gliomas*. DOI: 10.1101/2023.10.24.563466. URL: <https://www.biorxiv.org/content/10.1101/2023.10.24.563466v1> (visited on 03/28/2024).
- Mirzaei, Reza et al. (Dec. 5, 2023). *Spatially resolved single-cell analysis uncovers protein kinase C δ -expressing microglia with anti-tumor activity in glioblastoma*. preprint. Immunology. DOI: 10.1101/2023.12.04.570023. URL: <http://biorxiv.org/lookup/doi/10.1101/2023.12.04.570023> (visited on 03/28/2024).
- Mishra, Prachi et al. (Jan. 2, 2018). "ADHFE1 is a breast cancer oncogene and induces metabolic reprogramming". In: *The Journal of Clinical Investigation* 128.1, pp. 323–340. ISSN: 1558-8238. DOI: 10.1172/JCI93815.
- Mittelbronn, M. et al. (Mar. 2001). "Local distribution of microglia in the normal adult human central nervous system differs by up to one order of magnitude". In: *Acta Neuropathologica* 101.3, pp. 249–255. ISSN: 0001-6322. DOI: 10.1007/s004010000284.
- Montagner, Sara et al. (May 17, 2016). "TET2 Regulates Mast Cell Differentiation and Proliferation through Catalytic and Non-catalytic Activities". In: *Cell Reports* 15.7, pp. 1566–1579. ISSN: 2211-1247. DOI: 10.1016/j.celrep.2016.04.044.
- Mortazavi, Armin et al. (Sept. 1, 2022). "IDH-mutated gliomas promote epileptogenesis through d-2-hydroxyglutarate-dependent mTOR hyperactivation". In: *Neuro-Oncology* 24.9, pp. 1423–1435. ISSN: 1523-5866. DOI: 10.1093/neuonc/noac003.
- Motevasseli, Meysam et al. (Aug. 16, 2024). "Distinct tumor-TAM interactions in IDH-stratified glioma microenvironments unveiled by single-cell and spatial transcriptomics". In: *Acta Neuropathologica Communications* 12.1, p. 133. ISSN: 2051-5960. DOI: 10.1186/s40478-024-01837-5.
- Mrdjen, Dunja et al. (Feb. 20, 2018). "High-Dimensional Single-Cell Mapping of Central Nervous System Immune Cells Reveals Distinct Myeloid Subsets in Health, Aging, and Disease". In: *Immunity* 48.2, 380–395.e6. ISSN: 1097-4180. DOI: 10.1016/j.immuni.2018.01.011.
- Mu, Luyan et al. (2018). "The IDH1 Mutation-Induced Oncometabolite, 2-Hydroxyglutarate, May Affect DNA Methylation and Expression of PD-L1 in Gliomas". In: *Frontiers in Molecular Neuroscience* 11, p. 82. ISSN: 1662-5099. DOI: 10.3389/fnmo1.2018.00082.
- Mühlhausen, C. et al. (Apr. 2008). "Membrane translocation of glutaric acid and its derivatives". In: *Journal of Inherited Metabolic Disease* 31.2, pp. 188–193. ISSN: 1573-2665. DOI: 10.1007/s10545-008-0825-x.
- Müller, Annett et al. (July 15, 2015). "Resident microglia, and not peripheral macrophages, are the main source of brain tumor mononuclear cells". In: *International Journal of Cancer* 137.2, pp. 278–288. ISSN: 1097-0215. DOI: 10.1002/ijc.29379.
- Müller, Sören et al. (Dec. 20, 2017). "Single-cell profiling of human gliomas reveals macrophage ontogeny as a basis for regional differences in macrophage acti-

- vation in the tumor microenvironment". In: *Genome Biology* 18.1, p. 234. ISSN: 1474-760X. DOI: 10.1186/s13059-017-1362-4.
- Murray, Peter J. et al. (July 17, 2014). "Macrophage activation and polarization: nomenclature and experimental guidelines". In: *Immunity* 41.1, pp. 14–20. ISSN: 1097-4180. DOI: 10.1016/j.immuni.2014.06.008.
- Myllyharju, Johanna and Kari I. Kivirikko (Jan. 2004). "Collagens, modifying enzymes and their mutations in humans, flies and worms". In: *Trends in genetics: TIG* 20.1, pp. 33–43. ISSN: 0168-9525. DOI: 10.1016/j.tig.2003.11.004.
- Nagai, A. et al. (Dec. 2001). "Generation and characterization of immortalized human microglial cell lines: expression of cytokines and chemokines". In: *Neurobiology of Disease* 8.6, pp. 1057–1068. ISSN: 0969-9961. DOI: 10.1006/nbdi.2001.0437.
- Nakatani, Tsunetoshi et al. (May 2015). "Stella preserves maternal chromosome integrity by inhibiting 5hmC-induced γ H2AX accumulation". In: *EMBO reports* 16.5, pp. 582–589. ISSN: 1469-3178. DOI: 10.15252/embr.201439427.
- Natsume, Atsushi et al. (Feb. 14, 2023). "The first-in-human phase I study of a brain-penetrant mutant IDH1 inhibitor DS-1001 in patients with recurrent or progressive IDH1-mutant gliomas". In: *Neuro-Oncology* 25.2, pp. 326–336. ISSN: 1523-5866. DOI: 10.1093/neuonc/noac155.
- Noel, Nicolas et al. (Aug. 2021). "Inflammatory demyelinating polyneuropathies and lymphoma: clues to diagnosis and therapy". In: *Leukemia & Lymphoma* 62.8, pp. 2000–2004. ISSN: 1029-2403. DOI: 10.1080/10428194.2021.1889535.
- Notarangelo, Giulia et al. (Sept. 30, 2022). "Oncometabolite d-2HG alters T cell metabolism to impair CD8+ T cell function". In: *Science (New York, N.Y.)* 377.6614, pp. 1519–1529. ISSN: 1095-9203. DOI: 10.1126/science.abj5104.
- Noushmehr, Houtan et al. (May 18, 2010). "Identification of a CpG island methylator phenotype that defines a distinct subgroup of glioma". In: *Cancer Cell* 17.5, pp. 510–522. ISSN: 1878-3686. DOI: 10.1016/j.ccr.2010.03.017.
- Núñez, Felipe J. et al. (Feb. 13, 2019). "IDH1-R132H acts as a tumor suppressor in glioma via epigenetic up-regulation of the DNA damage response". In: *Science Translational Medicine* 11.479, eaaq1427. ISSN: 1946-6242. DOI: 10.1126/scitranslmed.aaq1427.
- O'Neill, Luke A. J. and Maxim N. Artyomov (May 2019). "Itaconate: the poster child of metabolic reprogramming in macrophage function". In: *Nature Reviews. Immunology* 19.5, pp. 273–281. ISSN: 1474-1741. DOI: 10.1038/s41577-019-0128-5.
- Ochocka, Natalia, Pawel Segit, Kacper Adam Walentynowicz, et al. (Feb. 19, 2021). "Single-cell RNA sequencing reveals functional heterogeneity of glioma-associated brain macrophages". In: *Nature Communications* 12.1, p. 1151. ISSN: 2041-1723. DOI: 10.1038/s41467-021-21407-w.
- Ochocka, Natalia, Pawel Segit, Kamil Wojnicki, et al. (Jan. 31, 2023). "Specialized functions and sexual dimorphism explain the functional diversity of the myeloid populations during glioma progression". In: *Cell Reports* 42.1, p. 111971. ISSN: 2211-1247. DOI: 10.1016/j.celrep.2022.111971.
- Oermann, Eric K. et al. (June 2012). "Alterations of metabolic genes and metabolites in cancer". In: *Seminars in Cell & Developmental Biology* 23.4, pp. 370–380. ISSN: 1096-3634. DOI: 10.1016/j.semcdb.2012.01.013.
- Okano, M. et al. (Oct. 29, 1999). "DNA methyltransferases Dnmt3a and Dnmt3b are essential for de novo methylation and mammalian development". In: *Cell* 99.3,

- pp. 247–257. ISSN: 0092-8674. DOI: 10.1016/s0092-8674(00)81656-6.
- Onodera, Atsushi et al. (June 22, 2021). “Roles of TET and TDG in DNA demethylation in proliferating and non-proliferating immune cells”. In: *Genome Biology* 22.1, p. 186. ISSN: 1474-760X. DOI: 10.1186/s13059-021-02384-1.
- Ostrom, Quinn T. et al. (Oct. 5, 2022). “CBTRUS Statistical Report: Primary Brain and Other Central Nervous System Tumors Diagnosed in the United States in 2015-2019”. In: *Neuro-Oncology* 24 (Suppl 5), pp. v1–v95. ISSN: 1523-5866. DOI: 10.1093/neuonc/noac202.
- Parry, Aled, Steffen Rulands, and Wolf Reik (Jan. 2021). “Active turnover of DNA methylation during cell fate decisions”. In: *Nature Reviews. Genetics* 22.1, pp. 59–66. ISSN: 1471-0064. DOI: 10.1038/s41576-020-00287-8.
- Pastor, William A. et al. (May 19, 2011). “Genome-wide mapping of 5-hydroxymethylcytosine in embryonic stem cells”. In: *Nature* 473.7347, pp. 394–397. ISSN: 1476-4687. DOI: 10.1038/nature10102.
- Picca, Alberto et al. (May 2024). “REVOLUMAB: A phase II trial of nivolumab in recurrent IDH mutant high-grade gliomas”. In: *European Journal of Cancer (Oxford, England: 1990)* 202, p. 114034. ISSN: 1879-0852. DOI: 10.1016/j.ejca.2024.114034.
- Pidsley, Ruth et al. (Oct. 7, 2016). “Critical evaluation of the Illumina MethylationEPIC BeadChip microarray for whole-genome DNA methylation profiling”. In: *Genome Biology* 17.1, p. 208. ISSN: 1474-760X. DOI: 10.1186/s13059-016-1066-1.
- Pirozzi, Christopher J. and Hai Yan (Oct. 2021). “The implications of IDH mutations for cancer development and therapy”. In: *Nature Reviews. Clinical Oncology* 18.10, pp. 645–661. ISSN: 1759-4782. DOI: 10.1038/s41571-021-00521-0.
- Platten, Michael et al. (Apr. 2021). “A vaccine targeting mutant IDH1 in newly diagnosed glioma”. In: *Nature* 592.7854, pp. 463–468. ISSN: 1476-4687. DOI: 10.1038/s41586-021-03363-z.
- Pombo Antunes, Ana Rita et al. (Apr. 2021). “Single-cell profiling of myeloid cells in glioblastoma across species and disease stage reveals macrophage competition and specialization”. In: *Nature Neuroscience* 24.4, pp. 595–610. ISSN: 1097-6256, 1546-1726. DOI: 10.1038/s41593-020-00789-y. URL: <http://www.nature.com/articles/s41593-020-00789-y> (visited on 04/07/2021).
- Pouget, Celso et al. (May 2020). “Ki-67 and MCM6 labeling indices are correlated with overall survival in anaplastic oligodendroglioma, IDH1-mutant and 1p/19q-codeleted: a multicenter study from the French POLA network”. In: *Brain Pathology (Zurich, Switzerland)* 30.3, pp. 465–478. ISSN: 1750-3639. DOI: 10.1111/bpa.12788.
- Prinz, Marco, Steffen Jung, and Josef Priller (Oct. 3, 2019). “Microglia Biology: One Century of Evolving Concepts”. In: *Cell* 179.2, pp. 292–311. ISSN: 1097-4172. DOI: 10.1016/j.cell.2019.08.053.
- Pusch, Stefan et al. (Feb. 14, 2014). “D-2-Hydroxyglutarate producing neo-enzymatic activity inversely correlates with frequency of the type of isocitrate dehydrogenase 1 mutations found in glioma”. In: *Acta Neuropathologica Communications* 2, p. 19. ISSN: 2051-5960. DOI: 10.1186/2051-5960-2-19.
- Qi, Shaohua et al. (Mar. 12, 2021). “X chromosome escapee genes are involved in ischemic sexual dimorphism through epigenetic modification of inflammatory signals”. In: *Journal of Neuroinflammation* 18.1, p. 70. ISSN: 1742-2094. DOI: 10.1186/s12974-021-02120-3.
- Qian, Jiawen et al. (July 12, 2021). *Dynamics of glioma-associated microglia and*

- macrophages reveals their divergent roles in the immune response of brain*. preprint. Immunology. DOI: 10.1101/2021.07.11.451874. URL: <http://biorxiv.org/lookup/doi/10.1101/2021.07.11.451874> (visited on 03/26/2024).
- Rasmussen, Kasper D. et al. (May 1, 2015). "Loss of TET2 in hematopoietic cells leads to DNA hypermethylation of active enhancers and induction of leukemogenesis". In: *Genes & Development* 29.9, pp. 910–922. ISSN: 1549-5477. DOI: 10.1101/gad.260174.115.
- Ravi, Vidhya et al. (July 26, 2021). *Oncometabolite R-2 hydroxyglutarate aids the inflammatory transformation of peritumoral astrocytes*. DOI: 10.21203/rs.3.rs-720962/v1. URL: <https://www.researchsquare.com/article/rs-720962/v1> (visited on 10/09/2024).
- Ravi, Vidhya M. et al. (June 13, 2022). "Spatially resolved multi-omics deciphers bidirectional tumor-host interdependence in glioblastoma". In: *Cancer Cell* 40.6, 639–655.e13. ISSN: 1878-3686. DOI: 10.1016/j.ccell.2022.05.009.
- Reilly, Steven K. et al. (Mar. 6, 2015). "Evolutionary genomics. Evolutionary changes in promoter and enhancer activity during human corticogenesis". In: *Science (New York, N.Y.)* 347.6226, pp. 1155–1159. ISSN: 1095-9203. DOI: 10.1126/science.1260943.
- Reitman, Zachary J. et al. (Feb. 22, 2011). "Profiling the effects of isocitrate dehydrogenase 1 and 2 mutations on the cellular metabolome". In: *Proceedings of the National Academy of Sciences of the United States of America* 108.8, pp. 3270–3275. ISSN: 1091-6490. DOI: 10.1073/pnas.1019393108.
- Réu, Pedro et al. (July 25, 2017). "The Lifespan and Turnover of Microglia in the Human Brain". In: *Cell Reports* 20.4, pp. 779–784. ISSN: 2211-1247. DOI: 10.1016/j.celrep.2017.07.004.
- Reuss, David E. et al. (June 2015). "IDH mutant diffuse and anaplastic astrocytomas have similar age at presentation and little difference in survival: a grading problem for WHO". in: *Acta Neuropathologica* 129.6, pp. 867–873. ISSN: 1432-0533. DOI: 10.1007/s00401-015-1438-8.
- Rica, Lorenzo de la et al. (2013). "PU.1 target genes undergo Tet2-coupled demethylation and DNMT3b-mediated methylation in monocyte-to-osteoclast differentiation". In: *Genome Biology* 14.9, R99. ISSN: 1474-760X. DOI: 10.1186/gb-2013-14-9-r99.
- Richard, Quentin et al. (Dec. 1, 2022). "New insights into the Immune TME of adult-type diffuse gliomas". In: *Current Opinion in Neurology* 35.6, pp. 794–802. ISSN: 1473-6551. DOI: 10.1097/WCO.0000000000001112.
- Rossi, M. L. et al. (1987). "Immunohistological study of mononuclear cell infiltrate in malignant gliomas". In: *Acta Neuropathologica* 74.3, pp. 269–277. ISSN: 0001-6322. DOI: 10.1007/BF00688191.
- Rustenhoven, Justin and Jonathan Kipnis (Dec. 20, 2019). "Bypassing the blood-brain barrier". In: *Science (New York, N.Y.)* 366.6472, pp. 1448–1449. ISSN: 1095-9203. DOI: 10.1126/science.aay0479.
- Sabogal-Guáqueta, Angélica María et al. (Oct. 13, 2023). "Species-specific metabolic reprogramming in human and mouse microglia during inflammatory pathway induction". In: *Nature Communications* 14.1, p. 6454. ISSN: 2041-1723. DOI: 10.1038/s41467-023-42096-7.
- Sardina, Jose Luis et al. (Nov. 1, 2018). "Transcription Factors Drive Tet2-Mediated Enhancer Demethylation to Reprogram Cell Fate". In: *Cell Stem Cell* 23.5, 727–741.e9. ISSN: 1875-9777. DOI: 10.1016/j.stem.2018.08.016.

- Sasaki, Masato, Christiane B. Knobbe, Momoe Itsumi, et al. (Sept. 15, 2012). "D-2-hydroxyglutarate produced by mutant IDH1 perturbs collagen maturation and basement membrane function". In: *Genes & Development* 26.18, pp. 2038–2049. ISSN: 1549-5477. DOI: 10.1101/gad.198200.112.
- Sasaki, Masato, Christiane B. Knobbe, Joshua C. Munger, et al. (Aug. 30, 2012). "IDH1(R132H) mutation increases murine haematopoietic progenitors and alters epigenetics". In: *Nature* 488.7413, pp. 656–659. ISSN: 1476-4687. DOI: 10.1038/nature11323.
- Sedgwick, J. D. et al. (Aug. 15, 1991). "Isolation and direct characterization of resident microglial cells from the normal and inflamed central nervous system". In: *Proceedings of the National Academy of Sciences of the United States of America* 88.16, pp. 7438–7442. ISSN: 0027-8424. DOI: 10.1073/pnas.88.16.7438.
- Seok, Junhee et al. (Feb. 26, 2013). "Genomic responses in mouse models poorly mimic human inflammatory diseases". In: *Proceedings of the National Academy of Sciences of the United States of America* 110.9, pp. 3507–3512. ISSN: 1091-6490. DOI: 10.1073/pnas.1222878110.
- Shan, Xia et al. (July 2020). "Prognostic value of a nine-gene signature in glioma patients based on tumor-associated macrophages expression profiling". In: *Clinical Immunology (Orlando, Fla.)* 216, p. 108430. ISSN: 1521-7035. DOI: 10.1016/j.clim.2020.108430.
- Silvin, Aymeric, Jiawen Qian, and Florent Ginhoux (Nov. 2023). "Brain macrophage development, diversity and dysregulation in health and disease". In: *Cellular & Molecular Immunology* 20.11, pp. 1277–1289. ISSN: 2042-0226. DOI: 10.1038/s41423-023-01053-6.
- Silvin, Aymeric, Stefan Uderhardt, et al. (Aug. 9, 2022). "Dual ontogeny of disease-associated microglia and disease inflammatory macrophages in aging and neurodegeneration". In: *Immunity* 55.8, 1448–1465.e6. ISSN: 1097-4180. DOI: 10.1016/j.immuni.2022.07.004.
- Smith, Amy M. and Mike Dragunow (Mar. 2014). "The human side of microglia". In: *Trends in Neurosciences* 37.3, pp. 125–135. ISSN: 1878-108X. DOI: 10.1016/j.tins.2013.12.001.
- Spitzer, Avishay et al. (May 2024). "Mutant IDH inhibitors induce lineage differentiation in IDH-mutant oligodendroglioma". In: *Cancer Cell* 42.5, 904–914.e9. ISSN: 15356108. DOI: 10.1016/j.ccell.2024.03.008. URL: <https://linkinghub.elsevier.com/retrieve/pii/S153561082400093X> (visited on 06/01/2024).
- Steffanoni, Sara et al. (Nov. 2022). "Impact of severe acute respiratory syndrome coronavirus-2 infection on the outcome of primary central nervous system lymphoma treatment: A study of the International PCNSL Collaborative Group". In: *British Journal of Haematology* 199.4, pp. 507–519. ISSN: 1365-2141. DOI: 10.1111/bjh.18396.
- Stroud, Hume et al. (June 20, 2011). "5-Hydroxymethylcytosine is associated with enhancers and gene bodies in human embryonic stem cells". In: *Genome Biology* 12.6, R54. ISSN: 1474-760X. DOI: 10.1186/gb-2011-12-6-r54.
- Stupp, Roger, Monika E. Hegi, et al. (May 2009). "Effects of radiotherapy with concomitant and adjuvant temozolomide versus radiotherapy alone on survival in glioblastoma in a randomised phase III study: 5-year analysis of the EORTC-NCIC trial". In: *The Lancet. Oncology* 10.5, pp. 459–466. ISSN: 1474-5488. DOI: 10.1016/S1470-2045(09)70025-7.
- Stupp, Roger, Sophie Taillibert, et al. (Dec. 19, 2017). "Effect of Tumor-Treating Fields

- Plus Maintenance Temozolomide vs Maintenance Temozolomide Alone on Survival in Patients With Glioblastoma: A Randomized Clinical Trial". In: *JAMA* 318.23, pp. 2306–2316. ISSN: 1538-3598. DOI: 10.1001/jama.2017.18718.
- Su, Rui et al. (Jan. 11, 2018). "R-2HG Exhibits Anti-tumor Activity by Targeting FTO/m6A/MYC/CEBPA Signaling". In: *Cell* 172.1, 90–105.e23. ISSN: 1097-4172. DOI: 10.1016/j.cell.2017.11.031.
- Suijker, Johnny et al. (June 20, 2015). "The oncometabolite D-2-hydroxyglutarate induced by mutant IDH1 or -2 blocks osteoblast differentiation in vitro and in vivo". In: *Oncotarget* 6.17, pp. 14832–14842. ISSN: 1949-2553. DOI: 10.18632/oncotarget.4024.
- Sulkowski, Parker L., Christopher D. Corso, et al. (Feb. 1, 2017). "2-Hydroxyglutarate produced by neomorphic IDH mutations suppresses homologous recombination and induces PARP inhibitor sensitivity". In: *Science Translational Medicine* 9.375, eaal2463. ISSN: 1946-6242. DOI: 10.1126/scitranslmed.aal2463.
- Sulkowski, Parker L., Sebastian Oeck, et al. (June 3, 2020). "Oncometabolites suppress DNA repair by disrupting local chromatin signalling". In: *Nature*. ISSN: 1476-4687. DOI: 10.1038/s41586-020-2363-0.
- Sun, Zhiyi et al. (Feb. 19, 2015). "A sensitive approach to map genome-wide 5-hydroxymethylcytosine and 5-formylcytosine at single-base resolution". In: *Molecular Cell* 57.4, pp. 750–761. ISSN: 1097-4164. DOI: 10.1016/j.molcel.2014.12.035.
- Suzuki, Takahiro et al. (Sept. 12, 2017). "RUNX1 regulates site specificity of DNA demethylation by recruitment of DNA demethylation machineries in hematopoietic cells". In: *Blood Advances* 1.20, pp. 1699–1711. ISSN: 2473-9529. DOI: 10.1182/bloodadvances.2017005710.
- Szulwach, Keith E. et al. (June 2011). "Integrating 5-hydroxymethylcytosine into the epigenomic landscape of human embryonic stem cells". In: *PLoS genetics* 7.6, e1002154. ISSN: 1553-7404. DOI: 10.1371/journal.pgen.1002154.
- Tarhonskaya, Hanna et al. (Mar. 5, 2014). "Non-enzymatic chemistry enables 2-hydroxyglutarate-mediated activation of 2-oxoglutarate oxygenases". In: *Nature Communications* 5, p. 3423. ISSN: 2041-1723. DOI: 10.1038/ncomms4423.
- Tateishi, Kensuke et al. (Dec. 14, 2015). "Extreme Vulnerability of IDH1 Mutant Cancers to NAD⁺ Depletion". In: *Cancer Cell* 28.6, pp. 773–784. ISSN: 1878-3686. DOI: 10.1016/j.ccr.2015.11.006.
- Tauziède-Espariat, Arnault et al. (Feb. 2024). "Brain metastasis of a urothelial neuroendocrine carcinoma: A double pitfall for neuropathologists and DNA-methylation profiling". In: *Neuropathology and Applied Neurobiology* 50.1, e12951. ISSN: 1365-2990. DOI: 10.1111/nan.12951.
- Tawbi, Hussein A. et al. (Aug. 23, 2018). "Combined Nivolumab and Ipilimumab in Melanoma Metastatic to the Brain". In: *The New England Journal of Medicine* 379.8, pp. 722–730. ISSN: 1533-4406. DOI: 10.1056/NEJMoa1805453.
- Terunuma, Atsushi et al. (Jan. 2014). "MYC-driven accumulation of 2-hydroxyglutarate is associated with breast cancer prognosis". In: *The Journal of Clinical Investigation* 124.1, pp. 398–412. ISSN: 1558-8238. DOI: 10.1172/JCI71180.
- Tewari, Manju et al. (Apr. 1, 2021). "Physiology of Cultured Human Microglia Maintained in a Defined Culture Medium". In: *ImmunoHorizons* 5.4, pp. 257–272. ISSN: 2573-7732. DOI: 10.4049/immunohorizons.2000101. URL: <https://www.immunohorizons.org/content/5/4/257> (visited on 05/21/2021).

- Thomas-Joulié, A. et al. (May 2024). "Prognosis of glioblastoma patients improves significantly over time interrogating historical controls". In: *European Journal of Cancer (Oxford, England: 1990)* 202, p. 114004. ISSN: 1879-0852. DOI: 10.1016/j.ejca.2024.114004.
- Timmerman, Raissa, Saskia M. Burm, and Jeffrey J. Bajramovic (2018). "An Overview of in vitro Methods to Study Microglia". In: *Frontiers in Cellular Neuroscience* 12, p. 242. ISSN: 1662-5102. DOI: 10.3389/fncel.2018.00242.
- Touat, M. et al. (May 2015). "Adapting the drivers to the road: a new strategy for cancer evolution?" In: *Annals of Oncology: Official Journal of the European Society for Medical Oncology* 26.5, pp. 827–829. ISSN: 1569-8041. DOI: 10.1093/annonc/mdv137.
- Touat, Mehdi et al. (Apr. 2020). "Mechanisms and therapeutic implications of hypermutation in gliomas". In: *Nature* 580.7804, pp. 517–523. ISSN: 1476-4687. DOI: 10.1038/s41586-020-2209-9.
- Tsai, Ya-Ping et al. (Dec. 3, 2014). "TET1 regulates hypoxia-induced epithelial-mesenchymal transition by acting as a co-activator". In: *Genome Biology* 15.12, p. 513. ISSN: 1474-760X. DOI: 10.1186/s13059-014-0513-0.
- Turcan, Sevin, Vladimir Makarov, et al. (Jan. 2018). "Mutant-IDH1-dependent chromatin state reprogramming, reversibility, and persistence". In: *Nature Genetics* 50.1, pp. 62–72. ISSN: 1546-1718. DOI: 10.1038/s41588-017-0001-z.
- Turcan, Sevin, Daniel Rohle, et al. (Feb. 15, 2012). "IDH1 mutation is sufficient to establish the glioma hypermethylator phenotype". In: *Nature* 483.7390, pp. 479–483. ISSN: 1476-4687. DOI: 10.1038/nature10866.
- Tyrakis, Petros A. et al. (Dec. 8, 2016). "S-2-hydroxyglutarate regulates CD8+ T-lymphocyte fate". In: *Nature* 540.7632, pp. 236–241. ISSN: 1476-4687. DOI: 10.1038/nature20165.
- Ugele, Ines et al. (Feb. 10, 2019). "D-2-Hydroxyglutarate and L-2-Hydroxyglutarate Inhibit IL-12 Secretion by Human Monocyte-Derived Dendritic Cells". In: *International Journal of Molecular Sciences* 20.3, E742. ISSN: 1422-0067. DOI: 10.3390/ijms20030742.
- Unruh, Dusten et al. (Dec. 2016). "Mutant IDH1 and thrombosis in gliomas". In: *Acta Neuropathologica* 132.6, pp. 917–930. ISSN: 1432-0533. DOI: 10.1007/s00401-016-1620-7.
- Utz, Sebastian G. et al. (Apr. 30, 2020). "Early Fate Defines Microglia and Non-parenchymal Brain Macrophage Development". In: *Cell* 181.3, 557–573.e18. ISSN: 1097-4172. DOI: 10.1016/j.cell.2020.03.021.
- Van Hove, Hannah et al. (June 2019). "A single-cell atlas of mouse brain macrophages reveals unique transcriptional identities shaped by ontogeny and tissue environment". In: *Nature Neuroscience* 22.6, pp. 1021–1035. ISSN: 1546-1726. DOI: 10.1038/s41593-019-0393-4.
- Vargas López, Antonio José (Mar. 25, 2021). "Glioblastoma in adults: a Society for Neuro-Oncology (SNO) and European Society of Neuro-Oncology (EANO) consensus review on current management and future directions". In: *Neuro-Oncology* 23.3, pp. 502–503. ISSN: 1523-5866. DOI: 10.1093/neuonc/noaa287.
- Venteicher, Andrew S. et al. (Mar. 31, 2017). "Decoupling genetics, lineages, and microenvironment in IDH-mutant gliomas by single-cell RNA-seq". In: *Science (New York, N.Y.)* 355.6332. ISSN: 0036-8075. DOI: 10.1126/science.aai8478. URL: <https://www.ncbi.nlm.nih.gov/pmc/articles/PMC5519096/> (visited on 04/06/2020).

- Walker, Douglas G. and Lih-Fen Lue (Aug. 19, 2015). "Immune phenotypes of microglia in human neurodegenerative disease: challenges to detecting microglial polarization in human brains". In: *Alzheimer's Research & Therapy* 7.1, p. 56. ISSN: 1758-9193. DOI: 10.1186/s13195-015-0139-9.
- Wang, Dongpeng et al. (Dec. 2, 2022). "Active DNA demethylation promotes cell fate specification and the DNA damage response". In: *Science (New York, N.Y.)* 378.6623, pp. 983–989. ISSN: 1095-9203. DOI: 10.1126/science.add9838.
- Wang, P. et al. (June 20, 2013). "Mutations in isocitrate dehydrogenase 1 and 2 occur frequently in intrahepatic cholangiocarcinomas and share hypermethylation targets with glioblastomas". In: *Oncogene* 32.25, pp. 3091–3100. ISSN: 1476-5594. DOI: 10.1038/onc.2012.315.
- Wang, Pu et al. (Dec. 22, 2015). "Oncometabolite D-2-Hydroxyglutarate Inhibits ALKBH DNA Repair Enzymes and Sensitizes IDH Mutant Cells to Alkylating Agents". In: *Cell Reports* 13.11, pp. 2353–2361. ISSN: 2211-1247. DOI: 10.1016/j.celrep.2015.11.029.
- Wang, Xiaomin et al. (July 2022). "SLC1A1-mediated cellular and mitochondrial influx of R-2-hydroxyglutarate in vascular endothelial cells promotes tumor angiogenesis in IDH1-mutant solid tumors". In: *Cell Research* 32.7, pp. 638–658. ISSN: 1748-7838. DOI: 10.1038/s41422-022-00650-w.
- Wang, Xue et al. (Dec. 29, 2017). "Identification of the histone lysine demethylase KDM4A/JMJD2A as a novel epigenetic target in M1 macrophage polarization induced by oxidized LDL". In: *Oncotarget* 8.70, pp. 114442–114456. ISSN: 1949-2553. DOI: 10.18632/oncotarget.17748.
- Wang, Zeshuai et al. (Sept. 28, 2023). "An immune cell atlas reveals the dynamics of human macrophage specification during prenatal development". In: *Cell* 186.20, 4454–4471.e19. ISSN: 1097-4172. DOI: 10.1016/j.cell.2023.08.019.
- Watanabe, Takuya et al. (Apr. 2009). "IDH1 mutations are early events in the development of astrocytomas and oligodendrogliomas". In: *The American Journal of Pathology* 174.4, pp. 1149–1153. ISSN: 1525-2191. DOI: 10.2353/ajpath.2009.080958.
- Weller, Michael et al. (Mar. 2021). "EANO guidelines on the diagnosis and treatment of diffuse gliomas of adulthood". In: *Nature Reviews. Clinical Oncology* 18.3, pp. 170–186. ISSN: 1759-4782. DOI: 10.1038/s41571-020-00447-z.
- Wen, Lu et al. (Mar. 4, 2014). "Whole-genome analysis of 5-hydroxymethylcytosine and 5-methylcytosine at base resolution in the human brain". In: *Genome Biology* 15.3, R49. ISSN: 1474-760X. DOI: 10.1186/gb-2014-15-3-r49.
- Wick, Antje et al. (May 15, 2021). "Phase I Assessment of Safety and Therapeutic Activity of BAY1436032 in Patients with IDH1-Mutant Solid Tumors". In: *Clinical Cancer Research: An Official Journal of the American Association for Cancer Research* 27.10, pp. 2723–2733. ISSN: 1557-3265. DOI: 10.1158/1078-0432.CCR-20-4256.
- Williams, Niamh C. et al. (Feb. 2022). "Signaling metabolite L-2-hydroxyglutarate activates the transcription factor HIF-1 α in lipopolysaccharide-activated macrophages". In: *The Journal of Biological Chemistry* 298.2, p. 101501. ISSN: 1083-351X. DOI: 10.1016/j.jbc.2021.101501.
- Wolf, Susanne A., H. W. G. M. Boddeke, and Helmut Kettenmann (Feb. 10, 2017). "Microglia in Physiology and Disease". In: *Annual Review of Physiology* 79, pp. 619–643. ISSN: 1545-1585. DOI: 10.1146/annurev-physiol-022516-034406.
- Wu, Meng-Ju, Hiroshi Kondo, et al. (July 12, 2024). "Mutant IDH1 inhibition induces

- dsDNA sensing to activate tumor immunity". In: *Science (New York, N.Y.)* 385.6705, ead16173. ISSN: 1095-9203. DOI: 10.1126/science.ad16173.
- Wu, Meng-Ju, Lei Shi, et al. (Mar. 1, 2022). "Mutant IDH Inhibits IFN γ -TET2 Signaling to Promote Immuno-evasion and Tumor Maintenance in Cholangiocarcinoma". In: *Cancer Discovery* 12.3, pp. 812–835. ISSN: 2159-8290. DOI: 10.1158/2159-8290.CD-21-1077.
- Wu, Xiaoji and Yi Zhang (Sept. 2017). "TET-mediated active DNA demethylation: mechanism, function and beyond". In: *Nature Reviews. Genetics* 18.9, pp. 517–534. ISSN: 1471-0064. DOI: 10.1038/nrg.2017.33.
- Xu, Wei et al. (Jan. 18, 2011). "Oncometabolite 2-hydroxyglutarate is a competitive inhibitor of α -ketoglutarate-dependent dioxygenases". In: *Cancer Cell* 19.1, pp. 17–30. ISSN: 1878-3686. DOI: 10.1016/j.ccr.2010.12.014.
- Xu, Yufei et al. (Dec. 7, 2012). "Tet3 CXXC domain and dioxygenase activity cooperatively regulate key genes for *Xenopus* eye and neural development". In: *Cell* 151.6, pp. 1200–1213. ISSN: 1097-4172. DOI: 10.1016/j.cell.2012.11.014.
- Yamaguchi, Shinpei et al. (Dec. 20, 2012). "Tet1 controls meiosis by regulating meiotic gene expression". In: *Nature* 492.7429, pp. 443–447. ISSN: 1476-4687. DOI: 10.1038/nature11709.
- Yang, Qunjun et al. (Mar. 2, 2022). "D2HGDH-mediated D2HG catabolism enhances the anti-tumor activities of CAR-T cells in an immunosuppressive microenvironment". In: *Molecular Therapy: The Journal of the American Society of Gene Therapy* 30.3, pp. 1188–1200. ISSN: 1525-0024. DOI: 10.1016/j.ymt.2022.01.007.
- Yeo, Alan T. et al. (June 2022). "Single-cell RNA sequencing reveals evolution of immune landscape during glioblastoma progression". In: *Nature Immunology* 23.6, pp. 971–984. ISSN: 1529-2916. DOI: 10.1038/s41590-022-01215-0.
- Yin, Yimeng et al. (May 5, 2017). "Impact of cytosine methylation on DNA binding specificities of human transcription factors". In: *Science (New York, N.Y.)* 356.6337, eaaj2239. ISSN: 1095-9203. DOI: 10.1126/science.aaj2239.
- Yokoyama, Ken Daigoro, Yang Zhang, and Jian Ma (Aug. 2014). "Tracing the evolution of lineage-specific transcription factor binding sites in a birth-death framework". In: *PLoS computational biology* 10.8, e1003771. ISSN: 1553-7358. DOI: 10.1371/journal.pcbi.1003771.
- Yu, Kai et al. (Aug. 2020). "Surveying brain tumor heterogeneity by single-cell RNA-sequencing of multi-sector biopsies". In: *National Science Review* 7.8, pp. 1306–1318. ISSN: 2053-714X. DOI: 10.1093/nsr/nwaa099.
- Yu, Miao et al. (June 8, 2012). "Base-resolution analysis of 5-hydroxymethylcytosine in the mammalian genome". In: *Cell* 149.6, pp. 1368–1380. ISSN: 1097-4172. DOI: 10.1016/j.cell.2012.04.027.
- Zeisel, Amit et al. (Mar. 6, 2015). "Brain structure. Cell types in the mouse cortex and hippocampus revealed by single-cell RNA-seq". In: *Science (New York, N.Y.)* 347.6226, pp. 1138–1142. ISSN: 1095-9203. DOI: 10.1126/science.aaa1934.
- Zhang, Lingjun et al. (Nov. 1, 2018). "D-2-Hydroxyglutarate Is an Intercellular Mediator in IDH-Mutant Gliomas Inhibiting Complement and T Cells". In: *Clinical Cancer Research: An Official Journal of the American Association for Cancer Research* 24.21, pp. 5381–5391. ISSN: 1557-3265. DOI: 10.1158/1078-0432.CCR-17-3855.
- Zhang, Xiaoran et al. (Oct. 2016). "IDH mutant gliomas escape natural killer cell immune surveillance by downregulation of NKG2D ligand expression". In: *Neuro-Oncology* 18.10, pp. 1402–1412. ISSN: 1523-5866. DOI: 10.1093/neuonc/now061.
- Zhao, Shimin et al. (Apr. 10, 2009). "Glioma-derived mutations in IDH1 dominantly

- inhibit IDH1 catalytic activity and induce HIF-1alpha". In: *Science (New York, N.Y.)* 324.5924, pp. 261–265. ISSN: 1095-9203. DOI: 10.1126/science.1170944.
- Zhong, Jianing et al. (Jan. 25, 2017). "TET1 modulates H4K16 acetylation by controlling auto-acetylation of hMOF to affect gene regulation and DNA repair function". In: *Nucleic Acids Research* 45.2, pp. 672–684. ISSN: 1362-4962. DOI: 10.1093/nar/gkw919.
- Zou, Zhongyu et al. (Oct. 2024). "RNA m5C oxidation by TET2 regulates chromatin state and leukaemogenesis". In: *Nature* 634.8035, pp. 986–994. ISSN: 1476-4687. DOI: 10.1038/s41586-024-07969-x.

Titre : Impact du D-2HydroxyGlutarate sur le micro-environnement tumoral des gliomes avec mutation IDH

Mots clés : Gliome diffus ; IDH ; D-2hydroxyglutarate ; Microglie ; Macrophages associés aux tumeurs

Résumé : Contexte : Les gliomes diffus sont les tumeurs primitives malignes du système nerveux central les plus fréquentes. Certains présentent une mutation du gène codant pour l'isocitrate déshydrogénase 1 ou 2 (IDH) qui leur confère la néo-activité de transformer l'alpha-cétoglutarate (α -KG) produit par l'enzyme non mutée en D-2hydroxyglutarate (D-2HG). L'accumulation de cet oncométabolite entraîne l'inhibition compétitive des dioxygénases dépendantes de l' α -KG, incluant la famille TET (Ten Eleven Translocase) des ADN hydroxylases, et les JmjC/KMDs histone déméthylases, qui conduit elle-même à l'hyperméthylation des histones et de l'ADN des cellules tumorales. Les macrophages et microglies associés aux tumeurs (TAMs) sont des cellules myéloïdes très abondantes dans les gliomes, dont le phénotype et la réponse immunitaire sont déterminés par l'ontogenèse et le microenvironnement. Les TAMs présentent des caractéristiques différentes en fonction du statut IDH du gliome, mais les mécanismes de régulation sous-jacents restent largement méconnus. Le D-2HG relargué dans le microenvironnement par les cellules de gliomes IDH-mutants (IDH-m) pourrait influencer le phénotype et la fonction de ces TAMs. Nous avons émis l'hypothèse que le D-2HG pourrait modifier l'épigénome des TAMs, comme dans le cas des cellules tumorales.

Matériel et méthodes : Nous avons comparé le méthylome (puce EPIC de méthylation) et le transcriptome des TAMs (CD11B+ isolés par tri cellulaire activé par magnétisme) de 25 gliomes IDH-m et 11 gliomes IDH-wildtype (IDH-wt), ainsi que de tissu cérébral contrôle non tumoral. Pour déterminer les effets directs du D-2HG sur la microglie, nous avons mis au point des cultures primaires de microglie humaine obtenues à partir d'une chirurgie de gliome ou d'épilepsie. Nous avons d'abord dosé le D-2HG dans la microglie traitée par D-2HG par spectrométrie de masse par chromatographie en phase liquide (LC-MS) afin d'évaluer l'entrée du métabolite dans ces cellules, et avons évalué l'activité enzymatique

de TET. Nous avons exposé ou non des cellules microgliales au D-2HG pendant 14 jours et analysé leur méthylome et leur transcriptome. Les ratios de 5mC/5hmC ont été analysés à une résolution de base unique. Nous avons évalué la réponse transcriptomique et la respiration mitochondriale après stimulation au LPS de la microglie pré-traitée par D-2HG. Enfin, nous avons analysé par snRNA-seq le transcriptome microglial d'un échantillon apparié de gliome IDH-m avant et après traitement par l'inhibiteur d'IDH-m ivosidenib, qui diminue les concentrations intratumorales de D-2HG.

Résultats : Nous montrons que les cellules myéloïdes CD11B+ des gliomes IDH-m humains présentent une hyperméthylation de l'ADN principalement au niveau des enhanceurs. Cette hyperméthylation est liée à une diminution de l'expression des gènes impliqués dans les réponses inflammatoires et le métabolisme glycolytique, et à l'inactivation des facteurs de transcription qui régulent la réponse microgliale aux stimuli environnementaux. L'exposition prolongée de la microglie primaire humaine au D-2HG inhibe l'oxydation de 5mC médiée par TET, ce qui entraîne une accumulation réduite des niveaux globaux de 5hmC. Nous avons observé des rapports 5mC/5hmC élevés, en particulier au niveau d'enhancers spécifiquement actifs dans ces cellules. Conformément à la modulation des enhanceurs, la microglie traitée au D-2HG présente une capacité pro-inflammatoire réduite et une augmentation de la phosphorylation oxydative. À l'inverse, la diminution des niveaux de D-2HG après traitement par ivosidenib chez un patient atteint de gliome IDH-m est associée à la restauration de l'expression génique liée à l'activation microgliale.

Conclusion : Nos résultats fournissent une base mécanistique de l'état hyporéactif de la microglie dans les gliomes IDH-m et élargissent le concept selon lequel les oncométabolites peuvent perturber la fonction des cellules immunitaires du microenvironnement tumoral.

Title: Impact of D-2HG on the Tumor Microenvironment of IDH-mutated Gliomas

Keywords: Diffuse glioma ; IDH ; D-2hydroxyglutarate ; Microglia ; Tumor associated macrophages

Abstract: Background: Diffuse gliomas are the most common primary malignant tumors of the central nervous system. A subset of these tumors harbors mutations in the genes encoding isocitrate dehydrogenase 1 or 2 (IDH), which confer a neo-activity that converts alpha-ketoglutarate (α -KG) produced by the wildtype enzyme into D-2-hydroxyglutarate (D-2HG). The accumulation of this oncometabolite competitively inhibits α -KG-dependent dioxygenases, including the TET (Ten Eleven Translocase) family of DNA hydroxylases and the JmjC/KDM family of histone demethylases. This ultimately leads to hypermethylation of both histones and DNA in tumor cells. Tumor-associated macrophages and microglia (TAMs) are abundant myeloid cells in gliomas, with their phenotype and immune responses shaped by ontogeny and the tumor microenvironment. The characteristics of TAMs differ depending on the IDH status of the glioma, yet the regulatory mechanisms underlying these differences remain poorly understood. D-2HG released by IDH-mutant (IDH-m) glioma cells into the microenvironment may affect the phenotype and function of TAMs. We hypothesized that D-2HG may influence the epigenome of TAMs, as in the case of tumor cells.

Materials and Methods: We compared the bulk DNA methylome (Methylation EPIC array) and transcriptome of TAMs (CD11B+ cells purified via magnetic-activated cell sorting) from 25 IDH-mutant (IDH-m) and 11 IDH-wildtype (IDH-wt) gliomas, as well as control tissues. To experimentally assess the direct effects of D-2HG, the oncometabolite produced and released by IDH-m glioma cells, we used primary cultures of human microglial cells obtained from glioma or epilepsy surgeries. We first measured D-2HG levels in D-2HG-treated microglia using liquid chromatography-mass spectrometry (LC-MS) to confirm metabolite uptake, and evaluated TET en-

zymatic activity. Bona fide IDH-m and IDH-wt cells were used as external controls. Microglia were exposed to D-2HG for 14 days, after which we analyzed their DNA methylome and transcriptome. Ratios of 5mC/5hmC were examined at single-base resolution. We evaluated the transcriptomic response and the mitochondrial respiration after LPS stimulation of microglia pre-treated with D-2HG. Lastly, we performed single-nuclei RNA sequencing (snRNA-seq) on microglial cells from a paired IDH-m glioma sample, before and after treatment with the IDH-m inhibitor ivosidenib, known to reduce intratumoral D-2HG levels.

Results: Our analysis revealed that CD11B+ myeloid cells in human IDH-m gliomas exhibit DNA hypermethylation predominantly at distal enhancers. This hypermethylation is associated with decreased expression of genes involved in inflammatory responses and glycolytic metabolism, as well as the inactivation of transcription factors critical for microglial response to environmental stimuli. Prolonged exposure of primary human microglia to D-2HG inhibited TET-mediated 5mC oxidation, leading to reduced global 5hmC accumulation. High 5mC/5hmC ratios were particularly prominent at lineage-specific enhancers. Consistent with this altered enhancer landscape, D-2HG-treated microglia demonstrated diminished proinflammatory capacity and enhanced oxidative phosphorylation. Conversely, depletion of D-2HG following ivosidenib treatment in an IDH-m glioma patient was associated with the restoration of microglial gene expression related to activation.

Conclusion: Our findings provide mechanistic insight into the hyporesponsive state of microglia in IDH-m gliomas and support the concept that oncometabolites, such as D-2HG, can disrupt the function of immune cells in the tumor microenvironment.

